Addis Ababa University

Addis Ababa Institute of Technology

School of Civil and Environmental Engineering

An Assessment of Long-term Overtopping of Dam under Climate Change (A Case of Baro I and II Hydropower Project)

By:

Bedasa Lemu

Advisor:

Dr.Ing. Dereje Hailu

Addis Ababa, Ethiopia

October 2019

Addis Ababa University

Addis Ababa Institute of Technology

School of Civil and Environmental Engineering

An Assessment of Long-term Overtopping of Dam under Climate Change (A Case of Baro I and II Hydropower Project)

A thesis submitted to the School of Graduate Studies of Addis Ababa University in Partial Fulfillment of the Degree of Masters of Science in Civil Engineering (Major Hydraulic Engineering).

By

Bedasa Lemu

Approval by Board of Examiners

______________________	____________	________
Advisor	Signature	Date
______________________	____________	________
Internal Examiner	Signature	Date
______________________	____________	________
External Examiner	Signature	Date
______________________	____________	________
Chairperson	Signature	Date

CERTIFICATION

The undersigned certify that I have read the thesis entitled: *An Assessment of Long-term Overtopping of Dam under Climate Change (In Case of Baro I and II Hydropower Project)* hereby recommend for acceptance by the Addis Ababa University in partial fulfillment of the requirements for the degree of Master of Science Hydraulic Engineering.

____

Dr.Ing. Dereje Hailu

(Supervisor)

____

Date

DECLARATION AND COPYRIGHT

I, Bedasa Lemu, declare that this thesis is my own original work and that it has not been presented and will not be presented by me to any other university for similar or any other degree award.

Signature: ________________________________

Date: ___________________

E-Mail Address: - badhookoo@gmail.com

Abstract

Current climate change is occurring in the world in serious cases, which affects all living and non-living things. Climate change will cause the problem of flooding, which damages the constructed structures (dam, road, buildings, bridge, etc.). This study assesses dam overtopping in case of Baro I and II under climate change on future projection representative concentration pathway (RCP) scenario RCP4.5 and RCP8.5 by using Regional Climate Model (RCM) and hydrological model by Arc SWAT model. The RCM data obtained from the Coordinated Regional Downscaling Experiment (CORDEX) Africa project using the driving force of General Circulation Model (GCM) of two institutions (MPI and CCLM). The downscaled RCM output bias-corrected by distribution mapping method and evaluated by the coefficient of determination (R^2), NSE (Nash Sutcliffe Efficiency (NSE) and Percent of Bias (PBIAS) results in 0.988, 0.969, and 6.485, respectively. The input data used for the model meteorological data, digital elevation model (DEM), land use land cover map 2018, and soil. The sensitivity analysis, calibration, and validation of the model is done by using SWAT-CUP model by using SUFI2 method. The model performance was evaluated using the coefficient of determination (R^2) and Nash-Sutcliffe Efficiency (NSE) results for calibration of the value of 0.75 and 0.71 respectively, for validation 0.84 and 0.82 respectively on a monthly basis.

Inflow hydrograph developed by Hershfield method and reservoir routing was done. The result obtained for two scenarios (rcp4.5 and rcp8.5) Baro I present future of peak inflow flow 3783.2 m^3/s and 5314.6 m^3/s, outflow 2244.9 m^3/s and 3004.9 m^3/s, mid future peak inflow 3892.9 m^3/s and 3314.6 m^3/s, outflow 2299.0 m^3/s and 2430.8 m^3/s and far future of peak inflow 3177.36 m^3/s and 3207.27 m^3/s, outflow 1903.01 m^3/s and 1918.68 m^3/s respectively. The result obtained for two scenarios (rcp4.5 and rcp8.5) Baro II present future of peak inflow flow 2233.5m^3/s and 2428.6 m^3/s, outflow 2081.4 m^3/s, and 2294.5 m^3/s, mid future peak inflow 3286.0 m^3/s and 3057.0 m^3/s, outflow 2871.4 m^3/s and 2544.19 m^3/s and far future of peak inflow 1882.85 m^3/s and 1898.42 m^3/s, outflow 1707.97 m^3/s and 1663.47 m^3/s respectively.

After frequency analysis, the simulated out of the RCM data result for two scenarios (rcp4.5 and rcp8.5) present future 6483.6 m^3/s and 6110.5m^3/s, mid future 5364.5m^3/s and 6304.7m^3/s, far future 5134.8 m^3/s and 4918.2m^3/s respectively.

Generally, the outflow above the projected RCM output for two scenarios (RCP4.5 and RCP8.5) result shown next future the spillway would not pass it. Hence, the dam at Baro I and II would be overtopped next future period.

Keywords: Baro-Akobo, dam, overtopping, climate change, spillway, RCM, Arc SWAT

Acknowledgment

First, I would like to thank the Almighty God for giving me all the things to finish this work successfully.

Secondly, I am deeply indebted to my advisor Dr.Ing. Dereje Hailu for his passionate and unreserved support, guidance, encouragement, and patience, which contributed to the success of this study. Thirdly, I would like to thank all organizations providing data to complete my work successfully. In addition, I would like to acknowledge the invaluable input of all individuals and organizations, in particular, those who provided materials, software and who helped me a lot during the data collection period. Finally, yet importantly, my thankfulness goes to all my families especially my wife Ms. Kulani Tesfahun for their support. All individuals and friends who have helped me in providing the required data and guiding me during my work.

.

ACRONYMS

AR4 - Assessment Report Four

AR5 - Assessment Report Five

CN – Curve Number

DEM - Digital Elevation Model

GCM - General Circulation Model

GIS – Geographic Information System

HEC- HMS - Hydrologic Engineering Center-Hydrologic Modeling System

HRU- Hydrologic Response Unit

ICOLD - International Commission on Large Dams

IPCC- Intergovernmental Panel on Climate Change

ITCZ – Inter-Tropical Convergence Zone

m.a.s.l. – Meters above Sea Level

MoWR- Ministry of Water Resources

MPI - Max-Planck-Institute for Meteorology Germany

NSE - Nash-Sutcliffe Efficiency

ºC - Degree Centigrade

OWDSE - Oromia Water Works Design and Supervision Enterprise

PMF - Probable Maximum Flood

PMP – Probable Maximum Precipitation

ppm - Parts Per Million

RCM – Regional Climate Model

RCP - Representatives concentration pathway

RMS - Root Mean Square Error

SNNP- Southern Nations, Nationalities, and Peoples

SRES - Special Report on Emissions Scenarios

SCS – Soil Conservation System

SWAT – Soil and Water Assessment Tool

US -United State

USACE - United States Army Corps of Engineers

UTM - The Universal Transverse Mercator

W.W.D.S.E-Water Works Design and Supervision Enterprise

WGEN - Weather Generator

WMO - World Meteorological Organization

Contents Page

List of Figures

List of Tables

1. Introduction

Dam is the most important component of water resource systems found in many places. Water is stored and regulated by dams for the development plans such that water supply, irrigation, manufacturing industry, energy generation, flood protection, recreation, etc. to meet required objectives for the required period.

A climate is a natural event, which describes the process of geographical weather condition. Climate and water have a positive and negative relationship. In the climate change Fourth Assessment Report of the Intergovernmental Panel (Ipcc, 2007), climate system warming is unequivocal, as is now evident from observations of increases in global average air and ocean temperatures, ice and snow melting, and rising global average sea level . In the fifth assessment, report (AR5) of the Intergovernmental Panel on Climate Change (IPCC) also says climate change is unequivocal (Intergovernmental Panel on Climate Change, 2014).

Impacts of climate change on water resources distribution has been projected as one of the major problems. However, the adaptations to the change still lack in many critical infrastructural systems. Embankment dams are very common in the world; hence, a large number of these dams will be affected due to climate change. Climate change can affect the dams and their performance through alterations of the hydrologic cycle.

Currently, impact of the climate change faces a wide range challenges on the reservoir management. Non- stationary nature of hydrological condition is one set of challenges, which in recent time an increase in frequency and severity of extreme weather events globally happening. This extreme event like flooding, increase the risk of dam care. One important concern is a probable maximum flood, which can significantly influence the sustainability and safety of the dam (Kunkel *et al.*, 2013). Gradual deposition of sediment reduces reservoir storage capacity, which affect functionality of reservoir and totally, the lifespan of the facility of the dam stopped. Moreover, if missing of flood control volume necessary to attenuate peaks in supply can compromise the safety of the dam structure. When flood levels exceed the designed spill capacity of reservoirs, the likelihood that dams will be overtopped increases (Manag, 2012).

Embankment dams are highly susceptible to failure due to their non-rigidity. Overtopping is one of eight codes developed in(ICOLD, 2014) for their survey reported in Bulletin on the safe passage of extreme floods. The reported finding of embankment dams, 35% have failed due to overtopping, 38% from piping and seepage, 21% due to foundation defects and 6% from other failure modes (as cited by (Abdellatif Mohamed and El-Ghorab, 2016). There have been several small and large-scale laboratory studies on embankment dam failures by overtopping, which provided useful discharge hydrographs for model validation (Manag, 2012; Amaral *et al.*, 2014). Overtopping has occurred due to inadequate spillway capacity, due to improper operation of spillway gates, failure of the body of the dam, upstream wave action, sedimentation, etc. In our country, Ethiopia, overtopping dams were occurred due to the determination of probable maximum flood result in a serious economic loss in case of Tendaho dam and Arjo dhidhessa cofferdam, etc. (Scale, Project and Report, 2017).

In the assessment of climate change, three critical change factors to be considered the magnitude and variability of rainfall and streamflow, the magnitude and severity of extreme flood and storm events, and the changes in vegetation and land use (Taye *et al.*, 2011).

Current climate change is already imposing a significant challenge to Oromia and South Nation Nationality and People region affecting food security, poverty reduction, energy supply, water supply, and sustainable development efforts, as well as by causing natural resource degradation and natural disaster. Baro-Akobo has a large watershed area, which is found in different weather condition; hence, there is a climate change impact on this river. These results increase or decrease in the amount of water in the basin, an increase in sediment amount, and fluctuation in flood in the basin. This study is to identify the effect of climate change on the life and stability dam in the study area.

1.2. Statement of the problems

Many studies investigated climate change effects on several hydropower dam during extreme flood in the present conditions and future scenarios through simulations of a hydrologic model using inputs of extreme precipitation. Overtopping is the major failure problem for the embankment dam in the world. Failures of earth/embankment dam due to overtopping 35% was failed, piping and seepage 38% was failed, foundation defects 21% was failed and 6% from other failure modes (Costa, 1985). The ongoing water projects and new water projects will have to concern with uncertainty associated with precipitation, which consequences in the inflow to the reservoir of the dam in climate change that will affect the life of the dam. Scientific evidence shows that the earth's climate is changing, climate change is real and happening (Nikulin *et al.*, 2018). The result of the negative temperature and very hot temperature at the start of 2019 on the world due to climate change. In our country, many of embankment dam was overtopped like Tendaho and Arjo dhidhessa cofferdam had been overtopped due to hydrologic extreme conditions (Scale, Project and Report, 2017). Particularly, the study made on climate change impact on Baro-Akobo River Basin reservoirs as cited in (Negassa, 2012) shown that inflow variability in the future emission scenarios. This shows that hydrological extremes condition may increase to the degree will be overtopping of dams and security of the downstream community by flooding disaster. All most all of the water resource projects feasibility study, and design of structure the effects of climate change was not considered. In this, the study key problems which initiate me is affect sustainability of the any structure due to climate change will produce the uncertainty associated with maximum precipitation will produce the maximum flood this result overtopping of dam risk under this condition. These problems affect management & performance Baro I & II embankment dam in the future.

1.3. The objective of the study

1.3.1. General Objective

The main objective of this study is assessing embankment dam overtopping under climate change for multipurpose hydropower project

1.3.2. Specific objectives

- Downscaling and bias correcting Coordinated Regional Climate Downscaling Experiment (CORDEX) regional climate model data
- Evaluation of the CORDEX data of future projection
- To evaluate the spillway adequacy for a long period
- To assess the sensitivity of the Baro I & II hydropower project on dam life under the climate change due to hydrological condition would be overtopped or not

1.4. Significance of the Study

This study mainly shows the significant effect of climate change on the hydraulic structures, especially on the dam. This study also gives information on the life of the dam under climate. Moreover, it enlightens is the climate change study considered in the design of a structure or not.

1.5. Research questions

- What are the effects of climate change on surface runoff?
- What is the effect of climate change on life dam of the under hydraulic condition?
- Is climate change result in the dam overtopping? If yes, what is measurement will be taken?

1.6. Limitation of the study

In this study, the climate change scenario considers only two representative concentration pathway RCP4.5 and RCP8.5 because of the other concertation emission scenario less effect than the others. The effect of the sedimentation of the reservoir, failure of the dam body due to seepage, failure of the spillway, other natural factors were not considered in the study. However, in the real world, the sediment inflow and some sort of leakage will occur due to natural and human influences. Hence, this study is open to be refined based on more regional climate models, emission and development scenarios considering sediment inflow, failure of the spillway, wind effect, land use land cover change and leakage losses.

2. Literature Review

2.1 Dam Overtopping

Dams are water packing, control or diversion structures that store water upstream in reservoirs. The water supplies for drinking, irrigation and industrial uses, flood control, hydroelectric power, recreation, and navigation are Aids provided by dams. At the similar period, dams also embody a risk to community safety.

The most common of the failures of the embankment dam is overtopping. The scientific research able to determinate the overtopping by using the analytical conceptual model coupling physical governing relationships with its scenarios (Lee and You, 2013) different factors and have gotten the would occurred. The driving force in dam overtopping is hydrological circumstances, mostly flood characteristics. Usually, engineering designs and hydrologic frequency analysis have depend on the assumption that hydrologic patterns (G. K, 2017). During dam failure, the flood results in a large devastating disaster which consequences include economic and human losses. Overtopping is the most common cause of failure in recent earth and earth-rock fill dams. According to the ICOLD report from a total of 33105 worldwide large dams 3/4 embankment dam corresponding 88% to earth dams and 12% to rock fill dams (ICOLD, 2014) based collecting dam failed in the world and analysis their problem. Embankment dams naturally cannot resist any of overtopping, due to imperfect erosion resistance of the material used in their construction. The extent of erosion is determined on material in the embankment, depth, and duration of the over-topping flow, the excellence and category of vegetation cover.

There were many embankment dams overtopped on worldwide. In our country, many of embankment dam was overtopped them like Tendaho and Arjo dhidhessa coffer dam overtopped due to miss forecasting of hydrological data and less estimation of probable maximum precipitation.

2.2 Cause of Dam Overtopping

There are many factor dam to be overtopped; those are flood frequency, spillway discharge capacity and other factors.

2.2.1 Flood Frequency

Non-stationary hydrological events will result from floods by producing a large amount of flow of water and increase water the level of the water bodies (stream, rivers, lakes, and oceans). The hydrological process as flood is has complex in natural events because it dependent on the catchment properties, rainfall and antecedent conditions. Flood events could be caused by long-lasting rainfall, failure of a dam, earthquake, landslide, human activities including the operation of flood control methods, etc. A set of challenges like severity of extreme weather event and increase the frequency, which arises from the non-stationary nature of hydrological conditions in recent decades. These extreme events, are flooding will increase the risk of reservoir and dam safety. Dam overtopping and failure the main factor is due to flood frequency (Prudhomme and Nick Reynard, 2002). To identify the depth duration of overtopping and duration require multiple routings of inflow hydrograph to minimize the impacts from these factors. (Prudhomme and Nick Reynard, 2002).

2.2.2 Probable Maximum Flood (PMF)

The Probable Maximum Flood (PMF) is the flood that combination of critical hydrological and meteorological conditions are reasonably possible in a particular drainage area. In critical meteorological condition if there is a finite limit on the atmosphere's ability to produce rain at any given location due to climate, topography and atmospheric moisture limits. The concept of a finite limit for precipitation from a single storm event is called the Probable Maximum Precipitation (PMP). On the other hand, the largest depth of rainfall for a given duration of storm that that is theoretically possible for a particular area and geographic location is probable maximum precipitation (PMP). The exceedance probability of the PMP by its nature is almost zero (i.e., it is an improbable event). In practice, the PMP exceedance probability and estimated return periods are in the range of 1 in 10,000 years to 1 in 1,000,000 years (Ouranos, 2015). It is the largest depth of precipitation for a given duration meteorologically possible for a design watershed or a given storm area, with no allowance made for long-term climatic trends (Project and Authority, 2014). PMP would result in the theoretical maximum flood, which give necessary information for the design of a given project in the targeted watershed. Climate projections using multi-model ensembles show increases in globally averaged mean water vapor, evaporation, and precipitation over the 21st century. Probable maximum flood is a flood from a given catchment with zero probability of exceedance and or it is an upper limit flood resulting from the severe combination of critical hydrologic and meteorological conditions (Pothwar *et al.*, 2015). There are two basic approaches, which help us to determine probable maximum flood (PMF). The first method is the deterministic approach and the second one is the probabilistic approach. In the first method, rainfall-runoff models are used and the second approach relies on flood or rainfall with a specified return period. In those, study rainfall-runoff model selected to determine the probable maximum flood.

Many dams were designed to accommodate floods based on the largest experienced local flood or a standardized PMF considered appropriate at that time. Overtopping the single most common cause of earthen or embankment dam. Typically, PMF is determined to design a spillway dam to minimize the risk of overflowing.

Spillway Adequacy

The spillway is a passage in a dam through which the design flood could be disposed of safely to the downstream. The spillway an important part of the dam that protects it from failure but the missing design of the spillway size results in the accident. An undersized spillway will lead to over-topping; therefore, design of spillway is serious to reservoirs (Tamirat Dessalegn & Awass, 2016). The spillway of embankment dam must be located away from the body such that discharge will not erode or destabilize the toe of the dam. The banks of spillway should be non-erosive unless provision must be made for protection. During peak flood, happen an emergency spillway must have adequate capacity to allow by considering the hazard to human life and potential property damage that may occur from the failure of the dam or too much flow rates through the spillway. (Manag, 2012).

2.2.2.1 Spillway Discharge Capacity

Discharge capacity under maximum reservoir level is determined from a hydrological study in which the hydrograph of the design flood flowing into the reservoir is the most important factor. Absolute accuracy cannot exist; it will depend on the amount and reliability of data collected in the past on river flow, flow pattern and meteorological aspect of major storms. In the words, the spillway design discharge refers to some intended maximum reservoir level. If the reservoir level is actually lower than expected flow, due to underestimated design flood in order to prevent the dam being overtopped with all disastrous consequences that may result from in (ICOLD, 2014).

Based on the inflow design flood determined in flow flood hydrograph to reservoir the discharge capacity of spillway is determined (Barker *et al.,* 2012). If the reservoir has significant and minimal storage volume the spillway capacity may be significantly less than the peak inflow discharge. When full size of the spillway is not available, dam overtopping can occur under more floods that are frequent. Dam failure from overtopping can lead to significant harm of life and downstream damages (Amaral *et al.*, 2014).

2.2.2.2 Spillway Configuration

The ultimate discharge and capacity reliability of a spillway affected by the configuration. When the spillway is uncontrolled or overflow, it steadfast with predictable discharges. Due to the mechanical and power failures of gated spillways can have inherent reliability concerns; the planned operations is differ from potential operations because of the incapability of an operator to access the gate controls hence an operator delay decision result downstream flooding concerns. In case IDF has significantly increased and the spillway is gated, the new spillway of dam flow may affect the gates, and reduce the capacity, and also when the flow stopped from weir orifice it has impact on access of the gate operations.

2.2.3 Reservoir Sedimentation

Amount of debris of some watersheds produce during rainstorms. Reservoir sediment distribution tends to increase the severity of sediment-related problems. Sediment yield predicting in reservoirs is extremely difficult due to the complication of the process like sediment transportation rate, production, type, mode of deposition, and reservoir operation, geometry, and stream variability (Morris *et al.*, 2004),(Walling, 2009). It is difficult to treat sediment estimation, as deterministic due to various uncertainties are inherent in the estimation of sedimentation and accumulation in reservoirs. Therefore, stochastic explanation ways for determining servitor sedimentation for a long period (Pothwar *et al.*, 2015); (Pothwar *et al.*, 2015)(Lee and You, 2013). Stochastic theory is used to evaluate the problem sedimentation. The probability of failure and life of reservoir modeled by probabilistic way of estimation in by considering the rainfall-runoff process, sedimentation, sediment conveyance, and reservoir storage and release (Garg and Jothiprakash, 2006). A better understanding of reservoir sedimentation and potential risk of failure could help to estimate the life span of reservoirs more effectively. Sediment deposition, transport and supply are the key aspects of sedimentation process but not linearly factor for estimation of annual reservoir sedimentation and accumulated through time. A comprehensive understanding of the dynamic nature of sediment yield or predictions to that end has yet to be achieved (Lee and You, 2013).

Generally, (Chanson, 2013) worldwide the design floods of numerous reservoirs were re-assessed and the revised discharge outflows of the many dams are typically larger than the previous design flow rate. Hence, during large flood events would produce dam overtopping due to inadequate storage or spillway capability is not available the this result catastrophic consequences in the case of embankment dams.

2.3 Climate Change

2.3.1 Global Climate Change

Climate usually defined as the average weather, or more rigorously, as the statistical description of the weather in terms of the mean and variability of relevant quantities over periods of several decades (typically three decades as defined by WMO). These quantities are most often surface variables such as temperature, precipitation, and wind, but in a wider sense, the "climate" is the description of the state of the climate system. The climate system consists of the following major components: the atmosphere, the oceans, the terrestrial and marine biospheres, the cryosphere (sea ice, seasonal snow cover, mountain glaciers, and continental-scale ice sheets) and the land surface. These components interact with each other, and through this collective interaction, determine the earth's surface climate. The complicity of the climate system shows different characteristics in time-to-time, and the specific phenomena involved in each one of the climate problems are quite diverse (Kovats *et al.*, 2014). All over the world climate, change is great occurring and it has an impact on stream flows, soil moisture, groundwater, and other hydrological parameters.

Between the start and end of 20th century, the global surface temperature was increased roughly by 0.74^{o}C (Shongwe *et al.*, 2015). It is now widely received that climate change is now happening and further change is unavoidable. The average global land and ocean surface temperature data calculated shows a warming of 0.85 ^{o}C in the period of 1880 to 2012 (Shongwe *et al.*, 2015). When multiple independently produced data sets exist, about 0.89 [0.69 to 1.08] °C the period from 1901 to 2012, and about 0.72 [0.49 to 0.89] °C the period from 1951 to 2012 (IPCC-Part A, 2014). Based on the IPCC report, these trends are set to continue to accelerate into the 21st century and will be accompanied by changes such as increases in extreme meteorological conditions events like a severe storm. In fact, based on the IPCC's latest findings, global average temperatures will probably raise a further 1.1 to 6.4ºC (2.0 to 11.5ºF) this century, depending on the extent of continued greenhouse gas emissions. This is more strongly after 1970; many studies discovery specifies that an increase in average global surface temperature over the past 50 years is attributable by human activities(Taylor and Pittock, 2011). Concentration of carbon dioxide (CO2), methane (CH4) and nitrous oxide (N2O) increase since 1750 by 40%, 150% and 20%, respectively (Intergovernmental Panel on Climate Change, 2014).

2.3.2 Climate Change in Ethiopia

For the past four decades, the average annual temperature in Ethiopia has been increasing by 0.37°C every ten years, which is slightly lower than the average global temperature rising (Osima *et al.*, 2018)(Emerta and Aragie, 2013). According to Emerita report, the greater part of the temperature rise was observed during the second half of the 1990s and temperature rise is more pronounced in the dry and hot spots of the country, which are located in the northern, northeastern, and eastern parts of the country.

Future temperature projection of the IPPC scenario show that the mean annual temperature will increase in the ranges of 0.9 to 1.1ºC at end of 2030, in the range of 1.7 to 2.1ºC at 2050, and in the range of 2.7 to 3.4ºC by 2080 in Ethiopia compared to the 1961 to 1990 (Emerta and Aragie, 2013). According to many studies, the precipitation projection in the next future shows an increase and decrease. Socio-economic and demographic development, technological change, energy, and land use, and emission of greenhouse gases and air pollutants are the driving force for the future climate change may occur concerning a range of variables (Ipcc, 2007). The future scenarios of driving agents (e.g. greenhouse gases and aerosols) are served into the climate models as input, and the output of these climate models is further used in climate change analysis and hence, the assessment of impacts, adaptation, and mitigation. In this work, climate change effects on the upstream watershed that will be producing high flood this result affects dam stability due to the amount of flood will come to the reservoir as compared to its capacity are studied.

2.4 Climate Model

Interaction between the atmosphere, land surface, ocean and cryosphere (glacier and ice sheets) process govern the earth's climate. These climate processes can be represented in mathematical terms based on physical laws such as the conservation of mass, momentum, and energy. The mathematical formulation is implemented in a computer program, which is referred to as a model. If the model includes enough of the components of the climate system to be useful for simulating the climate, it is commonly called a climate model (IPCC, 1999).

2.4.1 General Circulation Models

General Circulation Models (GCMs) have significant implications for climate at global and regional scales by indicating that rising concentration of greenhouse gases. In order to evaluate the effects of climate change on natural resources and maintain ecosystem integrity at the local and territorial scales, further studies should be conducted within the context of water resource management. One of the best tools for simulating current and future predictions of climate change scenarios is a global circulation model (GCM) (Tang, Xu and Xu, 2012)). Projections of climatic variables globally have been performed with General Circulation Models (GCMs) that provide projections at large spatial scales. Unfortunately, due to its coarse spatial GCMs are restricted in their usefulness for local studies (typically of the order 50,000 km^2) and inability to resolve essential sub-grid scale features like topography and clouds (Arritt *et al.*, 2002) . A GCM is composed of many grid cells that represent horizontal and vertical areas on the earth's surface in each of the cells. It compute the following things: water vapor and cloud atmospheric interactions, direct and indirect effects of aerosols on radiation and precipitation, changes in snow cover and sea ice, the storage of heat in soils and oceans, surfaces fluxes of heat and moisture, and large-scale transport of heat and water by the atmosphere and oceans (Arritt *et al.*, 2002).

Downscaling global-scale climatic variables to local-scale hydrologic variables and computing hydrological components for water resources variability and risks of hydrologic extremes in the future are the major components.

2.4.2 Regional Climate Model

Regional climate models (RCMs) have become important tools for providing detailed estimates of future climate change, to support a range of studies concerned with the regional impacts of climate change on natural ecosystems, society and even government and large utility planning(Giorgi, Jones and Asrar, 2009)(Abbasa, Wasimia and Al-Ansari, 2016). In today RCMs act as an important link between the global climates modeling for downscaling local climate and climate, change issues [38]. Many studies of regional effects of different global warming levels are based on ensembles of coarse-resolution global models, however, for impact assessment and adaptation planning, high-resolution regional climate information is necessary (Osima *et al.*, 2018). High-resolution regional climate projections generated by Regional Climate Models (RCMs) within the Coordinated Regional Climate Downscaling Experiment (Sanjay *et al.*, 2012)(Gutowski *et al.*, 2016). The Coordinated Regional Downscaling Experiment (CORDEX) was set up by the World Climate Research Program (WCRP) in 2009 to coordinate Regional Climate Downscaling and provide a set of high-resolution regional climate projections for the majority of global land regions. The spatial resolution of Regional Climate Models (RCMs) provides more reliable results on the regional scale as compared to General Circulation model(GCMs) which provide a new opportunity for climate change effects analysis (Nikulin *et al.*, 2018)(Muerth *et al.*, 2013). Additionally making this data available, and importantly useable, to impact and adaptation communities was a fundamental goal. Coordinated Regional climate Downscaling Experiment (CORDEX) is initially focused on Africa, which is particularly vulnerable to climate change and in general, has a low adaptive capacity. Multi-model CORDEX- Africa ensembles utilize for assessment of climate change in Africa applying the standard framework with a focus on fixed period (Osima *et al.*, 2018). The regional climate model requires the driving force of the global climate model to downscale the global climate data to the local area. Two RCMs (REMO2009 and CCLM-4-8-17) applied selected for this study based on the previous study on Africa by other researchers and literature (Lennard *et al.*, 2018). The simulated data of the models were averaged and used for the analysis of the study area.

2.4.3 Downscaling

The process of the Global Circulation model output to a local or particular location of interest by using models (dynamic or statistical) to increase the resolution is known as downscaling. Downscaling may use to increase the temporal resolution (e.g. from monthly to daily values of Precipitation and Temperature) or the spatial resolution (e.g., from a GCM grid cell size down to the weather station scale). Dynamic and statistical downscaling are the two main approaches to developing local or regional scales information from the global climate scenarios applying general circulation model. Dynamic downscaling which involves a nested or higher spatial resolution of 10-50 km of regional climate model (RCM) through the inclusion of more realistic topography and land use/vegetation (Chen, Brissette and Leconte, 2012). Statistical downscaling techniques, which employ a statistical relationship between the large-scale climatic data and local variations derived from historical data (Chen, Brissette and Leconte, 2012). In dynamic downscaling systematic errors will occur due to RCMs, require statistical corrections to provide realistic output. The main drawback of RCMs is that they are computationally costly complex models (Murphy, 1999). As such, RCM data is relatively scarce; fewer greenhouse gas emission scenario run and, except for a few inter-comparison studies, data from more than one model is rarely available for climate change uncertainty study. Moreover, despite improvements, the output of RCMs is still too coarse for several practical applications, such as smaller watersheds and site-specific agricultural impact studies, which may need local and site-specific climate scenarios. The relationships between GCM output and historical data to produce a finer spatial and temporal resolution of climate data at the regional level by statistical downscaling. It more effective as and less expensive than dynamical downscaling. Especially useful for temporal downscaling (from monthly to daily values). A diverse range of statistical downscaling techniques are available each method lies, generally, in one of the three categories, namely regression (transfer function) methods, stochastic weather generators, and weather classification schemes (Arritt *et al.*, 2002). The goal of dynamic downscaling, i.e., to extract local-scale information from large-scale GCM data, is achieved by developing and using the limited area models (LAMs) or regional climate models (RCMs) (Tang, Xu and Xu, 2012). For the climate change data RCMs data simulation, dynamic downscaling is applied for this study.

For classification of the present or recent climate in a region, good quality observed climatological data are required for a given baseline period. The criteria should be to consider in the selection of climatological baseline consists of the types and sources of data, duration of the baseline period, and sources of the data and how they can be applied in an impact assessment.

The baseline period is usually selected according to the following criteria (Intergovernmental Panel on Climate Change (IPCC), 1999).

- In the study region of a adequate encompass a range of climatic variations and several weather anomalies (e.g. severe droughts or cool seasons) should a representative of the present-day or recent average climate.
- All major climatological variables adequately distributed, abundant and readily available and including a period of data
- The baseline period should high quality of data and non-overlapping 30-year is normal as defined by World Meteorological
- It represents the recent climate, to which many present-day human or natural systems are likely to have become reasonably well adapted (though there are exceptions, such as vegetation zones or groundwater levels that can have a response lag of many decades or more relative to the ambient climate)
- In most countries, the observed climatological data are most readily available for this period, especially in the computer-coded form at a daily time resolution in evaluating impacts;
- Reliable or readily equivalent with baseline climatologists used in other influence assessments

In this study the baseline period for this 1981-2013 due to the observed meteorological data availability in the study area.

2.4.4 Global Emission Scenarios

In 1996, the IPCC began the development of a set of emission scenarios adapted, effectively to substitute the famous IS92 scenarios. The approved new set of scenarios is described in the IPCC special report on emission scenarios (SRES) until IPCC AR4. There are four different storylines where established to describe consistently the relationship between the forces driving emission, their evaluation and to add context for the scenario quantification to show the global integration, economic emphasis, environmental emphasis, and regional emphasis. Reducing of income alterations between world regions technology is the main driving force for demographic and economic development is assumed in all SRES scenarios. In four scenarios change in technological, demographic and economic are driving force of the future the greenhouse gas and Sulphur emission. From one of all storylines, each scenario contribute the specific quantification. The same storyline have families of scenarios which mainly express the properties of four SRES storylines (Ipcc, 2007). The A1 storyline and scenario family describe the global population reach peak in mid-century very rapid economic growth and new and more efficient technology in the future. The A2 storyline and scenario family describe a very heterogeneous world. Economic growth, per capita and technological advancement is primarily regionally oriented but more fragmented and slower than in other storylines. The B1 storyline and scenario family describe the global solution to environmental and social sustainability, quality improvement, but no additional to climate initiative. The B2 storyline and scenario family describe for the regional solution to social, economic and environmental sustainability. However, the world population increasing slower rate than A2, those scenarios work until the intergovernmental panel for climate change assessment report fourth.

2.4.5 Representative Concentration Pathways

The Representative Concentration Pathways (RCPs) describe four different 21st-century pathways of greenhouse gas (GHG) emissions and atmospheric concentrations, air pollutant emissions and land use. The RCPs represent the four range of GHG emissions scenario include a severe mitigation scenario (RCP2.6), two intermediate scenarios (RCP4.5 and RCP6.0), and one scenario with very high GHG emissions (RCP8.5). Scenarios without additional efforts to constrain emissions (‘baseline scenarios’) lead to pathways ranging between RCP6.0 and RCP8.5. The aim of RCP2.6 is to protect the global warming below 2°C above pre-industrial temperatures. Many models shown the RCP2.6 meeting level of substantial net negative emission by 2100 on average around 2 Gt CO_2/yr.(IPCC-Part A, 2014). According to the Special Report on Emission Scenarios (SRES) in IPCC AR4, by the year 2100, the minimum atmospheric concentration of CO_2 is projected to reach about 490ppm, 650ppm, 850ppm, and 1370ppm for the RCP2.6, RCP4.5, RCP6.0 and RCP8.5 scenario respectively. For air pollutants such as sulfur dioxide (SO_2), the RCP scenarios assume a there is decrease in emissions because of assumed air pollution control and GHG mitigation policy. Importantly, it does not consider the natural forcing i.e. volcanic eruptions (IPCC, 2014). From the four representative concentration pathway (RCP2.6, RCP4.5, RCP6. and RCP8.5) dynamically downscaled regional climate multi-model outputs of CORDEX-Africa, the RCP4.5, and RCP8.5 selected because the concentrations emission of CO_2 is RCP4.5 is higher than RCP2.6, for RCP8.5 higher than the RCP6.0 when compared with each other. The present analysis is based on multi-model downscaled products out from CORDEX Africa project (Kim *et al.*, 2014). To more understand present-day climate changes as compared to observations and the future projections of climate changes impact under under a medium stabilization scenarios (RCP4.5) and a very high baseline emission scenarios (RCP8.5) (Kunkel *et al.*, 2013). Comparison of CO2 concentrations by RCP emission scenarios are indicated in figure 2.1.

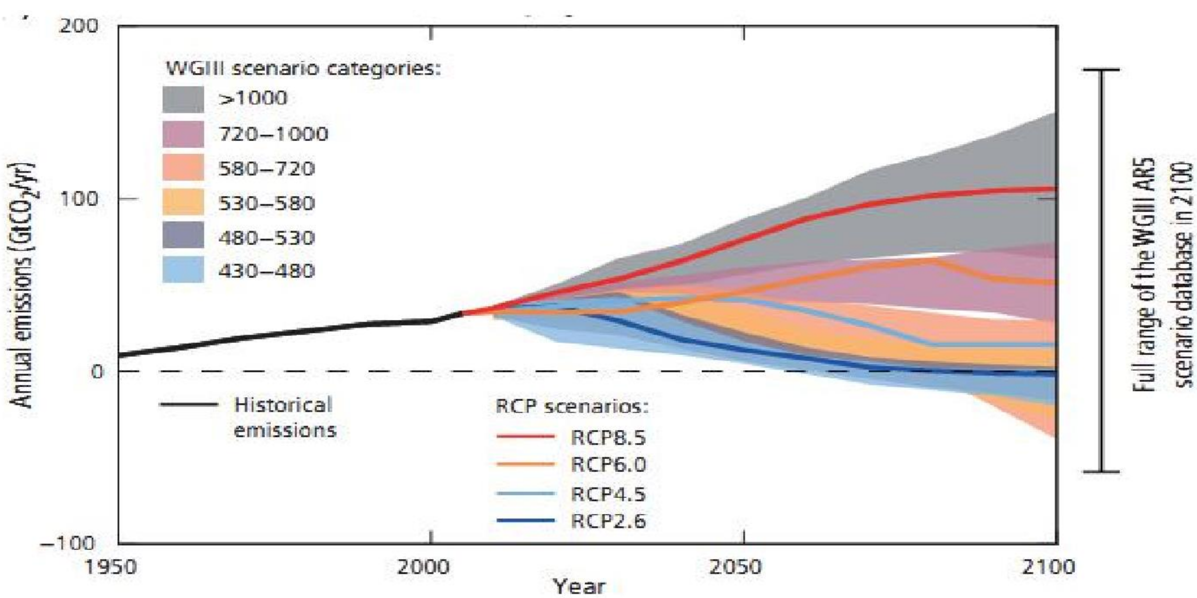

Figure 2:1 Representative concentration pathway (adapted from (Intergovernmental Panel on Climate Change, 2014))

2.4.6 Criteria for selecting climate scenarios

Depending impact on the researcher and policymakers climate scenarios should meet five criteria as suggested in(Mearns *et al.*, 2003)(Feenstra *et al.*, 1998):

- **Criterion 1:** Consistency with global projections. Based on an increased concentration of greenhouse gases all scenario should be consistent with broad range of global warming projections. This range is variously cited as 1.4°C to 5.8°C by 2100 (IPCC-Part A, 2014), or 1.5°C to 4.5°C for a magnifying of atmospheric CO_2 concentration - else known as the "equilibrium climate sensitivity" (IPCC, 2014).
- **Criterion 2:** Plausibility of physical. The scenario should obey the laws of physics, Hence, when there is changes in one region this change should be physically consistent change of another region and globally. Besides, the combination of changes in different variables which are often correlated with each other) should be physically consistent.
- **Criterion 3:** Applicability in impact assessments. Spatial and temporal scale variables should allow to for impact assessment. Input data for impact model variables like solar radiation, humidity, wind speed and precipitation at spatial scales from global and at temporal scales from annual to daily or hourly values
- **Criterion 4:** Representative. Scenario have the potential representative of future regional climate change and the ability to determine realistic impacts of estimation.
- **Criterion 5:** Accessibility. They should be easy to obtain, interpret and apply for impact assessment.

2.4.7 Bias Correction

The GCM outputs data have abundant biases that related to model-related uncertainties. Before using the model output data it is important bias correction data for impact assessments (Ahmed *et al.*, 2013). Bias correction is widely used in climate impact modeling. The main role of bias correction to correlate selected statistics of climate model data to better match observed statistics of climate data with the reference period. Bias correction might or might not include a downscaling step; it might y or might not adjust the simulated climate change; and it might adjust marginal aspects only, or also spatial, temporal and multi-variable aspects. The basic principle of bias correction is that selected climate model steps skillful input for a bias correction including a plausible representation of climate change (Maraun, 2016). GCM is the best tool available for projection of climate into the future, but are biased in GCM outputs. This bias output data is simply explained as the deviation from the observations data. However, in another expression, incorrect reproduction of extreme temperatures, prediction of excess number of wet days with low-intensity rainfalls, under or over-prediction of climatic variables, incorrect seasonal variations and so on are some of the forms of biases prevailing in GCM out-puts (Teutschbein and Seibert, 2013). According to (Lafon *et al.*, 2013), GCMs often incorrectly estimate the occurrences and intensities of precipitation. The limited understanding of the atmosphere and the simplified representation of the atmospheric processes in GCMs are regarded as the main causes of GCM bias. In general, prognostic variables of a GCM contain relatively less bias than the diagnostic variables that are derived from the prognostic variables. Since prognostic variables do not always show good relationships with the predictands of interest, diagnostic variables are also used in developing the downscaling models despite their larger bias (Shuma, 2015). This correction is used to correct the bias of predictands (e.g. precipitation and temperature) which were downscaled from GCM driving force of the RCMs outputs. Bias-correction has no direct connection with the internal functions of the GCM.

There are many different bias-correction techniques. Those techniques could be applied to the outputs of downscaling models, irrespective of whether the downscaling approach is dynamic or statistical. (Teutschbein and Seibert, 2013) used multiple bias correction techniques (linear scaling, local intensity scaling, power transformation, variance scaling, distribution mapping, Empirical quantile mapping, and delta-change approach) on dynamically downscaled precipitation and temperature.

2.5 Hydrological Modeling

2.5.1.General

Goodman (1984) defines systems analysis as "in a generic sense, systems analysis can refer to an orderly and scientific approach to problem-solving". Mathematical modeling is an essential tool in modern water resources planning and management. The selection of models is generally determined by the objective at hand, resources available, and detail and scale of investigation required. Because it is difficult to reliable apply most of the models developed in the "data-rich".

2.5.2. Hydrologic Model Selection Criteria

There were numerous criteria, which could be used for choosing the right hydrologic model. These criteria are always projected dependent since every project has its specific requirements and needs.

Further, some criteria are also user-dependent, such as personal preference for computer operation system, input/output management, and structure, or users add on expansibility. Among the various project-depended selection criteria, four main common, fundamental ones must always be considered (Cunderlik, 2003):

- Required model outputs important for the needed purpose and therefore to be estimated by the model: - Does the model predict the variables required by the project such as peak flow, event volume, hydrograph, and long term flows?
- Hydrologic processes that need to be modeled to estimate the desired outputs adequately: - is the model capable of simulating regulated reservoir operation, single event or continuous processes?
- Availability of input data: - can all the inputs required by the model be provided within the time and cost constraints of the project?
- Price: - does the investment appear to be worthwhile for the objectives of the project?

HEC-HMS Model

The hydrologic Modelling System developed by the US Army Corps of engineering Hydrologic Engineering center is designed for both continuous and event-based hydrological modeling, this software simulates the precipitation runoff process of the dendritic watershed system.

Arc SWAT

The Soil and Water Assessment Tool is a semi-distributed, physically based, and continues time step hydrologic model that is used for rainfall-runoff modeling as well as forecasting the effect of climate change on the hydrology and water quality of the rivers and watershed.

Considering the above issues, the physically based distributed model ArcGIS interface Soil and water assessment tool (SWAT) was applied in this study. ArcGIS interface with Soil and Water Assessment Tool (Arc SWAT) is a physical process-based, continuous, semi-distributed model to simulate the process at a catchment scale. It divides a catchment or basin into sub-basins by hydrological response unit (HRU) based on soil type, land use and management practice for this study is used.

2.5.3. Soil and Water Assessment Tool (Arc SWAT)

SWAT is the Soil and Water Assessment Tool**,** which is used to model a river basin, or watershed developed by Dr. Jeff Arnold for the USDA Agricultural Research Service (ARS). Since SWAT was created in the early 1990s, it has undergone continued to review and it has a different version. Different versions are SWAT94.2, SWAT96.2, SWAT98.1, SWAT99.2, SWAT2000, SWAT2009, etc. In each version, there are many improvements in Arc SWAT. This model was created to forecast the impact of sediment, chemicals amount in agricultural land when there is different soil, land use and management and use of water over long period (Neitsch *et al.*, 2011).

2.5.3.1. Overview of Soil and Water Assessment Tool(SWAT)

Soil water assessment tool allows several different physical processes to be simulated in watershed. This model is physical based it requires about soil properties, topography, vegetation, land management and weather information of the watershed. It model the sediment movement by water, water movement, crop growth, nutrient cycling, etc. In modeling purposes, a watershed might be partitioned into several sub-watersheds or subbasins. The dividing watershed subbasins in a during simulation is particularly beneficial when different areas of the watershed are dominated by one watershed properties that result impact to hydrology. When the watershed is subdividing into subbasin, which requires to distinguish the watershed spataily from one other. For each subbasin the necessary input data must be arranged are hydrologic response unit, groundwater, wetland/pond, climate, and main channels, or reach and draining the sub-basin. Hydrologic response units are lumped land areas within the sub-basin that are included of single land cover, soil, and management combinations.

2.5.3.2. Simulation of Arc SWAT

For any type of the problem studied by SWAT, what happens in the watershed water balance is a very important application to accurately forecast the movement of sediment, nutrients, pesticides, the hydrologic cycle as simulated by the model. Hydrologic cycle watershed simulation has two major division. The first one is land phase of the hydrologic cycle. In this division controls the amount of nutrients, sediments and pesticide loadings to the main channel in each sub-basin. The second division is the hydrologic cycle routing phase which well-defined as the movement of sediments, water, etc. through the channel networks of the watershed to the outlet point (Neitsch *et al.*, 2011).

Land Phase of the Hydrologic Cycle

The land phase of the hydrologic cycle is used to determine or control the amount of water in the watershed and different input data are required in this phase; climate, hydrology and overland cover. The hydrologic cycle governed by the water balance equation , its components of which consider the final soil water content, initial soil water content, precipitation, surface runoff, evapotranspiration, water entering the vadose zone from the soil profile and return flow. In the hydrologic cycle there different inputs and process that involved. For each HRU runoff is analysed then routed to get the total runoff for watershed. This increases accuracy and gives a much better a lot of the water balance.

In SWAT there are provides two methods to determine the surface runoff, the SCS curve number procedure (Mckeever, 1972) and Green & Ampt Infiltration method. SWAT simulates surface runoff volumes and peak runoff rates for each HRU using daily or sub-daily precipitation. Green & Ampt Infiltration method (1911) requires the sub-daily rainfall data and SCS requires daily data. Therefore, SCS curve number method is selected in the study. Rainfall depth, initial abstraction (surface storage, interception, and infiltration), retention parameter. The retention parameter varies spatially due to changes in soil, land use, management, and slope and temporally due to changes in soil water content.

The SCN curve number is a function of land use, permeability of soil, and antecedent soil water conditions. The three SCS describes antecedent moisture conditions: I – dry (wilting point), II – average moisture, and III- wet (field capacity). The U.S. Natural Resource Conservation Service(NRCS) classifies soil into four hydrological groups based on infiltration characteristics of the soils. Those are A, B, C, and D groups of soils or three dual classes, A/D, /D, and C/D. Definitions of classes are:- A(low runoff potential) the soil has a high infiltration rate even when all wetted and they have a high rate of water transmission. e.g sand or gravels. B(The soils have a moderate infiltration rate when all wetted). They have a moderate rate of water transmission. E.g soil has moderately fine to moderately coarse textures. C: The soils have a slow infiltration rate when all wetted. They have a slow rate of water transmission. They have a slow rate of water transmission. E.g soil has moderately fine to a fine texture. D(High runoff potential). Soils having slow infiltration rate when carefully wetted. This group of siol high swelling potentail due to large consist of clay soil, soils that clay layer at surface less water trasmision. Dual hydrologic groups are given for certain wet soils that can be sufficiently drained. The first letter applies to the drained condition, the second to the undrained.

For any type of soil curve number moisture condition II is defined but for the other soil moisture conditions determined from curve number two.

Typical curve numbers for moisture condition II are listed in various authors that are proper to slope less than 5%. However, for areas with slopes greater than 5%, the curve number is adjusted (Williams, 1995). The adjustment of the curve is not conducted in the SWAT for the slope but if required by the user must do before entering the curve number file to the model.

Peak Runoff Rate

The peak runoff rate obtained when there is event rainfall happened. This peak runoff rate is a function of fraction of daily rainfall, the surface runoff; area is the sub-basin area and the time of concentration

The average rainfall intensity have a duration equal to the critical storm duration, normally taken as the time of concentration (Yilma Shileshi (Dr.), 2005). Time of concentration is the time taken for a drop of excess rainfall on the most remote point of a drainage basin to reach the outlet, where remoteness tells to the time of travel rather than distance. In other words, it is the time after the start of rainfall excess when all parts of the drainage basin are donating concurrently to flow at the outlet. The time of concentration includes the overland flow and channel flow time.

ii. Routing Phase of Hydrologic Cycle

In this routing phase of the hydrologic cycle in Arc SWAT is the way to determine the movement of water in the watershed. The routing phase has two parts in the channel and reservoir routing of the watershed.

Channel Routing

In SWAT model, water in sub-basin channel network routed using variable storage or Muskingum River routing method. The variable storage method uses a simple continuity equation, whereas the Muskingum routing method uses wedge and prism storage of channel length. In addition to the wedge storage, the reach section covers a prism of storage shaped by a volume of the constant cross-section along the reach length. The variable storage routing method was developed by Williams (1969) and used in the HYMO (Williams and Hann, 1973) and (routing outputs to outlets) ROTO (Arnold et al., 1995). SWAT uses Muskingum routing method.

Reservoir Routing

Flow into the reservoir should be routing to determine of the hydrograph, spillway capacity and capacity of the reservoir. The application of reservoir routing based on the application of the continuity equation. The continuity equation considers the inflow, outflow, and storage with time. When the reservoir volume exceeds the principle storage, the extra water is released at the specified rate. The spillway capacity could be determined in this case.

2.5.3.3. Evapotranspiration

Evapotranspiration is the main ways by which water is removed from a watershed. Exact determination of evapotranspiration is critical in the valuation of water resources and the impact of climate and land-use change on those resources. There are many methods to calculate evapotranspiration. However, each method vary based on climatic variables required for calculation those are Penman-Monteith Method, Priestley-Taylor Method, Hargreaves Method (Neitsch *et al.*, 2011)

The Penman_Monteith method is recommended as the sole ET0 method for determining reference evapotranspiration when the standard meteorological variables including air temperature, relative humidity, and sunshine hours are available (Allen *et al.*, 1998).

2.6. Previous Study

The Baro I and II hydropower project were studied to pre-feasibility level in 1999 by NORPLAN-Norconsult. The study shows feasible for hydropower plant by evaluating the river discharge as well as the topography of the basin. Under the feasibility study of the project for the basin, the study considers the evaluation of the environmental impact and detain design of the project (International Monetary Fund, 2006).

Another study on the Baro I and II hydropower was climate change impact on reservoir operation under future projection future scenarios by considering the emission scenario for A1B using the RCM model. The result shows an increasing trend for both maximum and minimum temperature and precipitation increasing and decreasing precipitation next century. The projected mean annual temperature increases from the baseline period by an amount of $1^{o}C$ and $3.5^{o}C$, respectively, in the 2030s and 2090s. In general, the precipitation experiences a mean annual decrease of 1.8% in the 2030s and shall increase by 1.8% in the 2090s (Negassa, 2012).

Therefore the feasibility study for hydropower and climate change impact on the reservoir operation by considering emission scenario A1B from RCM data simulation which was the old emission scenario of climate change according to the assessment report five of IPPC and also the study didn't analysis is the overtopping of the dam in next century of climate projection.

3. Description of Study Area

3.1. Location

Baro Akobo river basin is located in the southwestern part of Ethiopia about approximately 600km from Addis Ababa, the Capital city of Ethiopia. The geographical location of the Baro-Akobo basin lies between latitudes of 5^0 31' and 10^0 54' north and longitude of 33^0 and 36^0 17'east and covers an area about 76,000km^2 of total drainage. The river basin flow through the four administrative regions of Benshangul-Gumuz, Gambella, Oromia and South nation Nationalities. This basin is the fourth largest river from the 12 major river basins in Ethiopia and neighboring with Abay river basin in the north and Omo-Gibe river basin in the south-west part of Ethiopia. It flows to the Sobat river basin in Sudan, which is tributary of the White Nile. The Baro I and II scheme hydropower projects are located along the Baro River in the Baro-Akobo Basin between Gore, Oromia, and Bonga, SNNPR(International Monetary Fund, 2006).

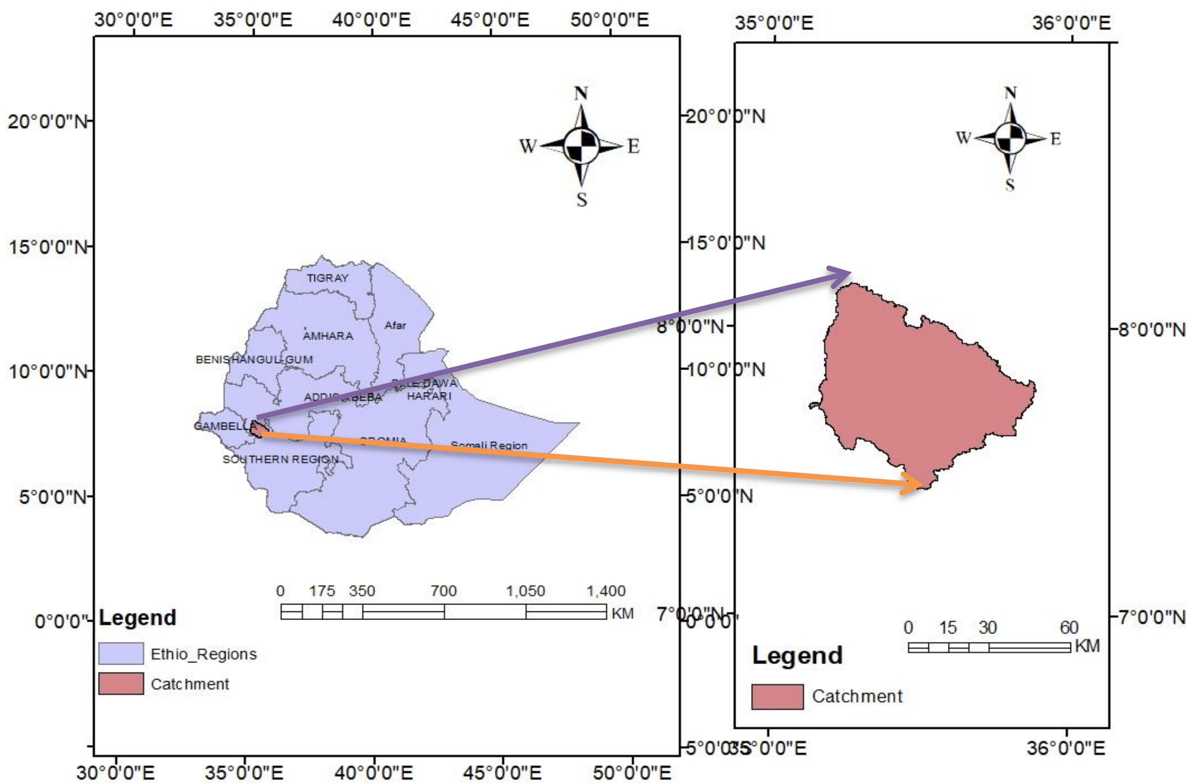

Figure 3:1 Location of the study area from Ethiopian map

3.2. Topography

The Baro-Akobo river basin covers highlands and lowland topographic area. Baro-Akobo Basin has elevation ranges from 390m.a.s.l. lowest and 3244m.a.s.l highest elevation. The basin divided into upper and lower Baro catchment by considering the hydropower project. The upper Baro catchment lies within the highlands of Illubabor and the lowlands of the Gambella plain with altitudes ranging from 550 to 2794 m.a.s.l. and with a mean elevation of 1883 m.a.s.l. as extracted from DEM data (figure 3.2). From the total drainage area of the basin the about 30,000km^2 drainage area in Baro river including Genji tributary used for hydropower development. The upper Baro catchment, sub-basin of the Baro-Akobo river basin, is located in the most eastern part of the basin. It lies in between 7^{o}27'8" N to 8^{o}17'30" N Northing and 34^{o}57'31" E to 35^{o}52'41" E Easting covering a total area of about 4828 sq.km. This hydropower project watershed covers parts of the highlands of Illubabor, lowlands of SNNPR and Gambella plain with altitudes ranging from 550 to 2794 m.a.s.l. From the slope map of the catchment, most of the area falls in the slope range of 0-67 % as shown in figure 3.2 obtained from the DEM of the Baro-Akobo river basin(International Monetary Fund, 2006).

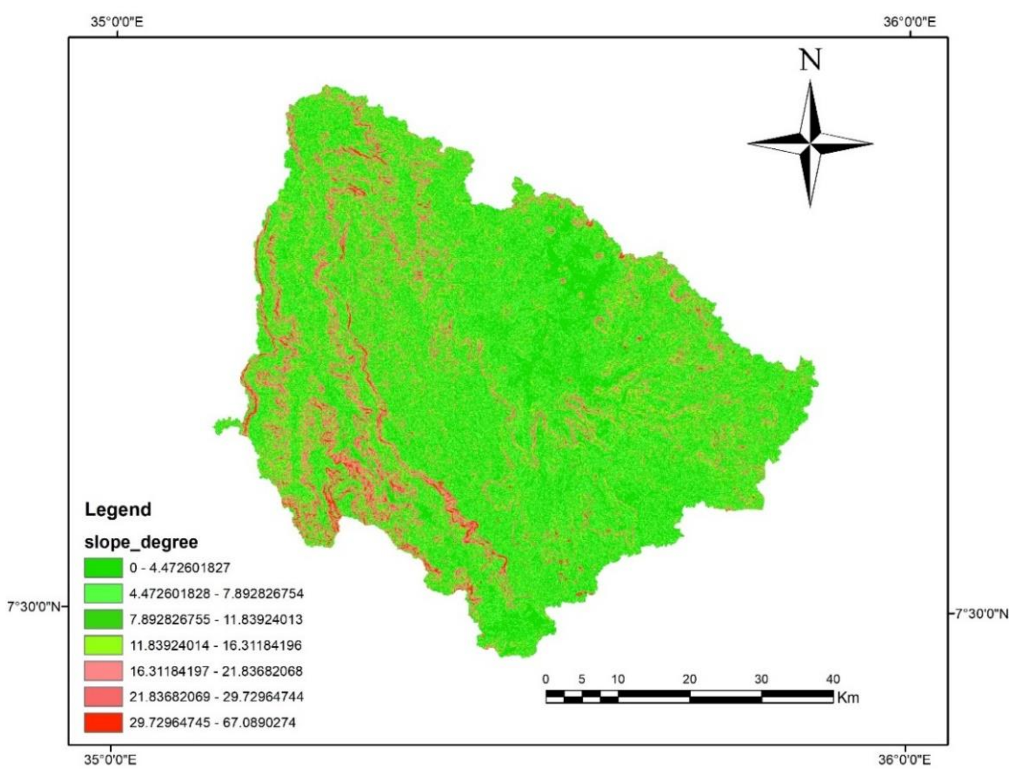

Figure 3:2 Topographic slope of the study area obtained from the DEM

3.3. Hydrology

The total mean annual flow from Baro-Akobo river basins is estimated to be 23.6 BMC. The Baro-Akobo basin is one of the most important basins in our country. There are many major rivers that flow to the Baro-Akobo river basin (Baro, Alwero, Gilo and Akobo rives). From major rivers, Baro and Akobo are Perennial River and they have different tributaries; the Baro rives tributaries (Birbir, Geba, Sor), Gilo tributaries (Gacheb, Bitun, Beg) and Akobo tributary (Kashu). The major tributaries of the upper Baro catchment are Gibo, Duchi, Birbir, Genji, Guracha, and Fano to form the Baro River. Dibo and Duchi tributaries are flows in a generally north-west direction with the total average drainage area of 14004 km^2 and an average elevation of 1700 m. Birbir river drains to north and eastern region with a total area of some 16,000 km^2, is actually the largest sub-basin within the Baro basin. Geba and Sor rivers are drains through the border of the Upper Baro catchment area; and the Genji, Guracha, and Fano Rivers are the other tributaries of the upper Baro river basin. The flow of major rivers closely matches the rainy season with peak discharge occurring during September (International Monetary Fund, 2006). The average annual flow for Baro I and II is 74.7m^3/s and 77.1m^3/s respectively(International Monetary Fund, 2006).

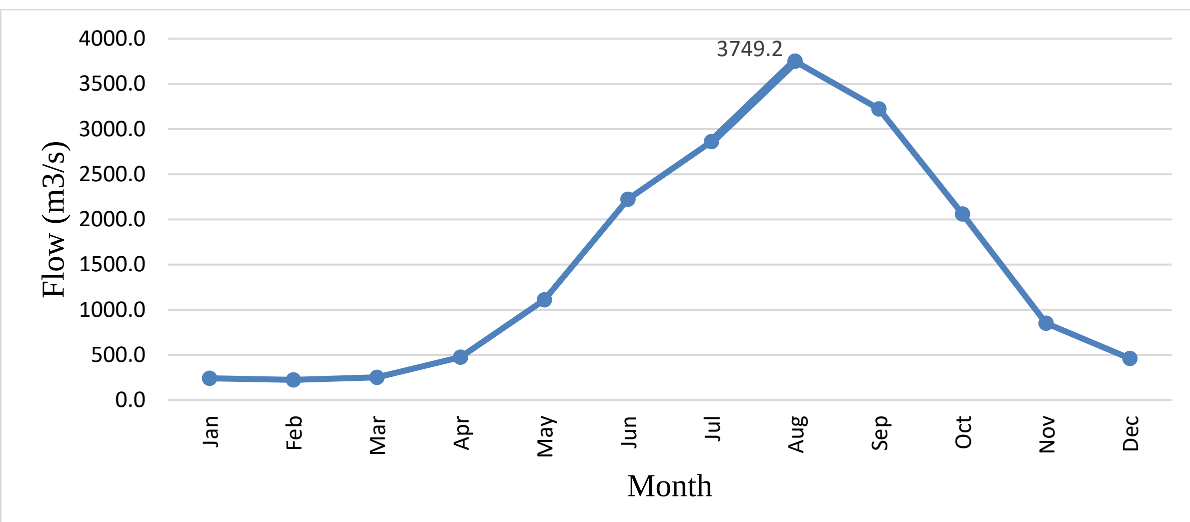

Figure 3:3 Monthly average flow of upper Baro River at Masha gauge

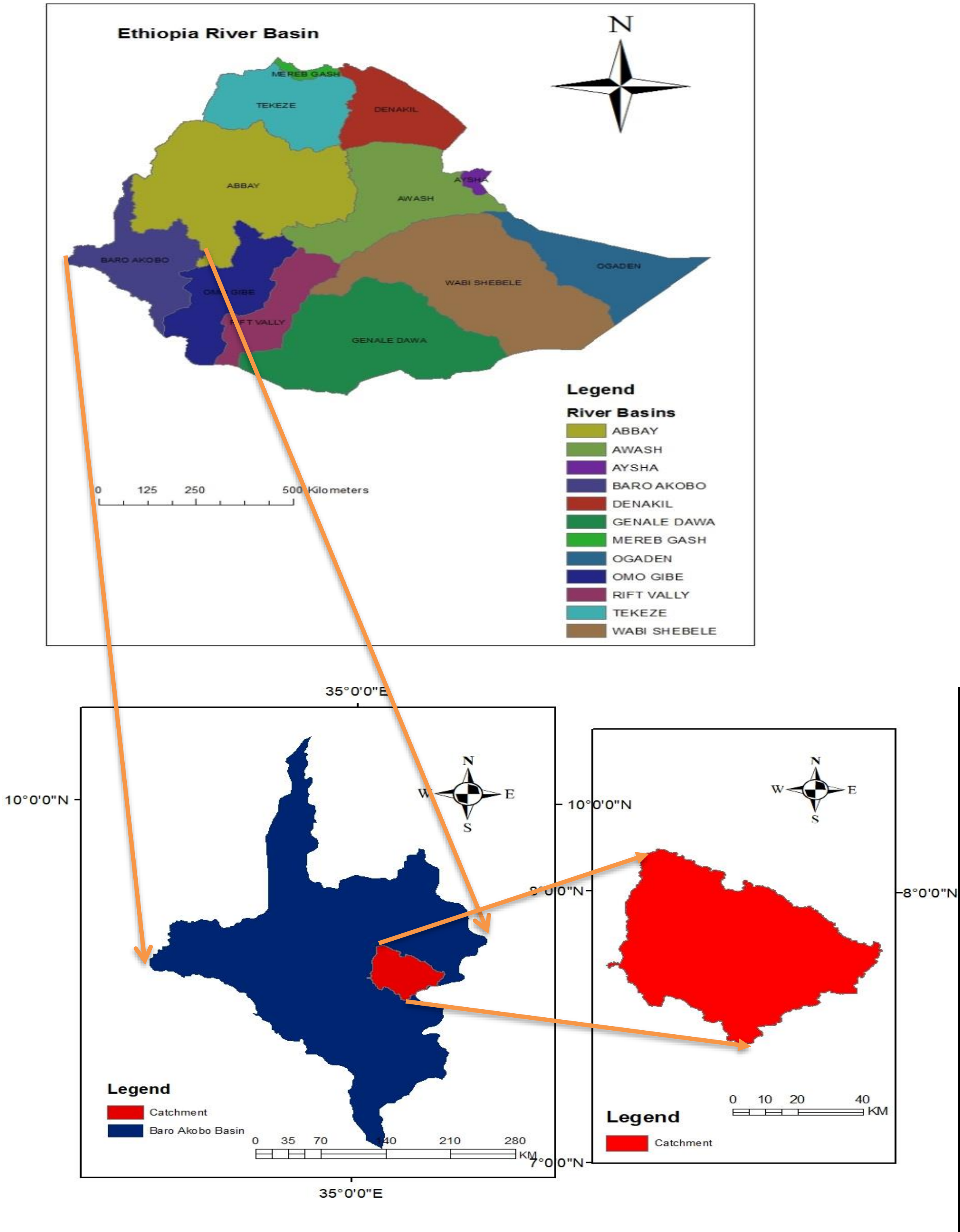

Figure 3:4 Upper Baro catchment from the Ethiopian river basin

3.4. Soil

The river basin covers a large area, due to this it has in different types of soil. The soil formation of the catchment area of this basin has different factors; those factors determine the soil types and their properties. A considerable part of the area was covered by residual soil derived from the underlying pre-Cambrian basement rocks. Alluvial deposits, sand, silt, and clay occur along the Baro River and its tributaries. The project area, except for parts of the Baro riverbed and steep sections of the slope up from the river, in general, covered by residual soil. The thickness varies, but general thickness is assumed of a few meters. Scattered deposits of alluvial materials are found along the riverbanks and in low gradient side valleys. The soil type mostly covers the watershed of the hydropower project are Dystric Cambisols, Haptic Acrisols, Humic Nitisols, Humic Alisols, Haptic Alisols, and Dystric Leptosols. Humic Nitisols and Dystric Cambisols the most types of soils cover the watershed of the study area, 67.2 %, and 15.7% respectively (International Monetary Fund, 2006) (Report, 2017).

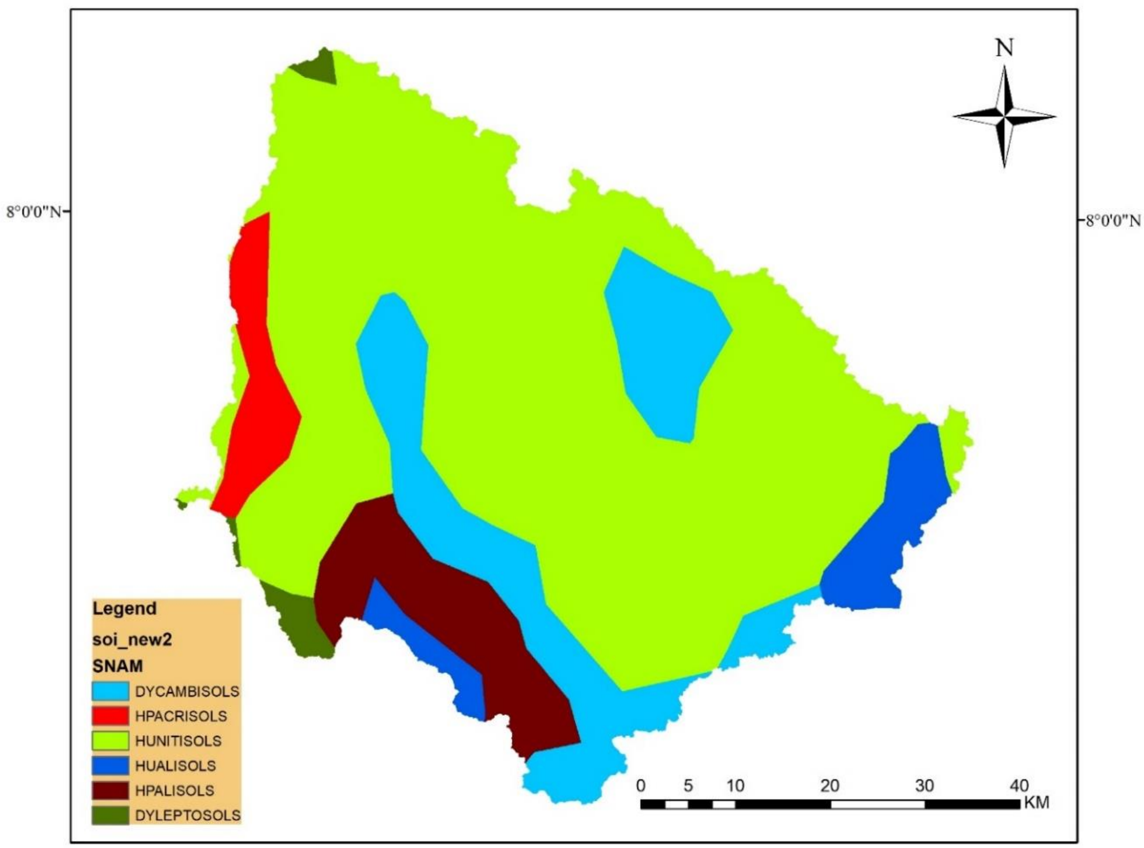

Figure 3:5 Soil type of the study area obtained from OWWDSE, 201

3.5. Land Use and Land Cover

Land use and land cover most of the time used interchangeably but they have a different meaning. Land use refers to the actual economic activity for which the land is used whereas land cover refers to the cover of the earth's surface. The land use of the study area was categorized mainly as agricultural, natural forest, waterbody, bush shrubland and woodland (MoA, 1990). The terms land use and land cover are often used even though the distinction between the two is important. The information contained in the land use map below shows how these different uses of the surface were distributed over the Upper Baro Basin. The land use land cover is a collective forest, agriculture, grasses land and bushland as shown in figure 2.6 (International Monetary Fund, 2006). This LULC map is not used for analysis but it is the input for image analysis of the study area.

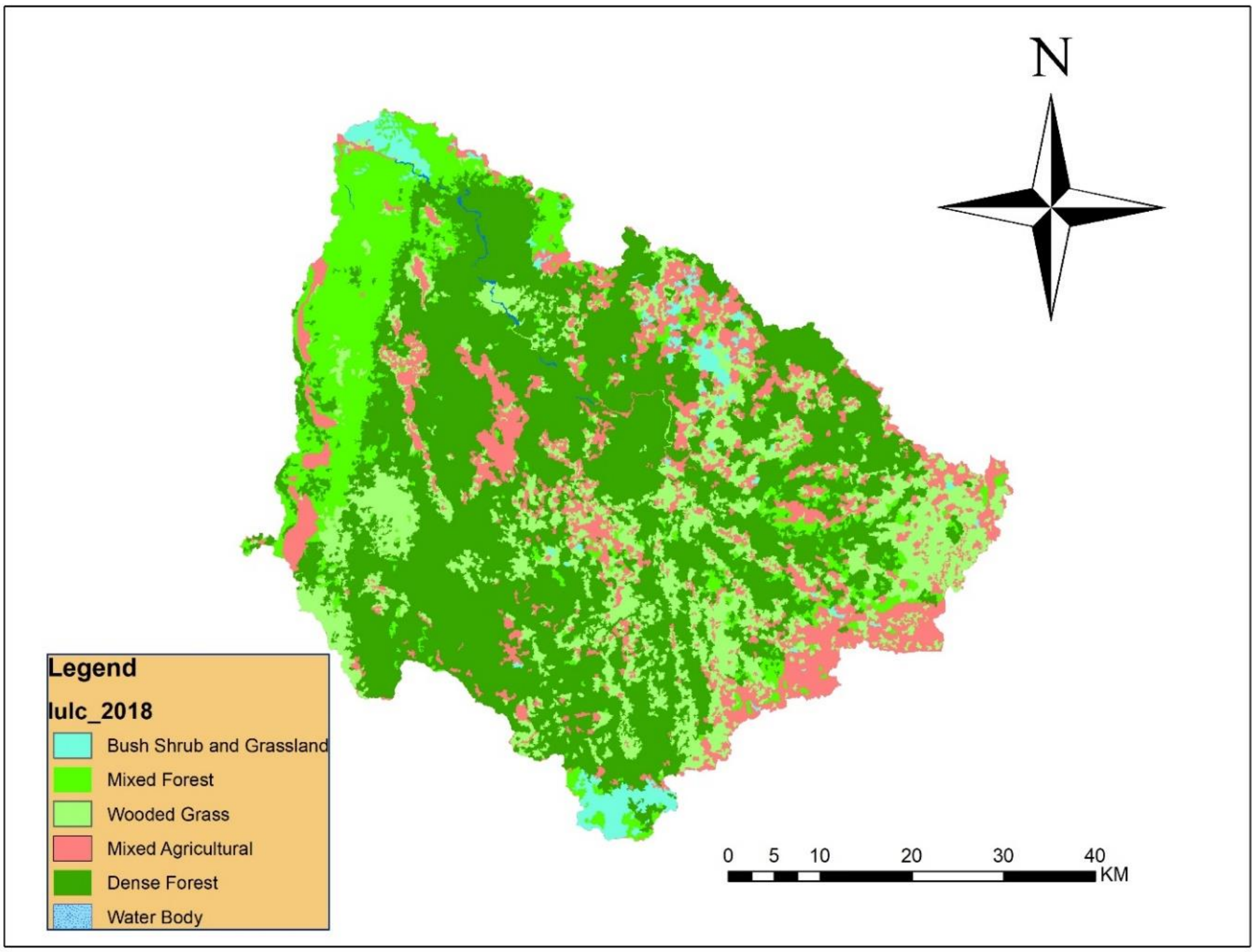

Figure 3:6 Land use land cover of the study area

3.6. Climate

Climate is the average weather condition of the area over a long period. The earth climate system influences changing temperature, precipitation, snowmelt, and a host of other natural phenomena, and it is also in turn influenced by the variability on earth(Fang *et al.*, 2015). In all parts of our country, Ethiopia, the elevation is highly affecting the climate characteristic and the river basin mainly connected with monsoon climate. On the other hand, almost all parts of the country climate are strongly influenced by the effects of elevation, which gives rise to distinct zones and characteristics.

The rainfall in the western part of Ethiopia likewise Upper Baro Basin mainly controlled by the Intertropical Convergence Zone (ITCZ) and the north or south different parts of the Upper Baro Basin experience different lengths of wet and dry seasons.

Through its northerly migration commencing in March, which is accompanied by a short wet-season in the south of the country. Around June, the ITCZ moves further north and produces the main wet season in most of the central and northern areas. The wet season here generally lasts until October, until the influence of the ITCZ diminishes as it moves southwards towards the equator.

The spatial variation of temperature circulation due to uneven distribution of land and ocean, coupled with different thermal properties. Temperature in basin shows warm and cold weather conditions along the elevation variation highland and lowland respectively. Traditional classifications based on altitude and temperature; show the presence of five zones, of which the following three are predominant in the Baro River Basin. Kola tropical hot and arid type, below 1500 m altitude with mean temperature in the range 20-28ºC. Woina Dega sub-tropical warm, between 1500-2500m.a.s.l altitudes with mean temperature in the range 16-20ºC. Dega temperate highland climate above 2500m.a.s.l. altitude with mean temperature in the range 6-16ºC (International Monetary Fund, 2006).

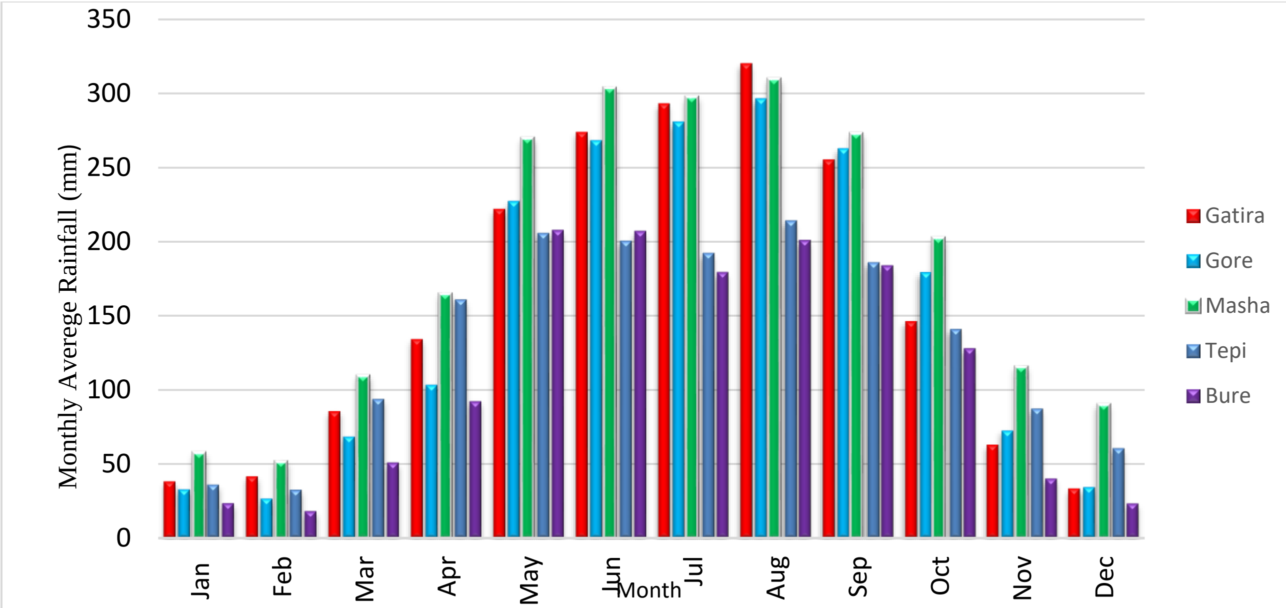

Figure 3:7 Monthly average rainfall of the watershed

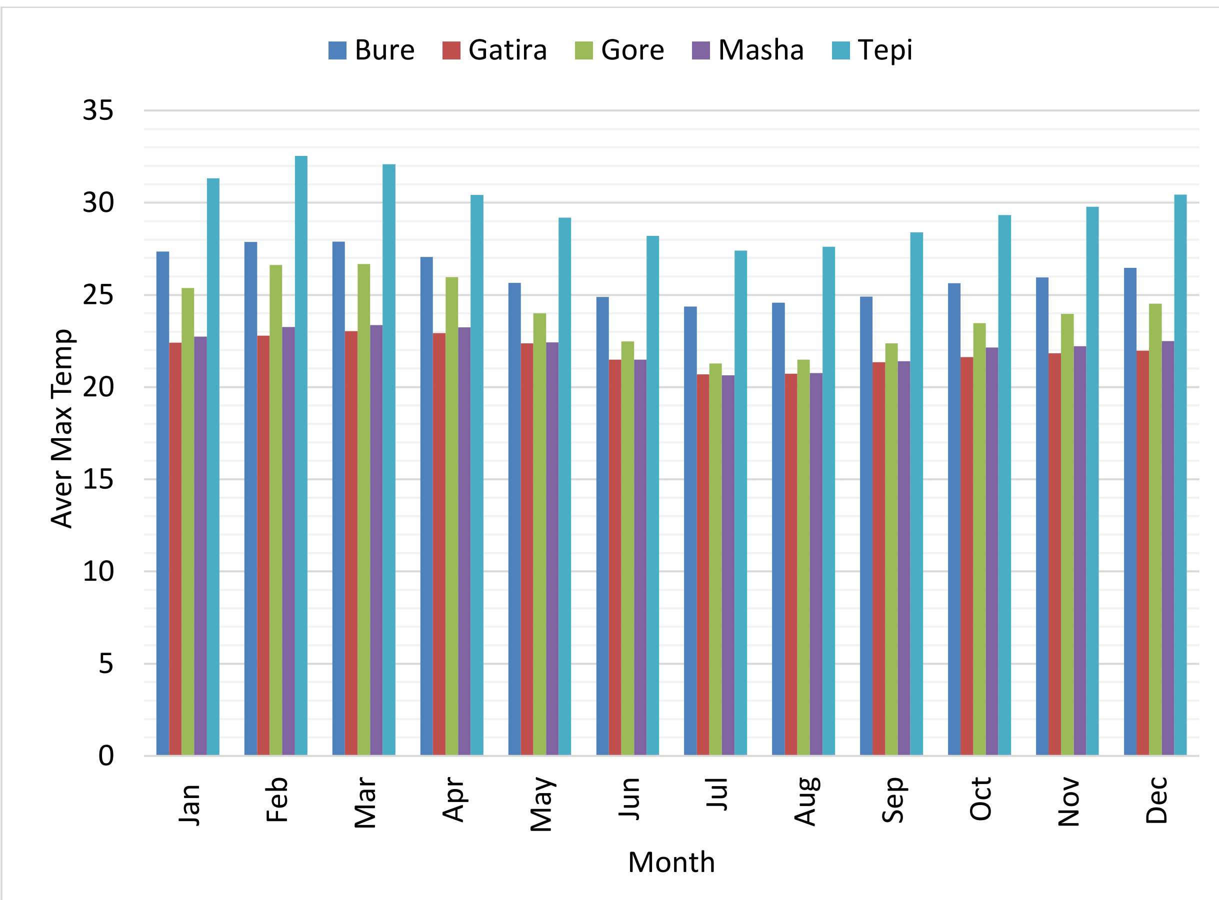

Figure 3:8 Monthly average maximum Temperature of the watershed

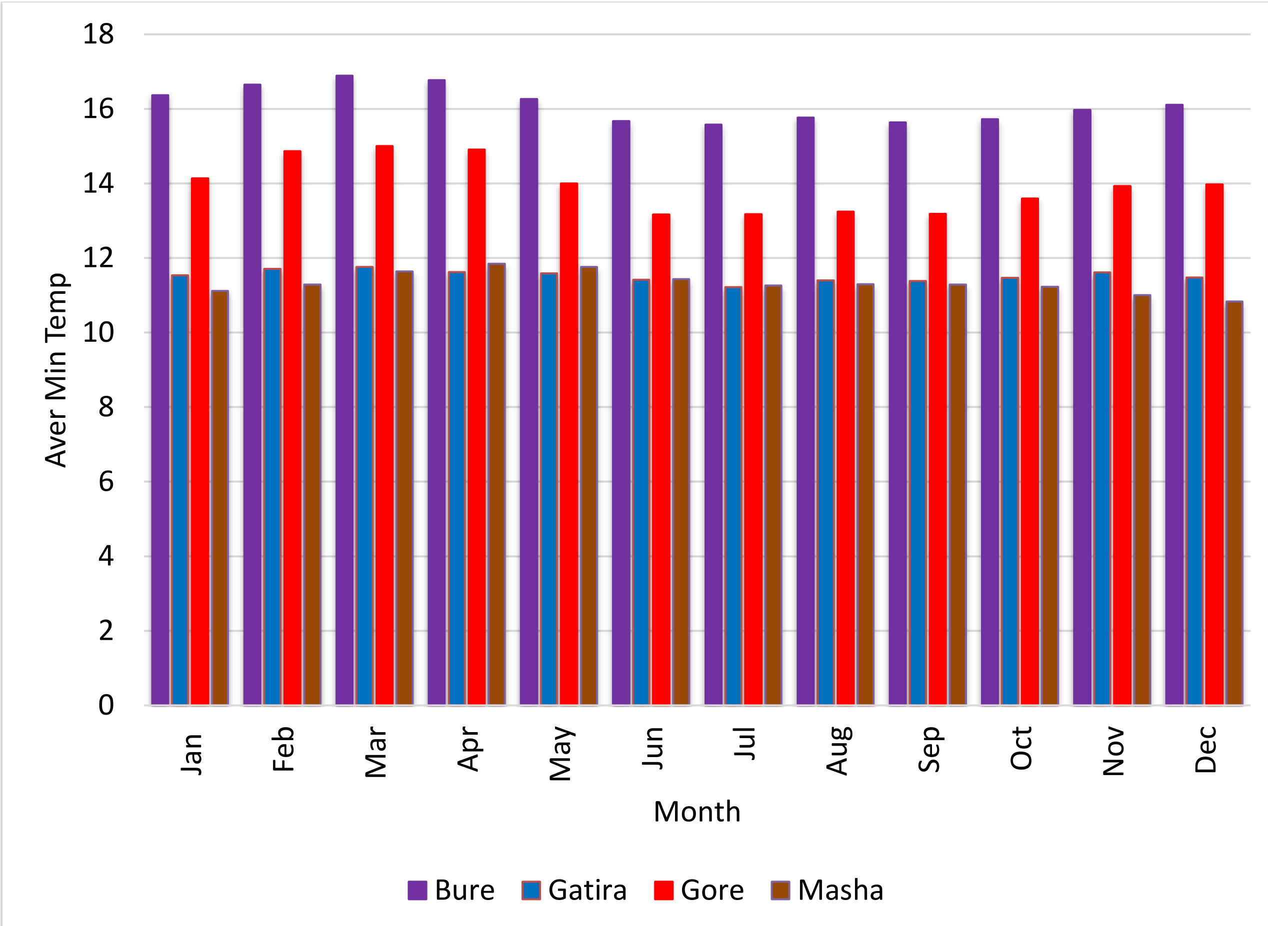

Figure 3:9 Monthly average maximum Temperature of the watershed

4. Materials and Methods

There are different materials to conduct the thesis those are, study area map, geographical information system (Arc GIS), Digital elevation model (DEM), soil and water assessment tools (Arc SWAT) model and Regional climate model (RCM).

4.1. Conceptual Framework of the Study

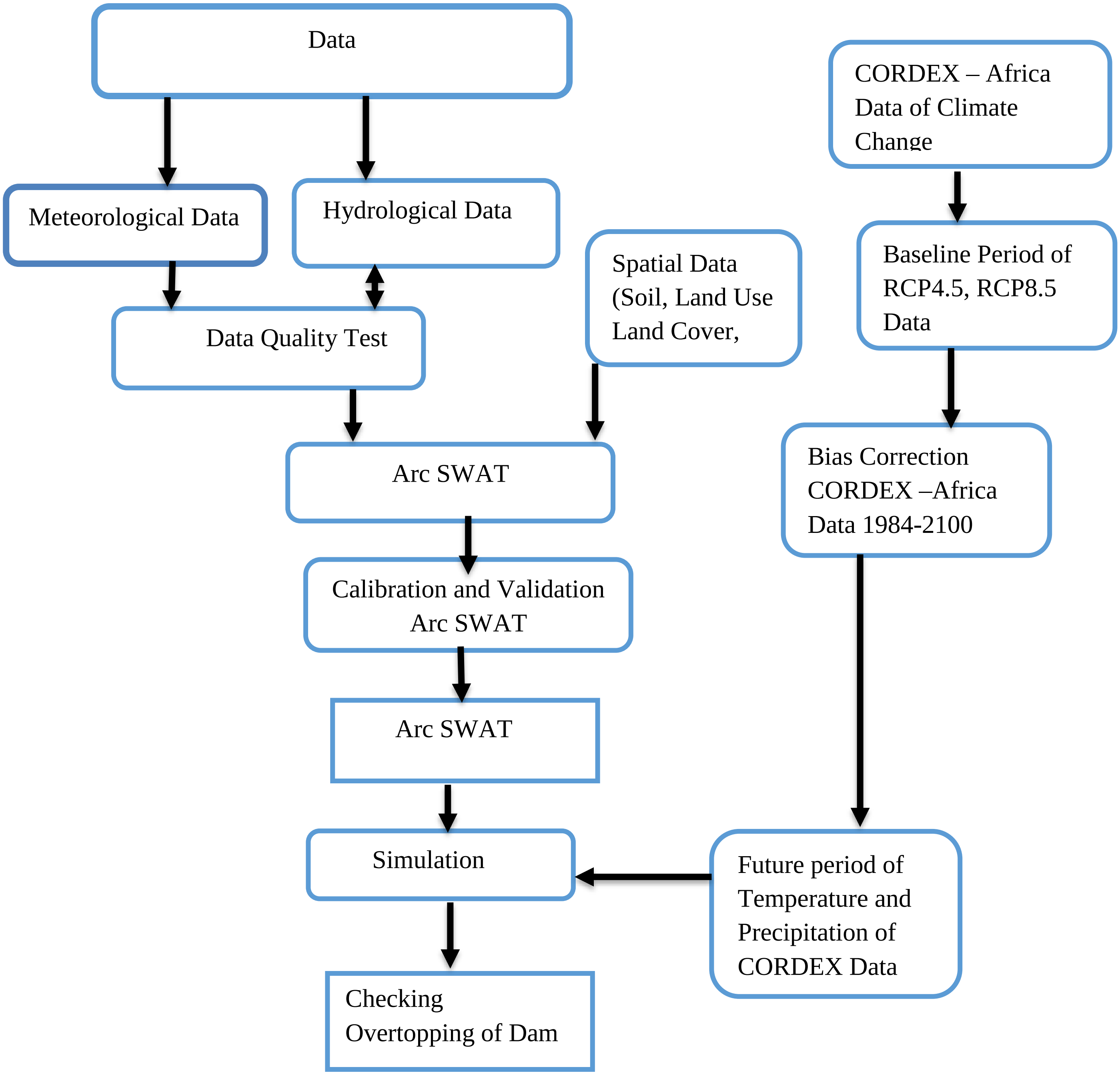

4.2. Data Collection

The primary requirement to conduct the research is data collection. Hence, there are different data are required to conduct this research. The data should be collected for the research are hydrological data, meteorological data, spatial data, catchment topographic data, the feasibility study of the Baro-Akobo hydropower plant data. Different hydrological, climatic, watershed, sediment data, and geospatial data of the study area are going to be considered during the research work.

4.3. Hydrological data

Hydrological data very important parameter to analysis any water resource development and management. The hydrological data is collected from the Ministry of Water Resources department of hydrology. From hydrological data observed daily time series of streamflow collected from this organization, and used for the calibration and validation of the Arc SWAT model. There are many gauging stations available in Baro-Akabo basin but for conducting this research three gauging stations were selected due considering the representativeness for study area watershed of the Baro-Akobo I and II hydropower plant. Observed hydrological data series of many gauging stations are Baro gauge near Masha, Genji gauge near Gecha, Baro Kella gauging and other stations are available in the upper Baro Basin. However, Baro Kella gauging station is located at the outlet of the upper Baro Basin, it has almost no data record and hence not used for study, but used for simulated basin outflow. Therefore, one gauging stations-Baro gauge near Masha has been used for the study. Other gauging stations in Baro River including Genji gauge near Gecha, Geba gauge near Bonga, and Sore gauge near Itang were used for comparison and filling missing data. The available data cover 20 years (1988- 2007) hydrological data which used for study.

4.4. Meteorological data

Meteorological data are the most important time series data necessary for hydrological design and analysis of water resources projects. The required meteorological data to conduct this research are precipitation, minimum and maximum temperature, relative humidity, sunshine duration, and wind speed were collected from National Meteorology Agency. Through the solar radiation recorded is not started in Ethiopia due to the solar radiation data calculated from the sunshine duration. The availability of data, the quality of data and the possibility of the station within the watershed or not, are the main criterions for the selection of the metrological station. The selected meteorological stations of the upper Baro catchment 5 stations (Bure, Gore, Masha, Tepi and Gatira) daily time series selected since they occur around Upper Baro Basin. The data collected covers a period of 1984-2013 years. Except few of the station, most of the station data are incomplete and short.

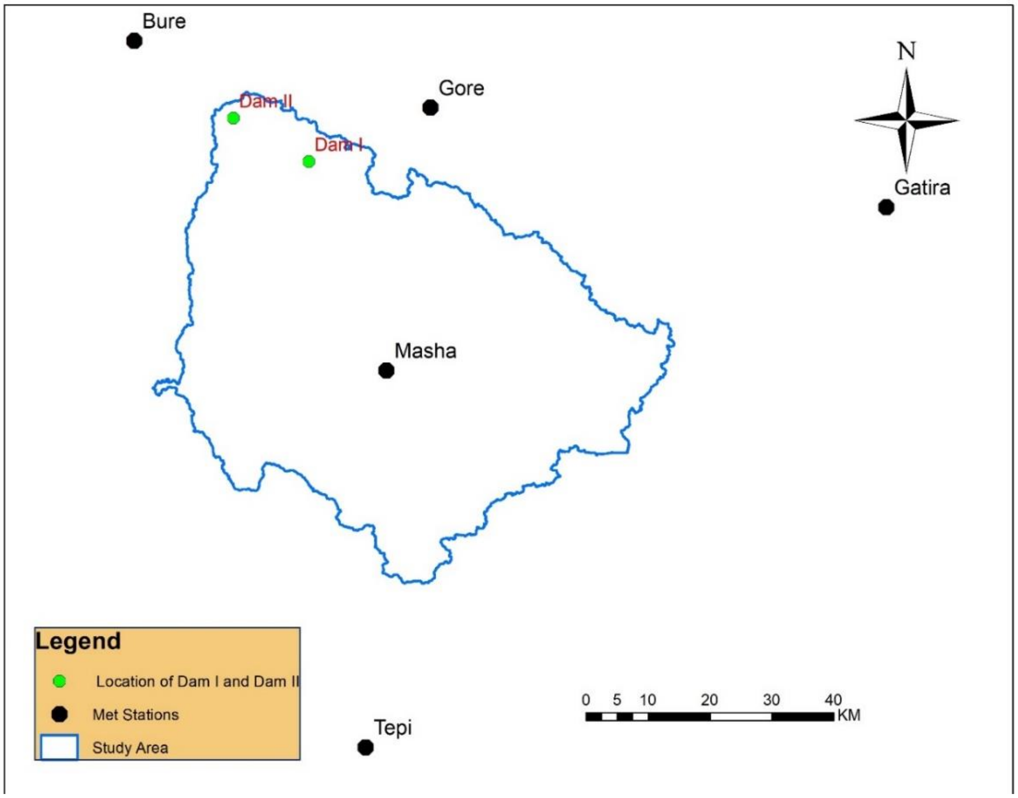

Figure 4:1 Meteorological stations of study area

4.5. Digital Elevation Model

A Digital Elevation Model (DEM) that describes the spatial resolution of any point in a given are of the topography of elevation as a digital file. A digital elevation model was needed for raster-based hydrological analysis in a GIS. DEM of the study area with the resolution of 30m by 30m is extracted from Ethiopian DEM and it is used to delineate the watershed properties of the study area. Watershed properties like sub-basin parameters such as slope, slope length and defining of the stream network, the outlet of each sub-basin with its characteristics such as channel slope, length, and width is derived from the DEM.

4.6. Soil and Land Use Land Cover

The soil database describes the surface and upper subsurface of a watershed and is used to determine a water budget for the soil profile, daily runoff, and erosion. Arc SWAT model requires textural properties and physio-chemical properties for each soil layer. Soil data is obtained from the Ministry of Water, Irrigation, and Energy bureau. Land Use Land Cover affects surface erosion, runoff, and evapotranspiration in a watershed. Land Cover Land Use map data used the map 2018. Design document of feasibility study of information concerning hydropower project of the study area obtained from this.

4.7. Regional Climate Model Downscaling Data

The regional climate model data downscaled from CORDEX Africa project, which is high resolution. CORDEX (Coordinated Regional Downscaling Experiment) obtained from two institutions; two RCM models of each have their GMC driving force model. This CORDEX Africa project RCM models have the 0.44^0 by 0.44^0 resolution. The key RCM model data of the hydrologic drivers (precipitation, maximum temperature and minimum temperature(Beyene, Lettenmaier and Kabat, 2010). This CORDEX dataset downloaded from climate impact4 and NASA Jet Propulsion Laboratory of California Institutes of Technology of climate by historical and RCP; their website https://climate4impact.eu/impactportal/data/esgfsearch.jsp and https://esgf node.jpl.nasa.gov/ac/list/ respectively for representative concentration pathway RCP4.5 and RCP8.5 scenarios. The climate change analysis categorized into historical, present future, mid future and far future period. RCM model data is classified into base period (1984-2013), present future (2014-2033), mid future (2034-2070) and far future or end of the 21st century (2071-2100) for analysis.

Table 4:1 CORDEX-RCMs and their driving GCMs used in this study

No	RCM Name	GCM driving Model	Institution Center
1.	REMO2009	MPI-ESM-LR	Max Planck Institute for Meteorology Climate Service Center, Germany
2.	CCLM-4-8-17	CNRM-CM5	Climate Limed -Area Modelling Community, USA

The procedure to downscale RCM data by using CORDEX data extractor software, meteorological station location of each station and with the help of the driving GCM driving force model. Many authors getting challenges to account the climate information and the existence of potential of the single model (Voldoire *et al.*, 2013)(Knutti, 2010) to focus on the multi-model methods (based on the combination of several models) in order to increase performance and reduce uncertainties simulations (Ezéchiel *et al.*, 2016). Hence, this study uses the average value of climate change of RCM simulated (output) data.

Downscaling and bias correction framework structure

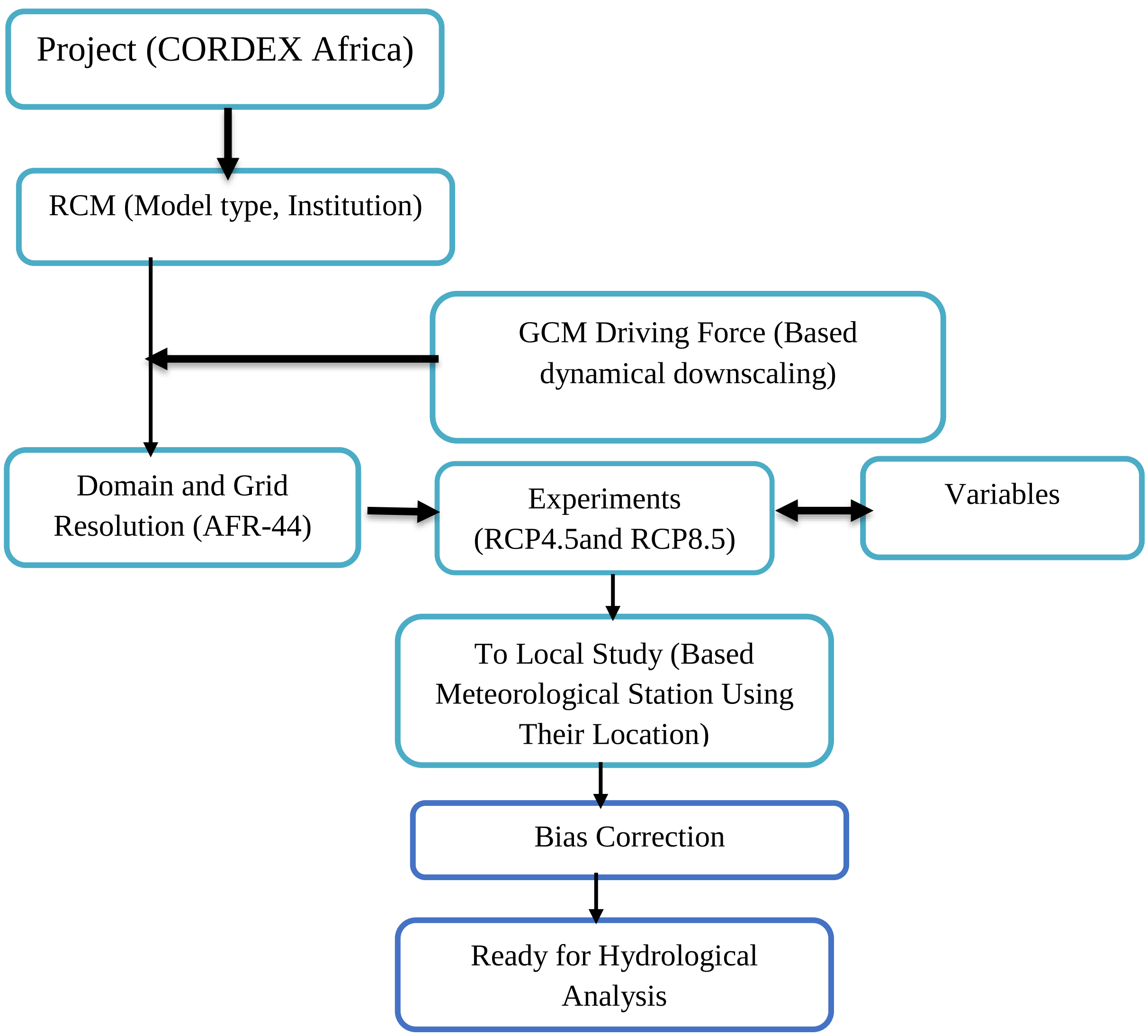

4.8. Bias Correction of CORDEX Data Output

Bias correction is widely used in climate impact aims to adjust selected statistics of a climate model simulation to better match between observed meteorological data (precipitation and temperature). Bias correction is usually needed as climate models often provide biased representations of observed time series data due to systematic model errors caused by imperfect conceptualization, discretization and spatial averaging within grid cells. Typical biases are the occurrence of too many wet days with low-intensity rain or incorrect estimation of extreme temperature in RCM simulations (S. Hansen *et al.*, 2013). Thus, the application of bias correction methods is recommended (Wigley and Wilby, 2000). Several techniques of bias correction for precipitation and temperature. The correction method is applied for precipitation (linear scaling approach, daily translation, delta change linear transformation, Power transformation, Distribution mapping, Empirical quantile mapping and others) and temperature correction methods (linear scaling, daily translation, variance scaling, distribution mapping, empirical quantile mapping, and others). For this study, distribution mapping selected for the correction precipitation and temperature RCM output data due to matches the statistical distribution of RCM-simulated climatic factors to the distribution of observations.

The distribution mapping adjust the RCM output data of mean, standard deviation, variance and higher moment distribution of climate variable to make more closely to observation data. This method considers computing parameters, the Gamma distribution, which considers shape parameter (α) and scale parameter (β) often, used for precipitation distribution.

$$f(p;\alpha,\beta)=p^{\alpha-1}\frac{exp^{\frac{-p}{\beta}}}{\Gamma(\alpha)\beta^{\alpha}} \quad p,\ \alpha,\ \beta >0\text{----------------------------}4\text{-}1$$

Where: Γ is the gamma function and P represents the simulated RCM daily precipitation. The raw RCM-simulated precipitation contains a large number of drizzle days, which may substantially distort the raw precipitation distribution. Here, parameters α and β estimated for each grid box for each month, using the method of moments:

$$\alpha = (\frac{\bar{p}}{\sigma_p})^2\text{---}4\text{-}2$$

$$\beta=\frac{{\sigma_p}^2}{\bar{p}}\text{---}4\text{-}3$$

Where: σ_p and $\bar{p}$ are the sample mean and standard deviation of P, respectively

The correction for daily precipitation applied with local intensity scaling which simultaneously corrected precipitation intensity and frequency. The correction is done as follows:

$$P_{cor,m,d} = F_r^{-1}(F_r(P_{LOCI,m,d} /\sigma_{LOCI,m}, \beta_{LOCI,m})/\sigma_{obs,m}, \beta_{obs,m}) \text{ -----------------4-4}$$

Where: $P_{cor,m,d}$ corrected precipitation (base and future), F_r cumulative distribution function, F_r^{-1} inverse of cumulative distribution function.

For the correction of temperature time series, the Gaussian distribution with location parameter μ, control the mean and scale parameter σ, control the standard deviation. Those parameters usually assumed to fit best for temperature.

$$f_N(x/\mu, \sigma^2) = \frac{1}{\sigma * \sqrt{2\pi}} * e^{\frac{-(x-\mu)^2}{2\sigma^2}}; x \epsilon R \text{---------------------------------------4-5}$$

Moreover, the corrected temperature is

$$T_{cor,m,d} = F_N^{-1}(F_N(T_{raw,m,d} /\sigma\mu_{raw,m}, \sigma_{raw,m})/\mu_{obs,m}, \sigma_{obs,m}) \text{ -----------4-6}$$

Where: F_N are Gaussian CDF and $F^{-1}{}_N$ inverse of it, $\mu_{raw,m}$ and $\mu_{obs,\ m}$ are observed means for the raw and observed precipitation series at a given month m, and σ raw, m and $\sigma_{obs,\ m}$ are the corresponding standard deviation respectively.

4.9. Spatial Data

Different spatial data are required for study such as Digital Elevation Model (DEM) of 30m*30m for Upper Baro Basin, Ethio-River Basin shapefiles, hydropower feasibility document of hydropower project of the basin, land use/land cover and soil data in the basin were collected from Ministry of Water Resource (International Monetary Fund, 2006), (Report, 2017).

4.10. Data Quality Test

4.10.1. Data Continuity Test

All most of the recorded data is not always continues due to the absence of observer or instrumental failure rainfall data record occasionally. The continuity of recorded data is broken by the missed value; to avoid this filling the missed data is very important. There are many meteorological stations found in the Baro- Akobo river basin. However the station selected for these study must be the station which is the first rank or should have five climate variables (precipitation, solar radiation, temperature, wind speed and relative humidity) and also depending on the location station in the study area or near to the study area, upper Baro catchment selected for this research. There are many missed values of rainfall in each station. These missed values filled by normal ration methods; this method selected due to the annual normal value of the missed station is greater than ten percent.

Normal ratio method

Normal ratio method is the most common method used to estimate missing rainfall data and it based on only past observation that rain gauge and its surroundings. However, this method does not consider the key factors such as aerial coverage of individual gauge, distances among rain gauges, etc. When normal annual precipitation of surrounding gauge exceeding 10% this method only used. This weighs of normal annual precipitation the effect of each surrounding station (Singh, 1994). The missing data are estimated by-

$$P_x = \frac{1}{n}\sum_{i=1}^{n} w_i P_i \text{------------------------------------4-7}$$

In which w_i is the weight for the rainfall depth $\boldsymbol{P_i}$ at gage ***i.*** The weight for station i is computed by:-

$$w_i = \frac{A_x}{nA_i} \text{--4-8}$$

In which $\boldsymbol{A_i}$ is the average annual catchment at gage i, **A,** is the average annual catchment at station x, and n is the number of stations.

Multiple Regression

Develop a fitting equation with different stations in the same rainfall regimes and orographic features and spatial distribution of the variables are considered Regression analysis is a procedure for fitting an equation to the absence of data. Specifically, given a set of measurements on two random variables, y, and x, regression provides a means for finding the values of the coefficients 'a' and 'b' for the straight line (y = a+ bx) that best fits the data. The coefficients 'a' and 'b' can be found using the least square method using the following two equations simultaneously(Bremer, 2012).Normal ration method selected to fill meteorological data and multiple regression method selected to fill hydrological data.

4.10.2. Homogeneity Test

Homogeneity analysis is the method used to identify separate change of statistical properties of time series data. Rainfall data for multiple time series at neighboring stations should ideally possess spatial homogeneity(Yilma Seleshi (Dr.), 2005). Data will be affected by either natural or man-made, those effects due to land use and relocation of the observation gauging station. Therefore, in order to select the representative meteorological station checking homogeneity of group stations is essential, the homogeneity of the selected gauging stations daily rainfall records were carried out by non-dimensional equation. The non-dimensional month's value is calculated as:- $P_i = \frac{\bar{p}_i}{\bar{p}} * 100$---------------------------------4-9

Where: - Pi = Non-dimensional value of precipitation for the month i, $\bar{p}_i$ = Over years averaged monthly precipitation for the station i, $\bar{p}$= Over year's average yearly precipitation of the station.

In order to select the representative meteorological station checking homogeneity of group, stations are essential. From figure 3.10, all station homogenous and representative from the catchment.

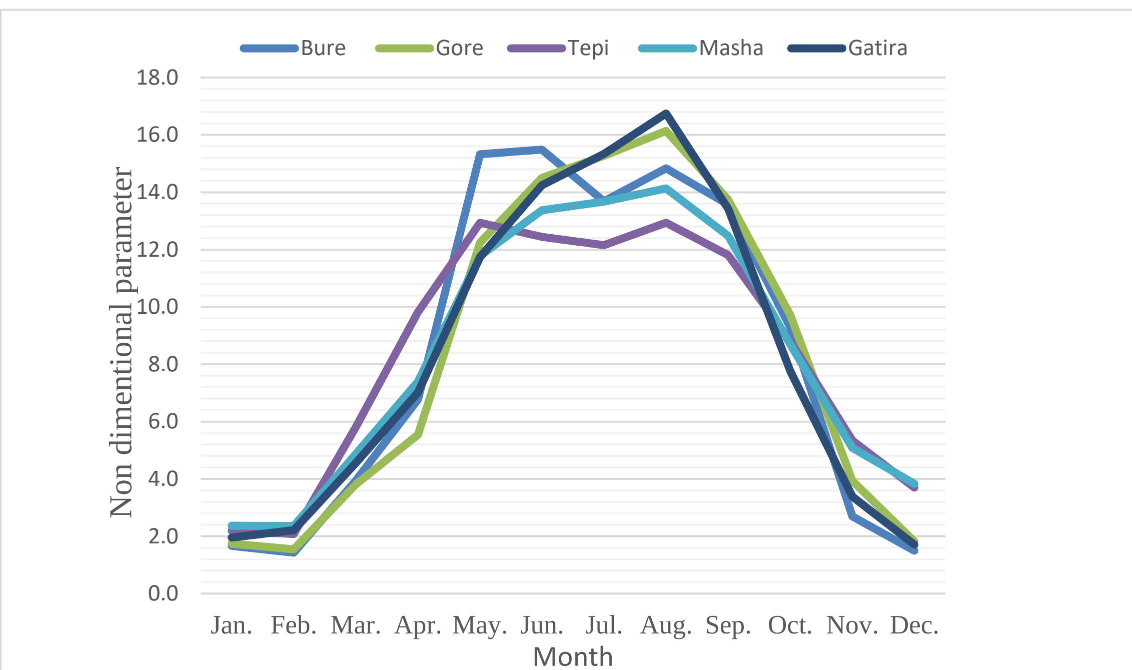

Figure 4:2 Homogeneity test of the all station

4.10.3. Data Consistency Test

The consistency of data shows the pattern of rainfall in the area by rain gauge during the recording of rainfall. If some significant change occurs during the recording of data inconsistency is happen. Data inconsistency happens due, shifting the rain gauge station to the new location, the neighborhood of the station undergoing a marked change, change of the ecosystem (forest fire, landslide, and earthquake) and the occurrence of the observation error. This data consistency is tested by using a double mass curve**.** It compares the accumulated annual rainfall at a given station with the concurrent accumulated values of average rainfall for a group of the surrounding stations. The double mass curve drawn by cumulative annual precipitation of station in the vertical axis to cumulative average annual precipitation of all stations in the horizontal axis. If the graph straight-line, it shows data is consistence.

Double mass is based on the principle that when each recorded data comes from the same parent population but if the data inconsistency occurs the correction of the data as follows. The data of the annual rainfall of the station 'X' selected and the group of average rainfall base stations in the neighborhood of the station covering a long period arranged in chronological order (i.e. the latest record period first entry and the oldest record is last entry). An accumulated rainfall of station X (i.e., ΣPx) and the accumulated values of the average of the base stations (i.e., ΣPav) are calculated starting from the latest record. The value of accumulated station X (ΣPx) values plotted against the average accumulated value of base stations ΣPav. A break in the slope of the resulting plot shown a change in the precipitation of station X. The rainfall values at station X above the period of change of regime corrected by using the relation given belew.

$$P_{cx} = P_x \frac{M_c}{M_a} \text{--4-10}$$

Where: P_{cx}=corrected precipitation at any time period t_1 at station X

P_x= original recorded precipitation at time period t_1 at station X

M_c= corrected slope of the double mass-curve

M_a= original slope of the double mass-curve

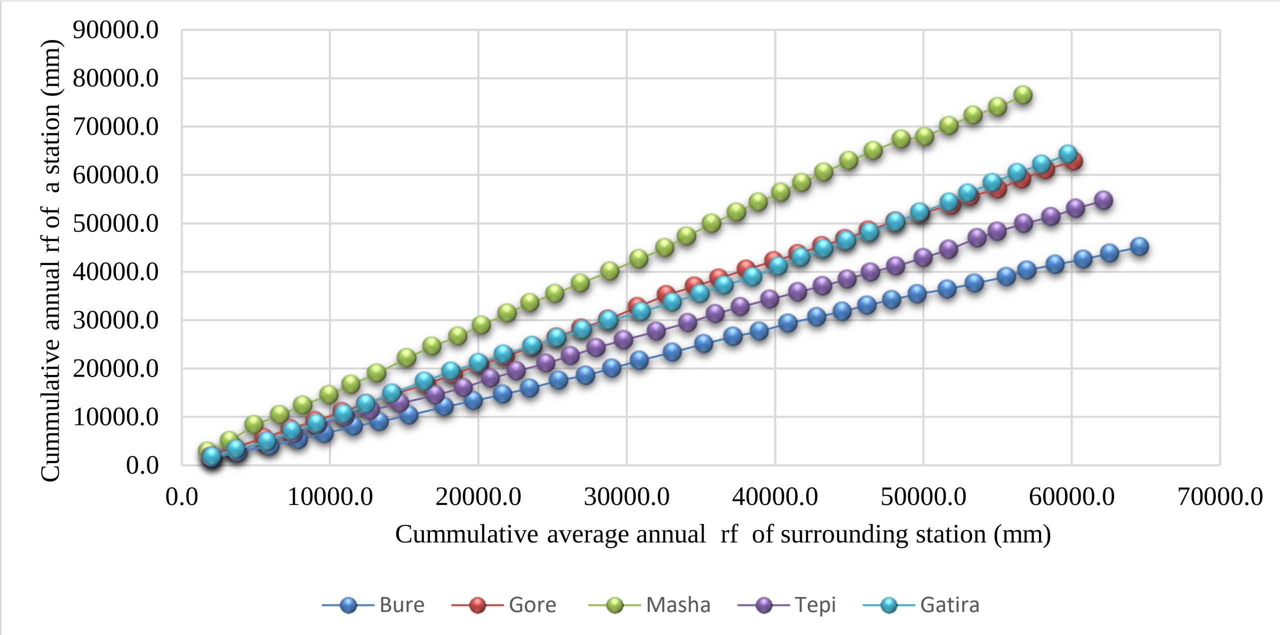

Figure 4:3 Double mass curve of all station

4.11. Areal Rainfall Determination

The rain gauge station in the area does not totally represent the value of rainfall in the catchment due to various reason. Rainfall records within the catchment and its immediate surroundings thus must be analyzed to take proper account of the spatial and temporal variation of rainfall over the basin (Yilma Seleshi (Dr.), 2005). Therefore, area rainfall is important, areal rainfall is the method to make an average value over a catchment of the point rainfall values of various stations. There are many methods to calculate areal rainfall. The first is the arithmetic mean method, the second is the Thiessen polygon method, and the third is the isohyet method.

Thiessen polygon method selected for determination of areal rainfall for this study for its sound theoretical basis and availability of computational tools. Nevertheless, the method is dependent on a good network of representative rain gauges and does not allow the hydrologist to consider factors, such as topography ('13. Applied Hydrology, Chow.pdf', no date). In this method, recorded the precipitation of each station was given a weightage based on an area closest to the station. The assumption in the method is that at any point in the watershed, the rainfall is the same as that at the nearest gauge so the depth recorded at a given gauge was applied out to a distance halfway to the next station in any direction.

The relative weights of each gauge are determined from the corresponding areas of application in a Thiessen polygon network, the boundaries of the polygons being formed by the perpendicular bisectors of the lines joining adjacent gages.

$$\bar{p} = \frac{1}{A}\sum_{j=1}^{n} A_j P_j \text{--4-11}$$

Where: A_j = the area of polygon j in the catchment (km^2), P_j = rainfall amount in polygon j (mm), $\bar{p}$= is average rainfall (mm) and A =is the total area of the catchment.

4.12. Input Data for Model

Arc SWAT model which is an ArcGIS interface requires many input files including the digital elevation model (DEM), land cove land use, soil, maximum and minimum temperature, precipitation, wind speed, relative humidity and solar radiation.

4.13. Hydrological Model Setup

The hydrological model used in this study soil and water assessment tool (SWAT) semi-distributed model that takes single value input produces a single value output. The interface between the model SWAT and ArcGIS is called Arc SWAT. There are different steps into model catchment in this model (watershed delineation, Hydrologic response unit, write input table, edit input table and simulation).

4.13.1. Watershed Delineation

It is the process to delineate the sub-watersheds in the basin from the large Baro-Akobo river basin based on an automatic procedure. The automatic watershed delineation tool was selected, which allows to preprocess the DEM of 30m by 30m data. In this, steps parameters should be specified which provide limits that influence the size and number of sub-watersheds created. The purpose of the watershed delineation is segmenting watershed into numerous hydrological linked sub-watersheds modeling with the SWAT model. The procedure of the watershed delineation is the following steps DEM setup, stream definition, outlet and inlet definition, watershed outlet(s) selection and definition, and calculation of sub-basin parameters. Burning in a stream network improves hydrographic segmentation and sub-watershed boundary delineation. After the watershed delineation, the initial stream network and sub-basin outlets are well-defined and defining streams based on a drainage area threshold, or, importing pre-defined watershed boundaries and streams. The point sources added is by default, have constant loading of zero for all water, sediment, and nutrient inputs. Inlet and outlet selection /definition are required after the stream definition is completed(Neitsch *et al.*, 2011).

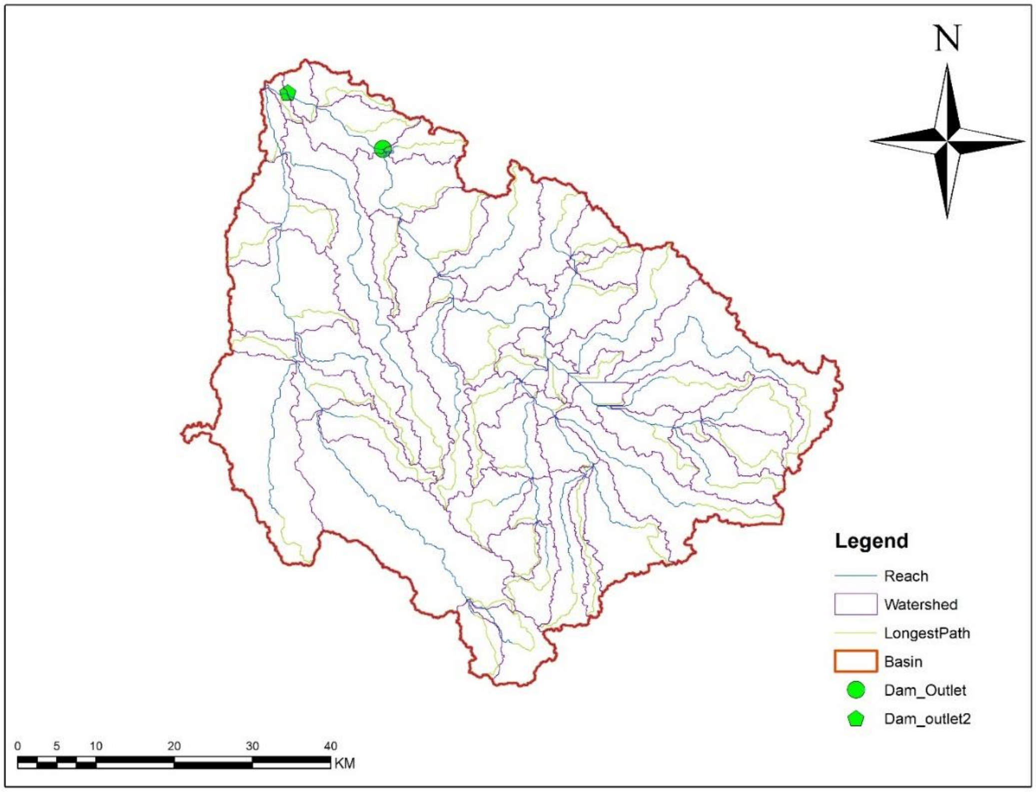

Figure 4:4 Study area watershed delineated

4.13.2. Hydrologic Response Unit

Land use land cover, soil, and slope characterization for a watershed is performed using commands from the HRU Analysis. Under the hydrologic response unit (HRU) analysis evaluate slope characteristics, and determine the land use/soil/slope class combinations and distributions for the delineated watershed(s) and each respective sub-watershed by loading land use/ land cover and soil layers. A unique combination of land use, soil layers, and slope classification that SWAT subsequently uses in defining the hydrologic characteristics of the sub-basins within a watershed is a hydrologic response unit. Subdividing the watershed into areas having unique land use and soil combinations aids the model to reflect different hydrologic conditions for different land covers and soils and evapotranspiration. The total runoff for watershed is obtained after predicting runoff for each HRU separately and routed. There are two options in determining the HRU distribution are assign a single HRU to each sub-watershed or assign multiple HRUs to each sub-watershed. If a single HRU per sub-basin is selected, the HRU is determined by the dominant land use category, soil type and slope class within each watershed. If multiple HRUs are selected, it may require specifying sensitivities for the land use, soil, and slope data that will be used to determine the number and kind of HRUs in each watershed. In this study, the multiple HRU is selected to determine the number and kind of HRs in watershed(Neitsch *et al.*, 2011). The HRU report shows the number of HRU 328 and 58 sub-basins.

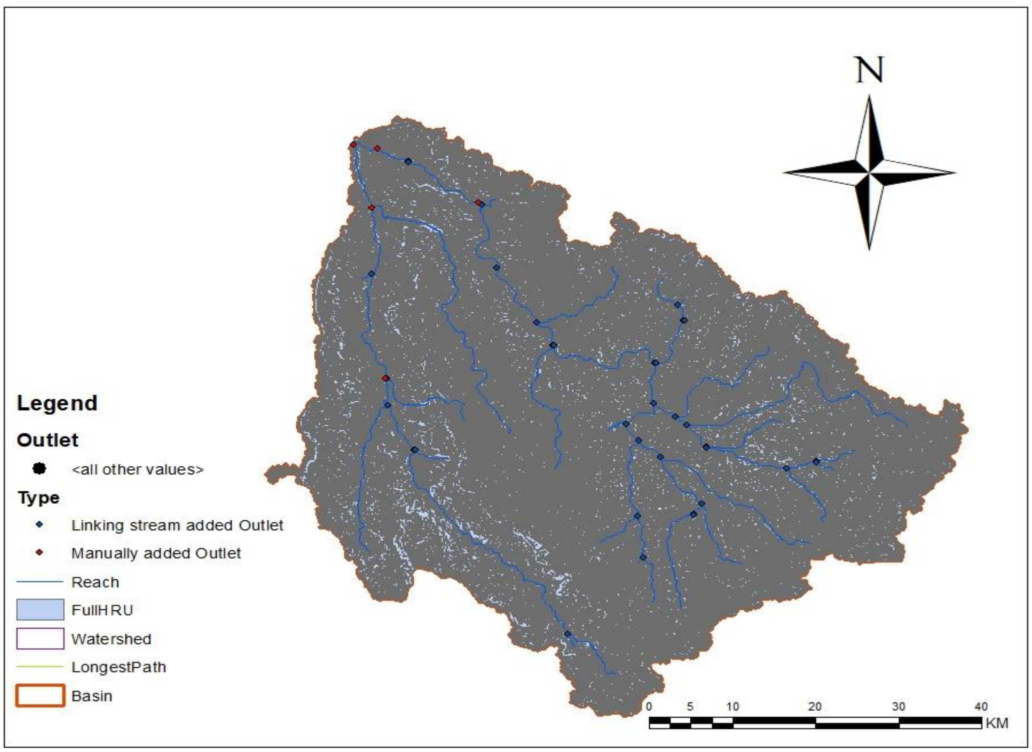

Figure 4:5 Hydrologic response unit of the study area

4.13.3. Import Data

Weather data used to model watershed imported after the HRU distribution defined. Weather data is loaded using the first command in the write input tables menu item on the Arc SWAT toolbar. This tool used to load weather station locations into the project and assign weather data to the sub-watersheds. In the weather data definition, it has six tab box weather generator data, rainfall data, temperature data, solar radiation data, wind speed data, and relative humidity data.

4.13.4. Simulation

After the HRU, analysis is completed, and five weather data stations (Masha, Bure, Gore, Tepi and Gatira) were added to the model and simulation is started. In the simulation step in Arc SWAT, the first step hydrologic cycle simulation by using the water balance equation. The water balance equation is:

$$SW_t = SW_o + \sum_{i=1}^{t}\left(R_{day} - Q_{surf} - E_a - W_{seep} - Q_{gw}\right) \qquad \text{4-12}$$

Where:- SW_t is the final soil water content (mm H_2O), SW_0 is the initial soil water content on day i (mm H_2O), t is the time (days), R_{day} is the amount of precipitation on day i (mm H_2O), Q_{surf} is the amount of surface runoff on day i (mm H_2O), E_a is the amount of evapotranspiration on day i (mm H_2O), w_{seep} is the amount of water entering the vadose zone from the soil profile on day i (mm H_2O), and Q_{gw} is the amount of return flow on day i (mm H_2O).

Next to hydrologic cycle simulation determination of peak runoff rate. The peak runoff rate is the maximum runoff flow rate that occurs with a given rainfall event. It is determined by the modified rational method in the SWAT model.

$$q_{peak} = \frac{\alpha_{tc} Q_{surf} Area}{3.6 t_{conc}} \qquad \text{4-13}$$

Where: q_{peak} is the peak runoff rate (m^3/s), α_{tc} is the fraction of daily rainfall that occurs during the time of concentration, Q_{surf} is the surface runoff (mm H_2O), Area is the sub-basin area (km^2), t_{conc} is the time of concentration for the sub-basin (hr.) and 3.6 is a unit conversion factor.

Surface runoff calculated by:

$$Q_{surf} = \frac{(R_{day} - 0.2S)^2}{(R_{day} + 0.8S)} \qquad \text{4-14}$$

Where: $\mathbf{Q_{surf}}$ is the accumulated runoff or rainfall excess (mm H_2O), $\boldsymbol{R_{day}}$ rainfall depth for the day (mm H_2O) and $\boldsymbol{S}$ is the retention parameter (mm H2O). The retention parameter defined as

$$S = 25.4\left(\frac{100}{CN} - 10\right) \qquad \text{4-15}$$

Where: CN is the curve number for the day. For any type of soil curve number moisture condition II is defined and the other soil moisture condition are calculated as(I and III):-

$$CN_1 = CN_2 - \frac{200(100-CN_2)^2}{(100-CN_2+exp[2.533-0.0636*(100-CN_2)])}$$ ------------------------------*4-16*

$$CN_3 = CN_2 * exp[0.0673 * (100 - CN_2)]$$ ---------------------------------------*4-17*

Where CN_1 is the moisture condition I curve number, CN_2 is the moisture condition of curve number II, and CN_3 is the moisture condition curve number III.

The time of concentration is obtained by:

$$t_{conc} = t_{ov} + t_{ch}$$ --4-18

Where: t_{conc} is the time of concentration for a sub-basin (hr.), t_{ov} is the time of concentration for overland flow (hr), and t_{ch} is the time of concentration for channel flow (hr.).

$$t_{ov} = \frac{L_{slp}^{0.6} * n^{0.6}}{18 slp^{0.3}}$$ ---*4-19*

Where: L_{slp} is the sub-basin slope length (m), *slp* is the average slope in the sub-basin (m/ m), and *n* is Manning's roughness coefficient for the sub-basin.

The channel flow time of concentration, t_{ch}, is also calculated as:

$$t_{ch} = \frac{0.62 L * n^{0.75}}{Area^{0.125} slp_{ch}^{0.375}}$$ -----------------------------*4-20*

Where: t_{ch} is the time of concentration for channel flow (hr.), *L* is the channel length from the most distant point to the sub-basin outlet (km), *n* is Manning's roughness coefficient for the channel, area is the sub-basin area (km^2), and slp_{ch} is the channel slope (m/m).

Routing phase

In watershed, the point source discharge and/ or drop of rain flow to the outlet of sub-basin through the channel, this flow in the channel routed in Arc SWAT model by using Muskingum routing method. In the Muskingum routing method models the storage volume in the channel length is a combination of wedge and prism storages. The Muskingum equation is given by

$$V_{stored} = K(X - q_{in}(1 - X)q_{out}))$$ --*4-21*

Where V_{stored} is the storage volume (m^3 H_2O), q_{in} is the inflow rate (m^3/s), q_{out} is the discharge rate (m^3/s), K is the storage time constant for the reach (s), and X is the weighting factor.

Potential Evapotranspiration (PET)

There are a number of methods to estimate potential evapotranspiration in arc SWAT model. However, the Penman-Monteith approach in both arid and humid climates and considers many climate variables (temperature, wind speed, solar radiation, and relative humidity). Because all climate variables for each station selected for analysis. The Penman-Monteith equation (Allen *et al.*, 1998)given by:-

$$ET_o = \frac{0.408\Delta[R_n - G]}{\Delta + \gamma(1+0.3u_2)} + \frac{\gamma \quad 900U_2(e_s - e_a)}{\Delta + \gamma(1+0.3u_2) * (T+273)} \text{---------------------------------} 4\text{-}22$$

Where, ET_o =Reference evapotranspiration, in mm/day, R_n= Net radiation, MJm^{-2} day^{-1}, G= Soil heat flux, MJm^{-2} day^{-1}, e_s = Saturated vapor pressure, KPa,, e_a= Actual vapor pressure, KPa, Δ = Slope of the saturation vapor pressure relationship, KPa°C, γ = Psychometric constant, $KPaC^{-1}$, U_2 = Wind speed, ms^{-1} and, T = Mean daily air temperature at 2m height (°C)

In this study, Penman-Monteith applied for the potential evapotranspiration for each weather station and for RCM simulated data of future projection.

4.14. Sensitivity Analysis

Sensitivity analysis is a technique of identifying the responsiveness of different parameters involving in the simulation of a hydrological process. For large hydrological models like SWAT, which involves a wide range of data and parameters in the simulation process, calibration is quite a cumbersome task. Sensitivity analysis is a method of minimizing the number of parameters to be used in the calibration step by making use of the most sensitive parameters largely controlling the behavior of the simulated process. This method reduce the time required for the overall calibration and validation process and also increases the accuracy of calibration by reducing uncertainty (van Griensven *et al.*, 2006). SWAT-CUP is a SWAT calibration uncertainties program, which was developed to analyze the prediction uncertainty, calibration, and validation of the model results (Khalid *et al.*, 2016).

4.15. Calibration and Validation of Model

The process of deriving characteristics equations, constants, weighting factors, and other parameters that serve to define the model for a particular watershed is termed ’calibration” (U.S Army Corps (U S Army Corps Of Engineers and Engineers, 1992). Model calibration involves establishing a statistical relationship between model parameters and observed characteristics of the watershed. Arc SWAT model can be calibrated both manually and automatically. The manual calibration is the most widely used calibration and involves the visual comparison of observed and simulated data. The SWAT-CUP can assimilate various calibration or uncertainty analysis procedures to decrease modeler uncertainty by removing some probable sources of modeling and calibration errors. It links Particle Swarm Optimization (PSO), Parameter Solution (ParaSol), Sequential Uncertainty Fitting ver.2 (SUFI-2), Generalized Likelihood Uncertainty Estimation (GLUE), and Markov Chain Monte Carlo (MCMC) algorithms to SWAT model.(Arnold *et al.*, 2012; Khalid *et al.*, 2016).

Whereas validation is a technique for testing, the performance of the calibrated model in order to decrease the gap between the observed values and simulated once.

4.16. Model Performance Evaluation

Model performance evaluation based on the extent of its accuracy, consistency, and adaptability of the model. Evaluation of a model’s ability to simulate catchment response accurately is vital before further application of the model (Seyoum, Milewski and Durham, 2015). A forecast efficiency criterion is, therefore, necessary to judge the performance of the model. Assessing the performance of a hydrologic model requires to estimates the closeness of the simulated behavior of the model to observations.

Three methods for goodness-of-fit to measure the model predictions during the calibration and validation periods were used, these three numerical model performance measures are coefficient of Correlation (R^2), the Nash-Sutcliffe simulation efficiency (NSE) and percent difference (D).

4.16.1. Nash-Sutcliffe Efficiency

The Nash-Sutcliffe Efficiency (NSE) is a measure of efficiency that relates the goodness-of-fit of the model to the variance of measured data. NSE can range from - ∞ to one value. When NSE indicates ‘1’ perfect match between observed and simulated discharges. When NSE is zero (0) shows simulations as poor as a constant value prediction, when NSE<zero represents very poor fit. Moreover, when NSE value between 0.75 and 1 indicates that the model performs very well while values between 0.6 and 0.75 indicate the indicate fair to good performance model (Rientjes *et al.*, 2008)(Fang *et al.*, 2015)(Roth, Nigussie and Lemann, 2016).

The NSE efficiency, proposed by Nash and Sutcliffe (Nash, 1970), is defined as

$$NSE = 1 - \frac{\sum_{i=1}^{n}(Q_o - Q_s)^2}{\sum_{i=1}^{n}(Q_o - \bar{Q}_o)^2} \text{---------------------------------} 4\text{-}23$$

Where, Q_o= observed flow, Q_s = Simulated flow and $\bar{Q}_o$ =Average of observed flow

4.16.2. Coefficient of Correlation

The coefficient determination measures the fraction of the variation in the measured data that is replicated in the simulated model results. An R^2 of zero means that the observed and simulated cannot fit the model. An R^2 value1 means the can be the model is perfect between the measured value and simulated. An R^2 between zero and one indicates that the model can be used. If values of R^2 outside the range 0 to 1, the model data does not fits the observed data. The range of values for R^2 is 1.0 (best) to 0.0 (bad)(Rientjes *et al.*, 2008). It is estimated by:

$$R^2 = \frac{[\sum_{i=1}^{n}[(Q_o - \bar{Q}_s)(Q_o - \bar{Q}_o)]^2}{\sum_{i=1}^{n}(Q_s - \bar{Q}_s)^2 \sum_{i=1}^{n}(Q_o - \bar{Q}_o)^2} \text{------------------------------------} 4\text{-}24$$

Where, Q_o= observed flow, Q_s = Simulated flow, $\bar{Q}_o$ = Average of observed flow and $\bar{Q}_s$= Average of simulated flow.

4.16.3. Percent Difference

The percent difference D measures the average difference between the simulated and measured values for a given quantity data over the entire calibration or validation period in the study or measures the average tendency of the simulated data to their observed counterparts.

$$D = 100 * \frac{\sum_{i=1}^{n} Q_s - \sum_{i=1}^{n} Q_o}{\sum_{i=1}^{n} Q_o} \text{------------------------------------} 4\text{-}25$$

Where, Q_o = Observed value, Q_s = Simulated value

The values of the percent difference (D) can be between ∞ and - ∞ but when a value 0 (zero) it performs best. Negative values “D” indicate an overestimation (i.e., the simulated dataset is higher than the observed dataset), while positive values indicate an underestimation (the simulated dataset lower than the observed dataset). The optimal value is 0.0, with low-magnitude values in both directions, possibly indicating accurate model simulations. The above indication defined as follow: A percent difference between ±5% indicates that a model performs well, while percent difference between +5% and +10%, and -5% and -10% indicates a model with reasonable performance (Obada *et al.*, 2017).

4.17. Overtopping Evaluation

Baro I reservoir minimum and maximum operation level are 1485m.a.s.l and 1520m.a.s.l respectively, giving an active storage of 993 Mm^3. The spillway is a free, ungated over-fall with crest elevation 1520m.a.s.l, corresponding to FSL. Considering the necessary surcharge height for the design flood discharge and sufficient allowance for a freeboard, a crest elevation of 5 m and the crest elevation for the structures (main dam and saddle dams) level is 1525m.a.s.l. The spillway is ungated, with crest elevation at FSL and the probable maximum flood (PMF) levels 1524.50m.a.s.l in reservoir at return period of 1000 years (International Monetary Fund, 2006).

Baro II reservoir maximum operation levels between an FSL of 1320m.a.s.l and a minimum operating level of 1318m.a.s.l corresponding active storage amounts to 18Mm^3, the spillway consists of a free, ungated over-fall, with crest at FSL (1320m.a.s.l). Consideration of the surcharge height for the design flood discharge and sufficient allowance for the freeboard resulted in a crest elevation of 5 m above FSL. The crest for the structures (main dam, saddle dams, and spillway) was thus fixed on 1325 m.a.s.l(International Monetary Fund, 2006).

Overtopping evaluation is the method to check the dam will be overtopped due to incoming of probable maximum flow to the reservoir. This maximum flow will occurs due to maximum depth of precipitation in future projection. The flow incoming to the reservoir will be evaluated by flow from future projection RCM simulated data of the under climate change presentative scenario (PCP4.5 and RCP 8.5). Under this future scenario, the peak flow or peak flood next century (present, mid and far future) will be obtained from reservoir routing and simulation of projected RCM output data by Arc SWAT. The evaluation of overtopping conducted comparing with elevation-area and elevation-volume relationships curve and outflow from the reservoir for Baro I and II hydropower dam developed before(International Monetary Fund, 2006). After obtaining peak flow to reservoir the spillway adequacy will be evaluated whether the dam will be overtopped or not.

4.17.1. Reservoir Routing

The reservoir elevation and outflow discharge varies with time due to flood wave entering a reservoir. Hence, knowing the volume-elevation characteristics of reservoir outflow-elevation relationship for the spillways is very important. To route reservoir level pool method is used; in this method outflow hydrograph calculated from a given inflow hydrograph and storage outflow characteristics(Yilma Seleshi (Dr.), 2005). The level pool method calculated as follows:

$$\left(\frac{I_1+I_2}{2}\right)\Delta t + \left(S_1 - \frac{Q_1\Delta t}{2}\right) = \left(S_2 + \frac{Q_2\Delta t}{2}\right) \text{-------------------------------} 4\text{-}26$$

Where: - I_1 inflow at first time, I_2 inflow at time second, Q_1 outflow at time first time, Q_2 outflow at second time, S_1 storage at first initial storage, S_2 is the second storage and Δt is change time.

Estimation of Inflow Hydrograph

Inflow hydrograph is obtained determined from the maximum rainfall or precipitation of the RCM out of RCP4.5 and RCP8.5 data for present future, mid future and far future period. Probable Maximum Precipitation is greatest depth of precipitation at a particular geographical location and at a particular time of year in duration, which is physically possible over a given size of storm area. Hence, the maximum precipitation is selected for each period (present future, mid future, and far future) of scenarios (RCP4.5 and RCP8.5). After the selection of maximum precipitation, the PMP is determined by using Hershfield, 1965 method. The mathematical representation Hershfield method for the one day for catchment is:

$$PMP = P_{ave} + K_m\delta_n \text{--} 4\text{-}27$$

Where;- PMP is the one-day probable maximum precipitation, P_{ave} is mean of annual 1-day maximum rainfall, δ_n is standard deviation of annual 1-day maximum rainfall maximum rainfall and K_m is the frequency factor which depends upon the number of observations, and obtained as follows

$$K_m = \frac{P_{max} - P_{ave(n-1)}}{\delta_{(n-1)}} \text{--} 4\text{-}28$$

Where:- P_{max} is the highest value in the series of annual daily maximum rainfall, $P_{ave\ (n-1)}$ is the mean of annual one-day maximum rainfall of n-1 observations excluding the highest rainfall, $\delta_{(n-1)}$ is the standard deviation of annual one-day maximum rainfall of n-1 observations excluding the highest rainfall.

Table 4:2 Probable maximum precipitation for RCP4.5

Present future(2014-2033)					
	Stations				
Parameter	Bure	Gatira	Gore	Masha	Tepi
P_{max}	169.60	154.07	166.98	258.54	128.10
P_{ave}	91.89	88.00	93.71	101.38	79.06
δ_n	31.71	34.80	32.77	45.64	29.85
$P_{ave\ (n-1)}$	75.64	72.42	89.86	93.10	76.48
$\delta_{(n-1)}$	24.64	27.30	28.63	27.47	28.28
k_m	3.81	2.99	2.69	6.02	1.83
PMP 24 Hr.	212.83	192.08	181.98	376.25	133.54

Mid future(2034-2071)					
	Stations				
Parameter	Bure	Gatira	Gore	Masha	Tepi
P_{max}	139.89	136.01	153.10	291.02	150.84
P_{ave}	80.61	82.16	88.43	96.20	83.39
δ_n	32.05	25.88	31.71	46.40	27.72
$P_{ave\ (n-1)}$	78.96	80.67	86.64	90.78	81.51
$\delta_{(n-1)}$	30.87	24.57	30.19	33.16	25.63
k_m	1.97	2.25	2.20	6.34	2.70
PMP 24 Hr.	143.85	140.45	158.24	390.51	158.37

Far future(2071-2100)					
	Stations				
Parameter	Bure	Gatira	Gore	Masha	Tepi
P_{max}	170.44	161.76	279.02	200.27	161.46
P_{ave}	89.64	86.84	107.79	110.69	97.12
δ_n	35.11	28.49	49.43	41.32	34.51
$P_{ave\ (n-1)}$	86.86	84.25	101.89	107.60	94.90
$\delta_{(n-1)}$	32.18	25.16	38.04	38.37	32.87
k_m	2.60	3.08	4.66	3.02	2.03
PMP 24 Hr.	180.83	174.59	337.94	235.64	167.00

Table 4:3 Probable maximum precipitation for RCP8.5

Present future(2014-2033)					
	Stations				
Parameter	Bure	Gatira	Gore	Masha	Tepi
P_{max}	222.38	214.50	235.14	321.12	152.31
P_{ave}	74.53	91.14	104.40	116.21	89.20
δ_n	40.40	38.68	45.24	59.22	35.44
$P_{ave\ (n-1)}$	66.74	84.64	97.52	105.43	85.88
$\delta_{\ (n-1)}$	21.07	26.25	34.08	35.31	33.06
k_m	7.39	4.95	4.04	6.11	2.01
PMP 24 Hr.	372.88	282.46	287.12	477.98	160.42

Mid future(2034-2070)					
	Stations				
Parameter	Bure	Gatira	Gore	Masha	Tepi
P_{max}	161.61	188.33	328.66	331.16	203.00
P_{ave}	89.07	87.58	107.53	111.79	91.07
δ_n	32.68	39.51	61.88	62.86	37.59
$P_{ave\ (n-1)}$	87.06	84.78	101.39	105.70	87.96
$\delta_{\ (n-1)}$	30.73	36.16	50.03	51.49	32.95
k_m	2.43	2.86	4.54	4.79	3.49
PMP 24 Hr.	168.37	200.72	388.64	412.58	222.31

Far future(2071-2100)					
	Stations				
Parameter	Bure	Gatira	Gore	Masha	Tepi
P_{max}	182.05	173.57	194.99	282.41	180.02
P_{ave}	92.59	102.19	105.85	123.50	104.76
δ_n	43.25	39.00	38.04	53.58	37.66
$P_{ave\ (n-1)}$	89.51	99.73	102.77	118.02	102.16
$\delta_{(n-1)}$	40.52	37.24	34.71	45.16	35.49
k_m	2.28	1.98	2.66	4.04	2.19
PMP 24 Hr.	191.37	179.51	206.90	340.20	187.37

For two RCP scenarios (RCP4.5 and RCP8.5) of the present future, mid future and far future the maximum PMP $_{24\ Hr.}$ is taken from each station. For RCP4.5 PMP $_{24\ Hr.}$ 376.25mm, 390.51mm and 337.90mm in present future, mid future and far future respectively and RCP8.5 477.98mm, 412.58mm and 340.20mm in present future, mid future and far future respectively.

The determined point probable maximum precipitation should be averaged areal design rainfall depth by areal reduction factor in order to represent throughout the determined PMP over the catchment(Tamirat Dessalegn & Awass, 2016). ARFs are estimated using either empirical and/or analytical methods. In many countries, the current ARF approaches are mostly based on empirical methods, using either storm-centered or geographically centered approaches. Hence, area reduction factor not calculated for Ethiopia but area reduction applied for east Africa 0.6 for large area of the watershed(Tamirat Dessalegn & Awass, 2016).

For the determination of the inflow hydrograph, other important data is unit hydrograph for the river basin of the Baro Akobo. This unit hydrograph developed by SCS synthetic unit hydrograph method. SCS synthetic unit hydrograph requires the catchment map properties (catchment area, elevation, length). Those catchment properties obtained from delineated watershed by arc GIS. The detail step to determine unit hydrograph from the catchment properties are basin lag time. Basin lag time the time lag, unit duration of rainfall, time to peak from the start, base time of triangular hydrograph . Basin lag time (hrs.) calculated (Linsley, et al).

$$t_p = 0.72 * \left(\frac{L * L_c}{\sqrt{S}}\right)^{0.385} \text{--4-29}$$

Where: - t_p basin lag time. L is the length of the length of the main stream from the outlet to upstream, L_c the distance from the outlet to the point stream nearest the centroid of the watershed and S slope of the catchment reach along the course.

Duration of the rainfall, time to peak from start and base time of triangular are calculated by;-

$$D = \frac{2t_p}{11} \text{---4-30}$$

$$T_p = t_p + \frac{D}{2} \text{---4-31}$$

$$T_b = 2.67T_p \text{---4-32}$$

Where: - D is duration of rainfall, t_p is basin lag time, T_p is time to peak from start and base time of triangular unit hydrograph.

From the principle of the area under unit hydrograph is equal with the unit depth of rainfall volume in upper Baro catchment the peak discharge under unit hydrograph is developed. From the above the parameter triangular unit hydrograph and smooth unit hydrograph is developed.

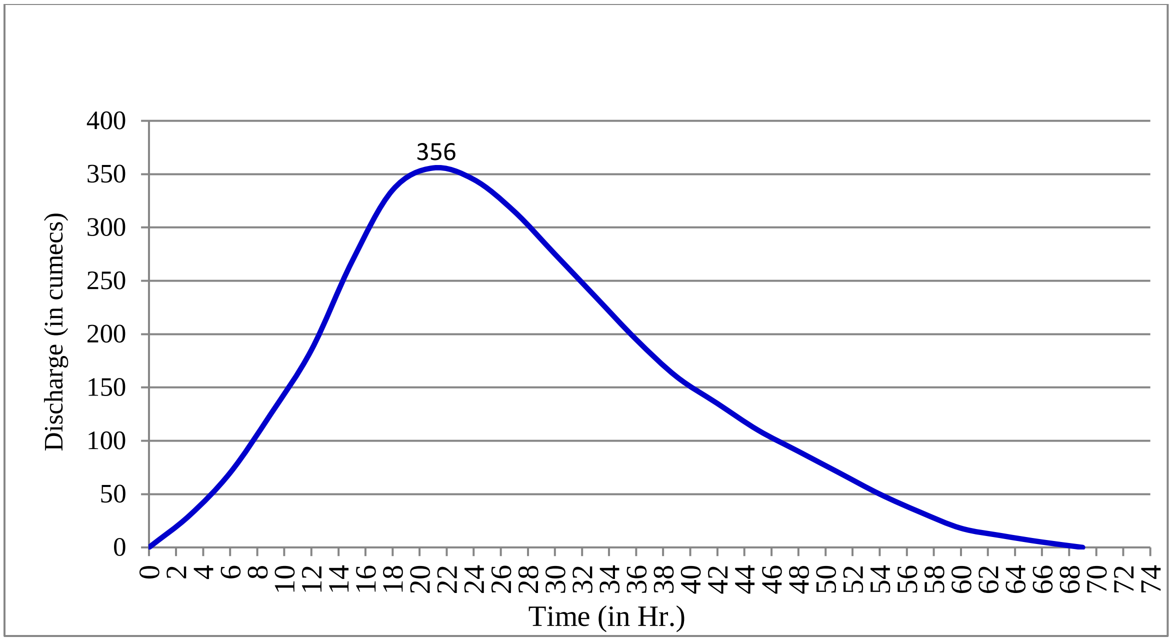

Figure 4:6 Upper Baro Ordinate unit hydrograph

Effective Rainfall Determination

The next step is effective PMP is determination referring the technical document from different projects the loss parameter taken and loss rate is determined for present future, mid future and far future. From effective PMP the PMF determined based on frequency storm. Since, hourly data is not available for this study-nested bell shaped or alternate block method was used to generate rainfall hyetograph. The discretization or disintegration of the PMP is based on the cubic root method of rainfall time to into 24 hours. By using the rainfall ration percentage the effective rainfall hyetograph. From the effective PMP determined, base flow and unit hydrograph the PMF inflow hydrograph is obtained for present, mid and far future for RCP4.5 and RCP8.5.

Outflow Hydrograph Estimation

Outflow versus elevation is determined for Baro I and II based the dimension of over fall spillway based on the discharge formula.

$$Q = C * L * (H - 1520)^{1.5}$$ --4-33

Where: - Q is discharge, C is coefficient of discharge, L is the length of the spillway and H elevation level above FSL of spillway and 1520 full supply of level of reservoir.

Baro II dam is the cascaded hydropower project located 11.7km downstream of the Baro I. Hence outflow from Baro I is the inflow for Baro II and outflow determined from the spillway formula. From inflow hydrograph, storage versus elevation, elevation outflow reservoir routing is done for the Baro I and II.

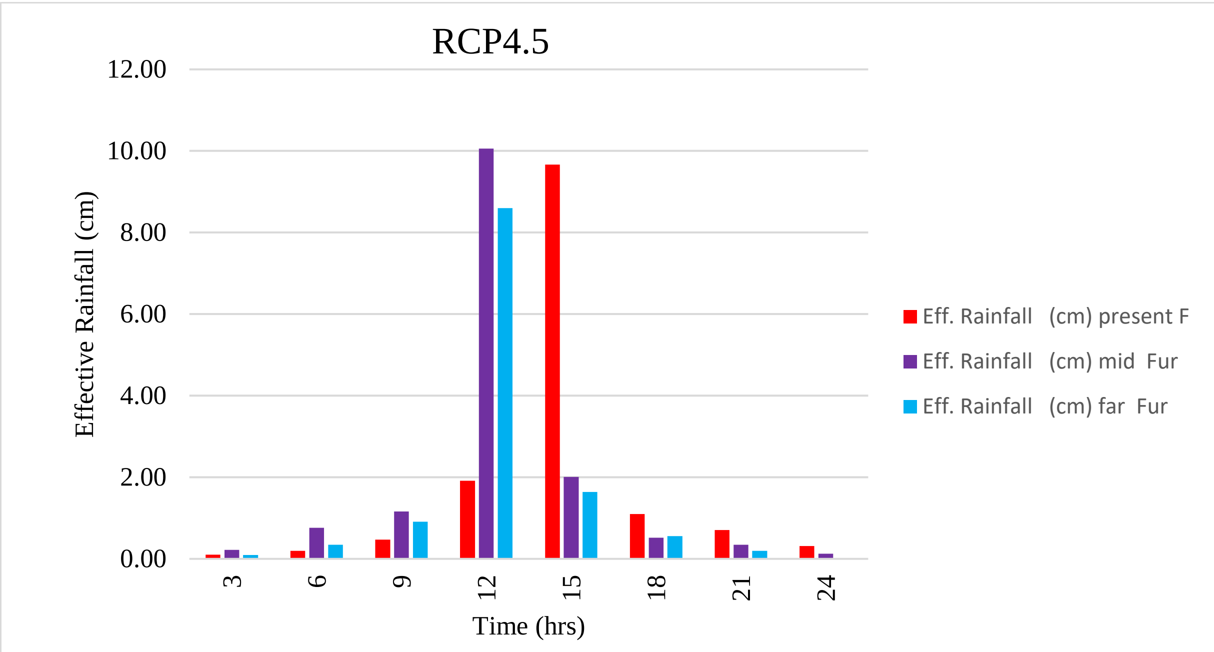

Figure 4:7 Effective PMP hyetograph RCP4.5

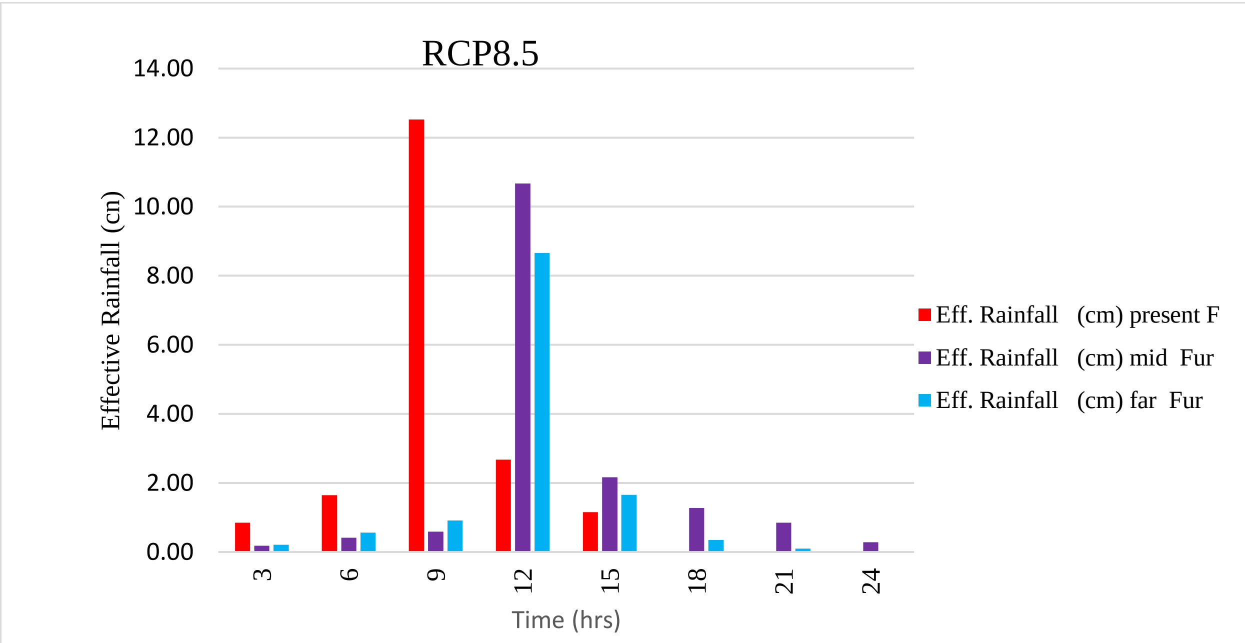

Figure 4:8 Effective PMF hyetograph RCP8.5

Table 4:4 Baro I elevation-volume relationships outflow

Reservoir Level (m)	Storage (MCM)	Outflow (m^3/s)
1520	1355.8	0
1520.5	1374.6	79.34
1521	1393.4	224.40
1521.5	1412.2	412.25
1522	1431.0	634.70
1522.5	1449.8	887.02
1523	1468.6	1166.02
1523.5	1487.4	1469.35
1524	1506.2	1795.20
1524.5	1525.0	2142.11
1525	1563.8	2508.87
1525.5	1602.8	2894.46
1526	0.0	3297.99

Table 4:5 Baro I elevation-volume relationships outflow

Reservoir Level (m)	Storage (MCM)	Outflow (m^3/s)
1320	46.0	0
1320.5	55.3	105.01
1321	64.7	297.00
1321.5	74.0	545.62
1322	83.4	840.04
1322.5	92.8	1174.00
1323	102.1	1543.26
1323.5	111.5	1944.73
1324	120.8	2376.00
1324.5	130.2	2835.14
1325	143.7	3320.56
1325.5	158.0	3830.90
1326	0.0	4364.99

Table 4:6 Baro I elevation-area and elevation-volume relationships (after (International Monetary Fund, 2006))

Elevation[m.a.s.l]	Area(km^2)	Volume(Mm^3)
1439	0	0
1440	0.5	0.2
1450	2.9	17.4
1460	5.6	59.3
1470	9.6	134.5
1480	15.2	259
1490	21.5	445
1500	27.4	690
1510	32.5	989
1520	36.8	1337
1525	38.7	1525

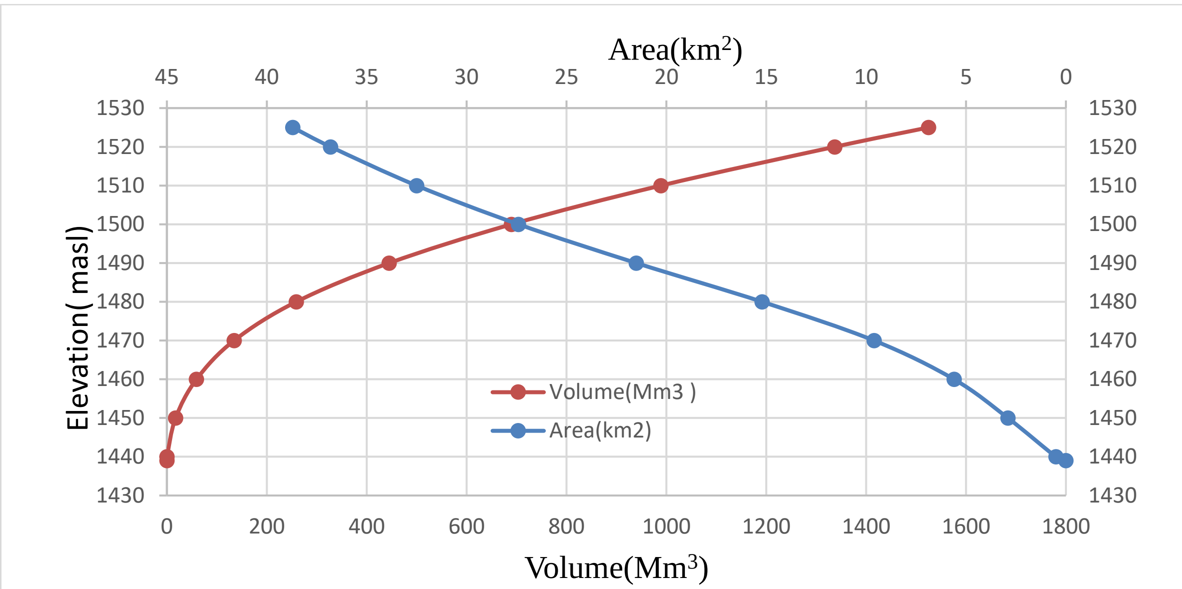

Figure 4:9 Baro I Reservoir, elevation-area and elevation-volume curves (After (International Monetary Fund, 2006))

Table 4:7 Baro I Elevation-area and elevation-volume relationships (after (International Monetary Fund, 2006))

Area(km^2)	**Volume(Mm^3)**	**Elevation[m.a.s.l.]**
0	0	1293
0.218	0.15	1295
0.78	2.5	1300
1.321	7.69	1305
2.613	17.4	1310
5.256	36.6	1315
9.617	73.3	1320
13.251	130.2	1325

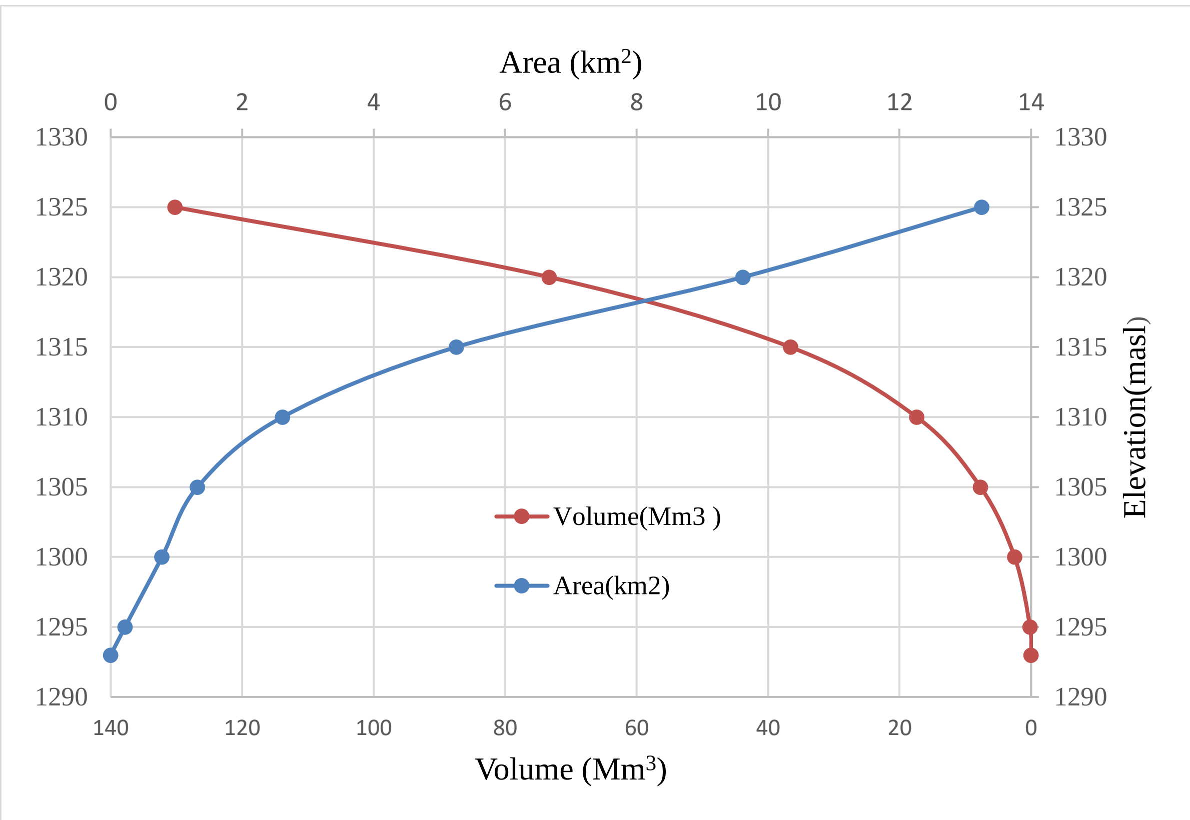

Figure 4:10 Baro I Reservoir, elevation-area and elevation-volume curves (After (International Monetary Fund, 2006))

4.18. Data Analysis

4.18.1. Data Continuity Test

There are many meteorological stations found in the Baro- Akobo river basin. However the station selected for these study must be the station which is the first rank or should have five climate variables (precipitation, wind speed, temperature and relative humidity) and also depending on the location station in the study area or near to the study area. Five meteorological stations are selected for this station like Masha, Gore, Tepi, Bure, and Gatira. There many missed values of rainfall in each station. These missed values filled by normal ration methods; this method selected due to the annual normal value of the missed station is greater than ten percent.

4.18.2. Continuity Test of Hydrological Data

The hydrological gauge stations selected (Masha, Genji, Sore and Geba) for this study area have not full-recorded data or there were many missed value in each station. Due to this continuity test is required, hence the missed value was filled by the multiple regression method. Masha gauge station selected for the analysis but other stations were used to fill missed value of data of Masha station. The random variables, y, and x, regression provides a means for finding the values of the coefficients ‘a’ and ‘b’ for the straight line (y = a+ bx) that best fits the data. The coefficients ‘a’ and ‘b’ obtained by using the least square method.

4.18.3. Areal Rainfall Analysis

Area rainfall analysis used obtain the areal representation of the point rainfall. Thiessen polygon method selected for determination of areal rainfall for this study for its sound theoretical basis and availability of computational tools. However, the method requires a good network of representative rain gauges. Figure 4.11 shows the created Thiessen polygon for the study area.

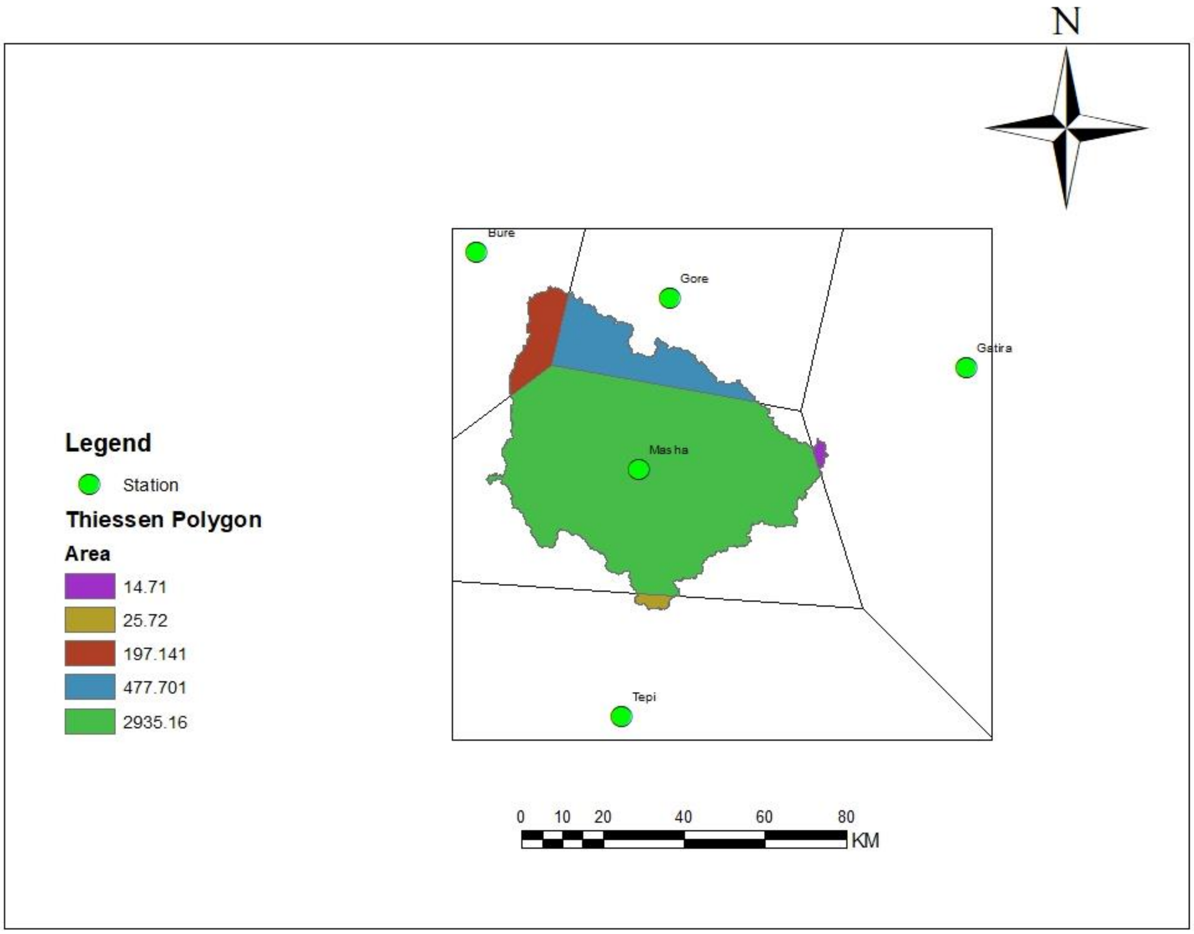

Figure 4:11 Created Thiessen polygon for area rainfall determination

4.19. Climate Change Data Analysis

The climate change data is obtained from the CORDEX Africa project dataset. Under this project, there are many RCM model each has their GCM driving model. The CORDEX dataset has its own realization of the framework to use the data for the specific study area. The RCM model used to downscale the climate change data are REMO2009 and CCLM4-8-7 and the average value of climate change projection for the RCP scenario (RCP4.5 and RCP8.5) is used. The average value RCM data to good value of climate change data for future analysis.

Downscaled climate change CORDEX dataset is divided into historical (1984-2005), present future (2014-2033), mid future (2034-2070) and far future (2071-2100). The baseline period, present future, mid future and future respectively for the RCP 4.5 and RCP8.5 for the analysis. The RCM simulated data categorized into historical and future projection scenarios data. The historical simulated data by RCM is used for the evaluation of the model with observation data.

4.19.1. Bias Correction CORDEX-RCM Simulated Data

The simulated or the output of the RCM data distribution as compared with the observed data is not the same. The original RCM outputs still contain considerable bias, which inherited from the driving of the GCMs or produced by systematic model error on output data. The distribution mapping method of the bias correction used avoid this error of simulated data. The correction is done for precipitation and temperature daily time series of simulated RCM baseline and by using the observation meteorological data, and the applied for future period of RCP scenarios time series of climate change of output RCM data.

4.19.2. Corrections Performance's Evaluation CORDEX- RCM Data

The evaluation of RCM data is the procedure to evaluate the corrected times series of data with historical simulated data with observed data. The model evaluation method is Nash- Sutcliffe efficiency (E_{NS}) and percent of bias (PBIAS). The performance evaluation of RCM data assessment was done as per the statistical measure with the corrected RCM precipitation and temperature data time series against observed precipitation and temperature data. As shown in the table below the precipitations and temperatures, data are accepted or fulfill the criteria of performance evaluation; can be used for hydrological analysis.

4.20. Sensitivity Analysis of Hydrological Model

The hydrological analysis by the SWAT model for determination of surface runoff involves a large number of parameters; around 23 parameters used for the sensitivity for model calibration and validation of the watershed. Hence, sensitivity analysis was performed to identify key parameters (Tang, Xu and Xu, 2012). Those parameters were selected based on the previous finding(Basin, 2016) on that area and the area similar characteristics with the study area. All parameters (Mechal, Wagner and Birk, 2015),(Khalid *et al.*, 2016) used in sensitivity analysis were shown table 5.1.

Those sensitive parameters were automatically calibrated using the Sequential Uncertainty Fitting (SUFI-2) algorithm (Yang *et al.*, 2008)(Abbaspour, Vaghefi and Srinivasan, 2017).

4.21. Regionalization of Parameter

There is no observed gauged station at the outlet of the study area; therefore, regionalization was applied to the model parameter. In parameter regionalization, parameter values are extended and/or extrapolated using calibrated values obtained from gauged watersheds located within the same region (Van Liew and Mittelstet, 2018). According to (Parajka, Merz and Blöschl, 2010), the watershed within the same geographic region and similar climatic condition having ungauged station can exhibit similar hydrologic behavior if they exhibit a high degree of similarity in their physical attributes and have received similar model parameter sets. This regionalization concept after calibrating the model at gauging station in catchment by using the sensitive parameter and then taking this sensitive parameter applied at the outlet of the catchment. The regionalization of the parameters is applied for the sub-basin, which has similar hydrologic response unit (HRU) (Van Liew and Mittelstet, 2018). Similar HRUs mean the sub-basin, which have similar soil type, land cover land use and slope. Each sub-basins at downstream of the ungauged sub-basin to the outlet of the catchment having similar HRUs with the upstream of the gauged sub-basin they have the same parameters. Hence, the parameters are shown in table 5.4 (CN2, GW_DELAY, ESCO, SOL_AWC, CH_K2, etc.) were used in the simulation to obtain a discharge of the projected inflow to the reservoir of Baro I and II hydropower reservoir.

4.22. Flood Frequency Analysis

Hydrologic data frequency analysis that used for the magnitude of extreme events to know the frequency of occurrence using probability distribution, the assumption made in during analysis the data should be independent and identically distributed. Flood frequency analysis is related to the magnitude of extreme events to their frequency of occurrence through probability distribution of hydrological data (i.e. flood) by assuming the data identically distributed and independent and hydrologic system considered stochastic, time independent and time independent. When stream flow peaks are arranged in the descending order of magnitude, they constitute a statistical array whose distribution can be expressed in terms of frequency of occurrence. The simulated output maximum annual flow from the hydrological model of the RCM data scenarios (RCP4.5 and

PCP8.5) used for frequency analysis. The annual series of this arranged in descending and the probability of each event equaled or exceeded. The return period or recurrence interval (*T*) is the average number of years during which a flood of given magnitude will be equaled or exceeded once and is computed by one of the following methods (Yilma Seleshi (Dr.), 2005). The return or recurrence interval (T) of annual maximum flood or flow-simulated output will be equaled or exceeded one is computed by Weibull method (1939):

$$T = \frac{n+1}{m} \text{--} 4\text{-}34$$

Where: - 'T' return period, 'n' total number of events in the data and 'm' is order numbers of the events.

The general equation for flood frequency analysis is which developed by proposed by Chow (1964).

$$X_T=\mu+k\,\delta \text{---} 4\text{-}35$$

Where: - 'X_T' is the value of variant (X) is random hydrologic series with return period (T), $'\mu'$ is mean data, $'\delta'$ standard deviation of data and 'k' is frequency factor which depends up on the return period (t) and assumed frequency factor distribution.

For the selection of best frequency method, the L-moment method Hosking and Wallis (1986) was used. This method gives the efficient result for determination of parent distribution. This method also improve the statistics for characterizing the shape of a probability distribution and estimating the distribution parameters(Seckin, Haktanir and Yurtal, 2011). The sampling properties of L-moment unbiased and normally distributed, and the L-moments are more convenient than other method because they can be directly interpreted as measures of scale and shape of probability distributions. In this respect, they are analogous to conventional moments. The unbiased parameter determined as follows:-

$\beta_o = \sum(X)/n$--4-36

$\beta_1 = \sum(((n-i)*X\,i)/(n*(n-1)))$--4-37

$\beta_2 = \sum(((i-1)(i-2)*Xi)/(n*(n-1)(n-2)))$--4-38

$\beta_3 = \sum (((i-1)(i-2)(i-3)*Xi)/(n*(n-1)(n-2)(n-3))$----------------------------4-39

$\lambda_1 = \beta o$ --4-40

$\lambda_2 = 2\beta 1 - \beta o$---4-41

$\lambda_3 = 6\beta 2 - 6\beta 1 + \beta o$--4-42

$\lambda_4 = 20\beta 3 - 30\beta 2 + 12\beta 1 - \beta o$---4-43

L-moment ratios, which are analogous to conventional moment ratios are defined by Hosking (1990) as follows:-

$\tau = \lambda_2 / \lambda_1$---4-44

$\tau_3 = \lambda_3 / \lambda_2$--4-45

$\tau_4 = \lambda_4 / \lambda_2$---4-46

Where: - λ_1 is a measure of location, λ_2 is a measure of scale and dispersion, τ_3 is a measure of Skewness and λ_4 is a measure of kurtosis.

To identification of the best-fitted distribution of data from the frequency distribution method the following equation are used three methods are selected (Seckin, Haktanir and Yurtal, 2011).

1. Log normal distribution ,

$\tau_4 = 0.12282 + 0.77518(\tau_3)^2 + 0.12279(\tau_3)^4 - 0.13638(\tau_3)^6 + 0.113638(\tau_3)^8$------------4-47

2. General extreme value,

$\tau_4 = 0.10701 + 0.1109(\tau_3) + 0.84838(\tau_3)^2 - 0.06669(\tau_3)^3 + 0.00567(\tau^3)^4\ 0.04208(\tau_3)^5 + 0.03763(\tau_3)^6$---4-48

3. Log Pearson type III

$\tau_4 = 0.1224 + 0.30115(\tau_3)^2 + 0.95812(\tau 3)^4 - 0.57488(\tau_3)^6 + 0.19383(\tau_3)^8$---4-49

The most commonly method Frequency distribution functions like Gumbel' s extreme-value distribution, log Pearson Type III distribution and Log normal distribution used for prediction extreme flood values.

4.22.1. Gumbel's Extreme Value Distribution Method

Gumbel's distribution was first introduced by Gumbel (1941) and is commonly known. This method widely used from probability distribution functions for extreme values determination in hydrologic and meteorological studies for estimate of maximum rainfalls, maximum wind speed , flood peaks, , , etc. Gumbel defined a flood as the largest of the 365 daily flows and the annual series of flood flows constitute a series of largest values of flows.

$$X_T=\mu+k\ \delta \text{---------------------------------}4\text{-}50$$

An extreme events like floods maximum rainfall depths and others have finite lengths of records; the above equation is modified to account for finite N as given below for practical use is:-

$$X_T=\mu+k\ \delta_{n-1} \text{------------------------------------}4\text{-}51$$

Where: - δ_{n-1} is standard deviation of the sample size N, K = frequency factor expressed and μ= mean of the data.

$\delta_{n-1} = \sqrt{\frac{\sum(X-\bar{x})^2}{N-1}}$, K = $\frac{y_T-\overline{y_n}}{S_n}$ and Y_T is the reduced variate $Y_T = -\left(ln.\,ln(\frac{T}{T-1})\right)$----------4-52

$\overline{y_n}$ = reduced mean, and S_n = reduced standard deviation they are a function of sample size N obtained from table.

4.22.2. Log-Pearson Type III Distribution

This type distribution is extensively used commonly in USA, and the variate is transformed into logarithmic from the base 10 and transformed data is then analyzed. If the variate of a random hydrologic series X, then the series of Z variates where first obtained by:-

$$z=logx \text{--}4\text{-}53$$

The Z variated of the any recurrence interval T

$$Z_T=\bar{z}+K_z\delta_z \text{--}4\text{-}54$$

Where: - K_z= a frequency factor which is a function of recurrence interval T and the coefficient of skew Cs and δ_z standard deviation of the Z variate sample

$$\delta_Z = \sqrt{\frac{\sum(Z-\bar{Z})^2}{N-1}} \text{ and } \frac{N\sum(Z-\bar{Z})^3}{(N-1)(N-2)\delta_Z{}^3} \text{--4-55}$$

Where: - $\bar{z}$ is the mean of the z values and N is ample size (number of years of record). The variations of K_z = f (Cs, T) is obtained from table. After finding the Z_T the corresponding, the value of X_T is determined by

$$X_T = antilog\ Z_T \text{--4-56}$$

4.22.3. Log-normal Distribution

When the skew is zero, i.e. C_S= 0, the log-Pearson Type III distribution reduces to log normal distribution. The lognormal distribution plots as a straight line on logarithmic probability paper.

5. Result and Discussion

The result and discussion have two major parts climate change model result and discussion, and hydrological modeling result and discussion. Each result was shown using graphical, tabular and graphically and discussed in detail as follows.

5.1. Regional Climate Model Output

After the bias correction was done on the climate change model data result, next is to see the change in the precipitation and temperature rainfall in climatological baseline or historical (1984-2005) with observed or recorded data a comparison was done. The comparison shows that the historical RCM out data after bias correction the result shows perfect fitted with the observed data for both temperature and precipitation. The downscaled RCPs data after bias correction can be used for impact assessment of climate change (Y and Kemal, 2017).

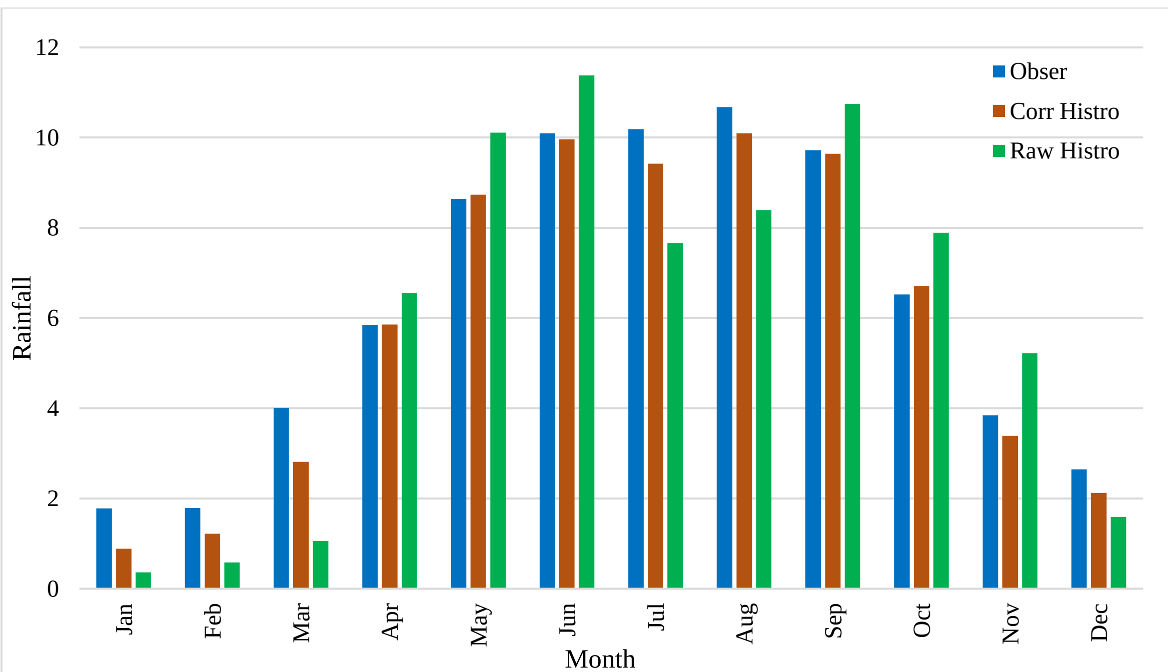

Figure 5:1 Observed and RCP after bias correction of rainfall in of Masha station

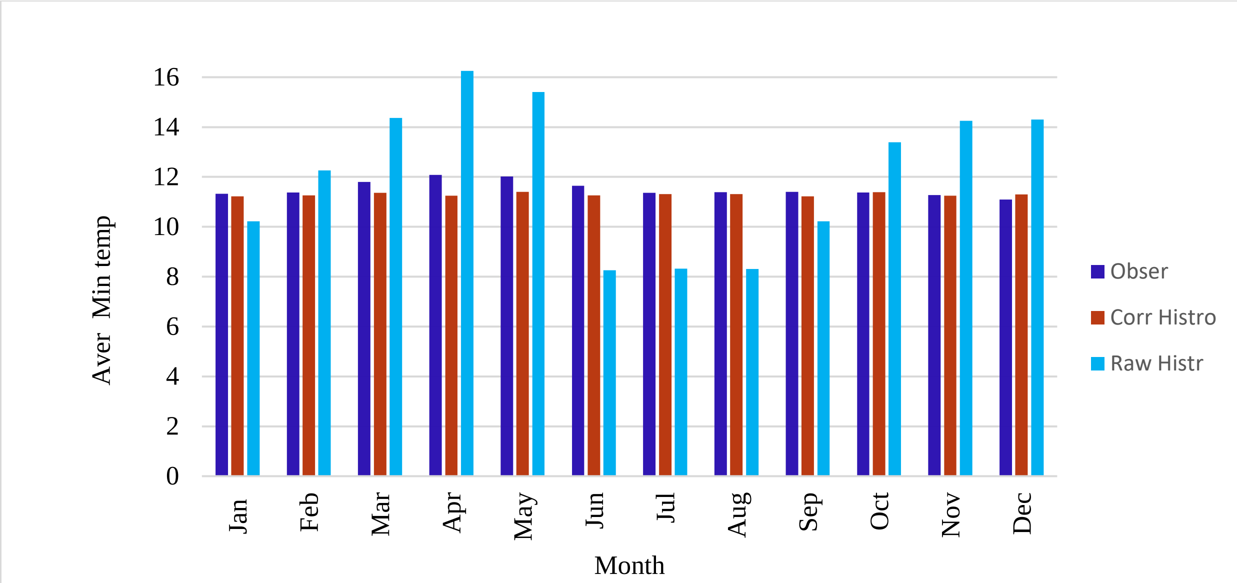

Figure 5:2 Bias correction of minimum temperature in of Masha station

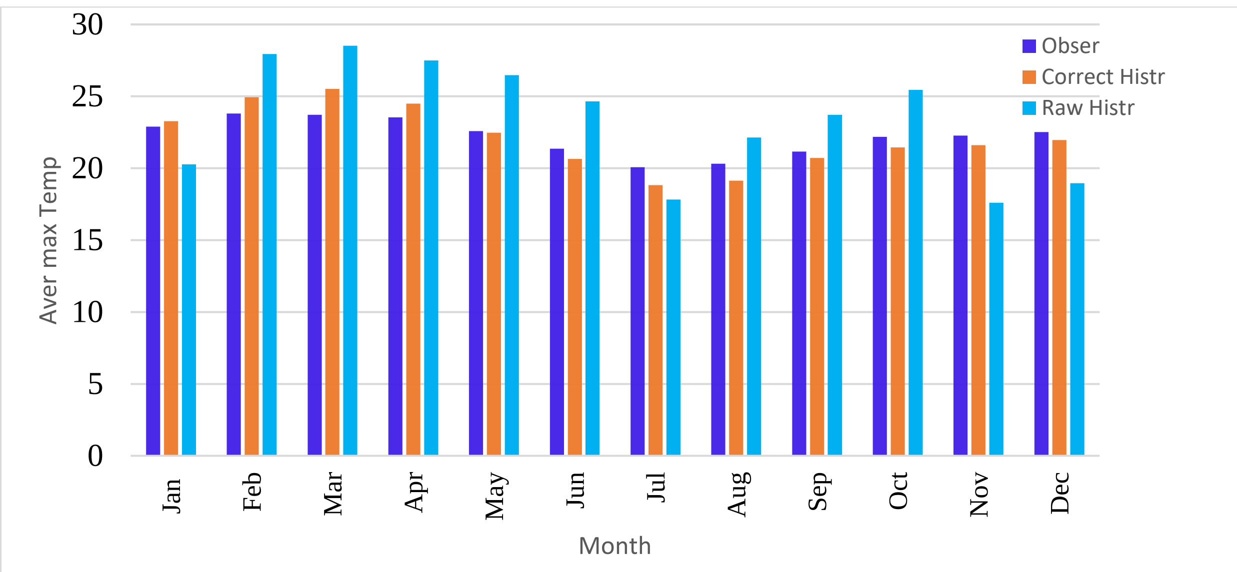

Figure 5:3 Bias correction of maximum temperature in of Masha station

From figure 5.1-5.3 the rainfall, maximum and minimum temperature of Masha station shown above, the figure shows an identical graph.

5.1.1. Regional Climate Model Output Evaluation

Coordinated Regional Climate Downscaling Experiment (CORDEX) Africa project data should be evaluated whether the conceded with observed data after downscaling and bias-corrected. The simulated data of the regional climate model evaluated under model performance evaluation criteria like coefficient of correlation, Nash-Sutcliff coefficient, and percent of bias. In performance criteria evaluation of each station, the coefficient of determination (R^2) has resulted more than 0.90 (Legesse Gebre, 2015; Lennard *et al.*, 2018) indicate better performance between the bias-corrected and observed values. The Nash-Sutcliffe coefficient resulted in more than 0.8 and percent of bias less than 10% (Legesse Gebre, 2015; Lennard *et al.*, 2018).

Table 5:1 Mean monthly-corrected RCM precipitation data sets

RCM data at station	Before Bias			After Bias		
	E_{NS}	PBIAS	R^2	E_{NS}	PBIAS	R^2
Masha	0.814	-7.335	0.869	0.969	-6.485	0.988
Gore	0.814	-7.335	0.869	0.969	-6.485	0.988
Tepi	0.236	-28.920	0.600	0.802	-18.635	0.943
Bure	0.417	-6.129	0.472	0.983	-5.813	0.992
Gatira	0.742	-16.484	0.833	0.947	-12.171	0.986

Table 5:2 Mean monthly-corrected RCM maximum temperature data sets

RCM data at station	Before Bias			After Bias		
	ENS	PBIAS	R2	ENS	PBIAS	R2
Masha	0.706	-0.497	0.953	1.000	0.003	1.000
Gore	0.152	-7.225	0.967	1.000	0.000	1.000
Tepi	-2.380	0.562	0.021	0.546	0.532	0.972
Bure	0.872	-0.137	0.879	0.997	0.105	0.999
Gatira	0.256	-4.063	0.956	0.961	-0.887	0.994

Table 5:3 Mean monthly-corrected RCM minimum temperature data sets

RCM data at station	Before Bias			After Bias		
	E_{NS}	**PBIAS**	**R^2**	**E_{NS}**	**PBIAS**	**R^2**
Masha	0.872	-1.068	0.997	0.872	-1.068	0.997
Gore	-1.507	-0.411	0.008	0.987	-0.411	0.994
Tepi	-2.380	0.562	0.021	0.546	0.532	0.972
Bure	-0.455	0.016	0.010	1.000	0.000	1.000
Gatira	1.000	0.016	1.000	1.000	0.016	1.000

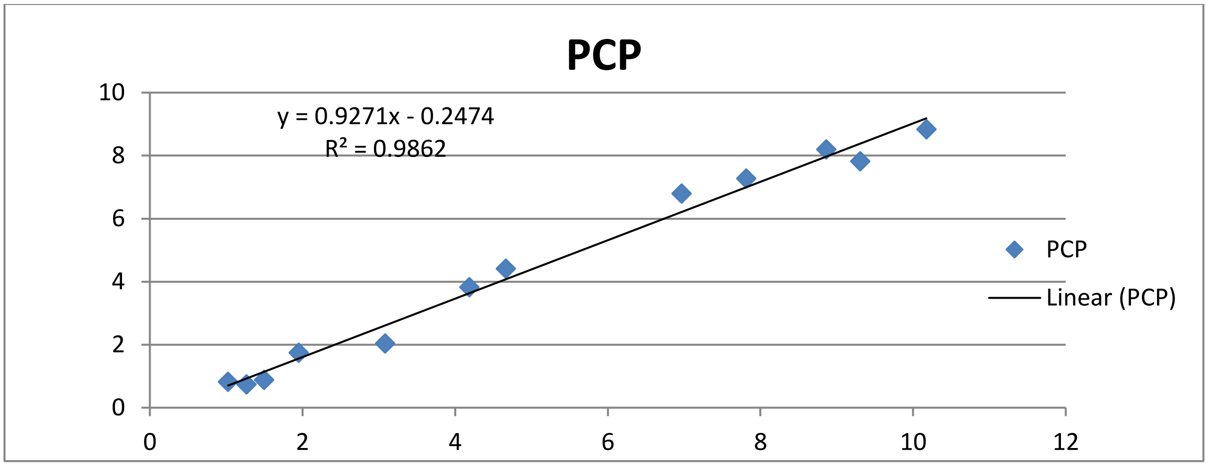

Figure 5:4 Precipitation RCM simulated evaluation result

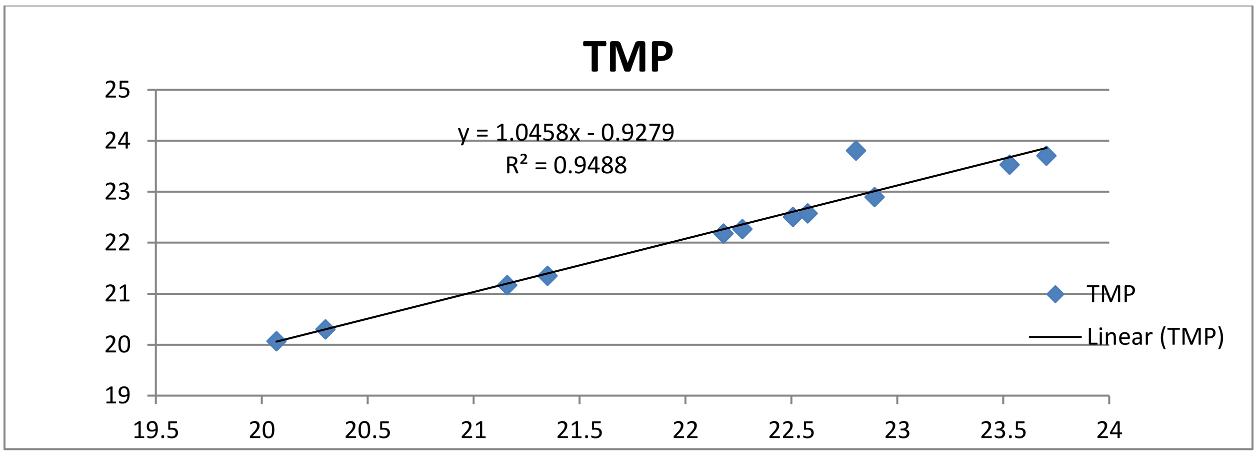

Figure 5:5 Maximum temperature RCM simulated evaluation result

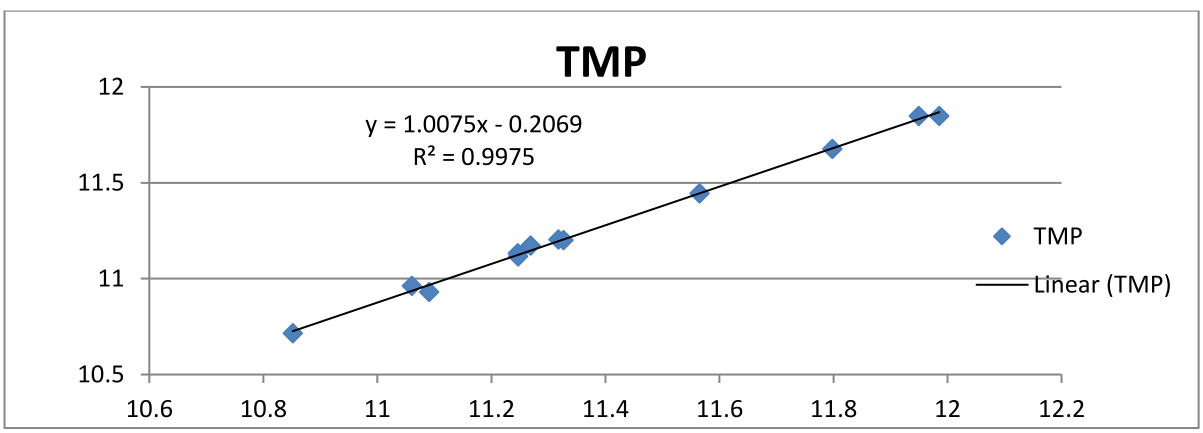

Figure 5:6 Minimum temperature RCM simulated evaluation result

Generally, all the RCMs output projected prediction of precipitation, maximum temperature, minimum temperature, wind speed, and solar radiation resembled in producing the observed data for the base period. Therefore, it is reasonable to use the RCMs data output for future prediction for the basin.

5.1.2. Future Climate Change Output Data

The future RCM output data of the RCP scenario (RCP4.5 and RCP8.5) of the daily precipitation and average temperature of the next century as discussed below.

5.1.2.1. Precipitation

The daily precipitation of next century of the regional climate models of the RCP scenario (RCP4.5 and RCP8.5) were evaluated for the study area but for simplification of evaluation of the precipitation increase or decrease the daily precipitation change to average monthly precipitation for comparison with the observation precipitation. The result shows of the average monthly precipitation for present future years (2014-2033) of RCP4.5 show increase in three months (April, May, and November) by 10.0% (Y and Kemal, 2017)and the other months show decreased by 23.4%. For mid future years, (2034-2070) in months (May, June, September and October) increased by of 3.7% and in others months decreased by 32.43%, in this scenario for far future (2071-2100) only four months (May, June, September, and October) shows increase by 9.1% and other months decrease by 33.4%. For RCP8.5 scenario of the average monthly precipitation of present future years (2014-2033) four months (May, June, September, and October) were shown increase by 7.9% and the others decrease by 34%. In the mid future years (2034-2070) three months (May, June, and November) were shown an increase by 8.85% and others decrease by 34.38%. In addition, for far future years (2071-2100) of this scenario, only two months (May and October) were shown to increase by 9.8% and others decreased by 30.0%.

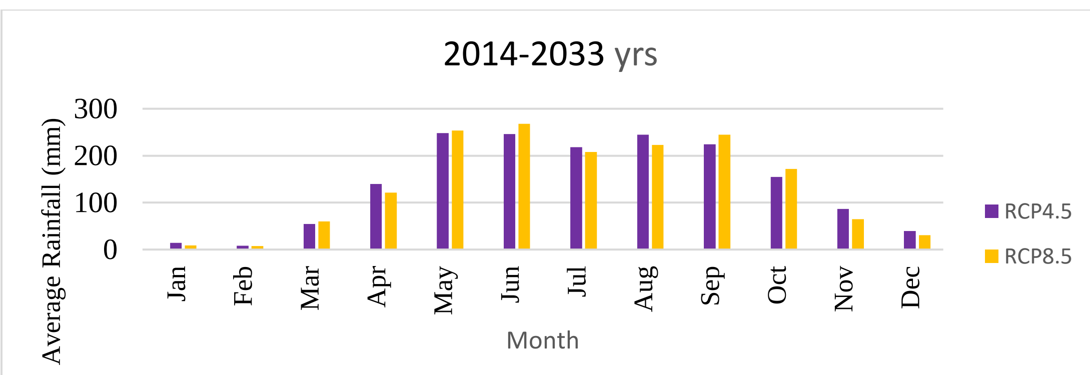

Figure 5:7 Average monthly precipitation result for present future (2014-2033)

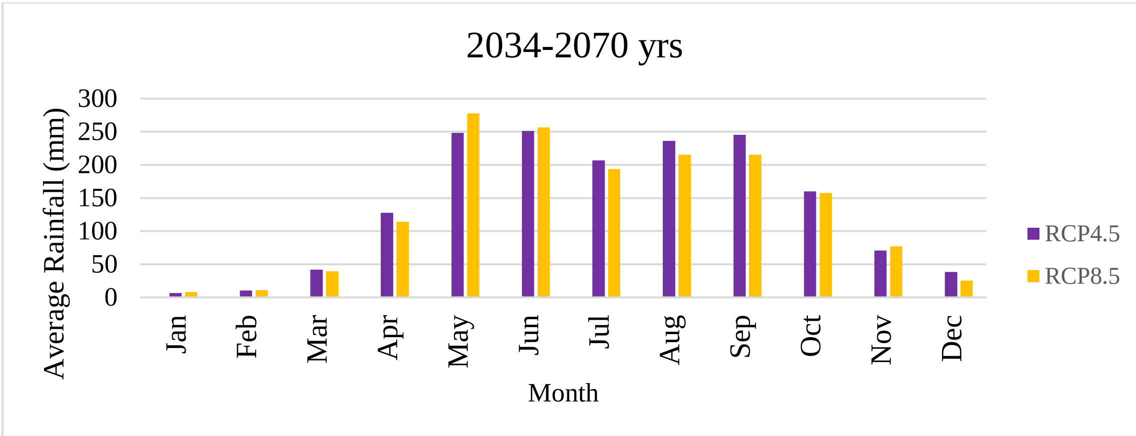

Figure 5:8 Average monthly precipitation result for mid future (2034-2071)

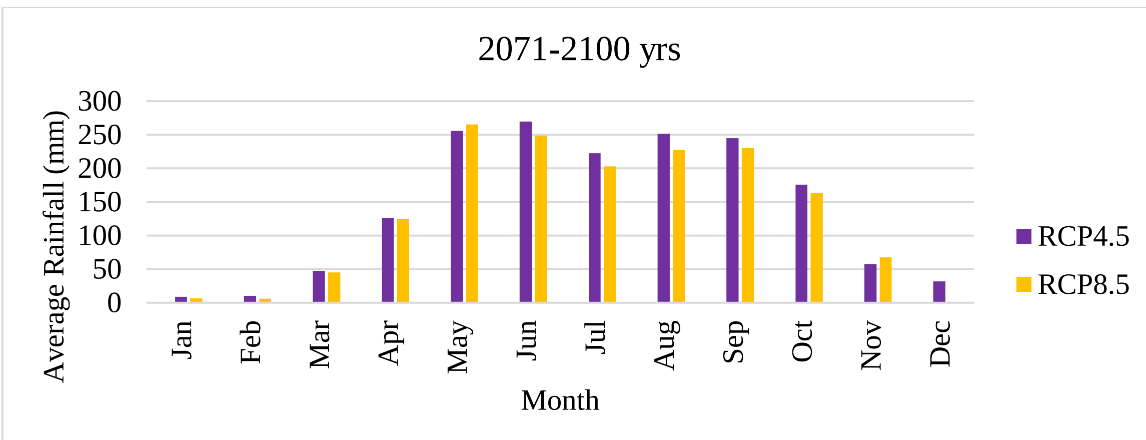

Figure 5:9 Average monthly precipitation result for far future (2071-2100)

5.1.2.2. Average Temperature Monthly Basis

The average monthly temperature for the RCP scenarios for the next century obtained from the simulated regional climate models. The present future years (2014-2033), mid future years (2034-2070) and far future years (2071-2100) for RCP4.5 scenario in all months were shown increase in values. Moreover, in the case of the RCP8.5 scenario also the present future years (2014-2033), mid future years (2034-2070) and far future years (2071-2100) were shown increase in throughout the year.

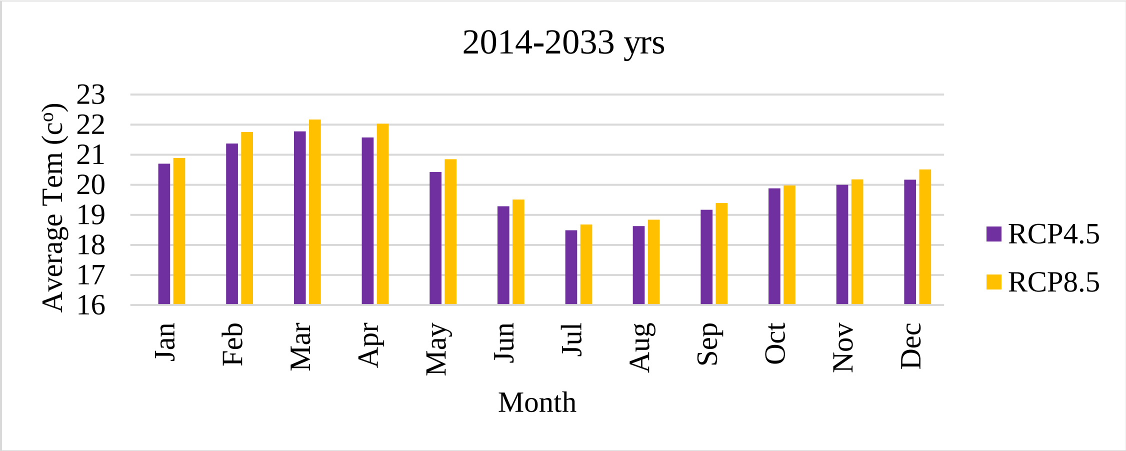

Figure 5:10 Average monthly temperature result for present future (2014-2033)

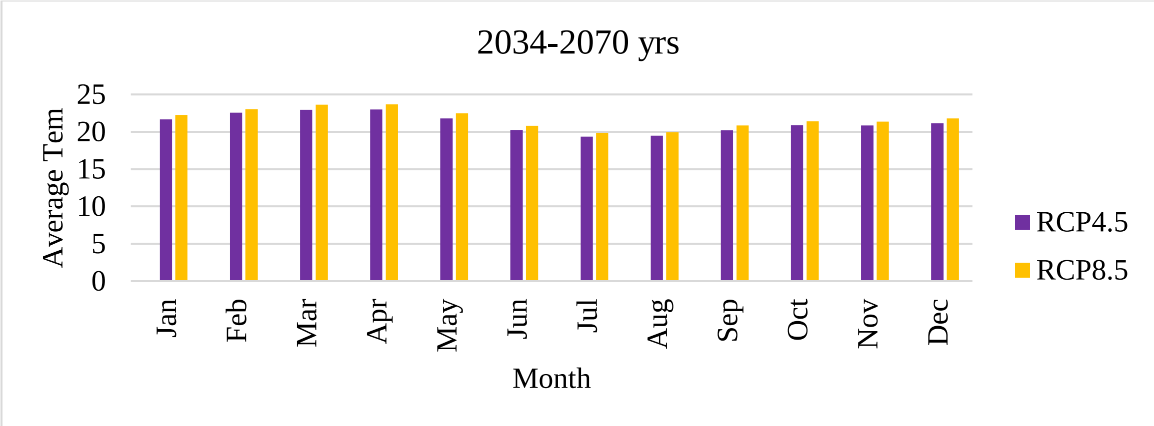

Figure 5:11 Average monthly temperature result for present future (2034-2070)

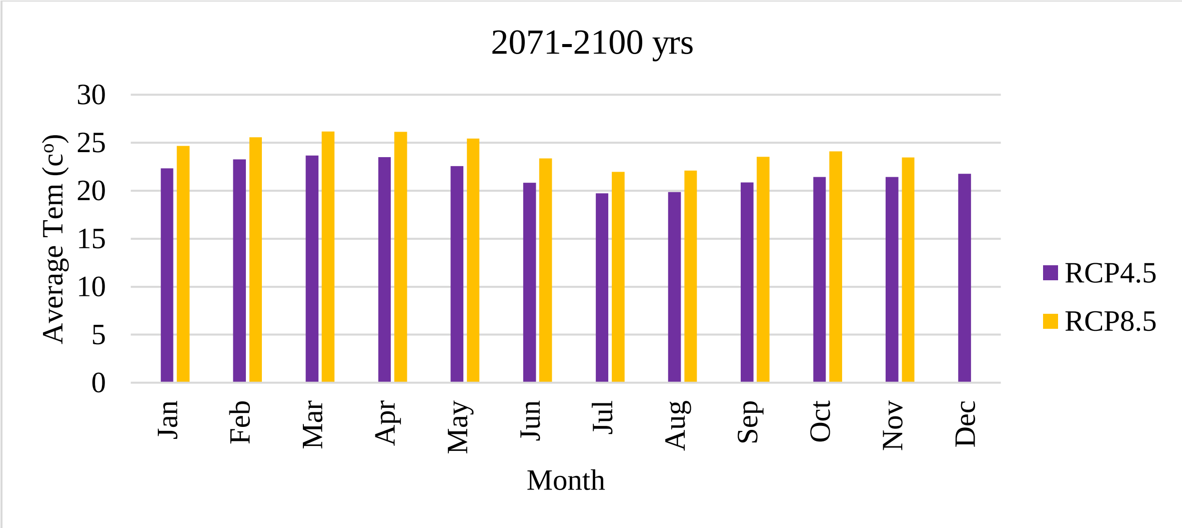

Figure 5:12 Average monthly temperature result for present future (2071-2100)

The annual summary of the precipitation of the projected the RCP of two scenarios were given in the annex B

5.2. Hydrological Modelling Output

5.2.1. Sensitive Analysis

The most sensitive parameters for flow were identified after many iterations and simulations considering the global sensitivity method using SWAT-CUP program. Identification of sensitive parameters enables us to focus only on parameters, which affect most of the model output during the simulation of the model. Hence, parameter reduction by filtering out the less influential parameters that have a significant impact on specific model output (Shoghli, Lim and Alikhani, 2016). The most sensitive parameters were ranked after many iterations using 23 numbers parameters were used for calibration and validation. Those parameters are: - SLSUBBSN, Curve number (CN2), HRU_SLP (hydrologic response unit slope), groundwater delay (GW_DELAY), channel effective hydraulic conductivity (CH_K2), SOL_K(soil hydraulic conductivity), Channel roughness coefficient (CH_N2), soil evaporation compensation factor (ESCO), base flow Alpha factor(ALPHA_BF), available water capacity SOL_AWC), etc. were shown in figure 4.13 according to the sensitivity of each that significantly affect flow. After identifying the more sensitive parameter model calibration was done for the model by using SWAT-CUP program (Abbaspour, Vaghefi and Srinivasan, 2017) SUFI2 method. The SFI2 method selected for due to easily implementation of the program, reduce the number of the model runs, it gives good prediction and allows manual adjustment of the parameter in the model.

Table 5:4 Sensitive parameters with their fitted value

S.No	Parameter Name	Minimum Value	Maximum Value	Calibrated Value
1	CN2.mgt	-0.25	0.25	0.1956
2	ALPHA_BF.gw	30	450	0.8300
3	GW_DELAY.gw	0	1	48.4000
4	GWQMN.gw	0	2	1.7533
5	GW_REVAP.gw	0.02	0.2	0.1898
6	REVAPMN.gw	0	500	18.3333
7	RCHRG_DP.gw	0	1	0.0367
8	SOL_AWC(..).sol	-0.25	0.25	-0.2183
9	SOL_K(..).sol	-0.25	0.25	-0.1383
10	SOL_ALB(..).sol	-0.25	0.25	0.1450

11	CH_N2.rte	-0.01	0.3	0.1047
12	CH_K2.rte	-0.01	500	34.9907
13	ALPHA_BNK.rte	0	1	0.1633
14	TLAPS.sub	-10	10	-8.6000
15	SLSUBBSN.hru	10	150	40.3333
16	HRU_SLP.hru	0	1	0.6304
17	OV_N.hru	0.91	31	2.2139
18	CANMX.hru	0	100	13.6667
19	ESCO.hru	0	1	0.4033
20	EPCO.hru	0	1	0.0033
21	SURLAG.bsn	0.05	24	1.2475
22	LAT_TTIME.hru	0	150	96.1000
23	PLAPS.sub	0	100	2.3333

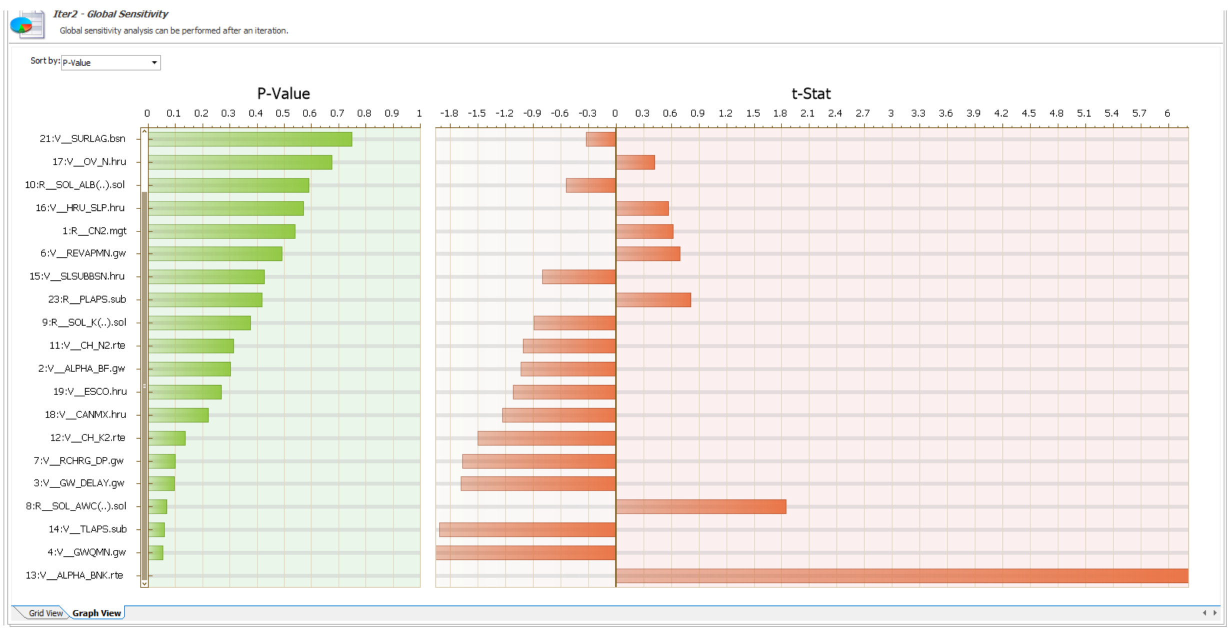

Figure 5:13 Sensitive parameter for calibration and validation of catchment from SWAT-CUP

5.3. Model Calibration and Validation

The model calibration and validation were done by using the SWAT-CUP software of SUFI2 method. After sensitive parameters are identified the calibration and validation of the model are done.

5.3.1. Calibration

The calibration of the SWAT model is done by selecting the Masha gauging station of the recorded data from 13 years (1988-2000) flow data taking 4 years (1984-1987) warm-up period for SWAT-CUP model order to set hydrologic processes to reach into equilibrium. The warm-up period used to model for initiation of the model for simulation. The calibration of the model conducted based on changing the daily time-series of data to monthly bases.

The selected parameters used to calibrate the model to decrease the gap between the observed flow data and simulated flow data. The procedure of calibration was done through the trial and error of changing parameter value to get the selected for model performance. Optimal model parameters were rarely found on the first attempt of automatic calibration. The automatic calibration and manual changing of the parameters value gives the successfully finish the calibration process.

The model performance evaluation criteria during the calibration period (close agreement between the goodness-of-fit criteria of the simulated and observed flow) should give the acceptable range. Coefficient of determination, which is best if $R^2 > 0.65$ and Nash-Sutcliffe (1970) coefficient of efficiency, which is best if NSE>0.6. Based on other documentation, NSE values greater than 0.75 signify good model performance, while those between 0.36 and 0.75 signify acceptable model performance (Teutschbein and Seibert, 2010)(Almeida, Pereira and Pinto, 2018)(S. Hansen *et al.*, 2013) (Tang, Xu and Xu, 2012). The calibration result of the study area satisfy above this criteria i.e. Nash-Sutcliffe coefficients of efficiency, NSE=0.71, coefficient of determination, R^2=0.76, which indicates goodness-of-fit criteria. (Negassa, 2012; Basin, 2016).

From the figure 5.14 of the observed data and simulated value during calibration show the goodness-of-fit on graph hence the model is successfully calibrated.

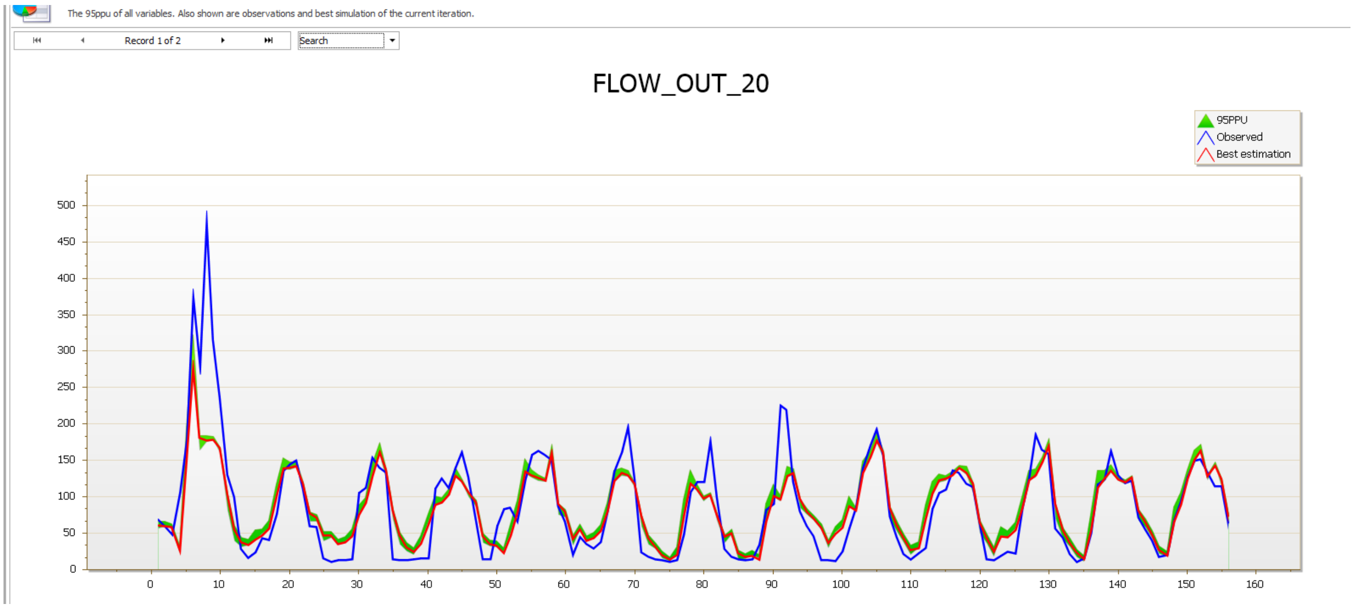

Figure 5:14 calibration result of the SWAT-CUP period (1988-2000)

5.3.2. Validation

After calibration of the model was completed, model validation was conducted. The model validation check illustrates the accuracy of the model for simulating time-periods outside of the calibration period and comparison of the model outputs with an independent data set without making further adjustments. Model validation confirmed the applicability of the watershed-based hydrologic parameters derived during the calibration process.

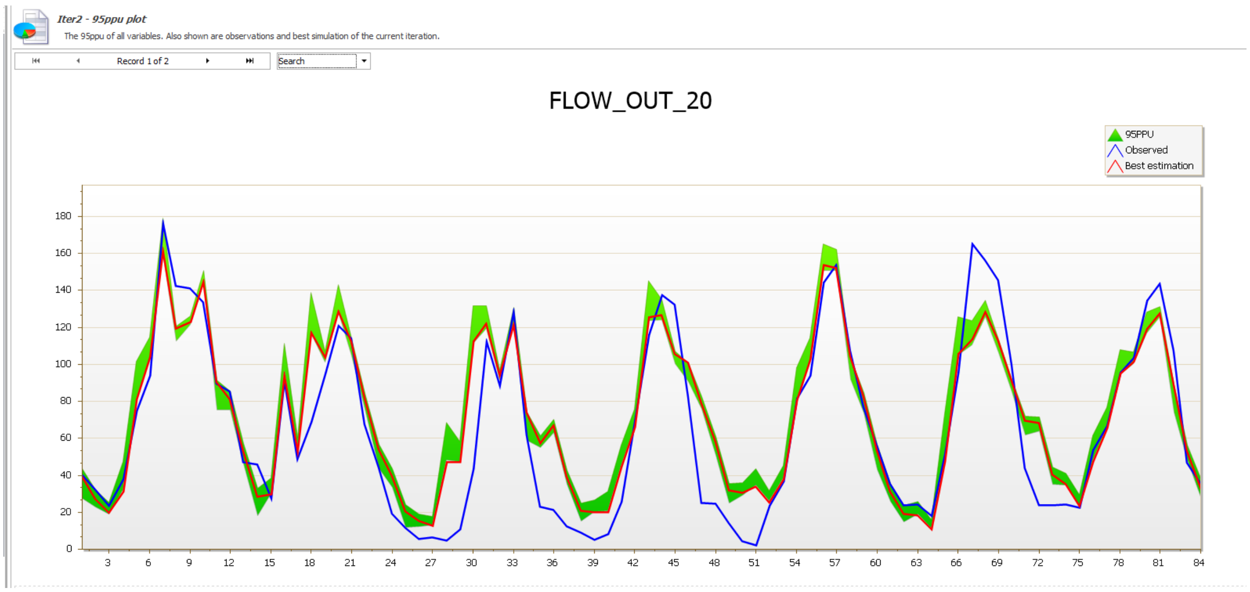

Figure 5:15 validation result of the SWAT-CUP period (2001-2007)

For the model validation seven years (2001-2007) data used for analysis by using the SWAT-CUP program. The result of the model validation was in the accepted range by model performance evaluation criteria when R^2 greater than 0.65, Nash-Sutcliffe greater than 0.6, percent of bias less than 15% which were recommended value(Tang, Xu and Xu, 2012; Abbasa, Wasimia and Al-Ansari, 2016; Shoghli, Lim and Alikhani, 2016; Almeida, Pereira and Pinto, 2018). The value coefficient of correlation (R^2) and Nash-Sutcliffe Efficiency (NSE) was in accepted range, which the R^2 = 0.84 and NSE= 0.82 (Basin, 2016).

5.4. Dam Overtopping Evaluation

The single most common cause of embankment dam failures is overtopping. An undersized spillway will lead to overtopping; therefore, spillway capacity is evaluated for future climate change result. The evaluation were based on the potential effect RCP scenario on the dam overtopping due to incoming flow to the reservoir. The outputs from this ensemble of regional climate model simulations were analyzed (Ouranos, 2015).

5.4.1. Hydrological Output of RCM Data

The hydrological evaluation of the RCM data output consider two cases are frequency analysis of the simulated of regional climate model output by Arc SWAT and routing of the inflow hydrograph of PMP to the reservoir for RCP scenario next century under climate change, and the trend of the land cover change conditions of 2018 is constant. The routed and simulated inflow by Arc SWAT divided into present future years (2014-2033), mid future years (2034-2070) and far future years (2071-2100). The frequency analysis of simulated flow (present future, mid future, and far future), and routing of inflow outflow from unit hydrograph to check the overtopping of the dam or potential under the most extreme conditions expected for life of embankment dam (Lee and You, 2013). The spillway capacity must be correctly estimated to prevent any overflow over embankment dam under any situation. The result of future simulated projected precipitation (see annual summary of precipitation annex B) used for reservoir routing and simulation in the model (Arc SWAT). Drainage of the watershed in Ethiopia were affected by due to the climate change (Osima *et al.*, 2018) Due to change in precipitation, the mean monthly inflow to reservoir for the A1B scenario in the two future time periods tends to decrease in the mid-century followed by an increase in the late century for Baro Basin (Negassa, 2012).

I. Reservoir Routing

After reservoir routing for Baro I present future period (2014-2033) for two scenarios (rcp4.5 and rcp8.5) of peak inflow flow are 3783.2 m^3/s and 5314.6 m^3/s, outflow 2244.9 m^3/s and 3004.9 m^3/s respectively. In the mid future period (2034-2070) for two scenarios (rcp4.5 and rcp8.5) of peak inflow are 3892.9 m^3/s and 3314.6 m^3/s, outflow 2299.0 m^3/s and 2430.8 m^3/s respectively. Moreover, for far future periods (2071-2100) for two scenarios (rcp4.5 and rcp8.5) of peak inflow are 3177.36 m^3/s and 3207.27 m^3/s, outflow 1903.01 m^3/s and 1918.68 m^3/s respectively. And also for Baro II present future period (2014-2033) for two scenarios (rcp4.5 and rcp8.5) of peak inflow flow are 2233.5m^3/s and 2428.6 m^3/s, outflow 2081.4 m^3/s, and 2294.5 m^3/s respectively. In the mid future period (2034-2070) for two scenarios (rcp4.5 and rcp8.5) of peak inflow are 3286.0 m^3/s and 3057.0 m^3/s, outflow 2871.4 m^3/s and 2544.19 m^3/s respectively. Moreover, for future periods (2071-2100) for two scenarios (rcp4.5 and rcp8.5) of peak inflow are 1882.85 m^3/s and 1898.42 m^3/s, outflow 1707.97 m^3/s and 1663.47 m^3/s respectively.

The routing result for the present future is shown in table 5.5 for Baro I and 5.6 for Baro II below, the others routing see under annex D.

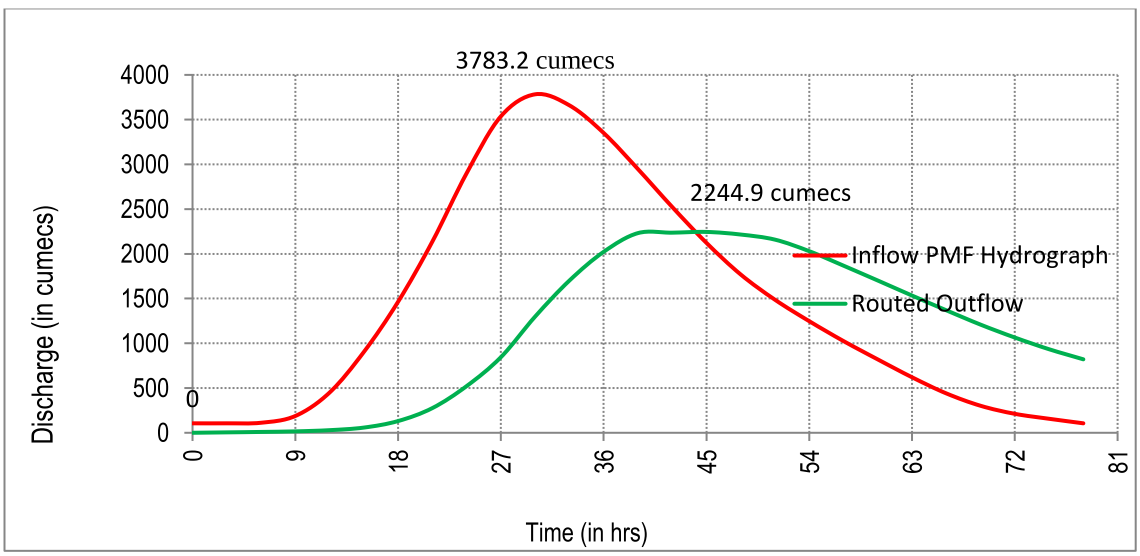

Figure 5:16 present future of RCP4.5 inflow PMF and routed outflow hydrograph of Baro I

Table 5:5 Present future (2014-2033) of RCP4.5 Reservoir routing Baro I

Time (hr.)	Δt (hr.)	Inflow I (cumes)	(I1+I2)/2	((I1+I2)/2)*Δt (MCM)	S-QΔt/2 (MCM)	S+QΔt/2 (MCM)	Elevation (m)	Outflow (cumec)
0.00		105.86				1355.80	1520.00	0.00

	3.00		105.86	1.14	1355.80	1356.94		
3.00		105.86					1520.03	4.72
	3.00		109.01	1.18	1356.89	1358.07		
6.00		112.16					1520.06	9.37
	3.00		149.99	1.62	1357.97	1359.59		
9.00		187.82					1520.10	15.63
	3.00		318.70	3.44	1359.42	1362.86		
12.00		449.59					1520.18	29.14
	3.00		676.50	7.31	1362.55	1369.85		
15.00		903.41					1520.37	57.98
	3.00		1183.99	12.79	1369.23	1382.01		
18.00		1464.56					1520.68	131.08
	3.00		1800.86	19.45	1380.60	1400.05		
21.00		2137.15					1521.14	275.93
	3.00		2518.97	27.20	1397.07	1424.27		
24.00		2900.78					1521.75	521.76
	3.00		3218.96	34.76	1418.64	1453.40		
27.00		3537.13					1522.47	844.81
	3.00		3660.14	39.53	1444.28	1483.81		
30.00		3783.15					1523.22	1299.28
	3.00		3721.39	40.19	1469.78	1509.97		
33.00		3659.62					1523.86	1701.25
	3.00		3505.21	37.86	1491.59	1529.45		
36.00		3350.81					1524.33	2022.66
	3.00		3149.10	34.01	1507.60	1541.61		
39.00		2947.39					1524.62	2231.65
	3.00		2735.55	29.54	1517.51	1547.06		
42.00		2523.71					1524.63	2236.45
	3.00		2323.03	25.09	1522.90	1547.99		
45.00		2122.35					1524.64	2244.86
	3.00		1945.74	21.01	1523.75	1544.76		
48.00		1769.12					1524.60	2215.80
	3.00		1627.97	17.58	1520.83	1538.41		
51.00		1486.82					1524.52	2158.71
	3.00		1367.07	14.76	1515.10	1529.86		
54.00		1247.32					1524.34	2029.61
	3.00		1136.11	12.27	1507.94	1520.21		
57.00		1024.90					1524.10	1867.68
	3.00		922.41	9.96	1500.04	1510.00		
60.00		819.92					1523.86	1701.86
	3.00		720.17	7.78	1491.62	1499.40		
63.00		620.41					1523.60	1533.82
	3.00		530.31	5.73	1482.84	1488.56		
66.00		440.21					1523.33	1368.87
	3.00		371.05	4.01	1473.78	1477.79		

69.00		301.89					1523.07	1208.93
	3.00		256.86	2.77	1464.73	1467.51		
72.00		211.83					1522.82	1064.47
	3.00		184.19	1.99	1456.01	1458.00		
75.00		156.55					1522.58	933.85
	3.00		131.21	1.42	1447.91	1449.33		
78.00		105.86					1522.37	821.19

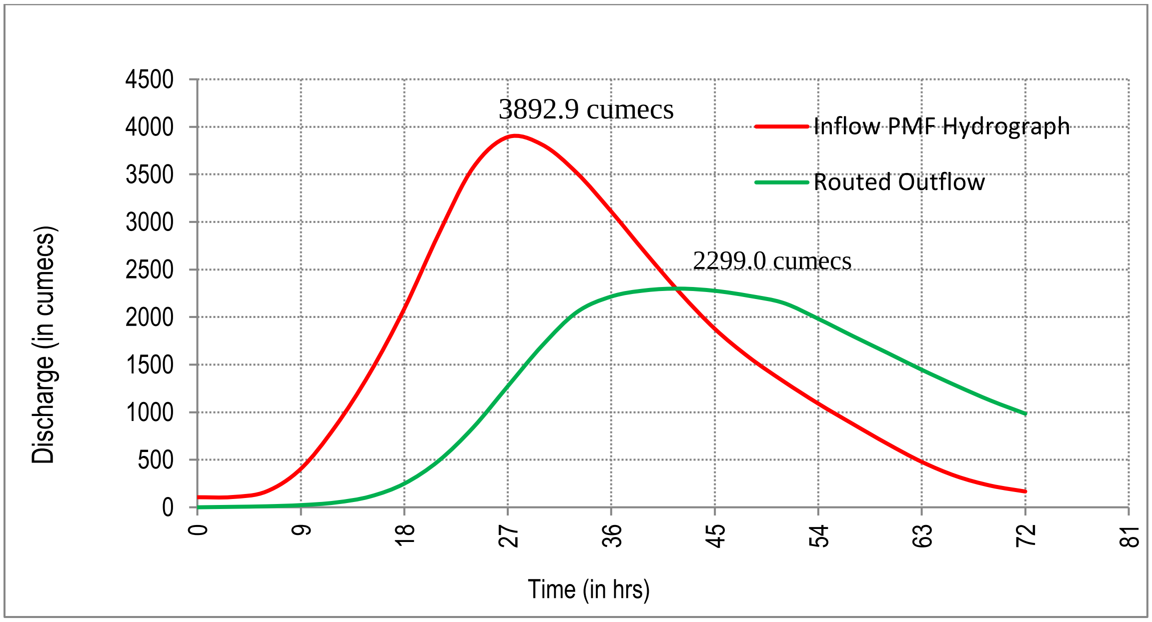

Figure 5:17 mid future RCP4.5 inflow PMF and routed outflow hydrograph of Baro I

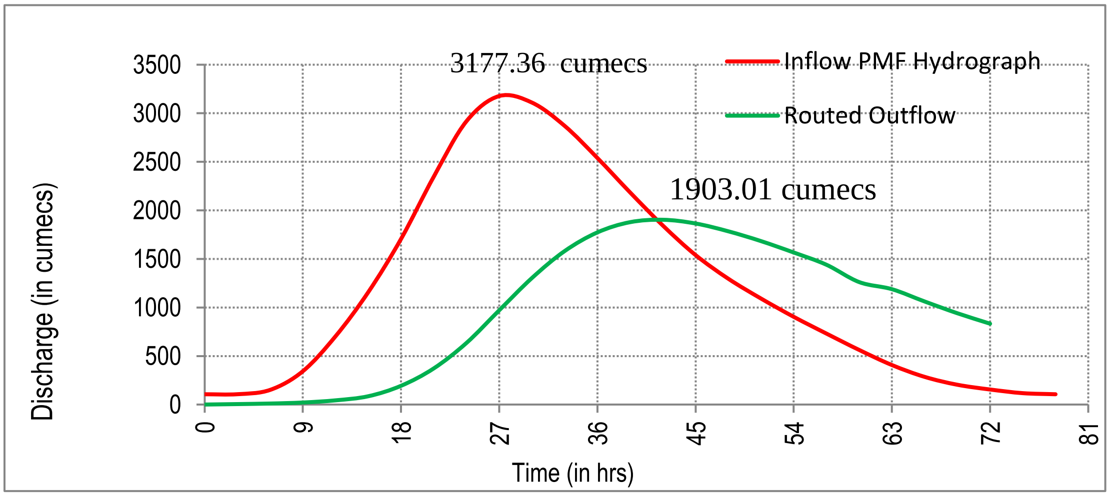

Figure 5:18 far future RCP4.5 inflow PMF and routed outflow hydrograph of Baro I

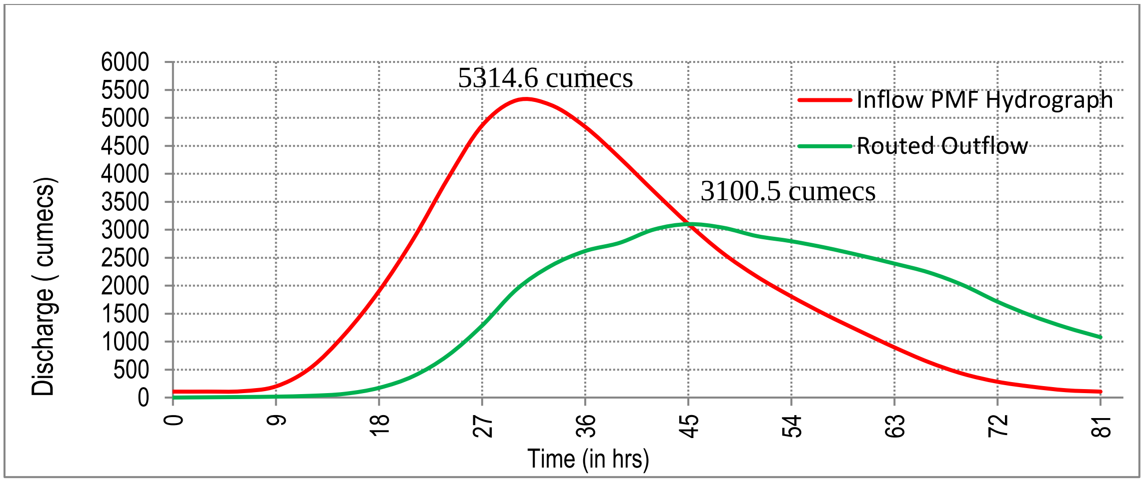

Figure 5:19 present future of RCP8.5 inflow PMF and routed outflow hydrograph of Baro I

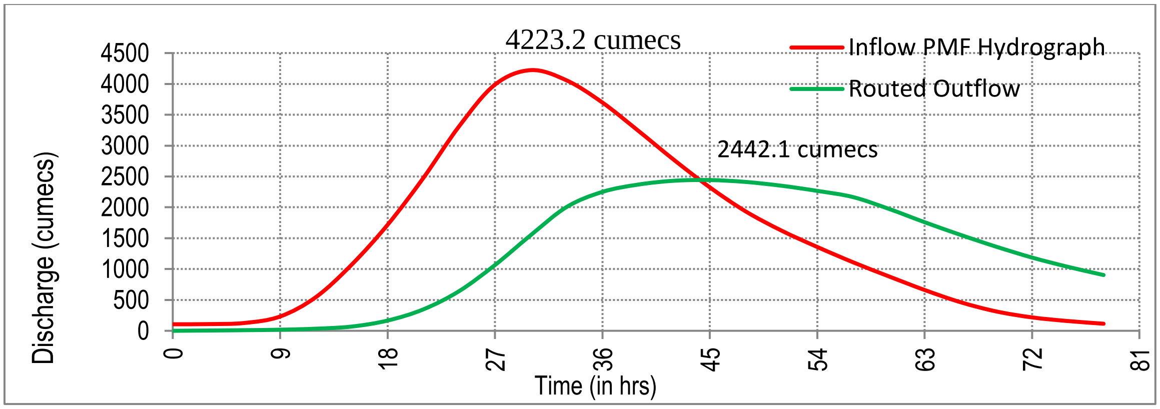

Figure 5:20 mid future of RCP8.5 inflow PMF and routed outflow hydrograph of Baro I

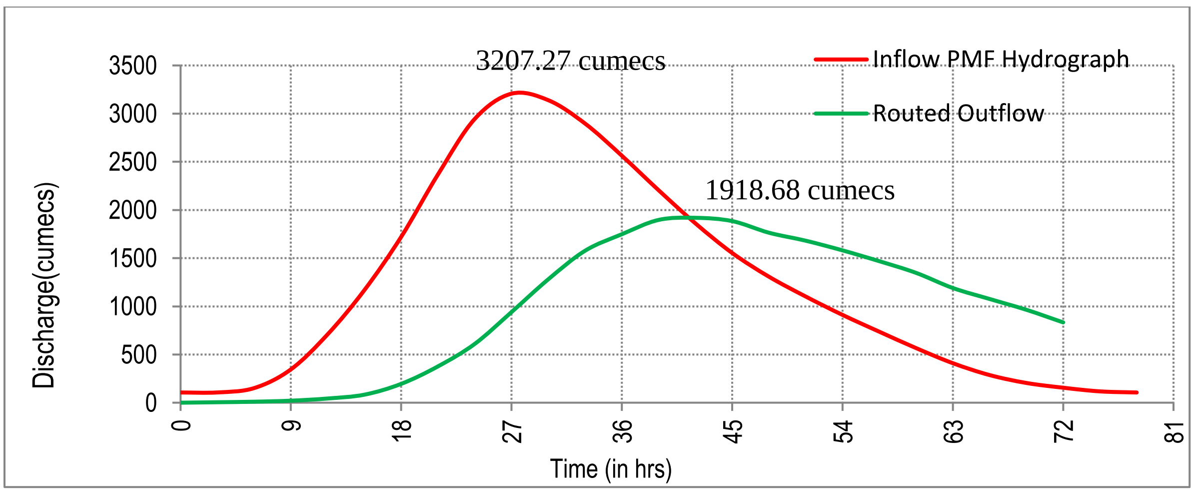

Figure 5:21 far future of RCP8.5 inflow PMF and routed outflow hydrograph of Baro I

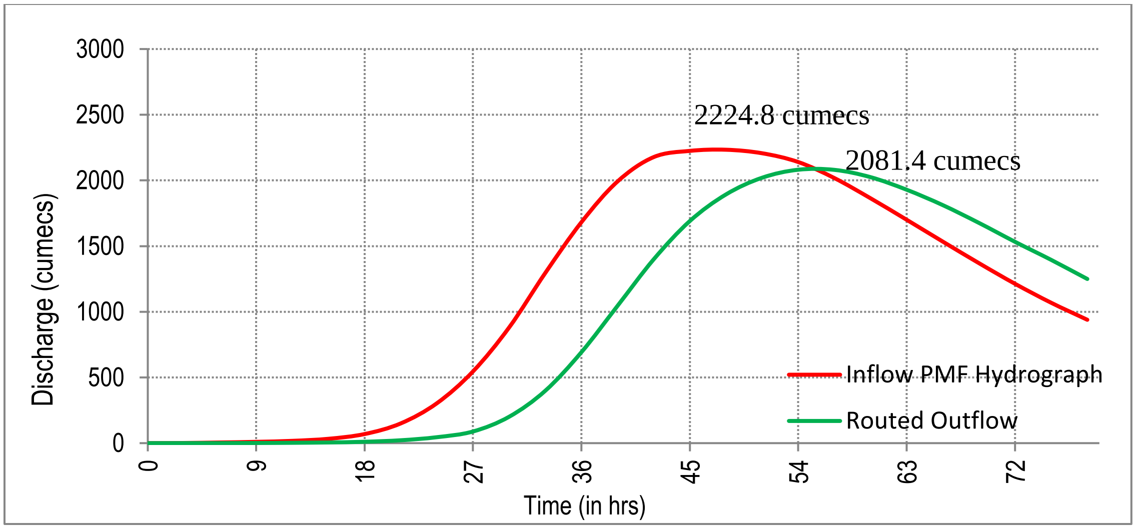

Figure 5:22 present future of RCP4.5 inflow PMF and routed outflow hydrograph of Baro II

Table 5:6 Present future of RCP4.5 inflow probable maximum flood and routed outflow hydrograph of Baro II

Time (hr.)	Δt (hr.)	Inflow I (cumes)	(I1+I2)/2	((I1+I2)/2)*Δt (MCM)	S-QΔt/2 (MCM)	S+QΔt/2 (MCM)	Elevation (m)	Outflow (cumec)
0		0.00				45.96	1320.00	0.00
	3		0.54	0.01	45.96	45.97		
3		1.09					1320.00	0.06
	3		3.02	0.03	45.97	46.00		
6		4.95					1320.00	0.40
	3		7.37	0.08	45.99	46.07		
9		9.79					1320.01	1.20
	3		13.60	0.15	46.06	46.21		
12		17.40					1320.01	2.61
	3		25.24	0.27	46.18	46.45		
15		33.09					1320.02	5.20
	3		51.10	0.55	46.40	46.95		
18		69.11					1320.05	10.44
	3		109.66	1.18	46.83	48.02		
21		150.21					1320.10	21.78
	3		226.93	2.45	47.78	50.23		
24		303.65					1320.22	45.21
	3		424.81	4.59	49.75	54.33		
27		545.98					1320.42	88.58
	3		713.35	7.70	53.38	61.08		
30		880.73					1320.75	200.93
	3		1088.09	11.75	58.91	70.66		
33		1295.46					1321.20	398.73

	3		1488.62	16.08	66.36	82.43		
36		1681.78					1321.75	692.09
	3		1837.00	19.84	74.96	94.80		
39		1992.22					1322.31	1045.34
	3		2084.87	22.52	83.51	106.03		
42		2177.51					1322.81	1399.25
	3		2201.15	23.77	90.91	114.69		
45		2224.78					1323.18	1690.66
	3		2229.15	24.07	96.43	120.50		
48		2233.52					1323.44	1893.20
	3		2220.12	23.98	100.06	124.03		
51		2206.72					1323.59	2020.40
	3		2173.35	23.47	102.21	125.68		
54		2139.99					1323.66	2081.35
	3		2078.85	22.45	103.21	125.66		
57		2017.71					1323.66	2080.36
	3		1940.88	20.96	103.19	124.15		
60		1864.04					1323.59	2024.78
	3		1782.27	19.25	102.28	121.53		
63		1700.50					1323.48	1929.07
	3		1617.36	17.47	100.70	118.17		
66		1534.22					1323.33	1811.83
	3		1452.17	15.68	98.60	114.28		
69		1370.12					1323.17	1676.56
	3		1291.45	13.95	96.17	110.12		
72		1212.79					1322.99	1532.48
	3		1140.67	12.32	93.57	105.89		
75		1068.55					1322.80	1394.86
	3		1003.75	10.84	90.83	101.67		
78		938.94					1322.61	1249.50

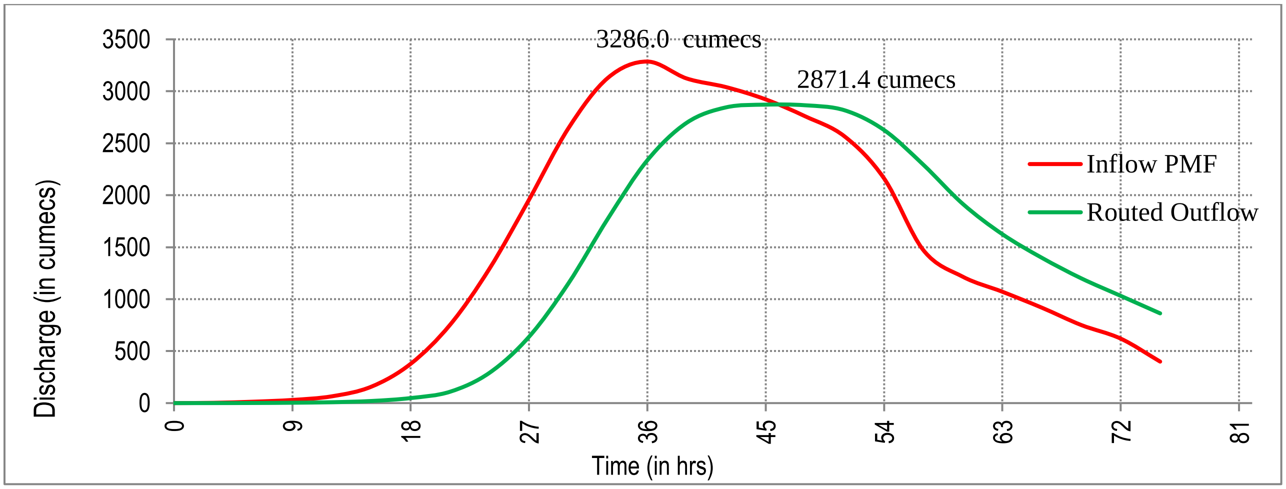

Figure 5:23 mid future of RCP4.5 inflow PMF and routed outflow hydrograph of Baro II

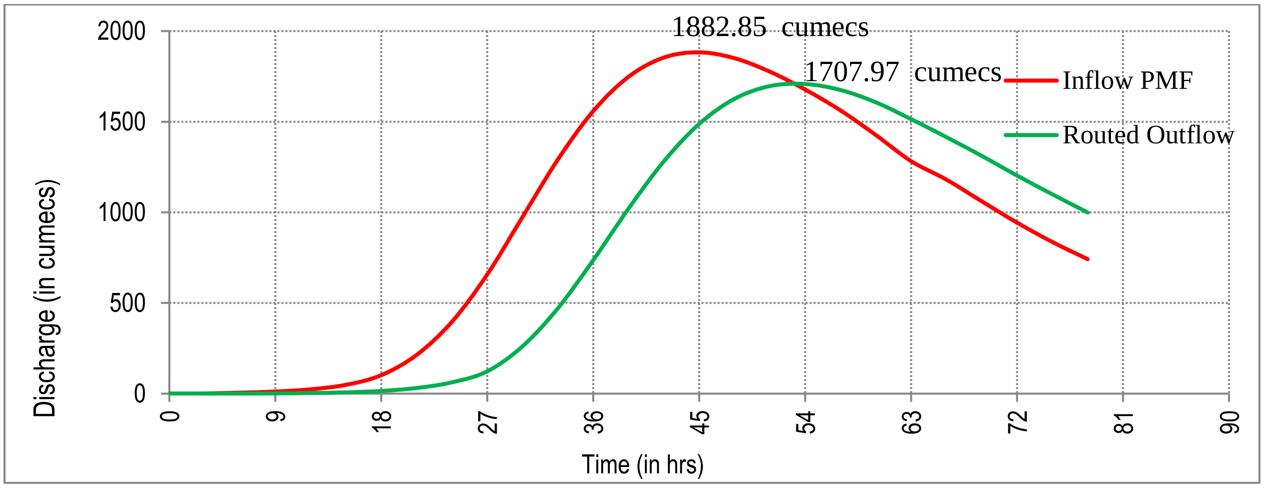

Figure 5:24 far future of RCP4.5 inflow PMF and routed outflow hydrograph of Baro II

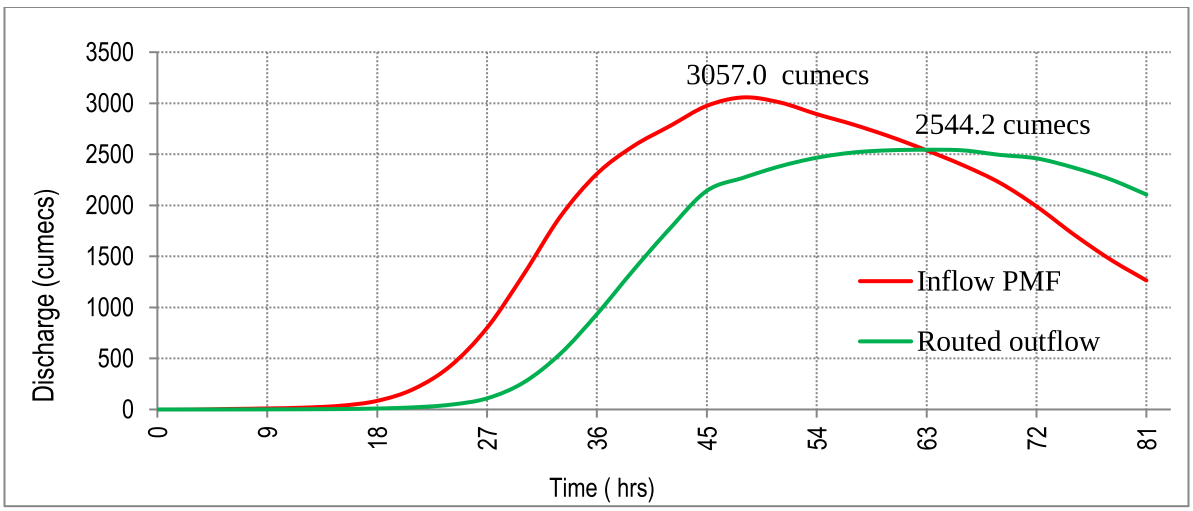

Figure 5:25 present future of RCP8.5 inflow PMF and routed outflow hydrograph of Baro II

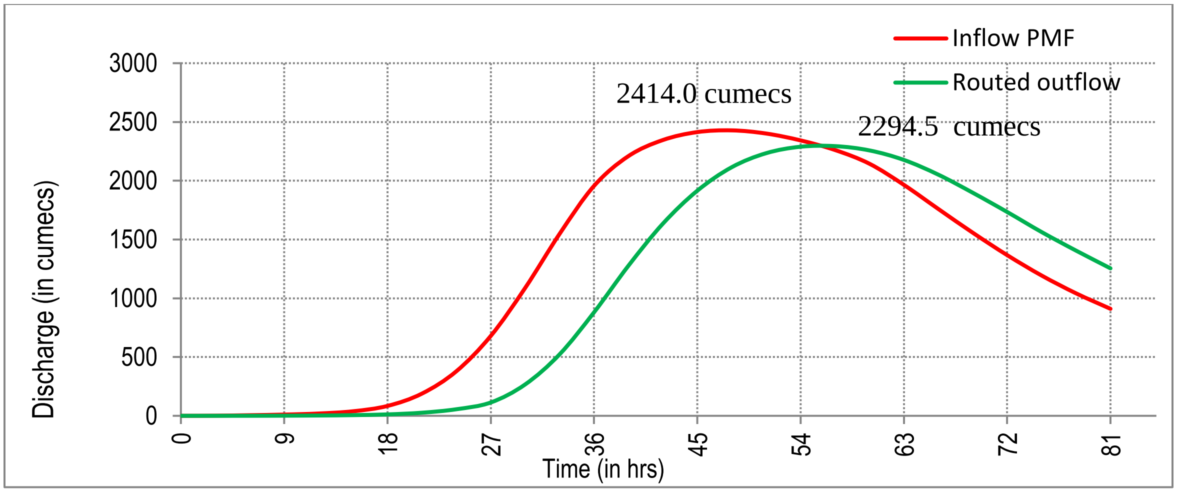

Figure 5:26 mid future of RCP8.5 inflow PMF and routed outflow hydrograph of Baro II

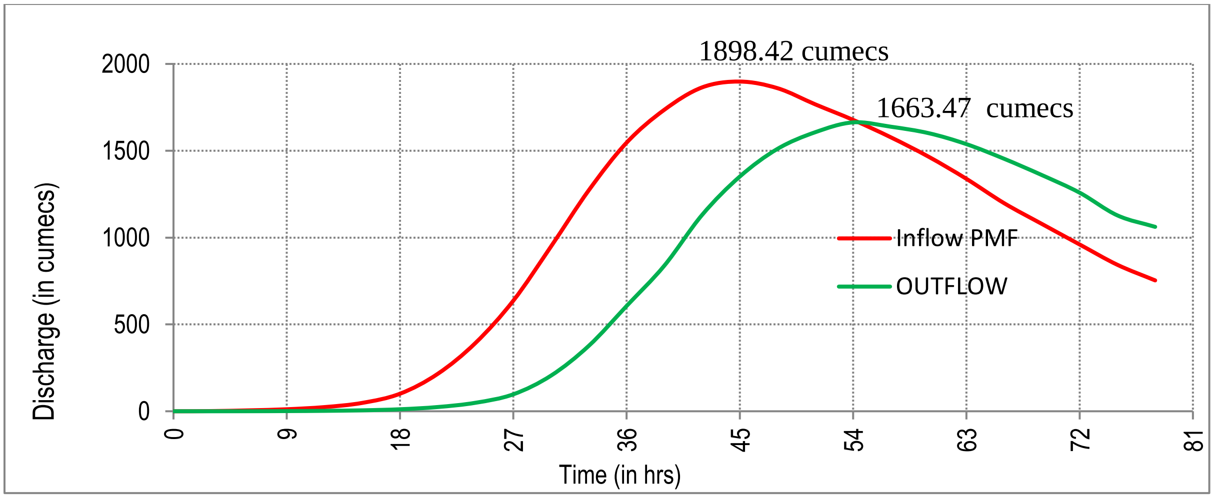

Figure 5:27 far future of RCP8.5 inflow PMF and routed outflow hydrograph of Baro II

II. Frequency Analysis Result

The two scenarios (RCP4.5 and RCP8.5) of RCM bias-corrected output simulated in the hydrological model Arc SWAT. The simulation result of the Baro I of the model for the RCP4.5 and RCP8.5 scenario, the frequency analysis of annual maximum daily (see annex E) output of model present future (2014-2033), mid future (2034-2070) and far future (2071-2100) best fit distribution using the L-moment distribution method. Hence, the best fit type of the frequency distribution for the present future and mid future of model output are Gumbel's Extreme Value, and far future of the model output was Log Pearson type III distribution method are shown in figure 5.28 to 5.33. (See annex F) detail calculation and result of the others.

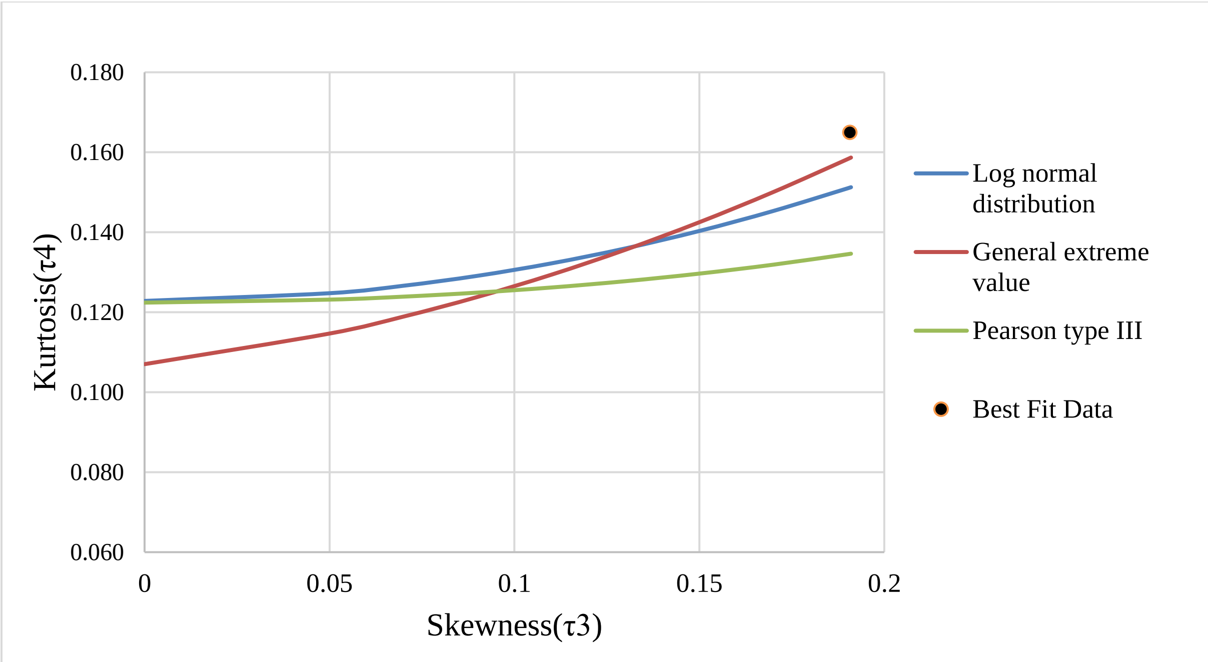

Figure 5:28 L-Moment ratio of best-fit distribution for present future RCP4.5

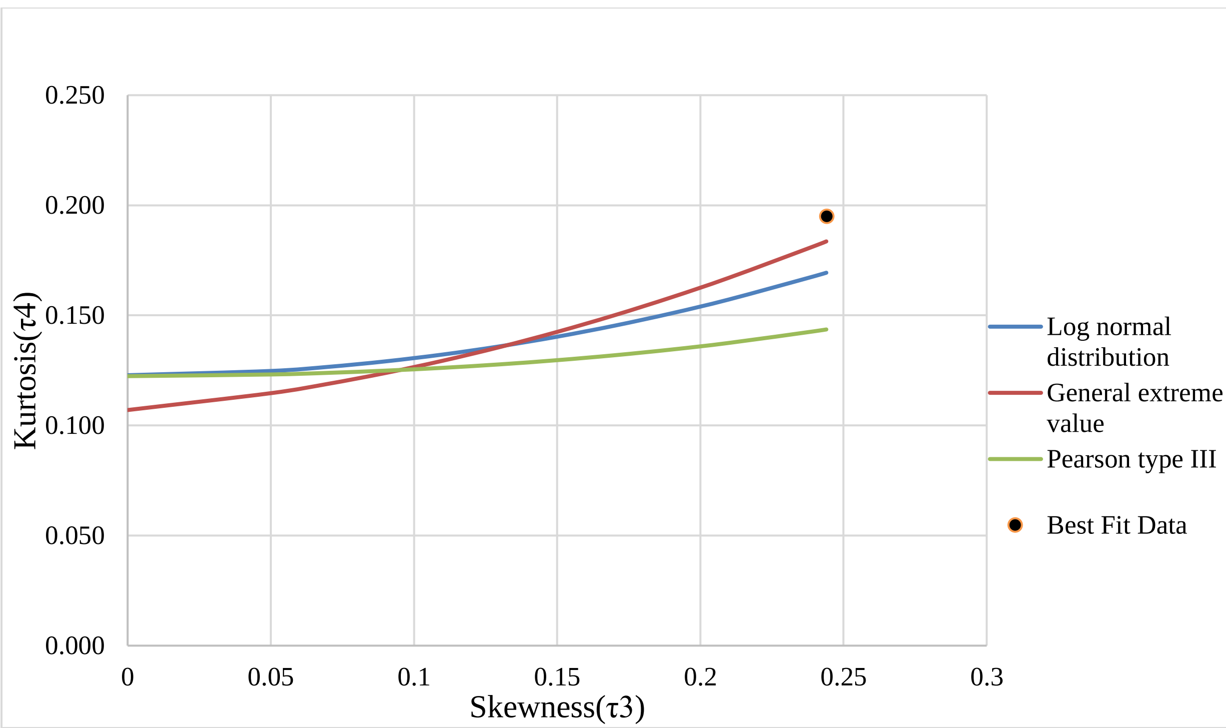

Figure 5:29 L-Moment ratio of best-fit distribution for present future RCP8.5

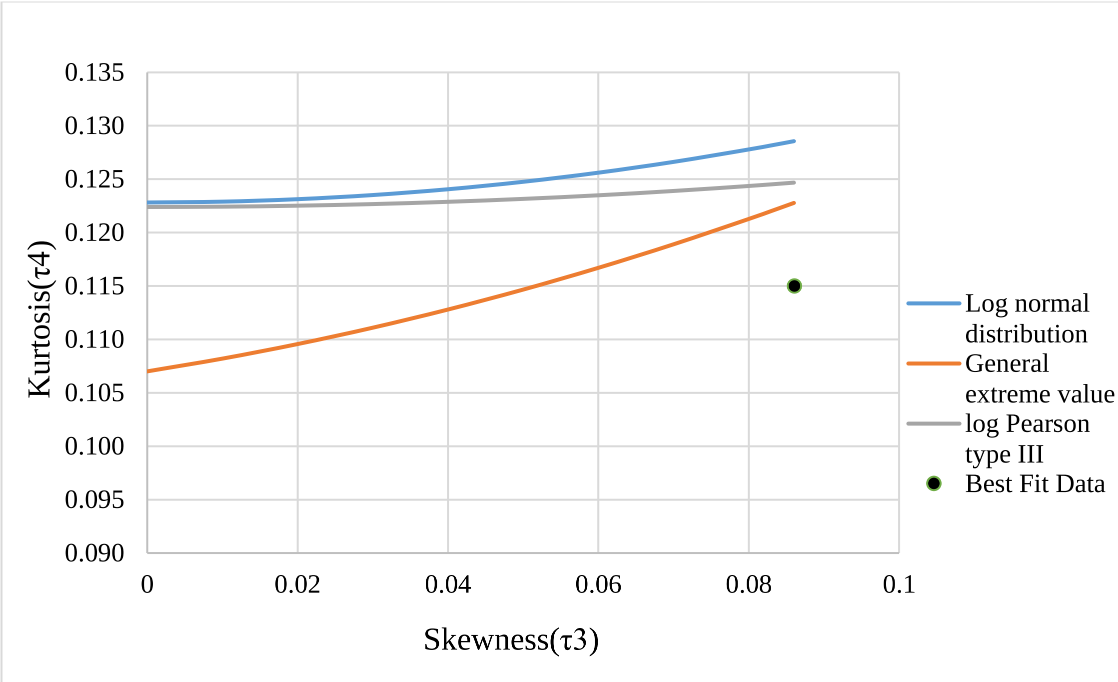

Figure 5:30 L-Moment ratio of best-fit distribution for mid future RCP4.5

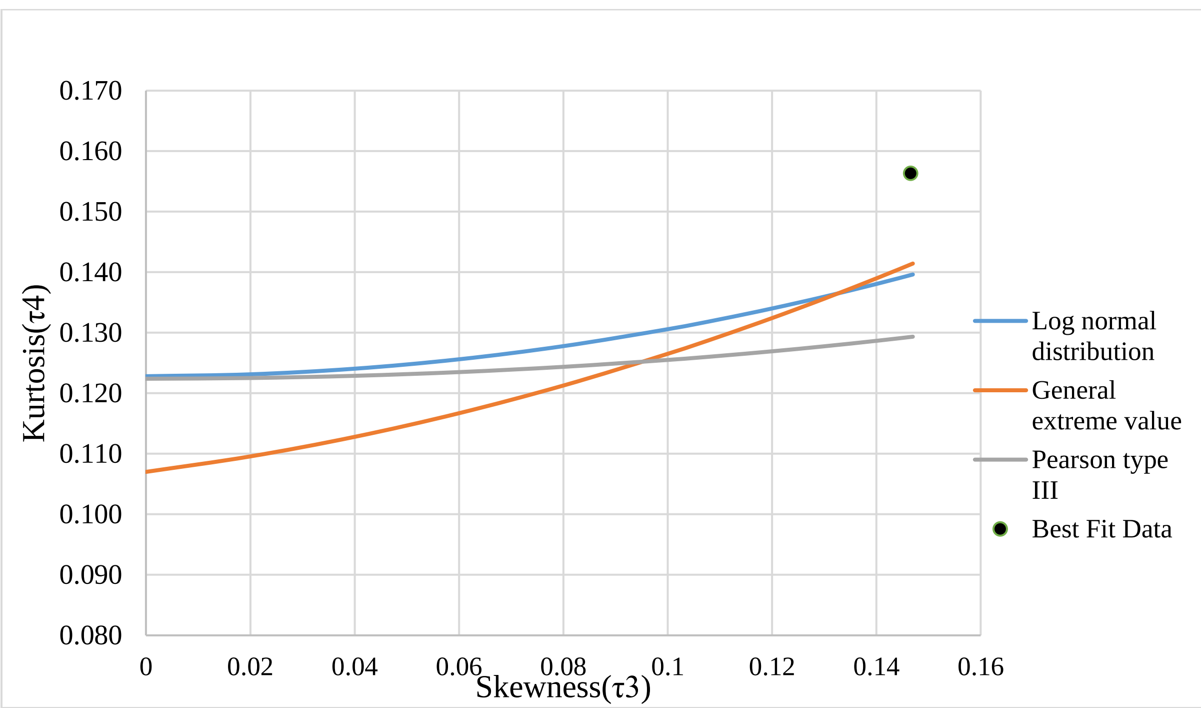

Figure 5:31 L-Moment ratio of best-fit distribution for mid future RCP8.5

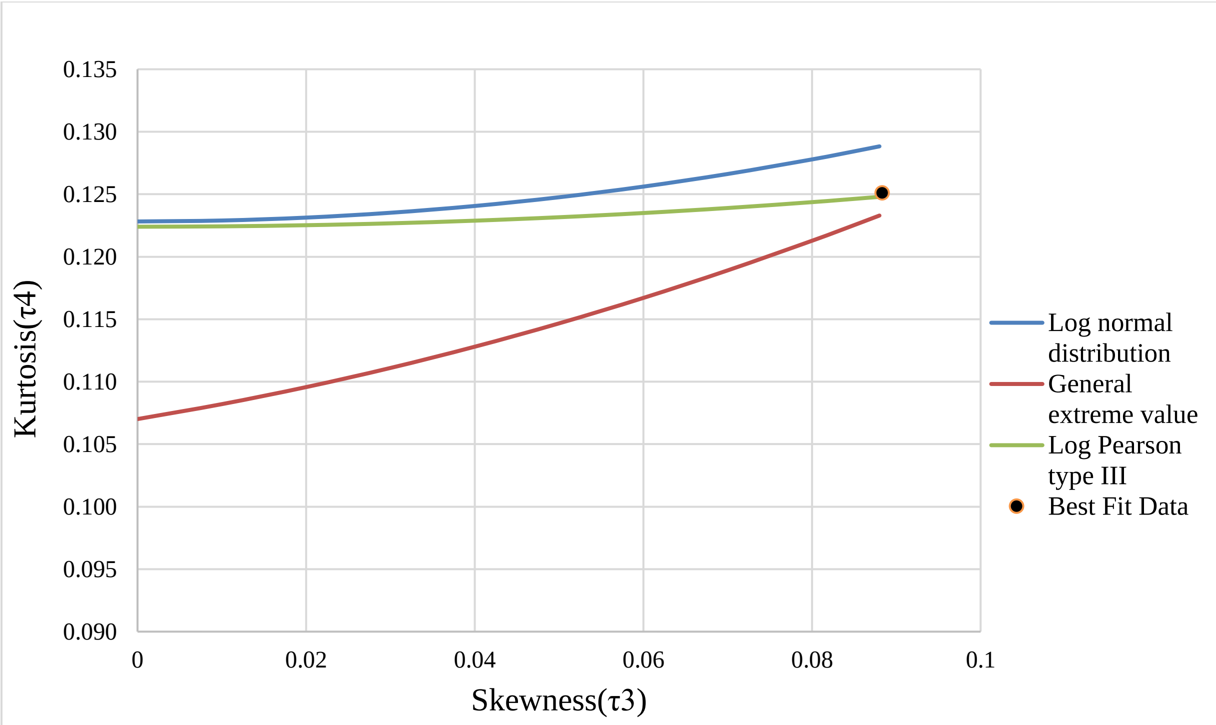

Figure 5:32 L-Moment ratio of best-fit distribution for far future RCP4.5

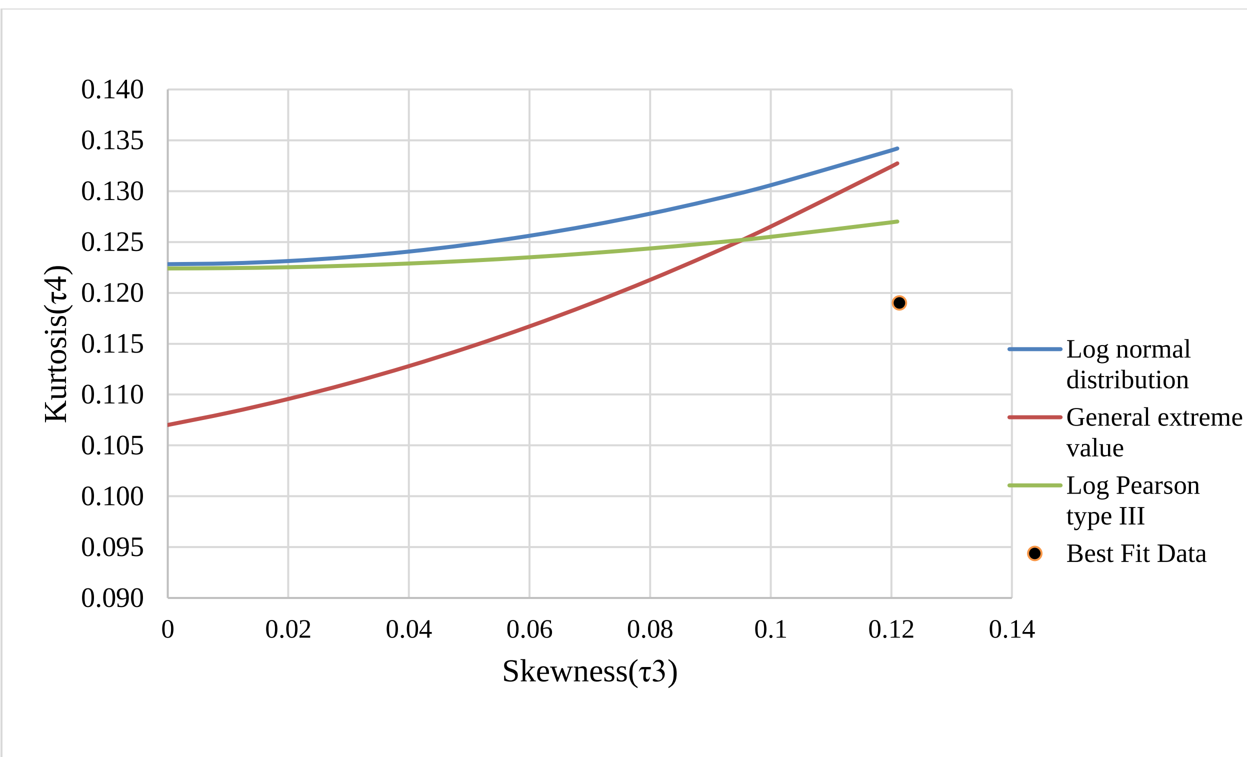

Figure 5:33 L-Moment ratio of best-fit distribution for far future RCP8.5

Based on the selected frequency method the maximum inflow to reservoir was calculated, the maximum inflow for the present and mid future for RCP4.5 scenario (Gumbel's Extreme Value method) 6483.6 m^3/s and 5364.5 m^3/s respectively and for far future (Log Pearson's Type III method) 5134.8 m^3/s. For the case of RCP8.5 scenario maximum inflow for the present and mid future (Gumbel's Extreme Value method) 6110.5m^3/s and 6304.7m^3/s respectively and for far future (Log Pearson's Type III method) 4918.2m^3/s.

Table 5:7 Present future of RCP4.5 scenario frequency analysis

Return Period T(yrs.)	**Probability (P), 1/T**	**% of probability occurrence**	Reduced Variate (Yt)	Reduced Mean (Yn)	Reduced Standard Devation (Sn)	Frequency Factor (Kt) =(Yt-Yn)/Sn	Ppt mean (Y)	Standard devation (σ)	Ppt @ T yrs Pt = Y + Kt*
10	0.1	10	2.250	0.524	1.063	1.625	1736.270	790.369	3020.410
25	0.04	4	3.199	0.524	1.063	2.517	1736.270	790.369	3725.530
50	0.02	2	3.902	0.524	1.063	3.179	1736.270	790.369	4248.628
75	0.013	1.333	4.311	0.524	1.063	3.563	1736.270	790.369	4552.673
100	0.01	1	4.600	0.524	1.063	3.836	1736.270	790.369	4767.864
200	0.005	0.5	5.296	0.524	1.063	4.490	1736.270	790.369	5285.206
500	0.002	0.2	6.214	0.524	1.063	5.354	1736.270	790.369	5967.740
1000	0.001	0.1	6.907	0.524	1.063	6.006	1736.270	790.369	6483.582

Table 5:8 mid future of RCP4.5 scenario frequency analysis

Return Period T(yrs.)	**Probability (P), 1/T**	**% of probability occurrence**	Reduced Variate (Yt)	Reduced Mean (Yn)	Reduced Standard Devation (Sn)	Frequency Factor (Kt) =(Yt-Yn)/Sn	Ppt mean (Y)	Standard devation (σ)	Ppt @ T yrs Pt = Y + Kt*
10	0.1	10	2.250	0.542	1.134	1.507	1586.170	673.047	2600.321
25	0.04	4	3.199	0.542	1.134	2.343	1586.170	673.047	3163.122
50	0.02	2	3.902	0.542	1.134	2.963	1586.170	673.047	3580.640
75	0.013	1.333	4.311	0.542	1.134	3.324	1586.170	673.047	3823.318
100	0.01	1	4.600	0.542	1.134	3.579	1586.170	673.047	3995.076
200	0.005	0.5	5.296	0.542	1.134	4.193	1586.170	673.047	4407.999
500	0.002	0.2	6.214	0.542	1.134	5.002	1586.170	673.047	4952.773
1000	0.001	0.1	6.907	0.542	1.134	5.614	1586.170	673.047	5364.500

Table 5:9 far future of RCP4.5 scenario frequency analysis

	Z mean	3.242	Standard Deviation	0.195
Return Period T(yrs.)				
	from table			
	Kz	$\delta_Z K_z$	Z=Zavrg+ $\delta_Z K_z$	X=antilogZ
10	1.216	0.2375	3.479	3014.928
25	1.567	0.306	3.548	3530.459
50	1.777	0.347	3.589	3880.131
100	1.955	0.382	3.624	4203.507
200	2.108	0.412	3.653	4502.921
1000	2.400	0.469	3.711	5134.819

Table 5:10 Present future of RCP8.5 scenario frequency analysis

Return Period T(yrs.)	**Probability (P), 1/T**	**% of probability occurrence**	Reduced Variate (Yt)	Reduced Mean (Yn)	Reduced Standard Devation (Sn)	Frequency Factor (Kt) =(Yt-Yn)/Sn	Ppt mean (Y)	Standard devation (σ)	Ppt @ T yrs Pt = Y + Kt*
10	0.1	10	2.250	0.524	1.063	1.625	1950.250	692.630	3075.589
25	0.04	4	3.199	0.524	1.063	2.517	1950.250	692.630	3693.512
50	0.02	2	3.902	0.524	1.063	3.179	1950.250	692.630	4151.923
75	0.013	1.333	4.311	0.524	1.063	3.563	1950.250	692.630	4418.368
100	0.01	1	4.600	0.524	1.063	3.836	1950.250	692.630	4606.948
200	0.005	0.5	5.296	0.524	1.063	4.490	1950.250	692.630	5060.314
500	0.002	0.2	6.214	0.524	1.063	5.354	1950.250	692.630	5658.443
1000	0.001	0.1	6.907	0.524	1.063	6.006	1950.250	692.630	6110.496

Table 5:11 mid future of RCP8.5 scenario frequency analysis

Return Period T(yrs.)	**Probability (P), 1/T**	**% of probability occurrence**	Reduced Variate (Yt)	Reduced Mean (Yn)	Reduced Standard Devation (Sn)	Frequency Factor (Kt) =(Yt-Yn)/Sn	Ppt mean (Y)	Standard devation (σ)	Ppt @ T yrs Pt = Y + Kt*
10	0.1	10	2.250	0.542	1.134	1.507	1797.959	802.799	3007.622
25	0.04	4	3.199	0.542	1.134	2.343	1797.959	802.799	3678.922
50	0.02	2	3.902	0.542	1.134	2.963	1797.959	802.799	4176.931
75	0.013	1.333	4.311	0.542	1.134	3.324	1797.959	802.799	4466.393
100	0.01	1	4.600	0.542	1.134	3.579	1797.959	802.799	4671.263
200	0.005	0.5	5.296	0.542	1.134	4.193	1797.959	802.799	5163.791
500	0.002	0.2	6.214	0.542	1.134	5.002	1797.959	802.799	5813.588
1000	0.001	0.1	6.907	0.542	1.134	5.614	1797.959	802.799	6304.689

Table 5:12 far future of RCP8.5 scenario frequency analysis

	Z mean	3.159	Standard Deviation	0.199
Return Period T(yrs.)				
	from table			
	Kz	$\delta_Z K_z$	Z=Zavrg+ $\delta_Z K_z$	X=antilogZ
10	1.25	0.25	3.41	2551.09
25	1.64	0.33	3.49	3062.45
50	1.89	0.38	3.54	3430.13
100	2.10	0.42	3.58	3784.19
200	2.29	0.46	3.62	4129.06
1000	2.68	0.53	3.69	4918.19

The spillways in the case of Baro I is ungated, free overflow, the crest elevation at FSL, and the flood in the reservoir is higher. From the design document of the dam, the probable maximum flood would inflow be 2800m^3/s and outflow 1750m^3/s (International Monetary Fund, 2006). In the case of Baro II, it is located at 12km from the Baro I and its spillway is also ungated

(International Monetary Fund, 2006) and the Baro II reservoir is controlled by outflow from the Baro I.

The output of simulated frequency analysis result from the model of two-scenario (RCP4.5 and RCP8.5) for the present future, mid future, and far future as compare with design data in the Baro I more than probable maximum inflow and outflow and the flood level 1524.5 m.a.s.l. Based on the results of routing also the peak inflow and outflow are higher than the probable maximum flood of the designed spillway for Baro I and Baro II in RCP4.5 and RCP8.5 for the present future, mid future, and far future; the dam will overtop under regional climate mode. Moreover, Baro I outflow controls Baro II inflow. Due to the above, the cases the Baro II will also overtop.

Generally, from the above result dam at Baro I and II would be overtopped under the projected outflow due to insufficiency of spillway capacity.

6. Conclusion and Recommendation

6.1. Conclusion

In this study, dam overtopping is assessed in the case of Baro I and II under climate change by using meteorological data, hydrological data, land use land cover change, RCM data, satellite data, and hydrologic modeling. The study expanded the analysis by incorporating the downscaled climate change data of the RCM based on probable maximum precipitation and hydrological modelling and frequency analysis modelled result of the RCM output. Depending on the data used, the analysis method and the result obtained the following conclusion are stated.

The effect of land use land cover change assume constant in the next scenario it does not affect the surface runoff in the watershed.

The downscaled RCP scenario and historical data of the climate change data bias correction is done using the distribution-mapping method based on observed meteorological data. The biased corrected data was evaluated by model performance evaluation criteria of RCM, all result above acceptable range R^2 and NSE more than 0.8 for criteria.

The magnitude of the simulated average temperature in the next future (2015-2033, 2034-2070, 2071-2100). For RCP4.5 scenario increased by 0.93 °C, 2.0 °C, and 2.5 °C respectively. For RCP8.5 scenario increased by 1.2°C, 2.5°C and 5.01°C respectively.

The result is shown of average monthly precipitation of the next future years increase in some months by 7.7% and decrease in others months by 29.9% in case of RCP4.5 scenario and 8.86 % increase in some months and 32.82% decrease in other months in case of RCP8.5 scenario as compare with the current recorded meteorological data.

The result of hydrological model calibration and validation indicated that the Arc SWAT model is capable to simulate the RCM output of climate change data of the study area to evaluate the spillway in the next future period. The routed and simulated frequency analysis result from the model were shown in case Baro I and II, the spillway capacity of each dam will not pass outflow. Hence, the dam at Baro I and II would be overtopped.

6.2. Recommendation

Based on the analysis and the result obtained in this study the following is recommended:-

- It is recommended that the study extended by considering changes in seepage from reservoirs, seepage through the dam, reanalysis of dam performance, sedimentation, and other water resource developments in the basin in addition to the climate variables.
- This study considers only what would be if climate change in the next future on the life of the dam and it gives clues and awareness on climate change with the design of the dam. Hence, this study is recommended to be included in other basins study for sustainable water resource development for any project to better emphasis on climate change.
- Continuing studies, however, should also consider the wide range of uncertainties associated with models and try to reduce these uncertainties through use of different RCM as well as institutions for CORDEX data to generate a more "reliable" ensemble, downscaling techniques, and all RCP scenarios.
- In order to decrease the effect on climate change on any project constructed before, it important if we conserve the watershed conservation or mitigation method. Hence, it is important if the continuing study consider the mitigation method of watershed to reduce the effect on the reservoir and dam structure because the hydrological system is uncertain.

7. Reference

'13. Applied Hydrology, Chow.pdf' (no date).

Abbasa, N., Wasimia, S. A. and Al-Ansari, N. (2016) 'Assessment of Climate Change Impacts on Water Resources of Al-Adhaim, Iraq Using SWAT Model', *Engineering*, 08(10), pp. 716–732. doi: 10.4236/eng.2016.810065.

Abbaspour, K. C., Vaghefi, S. A. and Srinivasan, R. (2017) 'A guideline for successful calibration and uncertainty analysis for soil and water assessment: A review of papers from the 2016 international SWAT conference', *Water (Switzerland)*, 10(1). doi: 10.3390/w10010006.

Abdellatif Mohamed, M. M. and El-Ghorab, E. A. S. (2016) 'Investigating scale effects on breach evolution of overtopped sand embankments', *Water Science*. National Water Research Center, 30(2), pp. 84–95. doi: 10.1016/j.wsj.2016.10.003.

Ahmed, K. F. *et al.* (2013) 'Statistical downscaling and bias correction of climate model outputs for climate change impact assessment in the U.S. northeast', *Global and Planetary Change*. Elsevier B.V., 100, pp. 320–332. doi: 10.1016/j.gloplacha.2012.11.003.

Allen, R. G. *et al.* (1998) 'FAO Irrigation and Drainage Paper No. 56. Crop Evapotranspiration (guidelines for computing crop water requirements)', *Irrigation and Drainage*, 300(56), p. 300. doi: 10.1016/j.eja.2010.12.001.

Almeida, R. A., Pereira, S. B. and Pinto, D. B. F. (2018) 'Calibration and Validation of the Swat Hydrological Model for the Mucuri River Basin', *Engenharia Agrícola*, 38(1), pp. 55–63. doi: 10.1590/1809-4430-eng.agric.v38n1p55-63/2018.

Amaral, S. *et al.* (2014) 'Failure by overtopping of earth dams. Quantification of the discharge hydrograph', *Proceedings of the 3rd IAHR Europe Congress: 14-15 April 2014, Portugal*, (1), pp. 182–193.

Arnold, J. G. *et al.* (2012) 'DigitalCommons@University of Nebraska-Lincoln SWAT: Model use, calibration, and validation', *Biological Systems Engineering: Papers and Publications*. doi: 10.13031/2013.42263.

Arritt, R. W. *et al.* (2002) 'Hydrological responses to dynamically and statistically downscaled climate model output', *Geophysical Research Letters*, 27(8), pp. 1199–1202. doi: 10.1029/1999gl006078.

Barker *et al.* (2012) 'SAN JACINTO RIVER BASIN , TX', (November).

Basin, T. R. (2016) 'Assessment of Surface Water Potential and Demands in Baro-Akobo', (December).

Beyene, T., Lettenmaier, D. P. and Kabat, P. (2010) 'Hydrologic impacts of climate change on the Nile River Basin: Implications of the 2007 IPCC scenarios', *Climatic Change*, 100(3), pp. 433–461. doi: 10.1007/s10584-009-9693-0.

Bremer, M. (2012) 'Math 261A -Spring 2012 Multiple Linear Regression', (1). Available at: http://mezeylab.cb.bscb.cornell.edu/labmembers/documents/supplement 5 - multiple regression.pdf.

Chanson, H. (2013) ‘Embankment dam spillways and energy dissipators’, *Labyrinth and Piano Key Weirs II*, pp. 23–37. doi: 10.1201/b15985.

Chen, J., Brissette, F. P. and Leconte, R. (2012) ‘Coupling statistical and dynamical methods for spatial downscaling of precipitation’, *Climatic Change*, 114(3–4), pp. 509–526. doi: 10.1007/s10584-012-0452-2.

Costa, J. E. (1985) ‘Open-File Report 85-560 Denver, Colorado 1985’.

Cunderlik, J. M. (2003) ‘Hydrologic model selection for the CFCAS project : Assessment of Water Resources Risk and Vulnerability to Changing Climatic Conditions’, *October*, (October), p. 40. Available at: http://www.eng.uwo.ca/research/iclr/fids/publications/cfcas-climate/reports/Report I.pdf.

Emerta, B. and Aragie, A. (2013) ‘C L I M AT E C H A N G E , G R O W T H , AND POVERTY IN ETHIOPIA’, (June).

Ezéchiel, O. *et al.* (2016) ‘Comparative study of seven bias correction methods applied to three Regional Climate Models in Mekrou catchment (Benin , West Africa)’, *International Journal of Current Engineering and Technology*, 6(5), pp. 1831–1840.

Fang, G. H. *et al.* (2015) ‘Comparing bias correction methods in downscaling meteorological variables for a hydrologic impact study in an arid area in China’, *Hydrology and Earth System Sciences*, 19(6), pp. 2547–2559. doi: 10.5194/hess-19-2547-2015.

Feenstra, J. *et al.* (1998) ‘Handbook on Methods for Climate Change Impact Assessment and Adaptation Strategies’, *Institute for Environmental Studies IVM Vrije Universiteit Amsterdam*, p. 464. doi: 10.1111/gcb.12365.

G. K, E. (2017) ‘Hydrological Analysis and Peak Discharge Determination’, *IOSR Journal of Mechanical and Civil Engineering*, 14(03), pp. 33–48. doi: 10.9790/1684-1403053348.

Garg, V. and Jothiprakash, V. (2006) ‘Estimation of useful life of a reservoir using sediment trap efficiency’, *Journal of Spatial Hydrology*, 6(2), pp. 1–14. Available at: http://www.spatialhydrology.com/journal/paper/2006/small_hydel/paper_josh.rar.

Giorgi, F., Jones, C. and Asrar, G. R. (2009) ‘Addressing climate information needs at the regional level: the CORDEX framework’, *World Meteorological Organization Bulletin*, 58(3), pp. 175–183. doi: 10.1109/ICASSP.2009.4960141.

van Griensven, A. *et al.* (2006) ‘A global sensitivity analysis tool for the parameters of multi-variable catchment models’, *Journal of Hydrology*, 324(1–4), pp. 10–23. doi: 10.1016/j.jhydrol.2005.09.008.

Gutowski, J. W. *et al.* (2016) ‘WCRP COordinated Regional Downscaling EXperiment (CORDEX): A diagnostic MIP for CMIP6’, *Geoscientific Model Development*, 9(11), pp. 4087–4095. doi: 10.5194/gmd-9-4087-2016.

ICOLD (2014) ‘Dam Surveillance Guide - Bulletin 158’, p. 109. Available at: http://www.icold-cigb.org/.

Intergovernmental Panel on Climate Change (2014) *Climate Change 2014 Mitigation of Climate Change*. doi: 10.1017/CBO9781107415416.

Intergovernmental Panel on Climate Change (IPCC) (1999) ‘General Guidelines on the Use of Scenario Data for climate impact and adaptation assessment’, *Finnish Environment Institute*, 312(June), p. 66. doi: 10.1144/SP312.4.

International Monetary Fund (2006) ‘The Federal Democratic Republic of Ethiopia:BARO 1 & 2 MULTIPURPOSE HYDROPOWER PROJECTS FINAL DRAFT’, *BARO 1 & 2 MULTIPURPOSE HYDROPOWER PROJECTS FINAL DRAFT*, 07(245), p. 1. doi: 10.5089/9781451812794.002.

IPCC-Part A (2014) *Climate Change 2014: Impacts, Adaptations, and Vulnerability. Part A: Global and Sectoral Aspects.Intergovernmental Panel on Climate Change. Cambridge University Press, UK.*

Ipcc (2007) *Climate Change 2007: impacts, adaptation and vulnerability: contribution of Working Group II to the fourth assessment report of the Intergovernmental Panel, Genebra, Suíça*. doi: 10.1256/004316502320517344.

IPCC (1999) *Technologies, Policies and Measures for Mitigating Climate Change, IPCC Technical Paper*. Available at: papers3://publication/uuid/9EE02C12-8F71-4F1C-A5F7-EE9127FD4E59.

IPCC (2014) *Climate change 2014. Synthesis report. Versión inglés, Climate Change 2014: Synthesis Report. Contribution of Working Groups I, II and III to the Fifth Assessment Report of the Intergovernmental Panel on Climate Change*. doi: 10.1017/CBO9781107415324.

Khalid, K. *et al.* (2016) ‘Sensitivity Analysis in Watershed Model Using SUFI-2 Algorithm’, *Procedia Engineering*. The Author(s), 162, pp. 441–447. doi: 10.1016/j.proeng.2016.11.086.

Kim, J. *et al.* (2014) ‘Evaluation of the CORDEX-Africa multi-RCM hindcast: Systematic model errors’, *Climate Dynamics*, 42(5–6), pp. 1189–1202. doi: 10.1007/s00382-013-1751-7.

Knutti, R. (2010) ‘The end of model democracy?’, *Climatic Change*, 102(3–4), pp. 395–404. doi: 10.1007/s10584-010-9800-2.

Kovats, R. S. *et al.* (2014) *Impacts, Adaptation, and Vulnerability. Part B: Regional Aspects. Contribution of Working Group II to the Fifth Assessment Report of the Intergovernmental Panel on Climate Change, Climate Change 2014*. doi: 10.1007/s13398-014-0173-7.2.

Kunkel, K. E. *et al.* (2013) ‘Probable maximum precipitation and climate change’, *Geophysical Research Letters*, 40(7), pp. 1402–1408. doi: 10.1002/grl.50334.

Lafon, T. *et al.* (2013) ‘Bias correction of daily precipitation simulated by a regional climate model: A comparison of methods’, *International Journal of Climatology*, 33(6), pp. 1367–1381. doi: 10.1002/joc.3518.

Lee, B. S. and You, G. J. Y. (2013) ‘An assessment of long-term overtopping risk and optimal termination time of dam under climate change’, *Journal of Environmental Management*. Elsevier Ltd, 121, pp. 57–71. doi: 10.1016/j.jenvman.2013.02.025.

Legesse Gebre, S. (2015) ‘Hydrological Response to Climate Change of the Upper Blue Nile River Basin: Based on IPCC Fifth Assessment Report (AR5)’, *Journal of Climatology & Weather Forecasting*, 03(01), pp. 1–15. doi: 10.4172/2332-2594.1000121.

Lennard, C. J. *et al.* (2018) ‘On the need for regional climate information over Africa under varying levels of global warming’, *Environmental Research Letters*, 13(6). doi: 10.1088/1748-9326/aab2b4.

Van Liew, M. W. and Mittelstet, A. R. (2018) ‘Comparison of three regionalization techniques for predicting streamflow in ungaged watersheds in nebraska, USA using SWAT model’, *International Journal of Agricultural and Biological Engineering*, 11(3), pp. 110–119. doi: 10.25165/j.ijabe.20181103.3528.

Manag, U. R. (2012) ‘IV-2 . Flood Overtopping Failure of Dams and Levees’, *USBR Risk*.

Maraun, D. (2016) ‘Bias Correcting Climate Change Simulations - a Critical Review’, *Current Climate Change Reports*, 2(4), pp. 211–220. doi: 10.1007/s40641-016-0050-x.

Mckeever, V. (1972) ‘Revisions by’, *Development*, (August).

Mearns, L. *et al.* (2003) ‘Guidelines for Use of Climate Scenarios Developed from Regional Climate Model Experiments’, *Development*, p. 38.

Mechal, A., Wagner, T. and Birk, S. (2015) ‘Recharge variability and sensitivity to climate: The example of Gidabo River Basin, Main Ethiopian Rift’, *Journal of Hydrology: Regional Studies*. Elsevier B.V., 4, pp. 644–660. doi: 10.1016/j.ejrh.2015.09.001.

Morris, M. *et al.* (2004) ‘CADAM / IMPACT / FLOODSITE What are CADAM , IMPACT and FLOODSITE ? The CADAM Concerted Action Project’, (November).

Muerth, M. J. *et al.* (2013) ‘On the need for bias correction in regional climate scenarios to assess climate change impacts on river runoff’, *Hydrology and Earth System Sciences*, 17(3), pp. 1189–1204. doi: 10.5194/hess-17-1189-2013.

Murphy, J. (1999) ‘An evaluation of statistical and dynamical techniques for downscaling local climate’, *Journal of Climate*, 12(8 PART 1), pp. 2256–2284.

Negassa, T. (2012) ‘Adaptive Reservoir Operation’.

Neitsch, S. L. *et al.* (2011) ‘Theoretical documentation SWAT’.

Nikulin, G. *et al.* (2018) ‘The effects of 1.5 and 2 degrees of global warming on Africa in the CORDEX ensemble’, *Environmental Research Letters*, 13 065003(6), p. 65003. doi: 10.1088/1748-9326/aab1b1.

Obada, E. *et al.* (2017) ‘Change in Future Rainfall Characteristics in the Mekrou Catchment (Benin), from an Ensemble of 3 RCMs (MPI-REMO, DMI-HIRHAM5 and SMHI-RCA4)’, *Hydrology*, 4(1), p. 14. doi: 10.3390/hydrology4010014.

Osima, S. *et al.* (2018) 'Projected climate over the Greater Horn of Africa under 1.5 °c and 2 °c global warming', *Environmental Research Letters*, 13(6). doi: 10.1088/1748-9326/aaba1b.

Ouranos (2015) 'Probable Maximum Floods and Dam Safety', p. 40.

Parajka, J., Merz, R. and Blöschl, G. (2010) 'A comparison of regionalisation methods for catchment model parameters', *Hydrology and Earth System Sciences Discussions*, 2(2), pp. 509–542. doi: 10.5194/hessd-2-509-2005.

Pothwar, O. F. *et al.* (2015) 'Estimation of Probable Maximum Flood (Pmf)':, 27(6), pp. 6471–6475.

Project, S. H. and Authority, A. E. (2014) 'PROBABLE MAXIMUM PRECIPITATION AND PROBABLE MAXIMUM FLOOD Historic Floods', (14241), pp. 1–11.

Prudhomme, C. and Nick Reynard, S. C. (2002) 'Downscaling of global climate models for flood frequency analysis: Where are we now?', *Hydrological Processes*, 16(6), pp. 1137–1150. doi: 10.1002/hyp.1054.

Report, B. S. (2017) 'OROMIA WATER WORKS DESING AND SUPERVISION'.

Rientjes, T. H. M. *et al.* (2008) 'Hydrological Balance of Lake Tana, Upper Blue Nile Basin, Ethiopia', *Nile River Basin*, (May 2008), pp. 69–89. doi: 10.1007/978-94-007-0689-7_3.

Roth, V., Nigussie, T. K. and Lemann, T. (2016) 'Model parameter transfer for streamflow and sediment loss prediction with SWAT in a tropical watershed', *Environmental Earth Sciences*, 75(19). doi: 10.1007/s12665-016-6129-9.

S. Hansen *et al.* (2013) 'Daisy: Model Use, Calibration, and Validation', *Transactions of the ASABE*, 55(4), pp. 1317–1335. doi: 10.13031/2013.42244.

Sanjay, J. *et al.* (2012) 'CORDEX Regional Climate Models Performance in Present-day Climate for South Asia', p. 2012.

Scale, A. L., Project, D. and Report, D. M. (2017) 'FEDERAL DEMOCRATIC REPUBLIC OF ETHIOPIA MINISTRY OF WATER , IRRIGATION AND ELECTRICITY ARJO DHIDHESSA DAM AND APPURTENANT STRUCTURES FINAL DESIGN MODIFICATION REPORT VOLUME II PART I JULY 2017', II(July).

Seckin, N., Haktanir, T. and Yurtal, R. (2011) 'Flood frequency analysis of Turkey using L-moments method', *Hydrological Processes*, 25(22), pp. 3499–3505. doi: 10.1002/hyp.8077.

Seyoum, W. M., Milewski, A. M. and Durham, M. C. (2015) 'Understanding the relative impacts of natural processes and human activities on the hydrology of the Central Rift Valley lakes, East Africa', *Hydrological Processes*, 29(19), pp. 4312–4324. doi: 10.1002/hyp.10490.

Shoghli, B., Lim, Y. H. and Alikhani, J. (2016) 'Evaluating the Effect of Climate Change on the Design Parameters of Embankment Dams: Case Studies Using Remote Sensing Data', (May), pp. 575–585. doi: 10.1061/9780784479872.059.

Shongwe, M. E. *et al.* (2015) 'An evaluation of CORDEX regional climate models in simulating precipitation over Southern Africa', *Atmospheric Science Letters*, 16(3), pp. 199–207. doi: 10.1002/asl2.538.

Shuma, D. (2015) 'Impact Assessment of Climate and Land Use Change on Tikur Wuha River', (March).

Tamirat Dessalegn & Awass, A. A. H. (2016) 'THE INTERNATIONAL JOURNAL OF SCIENCE & TECHNOLEDGE Embankment Dam Spillway Adequacy Evaluation under Probable', 4(9), pp. 89–98.

Tang, F. F., Xu, H. S. and Xu, Z. X. (2012) 'Model calibration and uncertainty analysis for runoff in the Chao River Basin using sequential uncertainty fitting', *Procedia Environmental Sciences*, 13(2011), pp. 1760–1770. doi: 10.1016/j.proenv.2012.01.170.

Taye, M. T. *et al.* (2011) 'Assessment of climate change impact on hydrological extremes in two source regions of the Nile River Basin', *Hydrology and Earth System Sciences*, 15(1), pp. 209–222. doi: 10.5194/hess-15-209-2011.

Taylor, P. and Pittock, J. (2011) *Lessons for climate change adaptation from better management of rivers Lessons for climate change adaptation from better management of rivers*. doi: 10.3763/cdev.2009.0021.

Teutschbein, C. and Seibert, J. (2010) 'Regional climate models for hydrological impact studies at the catchment scale: A review of recent modeling strategies', *Geography Compass*, 4(7), pp. 834–860. doi: 10.1111/j.1749-8198.2010.00357.x.

Teutschbein, C. and Seibert, J. (2013) 'Is bias correction of regional climate model (RCM) simulations possible for non-stationary conditions', *Hydrology and Earth System Sciences*, 17(12), pp. 5061–5077. doi: 10.5194/hess-17-5061-2013.

U S Army Corps Of Engineers and Engineers, U. S. A. C. O. (1992) 'Hydraulic Design of Spillways', *Design*, (EM 1110-2-1603), p. 170.

Voldoire, A. *et al.* (2013) 'The CNRM-CM5.1 global climate model: Description and basic evaluation', *Climate Dynamics*, 40(9–10), pp. 2091–2121. doi: 10.1007/s00382-011-1259-y.

Walling, D. E. (2009) 'The Impact of Global Change on Erosion and Sediment Transport by Rivers : Side publications series The United Nations World Water Development Report 3', *The United Nations World Water Assessment Programme*, 81, p. 26 p.

Wigley, T. M. L. and Wilby, R. L. (2000) 'Precipitation predictors for downscaling: observed and General Circulation Model relationships', *International Journal of Climatology*, 661, pp. 20: 641-661.

Y, B. and Kemal, A. (2017) 'The Impacts of Climate Change on Rainfall and Flood Frequency: The Case of Hare Watershed, Southern Rift Valley of Ethiopia', *Journal of Earth Science & Climatic Change*, 08(01), pp. 1–5. doi: 10.4172/2157-7617.1000383.

Yang, J. *et al.* (2008) 'Comparing uncertainty analysis techniques for a SWAT application to the

Chaohe Basin in China', *Journal of Hydrology*, 358(1–2), pp. 1–23. doi: 10.1016/j.jhydrol.2008.05.012.

Yilma Seleshi (Dr.) (2005) 'Engineering hydrology', *Journal of Hydrology*, 27(1–2), p. 169. doi: 10.1016/0022-1694(75)90105-5.

8. Annex

A. Input Data for SWAT Model

A.1. Soil

1	4	7	8	9
S.No	Soil Name	NLAYERS	HYDGRP	SOL_ZMX
0	DYCAMBISOLS	3	A	1000.00
1	HPACRISOLS	3	D	1000.00
2	HUNITISOLS	3	B	1000.00
3	HUALISOLS	3	B	1000.00
4	HPALISOLS	3	B	1000.00
5	DYLEPTOSOLS	3	A	300.00

10	11	12	13	14	15	16	17	18
ANION_EXCL	SOL_CRK	TEXTURE	SOL_Z1	SOL_BD1	SOL_AWC1	SOL_K1	SOL_CBN1	CLAY1
0.50	0.50	SL	100.000	1.580	0.015	180.000	0.700	10.000
0.50	0.50	CL	100.000	1.310	0.150	1.800	1.630	39.000
0.50	0.50	L	100.000	1.390	0.150	18.000	2.250	24.000
0.50	0.50	L	100.000	1.380	0.150	18.000	2.830	26.000
0.50	0.50	L	100.000	1.390	0.100	18.000	1.160	23.000
0.50	0.50	SL	30.000	1.580	0.015	180.000	0.650	10.000

19	20	21	22	23	24	25	26	27
SILT1	SAND1	ROCK1	SOL_ALB1	USLE_K1	SOL_EC1	SOL_Z2	SOL_BD2	SOL_AWC2
15.000	75.000	10.000	0.226	0.157	0.100	200.000	1.500	0.160
18.000	43.000	11.000	0.226	0.112	0.000	200.000	1.000	0.038
31.000	45.000	9.000	0.226	0.127	0.100	200.000	1.100	0.085
28.000	46.000	1.000	0.226	0.123	0.000	200.000	1.300	0.145
37.000	40.000	8.000	0.226	0.153	0.100	200.000	1.600	0.140
14.000	76.000	23.000	0.226	0.156	0.000	100.000	1.500	0.175

28	29	30	31	32	33	34	35	36	37
SOL_K2	SOL_CBN2	CLAY2	SILT2	SAND2	ROCK2	SOL_ALB2	USLE_K2	SOL_EC2	SOL_Z3
5.300	0.5	32.0	17.0	51.0	0.0	0.187	0.253	0.0	1000.000
37.210	0.8	22.0	31.0	47.0	0.0	0.105	0.301	0.0	1000.000
22.040	2.8	36.0	26.0	37.0	0.0	0.002	0.269	0.0	1000.000
8.640	1.1	47.0	26.0	27.0	0.0	0.059	0.233	0.0	1000.000
1.740	0.9	45.0	29.0	26.0	0.0	0.086	0.218	0.0	1000.000
2.340	0.9	32.0	39.0	28.0	0.0	0.086	0.353	0.0	1000.000

38	39	40	41	42	43	44	45	46	47
SOL_BD3	SOL_AWC3	SOL_K3	SOL_CBN3	CLAY3	SILT3	SAND3	ROCK3	SOL_ALB3	USLE_K3
1.600	0.160	2.57	0.3	40.0	17.0	42.0	0.0	0.275	0.253
0.900	0.038	56.55	0.9	22.0	28.0	49.0	0.0	0.086	0.301
1.200	0.085	13.23	1.0	37.0	29.0	35.0	0.0	0.071	0.269
1.200	0.145	11.44	0.5	58.0	21.0	21.0	0.0	0.187	0.233
1.600	0.140	1.88	0.5	51.0	27.0	21.0	0.0	0.187	0.218
1.400	0.175	3.92	0.4	34.0	41.0	25.0	0.0	0.227	0.353

B. Regional Climate Model Projected Output Data

B.1. Bias Correction Result Graph

At Gatira Station

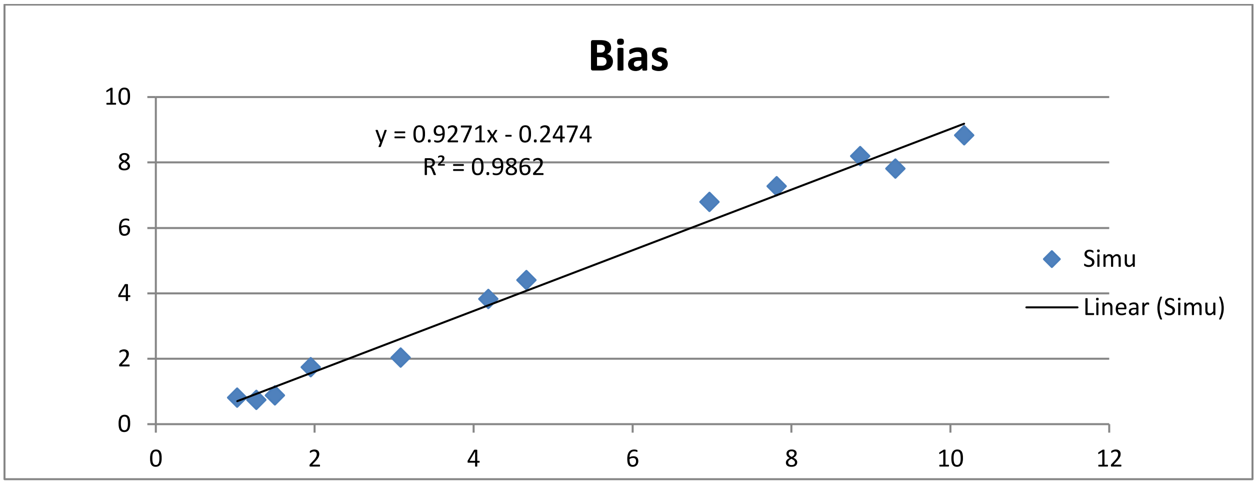

At Gore station

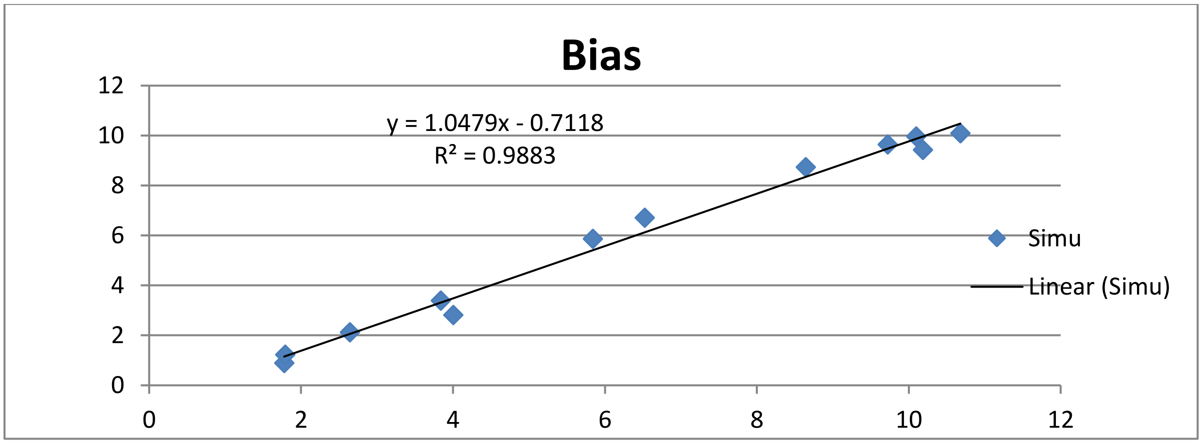

At Tepi station

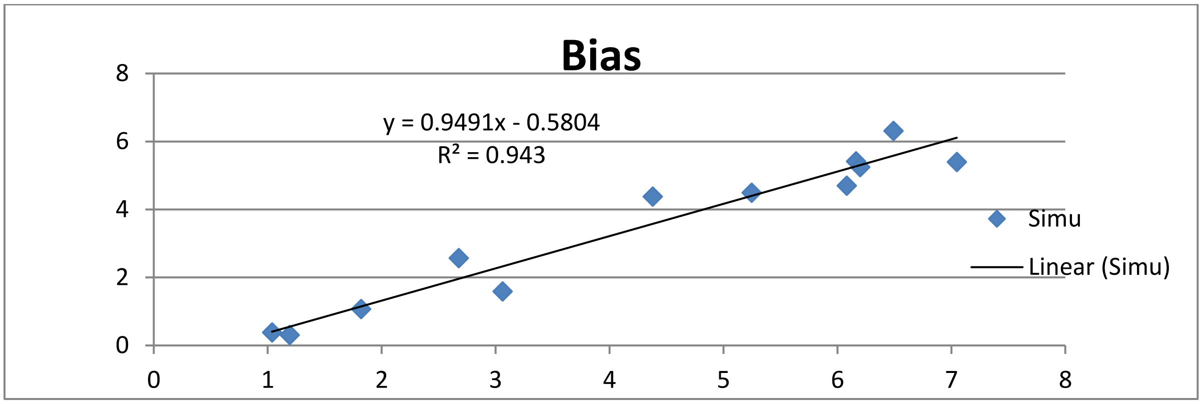

At Bure station

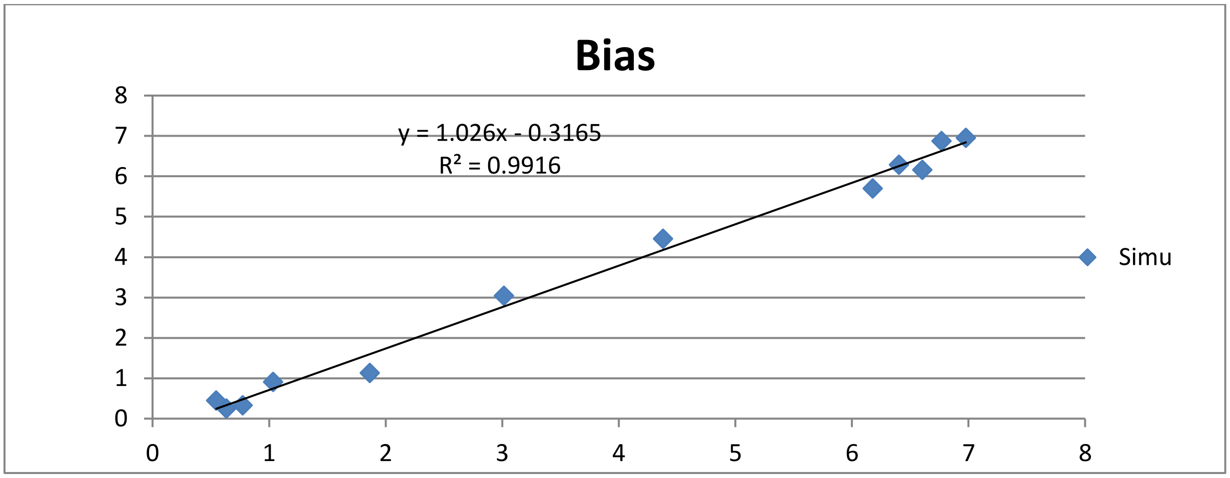

At Masha station

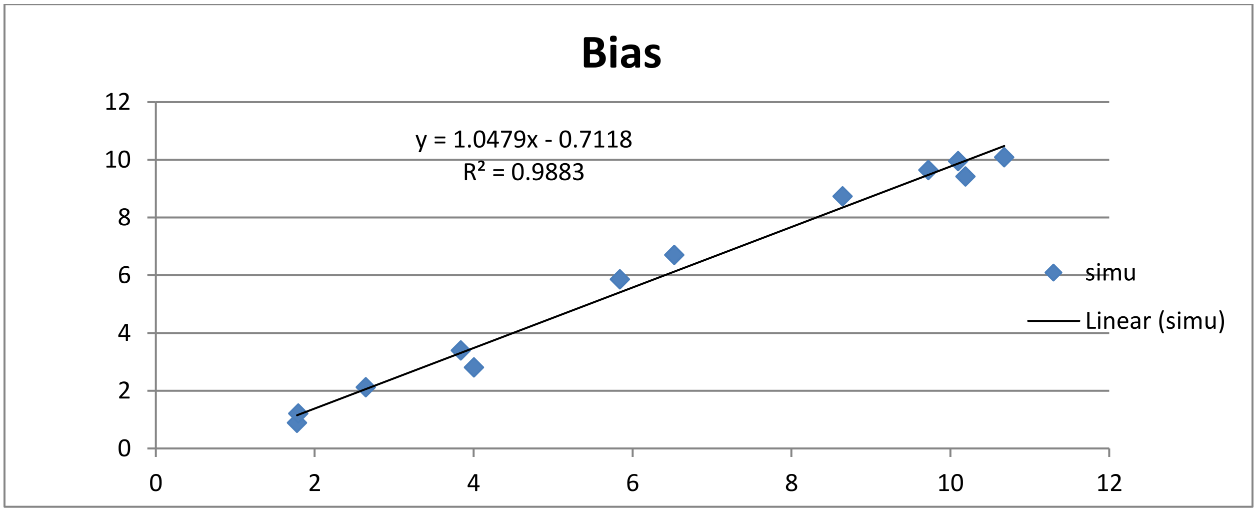

B.2.RCP4.5 data

Precipitation at Bure station (mm)

	Jan	Feb	Mar	Apr	May	Jun	Jul	Aug	Sep	Oct	Nov	Dec
2014	0.0	20.6	69.0	49.8	371.7	144.6	183.7	127.9	148.7	123.5	71.6	3.8
2015	0.0	0.0	12.2	104.0	140.5	171.4	137.7	128.6	210.9	116.8	49.7	44.2
2016	0.0	0.0	14.1	53.7	202.5	215.9	193.3	365.7	210.7	236.4	80.3	17.8
2017	0.0	0.0	13.0	96.5	226.5	247.7	136.7	164.8	150.7	67.3	16.6	5.3
2018	0.0	3.1	182.9	87.2	319.8	182.9	110.1	236.3	114.8	116.8	73.2	10.7
2019	20.5	0.0	35.1	169.9	179.4	286.6	111.8	136.6	138.4	186.2	16.6	45.1
2020	0.0	0.0	199.1	58.7	265.0	286.4	262.4	140.8	160.5	127.3	31.2	11.7
2021	0.0	0.0	0.0	170.7	308.8	252.2	171.2	204.8	229.9	115.9	60.1	5.4
2022	0.0	0.0	26.6	94.2	225.7	197.0	101.6	279.2	219.9	230.1	26.3	5.4
2023	9.0	0.0	8.1	57.4	162.8	138.9	247.1	151.1	182.9	118.8	22.4	0.0
2024	0.0	0.0	47.7	61.0	251.6	219.9	120.4	147.2	284.3	195.7	60.2	6.3
2025	0.0	0.0	13.3	279.6	204.4	335.3	241.3	212.3	155.7	185.0	62.2	13.2
2026	0.0	11.0	17.6	91.6	177.8	155.2	99.0	226.3	257.9	131.9	20.8	4.7
2027	21.6	0.0	8.3	144.9	162.1	113.5	203.2	114.3	103.8	128.0	10.4	15.6
2028	0.0	0.0	45.9	98.2	239.9	149.6	161.0	170.0	155.2	63.3	98.4	14.2
2029	0.0	0.0	89.7	33.5	228.0	245.9	169.3	198.5	346.7	101.1	16.6	0.0
2030	0.0	0.0	37.4	15.5	162.9	157.8	180.1	185.5	161.2	27.4	8.1	9.7
2031	5.4	3.7	6.7	69.7	353.0	166.8	131.1	233.0	288.2	103.5	4.1	23.3
2032	12.8	0.0	42.2	104.6	180.6	219.1	104.9	188.8	131.0	62.0	39.0	20.1
2033	0.0	0.0	0.0	86.1	399.9	73.8	184.7	143.6	138.3	113.0	3.3	1.0
2034	0.0	7.0	9.9	38.4	172.5	187.7	339.6	238.1	320.8	60.9	38.3	1.9
2035	0.0	0.0	18.3	40.0	415.2	133.5	216.1	275.1	255.6	293.5	20.5	4.2
2036	0.0	3.1	9.5	64.8	124.7	239.7	150.9	199.9	129.9	177.7	31.9	8.0
2037	0.0	0.0	103.9	56.4	209.3	144.4	154.5	210.4	202.8	37.4	36.1	25.4
2038	0.0	0.0	69.9	87.2	314.9	195.7	212.2	206.1	249.4	131.8	20.9	8.8
2039	0.0	13.5	17.6	97.0	196.7	269.7	98.7	94.8	309.6	168.8	12.8	5.2
2040	0.0	4.1	30.5	188.2	258.7	142.4	136.4	199.5	198.0	82.3	22.3	6.0
2041	0.0	0.0	0.0	38.1	167.4	182.2	165.9	169.2	311.8	110.6	48.4	47.9
2042	0.0	2.6	48.0	97.4	134.8	239.9	181.7	149.1	158.1	110.8	17.4	6.5
2043	0.0	3.9	83.6	26.1	259.9	205.2	86.5	91.1	144.7	114.4	50.0	4.2
2044	0.0	0.0	15.6	174.9	293.3	442.0	213.8	178.9	279.0	95.3	49.6	12.5
2045	0.0	0.0	32.0	52.7	424.0	201.3	193.1	236.1	531.4	173.2	27.4	8.9
2046	0.0	0.0	28.8	120.0	205.9	181.7	176.3	293.0	185.9	71.6	28.6	3.7
2047	0.0	0.0	37.9	253.7	248.8	200.9	66.6	163.2	128.0	124.6	92.8	27.9
2048	0.0	30.2	0.0	85.5	358.7	255.7	151.3	247.6	208.7	116.5	10.3	0.8
2049	0.0	0.0	0.0	69.3	255.5	246.7	103.0	119.0	123.5	179.1	10.3	0.0
2050	0.0	3.3	0.0	19.4	283.3	102.0	193.3	268.3	141.9	44.8	42.2	4.2
2051	0.0	0.0	8.9	42.1	281.9	169.3	137.8	132.2	101.2	218.7	9.9	1.1
2052	0.0	0.0	18.2	148.8	337.4	263.7	118.1	185.3	263.4	195.5	45.7	16.8

2053	16.4	0.0	185.8	231.4	129.0	353.6	119.2	219.0	89.7	157.5	75.8	14.4
2054	7.8	0.0	51.9	43.9	166.4	262.2	132.6	158.6	170.4	254.4	42.2	46.9
2055	0.0	0.0	17.1	56.9	144.4	118.4	205.7	98.5	128.3	73.5	31.0	17.0
2056	0.0	0.0	10.9	164.0	330.5	207.7	188.8	380.3	381.3	127.9	18.9	5.6
2057	0.0	4.5	0.0	34.7	149.6	218.5	203.2	147.9	284.8	121.0	17.4	6.8
2058	0.0	2.5	26.8	85.4	207.4	115.4	132.6	103.6	153.1	107.4	32.6	4.5
2059	0.0	0.0	0.0	101.0	126.2	280.5	115.0	130.9	230.6	233.9	44.6	0.0
2060	0.0	0.0	34.5	59.5	272.5	201.2	110.5	159.4	164.4	67.1	14.4	5.6
2061	0.0	33.2	41.2	45.8	235.6	176.9	242.6	254.3	223.6	146.8	3.5	7.7
2062	0.0	0.0	0.0	132.4	211.7	216.2	158.7	125.7	159.9	264.0	56.3	2.4
2063	0.0	0.0	19.3	83.2	289.7	147.6	150.7	117.0	171.4	167.4	76.2	13.1
2064	0.0	0.0	29.2	13.8	168.5	182.8	179.1	115.9	146.4	93.0	5.0	5.7
2065	0.0	0.0	7.4	4.1	179.3	113.9	88.1	149.0	196.8	99.7	12.6	1.5
2066	0.0	0.0	9.7	267.4	324.2	166.4	157.7	118.2	226.0	136.7	10.6	9.7
2067	0.0	0.0	0.0	67.7	163.1	117.6	232.9	115.1	149.6	152.0	33.7	6.2
2068	0.0	0.0	0.0	48.5	354.0	209.7	201.1	189.4	158.0	86.6	6.9	0.7
2069	0.0	0.0	2.8	81.0	182.1	279.8	65.3	199.4	195.2	302.4	22.6	51.4
2070	45.3	4.4	24.0	169.6	290.6	249.4	112.9	183.7	230.5	348.6	23.8	14.6
2071	0.0	0.0	0.0	121.5	176.6	366.7	183.6	197.0	172.1	205.0	24.2	0.0
2072	0.0	0.0	12.6	28.1	136.4	172.5	204.1	170.4	241.8	107.7	13.3	16.7
2073	43.1	18.9	12.6	66.8	120.7	206.0	75.0	189.7	307.9	247.1	16.2	1.3
2074	0.0	2.6	32.5	178.2	301.2	184.6	132.6	112.6	306.6	87.8	18.3	2.7
2075	0.0	0.0	26.2	85.5	187.5	153.1	286.8	176.0	230.7	88.7	10.3	13.2
2076	5.1	6.8	0.0	50.0	133.9	173.5	146.7	292.0	339.3	161.9	26.2	50.0
2077	0.0	12.9	9.7	26.9	408.5	142.9	237.7	153.8	160.4	348.1	21.2	10.3
2078	0.0	0.0	18.6	82.0	347.6	183.9	147.7	136.0	294.9	169.9	28.6	9.8
2079	0.0	10.7	46.8	30.7	319.3	396.4	235.3	207.2	238.7	250.5	26.5	0.0
2080	14.9	3.4	30.2	26.7	244.4	126.5	174.0	134.9	319.8	203.9	25.0	6.7
2081	0.0	0.0	25.5	187.3	448.2	337.2	131.9	95.6	267.2	253.5	29.1	10.1
2082	0.0	0.0	9.7	178.3	224.6	206.7	195.3	162.1	131.5	53.6	17.8	3.9
2083	0.0	5.7	6.4	30.4	151.5	197.3	214.8	165.8	189.0	87.3	7.3	2.5
2084	0.0	0.0	24.5	133.2	140.2	88.4	134.9	300.9	209.9	140.0	35.0	14.2
2085	0.0	0.0	205.6	61.1	316.7	173.6	195.9	199.7	245.4	119.8	62.7	3.6
2086	0.0	0.0	40.9	28.3	107.3	163.4	102.7	187.9	206.5	195.2	11.2	8.5
2087	23.5	2.4	16.5	111.1	211.5	245.3	126.6	233.2	237.7	110.6	10.8	5.6
2088	0.0	0.0	113.3	32.6	155.5	202.6	117.2	201.2	183.7	84.7	31.8	1.0
2089	0.0	0.0	5.1	55.4	217.5	168.3	277.2	239.0	322.2	144.3	44.7	8.0
2090	0.0	0.0	66.1	134.8	108.7	391.9	122.9	161.2	62.5	197.0	38.2	0.0
2091	0.0	0.0	8.2	111.3	168.9	184.8	155.9	212.8	273.5	108.8	38.7	11.6
2092	0.0	0.0	22.1	55.3	291.6	134.9	224.5	384.0	272.7	134.3	77.4	0.0
2093	7.9	0.0	35.8	259.4	117.7	174.6	259.4	237.2	271.1	79.6	6.7	3.4
2094	0.0	0.0	100.8	165.7	259.2	240.7	158.6	73.8	136.1	157.0	70.4	5.8
2095	0.0	113.3	47.5	14.2	273.1	203.2	154.6	286.0	270.8	179.8	5.6	0.0
2096	0.0	0.0	3.3	31.3	277.9	310.1	143.7	259.5	254.7	73.0	3.1	3.2
2097	0.0	0.0	0.0	124.7	169.8	186.2	336.7	285.0	223.5	206.1	20.7	60.8

2098	0.0	0.0	7.2	136.4	176.9	131.9	89.1	133.6	153.6	76.8	6.9	0.0
2099	0.0	0.0	10.4	48.3	252.0	315.4	189.1	155.0	167.7	215.2	19.9	33.1
2100	7.5	0.0	27.3	130.7	171.4	228.0	104.0	136.8	96.1	233.5	15.4	8.6

Precipitation at Gatira station (mm)

	Jan	**Feb**	**Mar**	**Apr**	**May**	**Jun**	**Jul**	**Aug**	**Sep**	**Oct**	**Nov**	**Dec**
2014	9.9	56.4	96.0	60.7	290.3	146.3	175.2	173.3	238.0	98.1	100.8	0.0
2015	3.8	0.0	73.9	330.1	140.9	253.2	213.0	221.2	176.6	96.6	99.4	26.2
2016	12.2	0.0	24.5	108.5	203.5	264.5	293.7	500.7	246.1	156.3	129.4	50.1
2017	25.9	3.7	37.1	149.2	147.5	202.8	110.2	232.2	176.6	16.5	29.6	12.6
2018	0.0	43.9	179.4	112.4	233.1	243.0	257.2	308.7	191.2	148.6	120.1	1.8
2019	14.9	8.4	43.5	110.4	139.8	340.5	214.6	279.8	120.7	228.4	12.9	73.4
2020	0.0	3.8	87.4	123.5	182.6	276.2	384.8	265.8	252.2	161.8	208.6	10.0
2021	27.3	14.3	34.2	141.5	187.9	283.5	282.6	328.6	231.3	182.4	161.8	4.5
2022	3.3	0.0	16.6	148.0	293.2	286.7	282.0	333.3	388.8	152.2	37.5	55.1
2023	30.8	16.5	0.0	109.3	195.4	274.8	242.2	235.1	233.5	147.8	32.0	0.0
2024	36.4	54.9	75.0	54.1	442.8	360.9	187.3	195.5	322.4	125.2	78.8	32.8
2025	0.0	4.8	22.5	247.0	100.8	272.2	358.0	320.3	133.4	174.9	383.3	8.8
2026	6.8	36.0	48.2	138.7	296.4	178.9	113.7	402.6	460.7	112.8	75.3	6.4
2027	0.0	0.0	15.9	290.6	183.5	337.5	277.9	232.4	162.0	170.4	29.7	29.8
2028	0.0	0.0	65.0	93.0	156.2	191.1	230.6	213.4	236.6	64.9	60.4	53.5
2029	1.8	11.2	203.5	99.5	235.2	434.0	242.1	223.8	145.7	193.9	48.5	0.0
2030	45.1	2.6	10.4	58.8	148.1	211.8	315.9	289.2	169.1	33.9	26.7	33.0
2031	56.8	10.1	16.1	93.0	197.1	118.2	223.8	355.7	236.4	190.2	14.5	50.0
2032	0.0	37.6	68.3	142.2	221.1	223.8	255.9	119.8	187.0	162.8	82.7	115.1
2033	11.6	12.5	40.5	146.0	244.6	119.9	217.0	311.1	250.9	96.2	0.9	4.9
2034	0.0	72.3	13.2	47.6	243.0	366.7	335.0	353.9	256.1	78.2	24.7	23.3
2035	5.6	3.0	60.3	88.3	241.5	225.4	221.7	232.3	293.7	178.3	13.1	3.2
2036	7.1	9.5	55.0	136.7	123.6	228.4	189.0	291.7	275.9	140.0	123.3	76.0
2037	33.2	4.6	103.2	68.4	337.5	173.4	295.0	279.9	205.8	30.8	39.1	7.3
2038	0.0	0.0	118.6	97.0	216.4	206.5	320.9	317.4	228.7	89.2	70.6	151.0
2039	35.3	22.1	93.3	139.2	131.1	256.4	223.2	163.5	255.7	103.6	20.7	34.1
2040	2.0	3.9	68.2	106.8	181.1	248.9	206.7	294.2	274.3	65.2	43.9	23.1
2041	0.0	0.0	0.0	113.7	116.1	267.4	174.2	291.8	376.1	162.1	90.5	146.1
2042	8.3	3.6	50.4	90.0	97.6	319.8	244.5	197.5	330.8	121.8	6.8	6.9
2043	26.0	10.8	103.4	37.8	138.7	226.9	213.2	144.4	155.4	67.4	85.2	1.4
2044	3.3	18.5	41.7	319.2	347.2	262.6	238.5	291.4	287.6	49.1	64.3	14.1
2045	0.0	60.8	79.7	58.0	388.2	393.9	228.7	354.0	327.8	69.2	31.3	2.3
2046	2.7	38.0	0.0	138.7	154.9	267.9	266.2	421.0	164.5	107.8	57.8	9.1
2047	12.7	28.1	77.6	188.7	392.5	220.4	148.2	300.8	218.0	206.1	38.5	71.3
2048	5.7	31.7	19.4	129.1	141.9	421.1	174.5	395.2	188.8	62.0	4.2	96.9

2049	0.0	0.0	32.1	116.3	271.1	332.5	201.1	296.1	190.8	182.1	107.8	4.0
2050	7.7	0.0	15.5	42.5	178.9	205.1	244.9	287.7	303.4	80.9	66.6	6.6
2051	0.0	29.0	37.9	104.1	252.1	276.9	162.4	183.9	147.0	151.7	15.6	61.9
2052	2.3	0.0	47.4	157.8	250.3	284.1	192.2	191.2	220.5	137.3	367.4	8.2
2053	86.7	8.9	124.3	113.2	49.3	437.5	145.4	380.8	196.9	155.5	80.3	18.9
2054	27.7	23.9	76.0	36.6	128.0	303.0	159.8	303.8	376.6	226.4	23.3	66.5
2055	2.3	39.4	38.4	134.7	163.6	181.9	160.5	197.6	285.4	194.8	113.9	95.2
2056	22.1	3.2	28.2	165.5	306.3	211.5	211.2	365.0	220.1	108.4	95.2	3.9
2057	0.0	41.4	36.4	40.5	170.6	233.8	340.4	317.7	198.1	103.1	6.7	26.8
2058	32.5	19.5	61.0	136.2	201.3	243.2	143.6	144.1	140.9	115.0	53.0	25.4
2059	10.4	10.7	18.6	142.9	172.2	304.7	253.9	202.6	226.3	215.8	61.3	3.3
2060	6.0	2.9	20.0	114.9	157.8	281.1	190.1	230.5	191.4	88.0	37.9	42.9
2061	50.6	30.6	46.9	160.6	223.6	328.9	261.9	274.3	303.5	127.9	64.6	27.1
2062	2.0	10.1	0.0	124.7	196.5	205.2	182.9	174.2	293.9	275.7	177.4	39.3
2063	24.0	25.7	2.2	184.0	326.8	221.2	207.3	187.1	411.5	121.2	279.9	5.3
2064	15.8	0.0	25.8	163.6	154.4	310.9	201.6	194.9	401.5	158.1	8.7	11.8
2065	5.1	0.0	0.0	5.0	289.3	242.7	156.9	201.9	218.9	62.1	7.2	0.0
2066	0.0	104.9	90.5	115.5	272.9	196.1	205.6	202.6	192.6	137.8	74.8	6.3
2067	0.0	23.8	0.0	103.1	269.2	241.9	269.0	235.4	157.6	166.1	18.8	10.2
2068	0.0	10.9	27.2	93.2	429.3	240.4	203.5	252.3	194.8	96.5	55.9	0.0
2069	0.0	0.0	7.4	246.4	240.4	175.1	199.5	264.6	257.9	343.7	34.1	95.4
2070	2.5	13.5	74.2	119.9	267.0	281.0	215.1	358.2	308.2	153.5	37.6	105.5
2071	0.0	0.0	7.2	59.7	202.3	437.5	212.5	283.9	195.3	275.9	45.2	0.0
2072	0.0	0.0	42.9	124.7	282.1	301.1	396.4	304.6	326.4	133.9	32.1	25.8
2073	81.5	42.0	17.9	121.8	186.1	244.2	149.4	212.5	143.7	141.2	0.0	6.4
2074	42.5	6.9	76.5	101.9	187.6	240.8	242.8	260.7	214.6	107.1	3.6	5.6
2075	0.0	6.1	21.6	56.3	280.9	145.6	423.4	259.5	163.5	123.8	15.5	138.1
2076	17.2	56.7	40.8	104.2	342.3	285.1	173.8	284.6	334.4	211.6	24.3	76.1
2077	0.0	12.0	8.9	59.7	199.1	254.9	225.1	223.2	580.1	230.0	20.7	79.3
2078	3.0	0.0	102.1	118.6	276.8	185.8	239.4	375.1	255.0	97.9	5.8	14.8
2079	7.5	37.4	63.2	128.5	358.3	385.1	322.1	287.6	197.3	280.6	54.4	34.6
2080	63.5	0.0	60.9	43.7	305.7	208.8	266.1	326.1	192.9	181.5	137.6	47.3
2081	2.1	0.0	49.9	205.0	222.3	473.2	198.7	216.9	199.5	154.8	76.1	8.2
2082	0.0	0.0	42.8	102.2	316.3	275.7	267.5	280.7	215.9	28.8	28.0	19.6
2083	0.0	48.0	29.6	149.4	142.5	191.3	423.5	249.8	187.3	113.7	23.1	30.3
2084	0.0	2.4	39.3	68.2	200.6	194.1	151.8	345.5	185.4	57.8	12.3	33.4
2085	0.0	36.4	144.8	95.5	297.4	327.3	172.0	310.9	203.3	110.5	67.7	0.0
2086	0.0	35.8	10.9	50.8	174.8	235.6	179.6	295.1	269.0	149.4	72.2	34.5
2087	11.7	0.0	85.3	140.3	190.8	243.8	221.0	132.3	316.4	140.0	10.1	0.0
2088	9.1	0.0	50.9	61.9	172.1	309.6	228.5	259.0	200.2	110.5	30.7	79.1
2089	0.0	0.0	32.7	56.3	311.1	260.0	191.3	299.1	233.6	197.4	20.0	36.2
2090	15.7	0.0	14.8	239.4	103.9	322.7	239.1	252.6	172.9	273.9	249.2	2.9
2091	17.7	0.0	162.2	199.1	75.7	384.6	288.6	383.2	207.5	110.1	39.9	11.7

2092	0.0	0.0	34.5	198.0	155.8	277.1	302.0	416.6	252.3	132.8	148.3	1.4
2093	21.5	16.0	97.3	221.8	43.2	302.8	281.3	405.7	196.1	250.6	19.4	6.4
2094	0.0	0.0	124.4	100.6	227.4	433.1	147.3	195.1	150.8	158.4	288.9	11.8
2095	19.1	38.7	22.0	79.3	165.5	208.9	259.0	356.3	199.1	118.3	14.5	0.0
2096	0.0	6.5	64.4	85.3	336.4	241.7	196.7	263.8	286.6	49.6	0.0	5.7
2097	0.0	2.3	79.4	125.1	175.4	406.9	190.9	287.4	272.7	139.3	31.4	90.3
2098	0.0	0.0	11.2	144.7	287.5	219.6	132.6	178.7	107.8	118.4	62.1	3.4
2099	0.0	17.6	2.8	93.7	343.7	403.7	243.4	327.9	258.3	61.3	46.8	13.4
2100	34.9	9.9	15.4	89.0	92.6	173.5	234.7	159.0	136.7	140.5	23.9	53.9

Precipitation at Gore station (mm)

	Jan	**Feb**	**Mar**	**Apr**	**May**	**Jun**	**Jul**	**Aug**	**Sep**	**Oct**	**Nov**	**Dec**
2014	42.3	38.7	67.8	92.8	273.6	140.4	159.7	215.9	218.8	139.6	124.7	19.3
2015	6.4	0.0	42.5	304.4	178.8	302.6	240.2	218.3	263.2	125.4	90.2	36.6
2016	12.4	0.0	6.7	85.1	225.9	296.5	302.6	591.6	270.9	222.6	86.4	99.3
2017	0.0	0.0	28.2	105.5	330.2	203.4	105.6	201.8	185.2	60.0	51.4	31.2
2018	0.0	0.0	163.2	86.6	258.0	266.2	223.9	269.5	177.9	233.5	152.4	13.5
2019	58.3	0.0	33.8	161.6	209.1	499.0	232.9	339.1	211.4	280.4	21.9	105.7
2020	0.0	2.0	109.1	173.2	193.6	351.7	404.6	260.2	261.5	200.6	87.3	16.9
2021	26.2	2.7	25.1	162.1	245.5	378.4	280.4	430.4	264.3	183.6	89.3	8.4
2022	0.0	2.0	17.4	88.4	333.0	258.9	189.8	367.5	280.8	298.5	34.1	14.6
2023	35.5	0.0	0.0	82.7	349.8	281.6	309.5	220.8	269.6	128.4	69.0	0.0
2024	43.1	10.5	51.6	49.9	336.7	299.0	185.7	161.8	341.0	163.7	77.8	21.7
2025	0.0	0.0	18.1	309.2	229.1	340.0	272.3	279.4	147.8	274.0	162.8	32.2
2026	16.8	37.9	59.5	126.2	239.0	187.9	130.9	402.5	412.0	335.5	59.9	1.2
2027	18.6	0.0	32.3	234.5	239.2	241.7	273.9	203.8	155.1	140.2	40.6	37.9
2028	0.0	0.0	29.9	82.6	196.7	217.5	300.0	313.7	276.8	96.8	151.0	40.1
2029	0.0	2.6	186.2	27.4	232.6	424.0	217.0	185.4	266.3	177.2	48.0	0.0
2030	68.8	0.0	45.8	21.1	240.5	240.4	293.9	270.4	224.6	50.3	31.2	32.2
2031	32.1	2.1	15.1	75.5	218.8	206.2	245.6	331.7	304.8	212.1	15.5	27.7
2032	5.9	5.8	47.9	126.7	204.7	261.8	301.0	217.0	248.7	156.1	83.2	59.5
2033	0.0	5.9	21.2	98.2	332.8	190.2	368.2	226.6	224.0	86.8	7.0	1.4
2034	0.0	24.5	2.4	39.3	266.5	416.9	377.8	261.3	262.3	82.5	39.8	17.5
2035	3.4	0.0	24.5	72.0	425.7	187.9	260.7	320.5	294.6	291.2	34.7	9.0
2036	0.0	10.7	19.2	127.1	242.5	278.2	188.3	264.6	279.4	178.7	77.7	37.1
2037	0.0	0.0	73.1	27.7	263.1	181.7	379.7	315.4	251.2	78.7	40.3	10.5
2038	0.0	6.6	58.3	82.3	235.5	261.4	239.7	264.9	271.1	155.2	60.6	59.1
2039	6.9	25.5	53.0	208.1	173.2	354.8	221.5	186.1	324.7	191.2	25.7	34.0
2040	12.8	3.9	59.9	195.5	253.7	239.8	245.6	270.5	322.6	130.7	50.7	14.4
2041	0.0	3.1	0.0	49.7	148.4	247.3	205.0	325.9	447.3	107.8	89.2	116.8

2042	0.0	3.3	32.9	76.1	160.0	339.7	195.5	173.7	303.9	125.7	21.2	20.9
2043	0.0	14.9	127.9	43.1	177.8	284.3	215.9	144.4	240.6	119.8	100.7	8.5
2044	0.0	5.8	34.1	334.9	362.5	441.5	374.7	214.6	342.4	103.9	64.3	15.8
2045	0.0	19.5	91.6	46.0	535.8	293.4	229.0	414.6	442.7	226.7	26.4	20.9
2046	0.0	10.2	26.4	184.7	173.5	303.5	223.7	335.9	208.6	180.8	65.0	1.3
2047	49.3	0.0	88.0	151.3	370.3	292.9	152.4	368.9	314.5	180.1	30.5	103.8
2048	0.0	27.1	14.4	105.4	254.4	341.0	187.6	350.3	170.5	99.4	8.1	30.8
2049	0.0	0.0	13.4	121.7	362.0	276.6	220.6	244.6	268.9	277.8	46.8	6.6
2050	0.0	0.0	26.1	46.9	260.7	191.1	307.8	247.4	252.3	78.4	113.0	4.1
2051	0.0	0.0	23.9	95.5	273.5	296.4	207.1	226.1	226.0	303.2	23.1	14.0
2052	0.0	0.0	34.9	126.9	233.9	329.1	209.8	243.0	285.3	288.0	125.3	20.7
2053	40.3	5.3	134.9	118.7	157.6	542.4	154.1	355.4	220.3	163.2	115.4	31.0
2054	28.7	9.5	93.7	79.2	285.0	294.6	166.6	274.8	305.3	198.5	64.4	77.3
2055	0.0	0.0	26.8	179.7	220.5	141.5	207.4	164.5	300.3	119.4	82.6	103.9
2056	4.1	3.8	14.9	205.9	328.0	175.0	189.7	427.2	353.3	180.2	75.7	25.5
2057	13.5	17.4	21.0	25.8	119.6	178.4	357.3	314.9	298.2	179.8	16.2	16.9
2058	0.0	7.3	49.8	69.0	197.3	304.6	213.5	216.2	207.8	166.9	59.3	18.6
2059	0.0	11.2	20.3	126.8	137.6	474.8	202.8	178.6	295.2	292.4	166.1	0.0
2060	0.0	0.0	46.9	88.4	249.3	316.0	232.0	241.3	323.1	124.6	31.3	21.5
2061	37.0	28.3	47.4	122.5	235.0	229.7	308.4	344.0	391.3	163.7	42.8	19.3
2062	0.0	12.5	2.6	89.8	192.2	328.9	336.6	224.2	246.0	221.7	201.2	25.0
2063	0.0	0.0	28.6	114.5	246.3	312.4	283.6	120.9	369.6	249.3	241.4	9.5
2064	0.0	0.0	33.6	73.1	181.6	339.1	268.3	175.9	294.8	133.9	29.3	12.3
2065	7.7	0.0	6.0	3.5	282.8	265.0	164.4	221.3	286.9	146.5	29.2	2.0
2066	0.0	27.4	88.0	152.3	223.1	195.0	171.6	262.5	224.1	196.7	24.9	20.7
2067	0.0	0.0	3.0	93.8	236.1	195.3	405.6	205.6	251.2	221.1	39.6	10.4
2068	0.0	6.8	16.8	81.2	457.3	271.5	340.3	266.3	252.4	132.5	26.6	2.2
2069	0.0	0.0	7.2	87.2	236.2	287.9	166.7	211.3	281.8	327.8	23.1	99.7
2070	21.7	4.9	63.2	179.2	277.1	369.1	181.6	342.1	264.3	341.2	43.9	39.2
2071	0.0	3.7	5.7	72.3	188.4	409.2	202.5	268.4	303.5	211.0	58.1	4.8
2072	0.0	0.0	49.8	58.1	195.4	278.3	323.7	356.8	357.2	195.7	43.4	46.6
2073	64.6	34.1	10.1	110.3	226.2	410.9	132.4	245.3	335.5	262.8	37.7	2.1
2074	29.3	0.0	37.1	56.0	188.0	344.4	281.8	230.0	324.0	190.8	17.8	8.0
2075	0.0	6.8	0.0	52.5	363.4	172.1	438.8	237.7	274.2	151.5	21.8	64.7
2076	6.0	36.5	25.6	88.8	168.2	257.3	183.2	300.6	558.5	239.9	46.6	123.0
2077	0.0	17.8	17.3	38.2	230.2	231.9	241.5	259.2	437.4	256.8	18.4	37.0
2078	0.0	0.0	54.8	136.9	449.0	264.1	319.8	255.0	238.7	153.5	36.5	6.8
2079	6.3	13.1	67.2	60.1	589.3	355.1	333.0	273.6	214.1	378.6	50.4	8.2
2080	109.7	0.0	81.0	73.0	238.0	285.5	353.3	280.0	313.4	206.3	64.9	30.4
2081	0.0	0.0	54.7	244.5	343.8	500.1	187.3	168.8	218.0	170.2	47.5	27.7
2082	0.0	0.0	19.5	148.6	485.0	247.5	289.6	223.0	210.5	59.9	20.8	14.7
2083	0.0	26.3	5.3	114.0	192.2	172.3	374.6	217.5	228.4	188.2	13.5	9.9

2084	5.6	3.2	45.5	177.5	191.1	122.2	185.8	457.2	296.9	177.9	71.4	20.0
2085	0.0	7.3	281.7	106.1	363.3	293.3	213.9	279.7	332.0	192.3	20.4	0.0
2086	0.0	16.5	35.7	31.8	141.2	250.5	268.5	311.2	328.1	165.0	33.1	12.9
2087	17.4	9.4	34.0	172.0	269.1	277.6	152.1	222.8	356.1	195.9	12.4	8.8
2088	26.8	0.0	71.3	40.9	294.0	279.6	212.5	288.8	243.1	121.3	57.1	3.0
2089	0.0	0.0	46.4	50.3	241.1	297.0	267.2	385.4	251.0	223.1	123.4	72.0
2090	0.0	4.8	41.5	191.3	298.6	377.0	273.8	267.4	175.0	277.0	114.4	0.0
2091	0.0	0.0	77.5	222.9	174.8	359.1	265.7	324.0	306.1	169.6	133.5	24.5
2092	0.0	0.0	26.6	222.5	330.0	271.4	312.5	472.1	322.5	199.7	160.6	0.0
2093	18.3	0.0	84.4	216.4	93.7	239.4	327.0	387.0	312.6	376.7	39.0	8.8
2094	0.0	0.0	123.0	183.9	286.1	545.6	215.4	141.2	224.7	160.2	152.1	21.7
2095	0.0	121.8	42.9	45.3	219.0	211.5	264.6	442.5	281.7	236.2	75.6	0.0
2096	0.0	0.0	39.4	81.7	372.8	342.6	247.7	288.2	337.7	139.0	4.0	10.1
2097	0.0	0.0	26.2	67.6	197.1	359.1	256.3	292.0	274.0	319.5	28.4	48.0
2098	0.0	0.0	16.8	198.8	317.8	247.2	118.2	233.6	220.1	163.4	27.9	0.0
2099	0.0	3.2	12.3	158.9	430.5	431.3	250.7	269.9	378.9	121.0	53.7	68.9
2100	35.9	8.5	54.3	106.9	186.9	321.3	255.7	231.2	154.0	188.4	27.7	34.5

Precipitation at Masha station (mm)

	Jan	Feb	Mar	Apr	May	Jun	Jul	Aug	Sep	Oct	Nov	Dec
2014	42.31	66.99	104.61	169.15	335.63	170.12	185.75	265.68	250.02	155.82	189.64	50.59
2015	7.60	0.00	57.09	459.28	225.61	351.26	283.56	262.49	289.20	142.51	151.90	105.52
2016	23.32	0.00	27.96	152.11	267.20	336.60	357.43	591.17	312.00	246.78	129.80	217.38
2017	9.87	2.58	47.74	189.59	385.82	241.47	129.79	228.25	203.37	74.23	77.68	66.42
2018	0.00	2.76	202.28	150.64	310.35	307.82	279.47	308.52	200.75	259.24	218.82	47.61
2019	62.19	2.53	51.50	256.71	273.48	531.21	275.11	363.84	238.00	304.87	35.86	246.27
2020	0.00	6.68	186.32	257.43	234.32	392.55	451.30	289.77	282.37	205.35	151.16	52.32
2021	39.28	4.80	36.47	270.03	291.07	420.13	344.12	446.14	287.09	215.71	127.13	18.17
2022	0.00	3.83	21.00	161.63	389.57	293.22	223.74	383.59	299.50	324.68	49.39	50.02
2023	45.14	14.42	2.30	147.60	395.86	314.71	339.72	266.06	298.92	143.55	112.65	0.00
2024	47.63	31.14	85.83	95.60	387.82	335.18	225.10	205.03	373.47	192.53	122.64	58.72
2025	0.00	0.00	27.60	452.59	272.05	385.37	323.31	320.08	174.05	287.05	230.75	80.61
2026	20.70	59.31	92.39	225.65	292.89	231.06	184.75	426.07	440.61	355.95	93.04	18.16
2027	19.66	0.00	57.89	358.75	293.90	275.17	316.02	230.86	177.93	161.39	69.05	85.51
2028	7.61	0.00	43.37	149.51	252.79	251.54	330.01	329.60	300.53	122.51	227.45	145.62
2029	0.00	18.08	220.37	63.05	284.56	460.51	262.37	234.49	296.34	191.44	70.76	0.00
2030	82.69	0.00	85.94	41.01	295.57	278.22	330.53	285.74	245.79	62.76	55.04	93.54

2031	36.80	6.57	25.41	124.85	254.27	251.23	273.12	359.11	326.74	230.64	29.68	68.05
2032	14.49	13.07	66.77	212.83	245.79	299.12	336.19	252.52	275.48	176.57	127.63	152.50
2033	0.00	9.15	39.75	167.37	387.26	229.56	405.35	248.36	249.51	105.71	14.43	7.90
2034	0.00	38.63	10.00	77.38	319.21	444.42	413.49	310.76	285.37	104.41	67.11	41.51
2035	7.18	0.00	37.88	120.17	467.95	218.52	305.97	351.38	317.66	307.84	59.81	36.15
2036	0.00	22.98	37.54	193.38	284.10	320.55	242.62	310.42	298.73	196.02	122.51	98.23
2037	6.47	0.00	113.34	53.96	307.56	222.25	398.39	335.12	287.87	89.23	74.38	27.69
2038	2.76	9.90	79.02	158.28	296.73	300.26	265.16	289.60	296.76	181.56	96.87	131.97
2039	8.04	48.32	71.31	329.07	229.11	383.76	253.24	231.81	349.76	212.87	41.87	102.40
2040	13.96	6.51	80.63	305.26	311.48	277.09	283.57	320.09	353.31	152.17	88.91	43.94
2041	0.00	5.33	5.36	88.87	189.64	284.04	247.82	347.43	476.28	128.46	140.45	266.02
2042	3.45	5.66	66.58	132.42	205.06	372.51	243.59	210.53	326.13	147.52	35.01	50.31
2043	4.09	37.12	160.12	81.49	223.68	315.16	257.93	165.56	267.19	145.68	156.44	18.28
2044	0.00	17.20	51.81	484.09	409.32	467.69	407.43	265.36	370.81	122.42	89.10	37.65
2045	0.00	34.24	118.39	93.00	590.55	321.52	267.80	430.06	471.33	239.34	49.08	57.39
2046	0.00	18.72	54.03	283.75	221.84	332.70	260.51	355.38	240.11	198.37	110.15	14.09
2047	68.25	8.89	114.50	245.21	418.99	331.62	212.80	392.54	342.02	205.10	66.35	188.68
2048	0.00	30.93	34.69	184.23	313.52	373.86	227.14	380.64	190.60	113.77	25.17	57.34
2049	0.00	0.00	18.21	179.53	417.75	307.39	247.30	290.98	301.24	302.20	73.40	17.71
2050	0.00	0.00	41.59	95.38	299.65	234.84	348.36	276.10	281.27	98.68	166.88	14.11
2051	0.00	0.00	33.76	159.63	327.53	327.83	241.21	256.43	246.75	322.82	41.00	32.13
2052	0.00	0.00	43.25	223.98	287.76	368.44	254.99	271.30	303.95	299.32	178.11	68.62
2053	64.09	11.08	164.10	206.25	190.11	564.20	190.86	380.09	251.14	192.57	172.62	70.22
2054	45.98	18.37	112.90	143.42	330.58	343.95	197.22	291.84	333.79	219.36	94.26	142.33
2055	0.00	11.75	46.39	283.15	272.40	174.04	248.63	205.08	328.44	138.05	120.82	155.45
2056	8.19	6.29	29.86	313.24	387.24	209.69	249.42	440.77	380.27	191.36	124.81	55.08
2057	13.68	27.30	40.02	49.31	159.28	209.27	382.06	343.07	327.11	196.21	32.29	48.56
2058	11.69	21.38	81.63	132.93	245.93	344.43	258.62	236.38	228.83	188.13	98.50	48.94
2059	0.00	14.93	30.71	198.50	173.62	498.05	237.70	215.52	321.35	315.53	238.15	6.14
2060	0.00	2.90	74.24	159.88	291.49	354.47	260.75	268.07	356.34	138.29	40.85	57.11
2061	47.04	41.35	62.34	197.15	283.16	267.02	371.73	368.48	417.56	173.28	64.98	45.59
2062	0.00	18.74	9.71	161.24	248.45	368.11	367.97	266.91	272.17	242.70	315.56	71.62
2063	0.00	14.25	58.19	195.26	280.57	338.53	314.77	163.92	401.91	270.51	365.14	29.23
2064	3.45	0.00	60.91	120.58	213.46	376.00	290.32	217.19	323.06	150.35	44.71	42.96
2065	8.86	0.00	8.44	11.96	314.72	310.60	210.40	254.65	316.02	168.37	44.31	8.31
2066	0.00	46.83	116.11	248.66	273.30	230.56	200.63	285.04	250.26	217.32	43.29	61.21
2067	0.00	0.00	14.00	161.23	278.50	221.18	436.69	242.27	275.34	247.58	74.74	54.11

2068	8.79	11.60	33.63	150.51	519.76	305.81	377.91	304.28	285.49	150.77	42.26	8.45
2069	0.00	0.00	10.28	152.87	288.60	317.88	204.20	235.45	308.18	318.54	45.53	228.29
2070	35.20	10.86	96.56	292.05	328.81	407.64	241.75	368.34	295.82	355.40	71.76	95.64
2071	0.00	6.24	10.86	133.76	223.69	443.19	244.90	287.90	329.26	239.54	87.60	10.46
2072	0.00	0.00	66.28	109.94	233.96	324.12	347.05	378.67	389.04	226.04	71.45	127.36
2073	69.69	49.68	20.08	176.24	276.35	443.47	176.04	268.87	367.84	278.48	52.65	6.19
2074	38.76	0.00	66.84	108.21	239.11	380.17	339.65	269.54	362.28	218.06	30.61	33.62
2075	0.00	10.16	31.00	91.34	416.29	208.92	476.14	267.06	317.96	161.42	33.88	142.18
2076	16.36	60.94	37.76	147.40	217.92	283.12	216.00	335.42	593.48	258.02	71.13	193.63
2077	2.64	21.70	27.23	76.42	287.37	269.55	282.36	282.66	473.56	281.27	37.99	79.96
2078	3.69	6.48	76.26	218.22	501.58	298.56	361.53	287.03	261.30	184.53	61.44	34.98
2079	11.53	24.31	81.04	113.17	647.75	387.31	360.68	298.39	239.32	404.96	72.45	24.73
2080	105.08	0.00	98.07	124.06	278.37	324.26	398.67	310.56	339.02	234.65	103.81	76.84
2081	3.31	0.00	62.06	362.20	400.58	533.08	227.70	207.33	245.49	192.11	69.59	64.61
2082	0.00	0.00	31.60	236.47	539.59	293.45	349.64	251.37	234.99	77.79	33.67	49.29
2083	0.00	42.85	19.17	191.80	232.94	205.21	396.29	261.67	260.50	201.24	29.89	39.78
2084	6.71	5.50	64.15	266.83	232.81	157.09	224.79	470.66	325.83	189.00	109.35	52.34
2085	0.00	15.77	283.52	176.65	411.36	331.57	257.97	316.10	358.32	212.24	36.86	5.78
2086	0.00	29.71	61.05	68.35	188.48	278.39	292.10	333.67	356.35	191.71	54.94	47.62
2087	25.31	17.18	49.14	278.10	324.14	316.35	176.11	252.89	393.35	221.80	24.47	19.09
2088	32.82	0.00	95.61	80.20	336.61	308.45	240.24	309.13	263.15	142.56	97.91	16.37
2089	7.00	0.00	62.77	94.83	286.01	337.08	298.96	412.33	275.30	243.82	177.94	166.81
2090	0.00	7.68	61.51	314.10	341.43	418.43	306.36	296.73	200.86	294.75	160.40	3.58
2091	0.00	0.00	95.25	340.34	225.38	395.28	306.95	342.66	329.20	184.46	192.91	58.64
2092	0.00	0.00	36.26	338.66	388.41	314.39	368.90	491.12	352.18	221.01	226.34	3.33
2093	24.65	0.00	102.91	315.49	124.86	277.81	373.48	420.63	335.97	392.64	68.58	18.97
2094	0.00	0.00	167.77	291.38	322.98	565.87	264.54	174.47	259.69	176.88	207.94	57.97
2095	5.74	130.89	65.32	82.47	234.71	257.26	308.91	450.43	305.84	256.90	106.88	2.91
2096	0.00	0.00	66.23	133.66	400.89	370.51	300.07	325.26	369.19	158.39	12.81	36.13
2097	0.00	0.00	39.07	124.51	247.23	407.65	284.25	333.96	308.22	321.77	53.83	121.57
2098	0.00	0.00	32.19	321.74	370.82	284.65	142.07	265.63	247.00	187.02	43.90	0.00
2099	0.00	5.52	16.52	250.69	471.98	460.04	294.62	310.96	406.63	141.56	78.24	148.74
2100	46.74	13.95	71.77	181.07	234.07	363.62	292.32	271.76	176.28	213.38	44.53	87.12

B.3 RCP8.5 data

Precipitation at Bure station (mm)

	Jan	Feb	Mar	Apr	May	Jun	Jul	Aug	Sep	Oct	Nov	Dec
2014	26.15	24.40	26.02	25.43	22.72	21.49	20.44	20.71	21.10	23.04	23.32	24.31
2015	25.41	25.39	26.30	24.72	22.80	21.67	20.42	20.25	21.47	22.76	23.62	24.10
2016	24.50	24.87	25.74	25.42	24.02	21.82	20.66	20.33	22.15	22.82	23.02	23.27
2017	23.69	24.91	24.68	24.77	23.36	20.11	20.14	20.32	21.22	23.44	23.31	23.28
2018	23.12	24.06	24.77	24.97	21.22	20.30	19.85	20.59	20.27	22.18	22.44	23.68
2019	24.28	25.55	25.89	24.46	23.30	21.06	21.01	21.07	21.87	22.64	23.68	23.83
2020	24.19	25.85	23.98	24.35	22.94	21.12	20.13	20.57	21.26	23.37	23.97	23.85
2021	24.00	25.16	25.70	24.99	22.71	21.03	19.78	20.07	22.09	22.99	23.41	24.01
2022	25.06	26.45	24.66	24.04	23.24	20.54	19.47	19.80	20.29	23.13	23.21	23.48
2023	24.05	25.13	25.29	26.84	23.77	20.53	19.63	20.27	21.01	23.36	22.98	23.23
2024	24.44	24.26	24.52	25.95	22.38	20.50	21.01	20.16	20.91	23.13	23.02	23.38
2025	24.46	25.57	26.92	25.54	23.11	21.69	20.42	19.89	21.07	22.79	23.34	23.87
2026	24.10	25.44	25.20	25.03	23.10	22.41	20.17	20.88	21.49	22.86	23.59	24.62
2027	25.48	25.72	25.56	24.77	23.62	21.09	19.69	20.30	21.23	22.29	23.10	24.38
2028	25.59	26.04	25.66	25.85	24.06	20.76	20.22	21.19	21.73	22.82	24.03	24.86
2029	24.42	26.39	26.44	24.76	23.98	21.74	20.71	20.56	20.85	23.05	24.27	24.54
2030	25.64	26.55	25.79	26.50	24.04	21.20	19.82	20.64	20.88	23.23	24.12	25.42
2031	26.29	26.08	27.09	27.55	22.91	21.78	21.10	19.77	21.25	22.94	22.69	24.98
2032	25.53	25.88	27.23	26.09	24.20	21.75	22.18	21.74	23.02	23.48	24.80	25.68
2033	25.10	27.01	27.02	25.73	24.06	23.05	22.48	20.67	22.55	23.57	23.89	25.17
2034	26.02	25.87	26.64	27.58	23.19	21.54	20.75	21.21	21.39	23.99	23.92	24.33
2035	26.26	26.53	26.49	27.35	25.15	21.92	20.31	20.26	21.49	23.84	23.62	24.06
2036	24.30	25.85	26.01	27.42	25.02	21.86	21.14	21.12	22.20	23.70	22.93	25.05
2037	25.37	25.46	25.74	27.09	23.11	22.21	21.46	20.82	22.46	23.66	23.82	24.11
2038	26.08	26.34	27.99	25.73	24.44	21.79	20.42	21.48	22.11	23.99	24.34	25.15
2039	26.84	27.15	27.58	26.01	24.96	22.68	22.36	21.81	22.55	25.07	24.78	25.05
2040	26.71	27.55	26.36	26.34	23.88	21.55	20.77	20.72	22.33	24.64	24.58	25.01
2041	26.09	27.60	26.70	28.61	26.68	21.95	21.00	21.49	22.07	24.47	24.69	25.37
2042	26.30	27.26	26.61	26.78	23.24	21.37	19.55	20.62	22.01	23.34	23.66	25.08
2043	25.67	26.54	25.10	26.14	25.19	22.97	21.92	21.48	22.39	24.46	24.22	25.69
2044	26.82	26.49	27.67	27.12	26.06	22.26	22.44	21.05	22.87	25.25	25.11	26.79
2045	26.50	27.27	26.32	27.42	23.33	20.96	19.68	21.04	21.18	24.33	24.36	23.86
2046	25.30	27.00	25.75	25.80	24.24	22.43	20.70	21.00	22.62	24.51	24.34	25.05
2047	26.43	26.77	27.25	25.64	24.20	23.64	21.89	21.28	23.23	24.51	24.27	24.44
2048	24.52	26.95	25.73	25.79	23.77	21.55	19.62	20.70	21.91	23.42	24.34	24.71
2049	27.11	26.77	28.41	27.90	25.40	22.19	22.18	21.55	23.45	25.13	24.88	25.13
2050	25.48	26.57	26.80	27.94	24.66	22.18	21.32	21.96	23.41	23.91	24.54	26.55
2051	26.87	27.23	28.30	27.89	25.18	22.72	22.15	22.13	24.04	25.00	25.53	27.00

2052	27.66	27.14	28.35	25.60	25.50	23.07	22.44	21.97	22.92	24.57	25.05	25.18
2053	24.65	27.07	25.93	25.37	25.66	22.10	21.79	21.34	23.00	25.66	25.21	26.47
2054	26.42	26.93	26.49	27.01	25.31	22.52	22.97	21.98	23.61	24.87	25.10	25.84
2055	26.97	28.14	27.87	26.57	26.14	23.51	21.93	22.58	23.18	24.80	24.84	25.69
2056	26.45	26.59	27.15	26.45	23.96	22.24	20.86	20.65	21.93	23.81	24.66	25.65
2057	26.04	27.28	26.45	29.08	25.94	22.06	21.27	21.59	23.73	24.34	24.89	25.65
2058	25.72	27.49	26.74	27.32	25.36	23.92	23.10	21.87	23.51	24.82	25.13	26.88
2059	27.19	27.55	28.75	27.66	27.49	22.48	22.38	21.80	23.50	24.69	24.87	25.32
2060	26.81	27.75	26.55	26.57	25.99	22.22	21.26	22.11	23.64	24.97	25.52	26.91
2061	26.99	26.64	27.51	28.93	25.76	21.76	22.03	21.78	23.23	24.57	24.30	26.47
2062	25.50	27.77	28.97	27.75	25.53	23.80	22.95	22.96	25.22	25.30	25.61	26.19
2063	24.45	28.00	27.76	27.36	24.79	23.86	23.91	22.51	24.44	26.67	25.71	26.66
2064	25.78	27.74	26.81	30.16	25.87	23.96	22.31	22.34	23.95	24.57	24.94	26.62
2065	28.33	30.02	29.00	31.05	27.42	23.82	22.29	21.70	22.00	24.60	24.78	25.91
2066	26.09	27.70	26.79	26.07	23.99	22.31	21.37	22.17	23.36	24.91	24.91	26.30
2067	26.65	26.88	27.97	28.09	25.46	22.46	21.49	21.28	23.28	24.90	24.05	25.57
2068	25.67	27.06	28.44	27.04	24.44	21.56	21.88	21.32	23.37	24.81	25.30	25.98
2069	26.03	28.53	30.68	28.67	26.33	23.33	22.97	22.14	23.57	26.31	26.20	26.13
2070	26.56	26.56	28.11	26.93	25.53	24.09	21.85	22.49	23.79	25.87	25.43	26.33
2071	26.98	28.12	27.95	28.13	26.40	21.94	21.56	21.73	23.85	24.57	24.96	25.95
2072	25.67	27.44	28.29	26.87	24.86	22.84	20.99	22.38	23.97	24.93	24.85	26.56
2073	26.53	27.16	27.72	28.44	25.93	23.61	22.58	21.58	24.44	25.07	25.58	27.01
2074	27.73	27.65	27.74	28.06	26.37	24.70	23.15	23.21	24.34	25.84	25.90	27.56
2075	29.70	28.78	30.28	29.50	26.78	23.69	22.72	22.11	23.69	25.85	25.11	26.98
2076	26.63	27.46	28.99	27.10	27.84	21.97	21.60	22.11	24.43	24.17	24.91	26.67
2077	27.58	28.28	27.35	28.64	26.26	23.63	21.48	22.31	23.41	24.34	25.14	26.05
2078	25.94	26.94	26.39	27.25	25.34	23.27	23.42	21.63	23.44	26.62	25.72	27.28
2079	27.79	28.81	28.10	28.93	25.46	22.56	22.13	21.15	22.92	25.78	25.81	24.64
2080	25.41	27.57	28.02	27.64	25.99	24.68	23.53	23.25	24.80	26.21	26.41	27.02
2081	29.04	29.79	30.07	27.78	27.12	23.65	22.11	22.18	23.73	26.27	24.86	27.38
2082	26.91	28.46	28.98	28.97	26.58	22.68	21.69	22.20	24.44	25.62	25.46	26.58
2083	27.26	28.96	28.57	28.89	28.04	23.48	21.78	22.04	23.71	24.27	25.11	26.33
2084	26.74	28.43	28.18	29.59	25.63	23.43	23.06	22.36	24.40	25.61	26.15	25.70
2085	27.89	28.12	28.29	28.25	25.57	23.98	21.73	20.99	23.93	25.70	25.99	27.08
2086	27.67	27.77	28.47	28.39	26.91	23.65	23.32	22.59	24.66	25.20	26.53	26.64
2087	28.26	28.70	28.65	27.08	27.60	24.90	22.43	21.85	24.28	26.11	25.63	27.04
2088	26.38	27.50	27.95	28.12	27.70	23.24	22.57	23.16	23.70	26.29	26.04	26.57
2089	28.03	28.91	28.92	28.62	26.90	23.05	21.95	21.70	23.69	25.05	25.99	26.38
2090	27.04	28.10	28.43	26.10	26.49	23.51	22.72	22.81	24.74	25.59	25.01	26.59
2091	26.86	28.05	27.76	27.84	25.82	23.23	21.81	22.51	23.96	25.59	25.93	26.44
2092	27.14	28.90	27.95	28.14	26.66	23.50	21.00	22.09	23.85	25.97	24.76	27.29
2093	27.39	28.40	26.20	27.70	26.60	24.42	22.40	22.18	24.13	24.93	25.50	25.60
2094	24.96	27.89	27.58	26.59	25.33	23.43	21.77	21.81	24.04	24.90	26.05	28.38

2095	27.81	28.24	26.94	27.80	26.46	23.59	21.92	23.25	24.19	26.24	26.57	27.35
2096	28.33	29.02	28.77	30.61	26.58	24.10	23.00	21.64	23.57	25.70	26.75	28.07
2097	27.37	27.60	28.64	27.06	26.80	23.86	22.73	21.97	23.90	26.22	25.36	26.72
2098	26.69	27.76	28.24	27.11	26.07	23.54	22.56	22.53	24.97	25.66	25.64	26.95
2099	27.81	28.72	28.69	28.14	26.72	22.44	21.50	21.79	23.94	26.05	26.02	28.26
2100	27.95	28.78	28.45	27.48	26.61	23.67	23.10	23.01	24.47	26.16	25.52	27.63

Precipitation at Gatira station (mm)

	Jan	**Feb**	**Mar**	**Apr**	**May**	**Jun**	**Jul**	**Aug**	**Sep**	**Oct**	**Nov**	**Dec**
2014	17.92	17.08	17.94	18.13	17.57	16.83	15.64	16.31	16.60	16.98	17.13	17.05
2015	17.95	17.95	18.51	18.02	17.32	16.98	15.93	16.01	16.50	17.00	17.21	17.27
2016	17.49	17.46	18.29	18.49	18.01	17.08	15.97	15.96	16.84	16.65	16.73	16.52
2017	16.81	17.42	17.70	18.09	17.89	16.48	15.85	15.96	16.72	16.87	16.72	16.57
2018	16.92	17.16	17.56	18.05	16.59	16.15	15.48	16.02	16.06	16.46	16.51	16.79
2019	17.01	17.82	18.24	17.66	17.83	16.90	15.97	16.11	16.93	16.84	17.26	17.27
2020	17.42	17.94	17.69	17.30	17.36	16.77	15.99	15.95	16.52	17.03	16.92	16.86
2021	17.01	17.18	17.96	18.09	17.60	16.71	15.71	15.70	16.76	16.69	16.95	16.92
2022	17.74	18.18	17.33	17.36	17.61	16.56	15.53	15.90	16.28	16.88	16.51	16.68
2023	17.17	17.34	17.76	18.69	18.10	16.69	15.46	15.89	16.21	16.92	16.68	16.60
2024	17.19	16.67	17.38	18.51	17.28	16.43	16.16	15.89	16.33	16.80	16.57	16.41
2025	16.95	17.61	18.43	18.21	17.53	17.32	15.97	15.96	16.63	16.62	16.63	16.43
2026	16.65	17.27	17.79	17.72	17.60	17.48	16.07	16.29	16.76	16.86	16.91	16.90
2027	17.76	17.76	18.25	18.17	17.64	16.62	15.35	15.84	16.60	16.64	16.53	16.80
2028	17.29	17.36	17.90	18.41	17.97	16.74	15.68	16.13	16.62	16.93	17.56	17.45
2029	17.22	18.06	18.44	17.73	17.94	17.15	16.21	16.02	16.64	16.99	17.35	17.06
2030	17.74	18.24	17.97	19.10	18.38	17.06	15.37	16.11	16.35	17.07	17.42	17.55
2031	18.07	18.16	19.00	19.57	17.56	17.02	16.22	16.08	16.80	16.74	16.55	17.14
2032	17.41	18.14	18.97	18.96	18.36	17.29	16.49	16.72	17.25	17.47	17.93	17.44
2033	17.79	18.57	18.54	18.09	18.03	17.67	16.84	16.26	16.91	17.03	17.21	17.19
2034	17.77	18.24	18.07	19.18	17.46	17.05	16.11	16.70	16.77	17.13	17.20	16.83
2035	17.97	18.37	18.30	19.00	18.16	17.01	15.77	15.85	16.45	16.96	16.98	16.87
2036	17.09	17.89	18.15	18.89	18.40	17.12	16.29	16.15	16.74	17.36	16.83	17.28
2037	17.69	17.62	18.01	18.47	17.70	17.26	16.24	16.58	17.13	17.17	17.10	17.14
2038	17.85	18.03	18.98	18.69	18.21	17.22	16.17	16.61	17.13	17.38	17.42	17.56
2039	18.16	18.44	18.77	18.76	18.79	17.77	16.91	16.95	17.59	17.73	17.69	17.29
2040	17.85	18.78	18.49	18.94	18.33	17.23	16.18	16.22	17.08	17.48	17.52	17.42
2041	18.06	18.98	18.90	19.37	18.64	17.38	16.43	16.73	17.17	17.15	17.53	17.23
2042	17.71	18.19	18.42	19.13	17.67	17.13	15.68	16.21	16.95	16.80	16.84	17.00
2043	17.56	18.13	17.82	18.66	18.70	17.91	16.82	16.93	17.06	17.45	17.31	17.52
2044	18.51	18.38	19.47	19.18	19.05	17.75	17.01	16.66	16.99	17.68	17.47	17.62
2045	17.83	18.47	18.33	19.46	18.16	16.63	15.68	16.39	17.04	17.40	17.10	16.86

2046	17.48	18.48	18.55	18.83	17.90	17.69	16.21	16.63	17.19	17.36	17.39	17.30
2047	18.17	18.35	18.92	18.39	18.05	18.07	17.05	16.77	17.43	17.59	16.97	17.10
2048	17.34	18.48	18.32	18.78	18.36	17.40	15.69	16.47	17.09	16.98	17.08	17.09
2049	18.34	18.10	19.16	19.54	18.97	17.44	16.83	16.71	17.46	17.55	17.47	17.41
2050	17.58	18.27	18.63	20.16	18.53	17.48	16.48	17.06	17.52	17.27	17.64	17.63
2051	18.55	19.26	19.41	19.92	19.02	17.85	16.70	17.16	17.94	17.84	18.00	17.81
2052	18.39	18.57	19.00	18.66	19.07	18.14	17.03	17.14	17.84	17.70	17.39	17.32
2053	17.12	18.16	18.20	18.46	19.22	17.54	16.89	16.70	17.51	17.97	17.77	17.65
2054	18.18	18.35	18.82	19.52	19.72	17.78	17.20	16.91	17.70	17.77	17.33	17.24
2055	18.06	19.01	19.12	18.95	19.53	18.12	16.63	16.94	17.53	17.58	17.55	17.44
2056	17.82	17.78	18.63	19.23	18.08	17.49	16.45	16.46	17.27	17.19	17.22	17.29
2057	17.77	18.50	18.30	20.03	18.94	17.57	16.72	16.68	17.74	17.41	17.58	17.59
2058	17.67	18.79	18.81	19.41	18.71	18.53	17.48	16.95	17.98	18.02	18.31	18.15
2059	18.40	18.84	19.76	20.00	20.15	17.77	17.01	16.86	17.72	17.59	17.41	17.10
2060	17.99	18.76	18.73	19.01	19.26	17.78	16.37	16.85	17.78	17.72	17.99	17.86
2061	18.20	18.47	19.36	19.87	18.82	17.52	16.96	16.80	17.72	17.37	17.06	17.67
2062	17.90	18.67	19.89	20.45	19.07	18.54	17.20	17.48	18.25	17.93	17.77	17.76
2063	17.56	18.72	19.37	19.40	18.70	18.13	17.52	17.35	18.24	18.04	17.71	17.64
2064	18.05	18.83	19.22	20.60	19.07	18.54	16.88	17.10	18.01	17.55	17.75	17.56
2065	18.59	19.92	19.93	20.85	19.75	18.24	16.90	16.86	17.22	17.62	17.78	17.83
2066	18.03	18.39	18.37	19.05	18.29	17.33	16.64	16.75	17.47	17.40	17.38	17.69
2067	18.45	18.75	19.52	20.01	18.68	17.52	16.44	16.81	17.60	17.43	17.38	17.55
2068	17.90	18.65	19.34	19.61	18.50	17.36	16.87	16.60	17.56	17.68	17.96	17.80
2069	18.09	19.40	20.84	20.47	19.45	18.28	17.45	17.13	18.04	17.87	17.67	17.44
2070	17.95	17.93	19.41	19.03	19.34	18.33	16.91	17.55	17.76	17.89	17.72	17.56
2071	18.00	18.98	19.24	19.81	19.34	17.34	16.53	16.75	17.85	17.41	17.53	17.73
2072	17.95	19.03	19.92	19.21	18.40	18.06	16.21	17.11	18.22	17.56	17.59	17.98
2073	18.25	18.37	19.10	19.72	19.01	18.42	16.80	16.69	18.12	18.02	18.21	18.36
2074	18.34	19.04	19.09	19.24	19.72	18.74	17.64	17.99	18.24	18.35	18.24	18.17
2075	19.25	19.40	20.52	20.72	19.49	18.33	17.19	17.04	17.85	17.82	17.74	17.99
2076	17.88	18.52	19.52	19.08	19.55	17.45	16.43	17.21	18.36	17.38	17.55	17.78
2077	18.66	18.92	19.17	20.06	19.52	18.32	16.73	17.28	17.88	17.45	17.44	17.43
2078	17.82	18.35	18.58	19.04	18.93	17.96	17.65	17.12	18.05	18.31	17.70	17.81
2079	18.64	19.48	19.61	20.06	19.23	18.03	16.66	16.76	17.83	18.02	17.72	17.20
2080	17.68	18.44	19.34	19.90	19.22	18.75	17.62	17.96	18.23	18.25	18.22	18.11
2081	19.07	19.86	20.49	20.33	20.27	18.46	17.25	17.29	17.96	18.11	17.54	17.97
2082	18.41	19.42	19.88	20.24	19.45	17.98	16.77	17.34	18.35	17.97	18.13	17.82
2083	18.94	19.91	19.81	20.06	20.29	18.39	16.82	17.32	17.97	17.41	17.82	17.86
2084	18.38	19.54	19.27	20.42	19.19	18.40	17.35	17.44	18.31	18.02	18.40	17.77
2085	18.95	19.33	19.49	20.11	18.97	18.74	16.85	16.64	17.96	17.87	17.92	17.94
2086	18.56	18.98	19.88	20.13	19.75	18.23	17.13	17.35	18.08	18.31	18.41	17.83
2087	18.69	19.82	19.73	19.60	20.13	18.78	17.04	17.12	18.11	18.15	17.96	18.00
2088	18.52	18.90	19.67	20.13	20.37	18.26	16.98	17.28	18.01	17.94	18.12	17.76

2089	18.75	19.34	19.97	20.42	19.46	18.16	16.70	17.21	18.00	17.79	17.92	17.79
2090	17.98	18.79	19.77	19.26	19.55	18.18	17.03	17.19	18.19	17.77	17.54	17.59
2091	18.39	18.89	19.22	19.33	19.14	18.23	16.74	17.31	18.28	17.95	17.89	17.75
2092	18.48	18.77	19.27	19.26	19.55	18.32	16.63	17.05	18.13	18.00	17.37	17.65
2093	18.57	19.54	18.44	19.70	19.41	18.90	17.52	17.42	18.15	17.90	17.66	17.68
2094	18.22	19.18	19.21	19.46	19.35	18.07	16.83	16.94	17.97	17.80	17.96	18.35
2095	18.43	19.05	19.24	19.63	19.72	18.40	17.01	17.81	18.50	18.37	18.15	17.93
2096	19.15	19.86	20.04	21.15	19.65	18.64	17.64	16.95	18.02	17.95	18.20	18.22
2097	18.72	18.87	19.77	19.43	19.35	18.55	17.34	17.24	18.02	17.96	17.55	17.67
2098	18.25	18.95	19.63	19.58	19.56	18.18	16.70	17.25	18.52	18.22	18.25	18.21
2099	18.84	19.44	19.74	20.28	19.69	17.63	16.58	17.14	18.05	18.18	18.25	18.35
2100	18.76	19.60	19.86	20.37	20.04	18.34	17.64	17.36	18.32	18.46	18.10	18.25

C. Hydrological data

C.1. Annual flow Masha gauge (m^3/s)

	Jan	Feb	Mar	Apr	May	Sep	Oct	Nov	Dec
1988	2155.207	1770.269	1570.206	3189.493	8624.201	15465.43	7342.098	5096.766	4356.624
1989	199.1568	502.746	775.649	1330.613	1284.798	4525.814	2852.519	622.593	1207.717
1990	197.369	180.155	111.756	115.679	477.031	3317.999	1034.708	225.603	242.925
1991	409.513	224.601	205.499	481.121	3479.565	5216.541	4893.829	2075.383	457.802
1992	180.555	1753.819	2586.129	2594.945	2140.962	4735.964	3106.672	1323.326	721.8868
1993	205.831	89.661	111.415	922.225	1208.553	5997.68	2392.904	1094.154	439.8392
1994	280.414	22.315	30.92	171.85	1518.614	5468.895	3106.672	891.0312	211.146
1995	91.1	101.895	130.624	1053.362	2569.843	3350.579	1861.994	630.645	825.486
1996	418.577	219.255	412.171	481.746	1149.582	5275.115	3972.09	414.037	311.624
1997	231.907	133.663	129.925	912.559	1972.362	4024.342	2127.076	3414.298	416.652
1998	202.306	53.834	473.184	482.365	722.481	4068.086	4329.773	810.497	239.704
1999	149.951	140.344	92.39	244.079	2151.885	2710.222	3192.588	678.79	269.213
2000	149.951	145.847	88.592	261.397	2249.091	2686.199	3154.005	637.197	263.737
2001	173.072	72.584	123.744	248.774	1089.941	4249.645	4143.733	1198.825	479.969
2002	538.636	170.127	267.092	398.841	304.667	3428.272	2097.824	1340.318	610.219
2003	367.887	167.023	208.236	153.154	337.012	3909.189	1914.093	702.937	672.266
2004	392.11	271.252	175.553	252.223	797.774	3971.583	2574.092	759.874	780.366
2005	440.209	124.63	82.572	414.175	833.877	4632.187	3329.526	1112.906	499.802
2006	166.796	114.299	135.987	135.876	676.689	4967.599	3106.672	1323.326	750.0779
2007	440.209	124.63	82.572	414.175	833.877	4632.187	3329.526	1112.906	499.802

D. Reservoir Routing

i. Mid (2034-2070) of RCP4.5 Reservoir routing Baro I

Time (hr)	Δt (hr)	Inflow I (cumes)	(I1+I2)/2	((I1+I2)/2)*Δt (MCM)	S-QΔt/2 (MCM)	S+QΔt/2 (MCM)	Elevation (m)	Outflow (cumec)
0.00		105.86				1355.80	1520.00	0.00
	3.00		106.80	1.15	1355.80	1356.95		
3.00		107.74					1520.03	4.76
	3.00		136.85	1.48	1356.90	1358.38		
6.00		165.95					1520.07	10.65
	3.00		285.33	3.08	1358.27	1361.35		
9.00		404.71					1520.14	22.89
	3.00		626.84	6.77	1361.10	1367.87		
12.00		848.98					1520.31	49.80
	3.00		1130.23	12.21	1367.33	1379.54		
15.00		1411.47					1520.62	112.74
	3.00		1749.80	18.90	1378.32	1397.22		
18.00		2088.12					1521.07	249.11
	3.00		2482.19	26.81	1394.53	1421.34		
21.00		2876.25					1521.67	489.82
	3.00		3225.46	34.83	1416.05	1450.88		
24.00		3574.67					1522.41	840.60
	3.00		3733.78	40.32	1441.80	1482.13		
27.00		3892.90					1523.18	1273.33
	3.00		3852.37	41.61	1468.37	1509.98		
30.00		3811.84					1523.86	1701.47
	3.00		3663.89	39.57	1491.60	1531.17		
33.00		3515.95					1524.37	2051.62
	3.00		3312.44	35.77	1509.02	1544.79		
36.00		3108.94					1524.60	2216.07
	3.00		2890.09	31.21	1520.86	1552.07		
39.00		2671.25					1524.69	2281.54
	3.00		2461.19	26.58	1527.43	1554.01		
42.00		2251.14					1524.71	2298.99
	3.00		2063.75	22.29	1529.18	1551.47		
45.00		1876.37					1524.68	2276.14
	3.00		1725.68	18.64	1526.89	1545.53		
48.00		1575.00					1524.61	2222.68
	3.00		1448.84	15.65	1521.52	1537.17		
51.00		1322.67					1524.51	2147.51
	3.00		1206.35	13.03	1513.98	1527.00		
54.00		1090.03					1524.27	1981.62
	3.00		983.23	10.62	1505.60	1516.22		
57.00		876.42					1524.01	1800.69
	3.00		772.52	8.34	1496.77	1505.12		
60.00		668.62					1523.74	1624.39

	3.00		573.13	6.19	1487.57	1493.76		
63.00		477.64					1523.46	1446.03
	3.00		402.48	4.35	1478.15	1482.49		
66.00		327.31					1523.19	1278.76
	3.00		277.27	2.99	1468.68	1471.68		
69.00		227.24					1522.92	1121.78
	3.00		196.74	2.12	1459.56	1461.69		
72.00		166.25					1522.67	984.52
	3.00		143.27	1.55	1451.05	1452.60		
75.00		120.28					1522.45	862.13
	3.00		113.07	1.22	1443.29	1444.51		
78.00		105.86					1522.25	761.78

ii. Far future (2071-2100) of RCP4.5 Reservoir routing Baro I

Time (hr)	Δt (hr)	Inflow I (cumes)	(I1+I2)/2	((I1+I2)/2)*Δt (MCM)	S-QΔt/2 (MCM)	S+QΔt/2 (MCM)	Elevation (m)	Outflow (cumec)
0.00		105.86				1355.80	1520.00	0.00
	3.00		106.13	1.15	1355.80	1356.95		
3.00		106.41					1520.03	4.73
	3.00		128.69	1.39	1356.90	1358.29		
6.00		150.98					1520.06	10.25
	3.00		247.07	2.67	1358.17	1360.84		
9.00		343.16					1520.13	20.81
	3.00		523.41	5.65	1360.62	1366.27		
12.00		703.66					1520.27	43.20
	3.00		931.06	10.06	1365.80	1375.86		
15.00		1158.45					1520.52	85.49
	3.00		1432.06	15.47	1374.94	1390.40		
18.00		1705.68					1520.89	193.22
	3.00		2026.33	21.88	1388.32	1410.20		
21.00		2346.98					1521.39	372.18
	3.00		2632.53	28.43	1406.18	1434.61		
24.00		2918.08					1522.00	634.70
	3.00		3047.72	32.92	1427.76	1460.67		
27.00		3177.36					1522.65	970.59
	3.00		3143.67	33.95	1450.19	1484.14		
30.00		3109.97					1523.23	1303.23
	3.00		2989.86	32.29	1470.07	1502.36		
33.00		2869.74					1523.67	1580.65
	3.00		2704.54	29.21	1485.29	1514.50		
36.00		2539.34					1523.97	1773.03
	3.00		2361.83	25.51	1495.35	1520.85		
39.00		2184.33					1524.12	1878.44
	3.00		2014.01	21.75	1500.57	1522.32		
42.00		1843.69					1524.16	1903.01

	3.00		1691.63	18.27	1501.77	1520.04		
45.00		1539.56					1524.10	1864.70
	3.00		1417.66	15.31	1499.90	1515.21		
48.00		1295.77					1523.98	1784.32
	3.00		1193.78	12.89	1495.94	1508.83		
51.00		1091.79					1523.83	1683.24
	3.00		997.55	10.77	1490.65	1501.42		
54.00		903.31					1523.65	1565.87
	3.00		816.94	8.82	1484.51	1493.34		
57.00		730.56					1523.45	1439.69
	3.00		646.32	6.98	1477.79	1484.77		
60.00		562.08					1523.24	1261.20
	3.00		484.52	5.23	1471.15	1476.38		
63.00		406.96					1523.04	1188.02
	3.00		345.94	3.74	1463.55	1467.28		
66.00		284.92					1522.81	1061.44
	3.00		244.41	2.64	1455.82	1458.46		
69.00		203.90					1522.60	940.20
	3.00		179.35	1.94	1448.31	1450.24		
72.00		154.81					1522.39	832.63
	3.00		136.02	1.47	1441.25	1442.72		
75.00		117.24					1522.21	738.48
	3.00		111.55	1.20	1434.74	1435.95		
78.00		105.86					1522.04	653.75

iii. Present future (2014-2034) of RCP8.5 Reservoir routing Baro I

Time (hr)	Δt (hr)	Inflow I (cumes)	(I1+I2)/2	((I1+I2)/2)*Δt (MCM)	S-QΔt/2 (MCM)	S+QΔt/2 (MCM)	Elevation (m)	Outflow (cumec)
0.00		105.86				1355.80	1520.00	0.00
	3.00		106.06	1.15	1355.80	1356.95		
3.00		106.25					1520.03	4.73
	3.00		109.43	1.18	1356.89	1358.08		
6.00		112.62					1520.06	9.39
	3.00		156.16	1.69	1357.97	1359.66		
9.00		199.70					1520.10	15.93
	3.00		363.60	3.93	1359.49	1363.42		
12.00		527.50					1520.20	31.42
	3.00		829.05	8.95	1363.08	1372.03		
15.00		1130.61					1520.42	66.97
	3.00		1517.12	16.38	1371.31	1387.69		
18.00		1903.64					1520.82	173.14
	3.00		2370.27	25.60	1385.82	1411.42		
21.00		2836.91					1521.42	383.76
	3.00		3374.90	36.45	1407.28	1443.73		
24.00		3912.89					1522.23	751.06

	3.00		4388.42	47.39	1435.61	1483.01		
27.00		4863.96					1523.20	1286.42
	3.00		5089.29	54.96	1469.12	1524.08		
30.00		5314.63					1524.20	1932.57
	3.00		5272.68	56.94	1503.21	1560.15		
33.00		5230.73					1524.79	2354.23
	3.00		5035.67	54.39	1534.73	1589.11		
36.00		4840.61					1525.14	2619.29
	3.00		4564.05	49.29	1560.82	1610.12		
39.00		4287.49					1525.40	2765.72
	3.00		3986.80	43.06	1580.25	1623.30		
42.00		3686.11					1525.64	3004.89
	3.00		3395.59	36.67	1590.85	1627.52		
45.00		3105.06					1525.76	3100.50
	3.00		2845.04	30.73	1594.04	1624.76		
48.00		2585.03					1525.68	3037.99
	3.00		2373.87	25.64	1591.95	1617.59		
51.00		2162.72					1525.49	2886.59
	3.00		1985.34	21.44	1586.42	1607.86		
54.00		1807.95					1525.37	2795.23
	3.00		1645.67	17.77	1577.67	1595.44		
57.00		1483.38					1525.22	2678.71
	3.00		1334.42	14.41	1566.51	1580.92		
60.00		1185.45					1525.04	2542.44
	3.00		1041.31	11.25	1553.47	1564.71		
63.00		897.16					1524.85	2395.23
	3.00		765.14	8.26	1538.84	1547.11		
66.00		633.12					1524.63	2236.90
	3.00		528.47	5.71	1522.95	1528.66		
69.00		423.82					1524.31	2009.36
	3.00		352.99	3.81	1506.96	1510.77		
72.00		282.17					1523.88	1713.95
	3.00		238.19	2.57	1492.26	1494.83		
75.00		194.22					1523.49	1461.86
	3.00		162.03	1.75	1479.04	1480.79		
78.00		129.85					1523.14	1253.51
	3.00		117.85	1.27	1467.25	1468.53		
81.00		105.86					1522.84	1078.50

Iv. Mid (2034-2070) of RCP8.5 Reservoir routing Baro I

Time (hr.)	Δt (hr.)	Inflow I (cumes)	(I1+I2)/2	((I1+I2)/2)*Δt (MCM)	S-QΔt/2 (MCM)	S+QΔt/2 (MCM)	Elevation (m)	Outflow (cumec)
0.00		105.86				1355.80	1520.00	0.00
	3.00		107.11	1.16	1355.80	1356.96		
3.00		108.37					1520.03	4.77

	3.00		117.46	1.27	1356.91	1358.17		
6.00		126.55					1520.06	9.79
	3.00		179.10	1.93	1358.07	1360.00		
9.00		231.65					1520.11	17.34
	3.00		389.04	4.20	1359.82	1364.02		
12.00		546.43					1520.21	33.90
	3.00		809.57	8.74	1363.65	1372.39		
15.00		1072.70					1520.43	68.47
	3.00		1394.62	15.06	1371.65	1386.72		
18.00		1716.54					1520.80	165.92
	3.00		2096.44	22.64	1384.92	1407.57		
21.00		2476.34					1521.33	347.21
	3.00		2895.47	31.27	1403.82	1435.09		
24.00		3314.60					1522.02	642.96
	3.00		3651.46	39.44	1428.14	1467.58		
27.00		3988.32					1522.82	1065.48
	3.00		4105.73	44.34	1456.07	1500.41		
30.00		4223.15					1523.62	1549.85
	3.00		4140.28	44.72	1483.68	1528.39		
33.00		4057.42					1524.30	2004.90
	3.00		3877.95	41.88	1506.74	1548.62		
36.00		3698.48					1524.65	2250.50
	3.00		3470.30	37.48	1524.31	1561.79		
39.00		3242.12					1524.81	2368.98
	3.00		3005.52	32.46	1536.21	1568.67		
42.00		2768.92					1524.89	2430.81
	3.00		2546.85	27.51	1542.42	1569.92		
45.00		2324.77					1524.91	2442.08
	3.00		2130.18	23.01	1543.55	1566.55		
48.00		1935.59					1524.87	2411.78
	3.00		1779.93	19.22	1540.51	1559.73		
51.00		1624.26					1524.78	2350.41
	3.00		1491.45	16.11	1534.34	1550.45		
54.00		1358.64					1524.67	2266.98
	3.00		1234.65	13.33	1525.97	1539.30		
57.00		1110.67					1524.53	2166.71
	3.00		996.44	10.76	1515.90	1526.66		
60.00		882.21					1524.26	1975.92
	3.00		771.65	8.33	1505.32	1513.66		
63.00		661.10					1523.95	1759.76
	3.00		562.40	6.07	1494.65	1500.73		
66.00		463.70					1523.63	1554.80
	3.00		388.85	4.20	1483.93	1488.13		
69.00		313.99					1523.32	1362.48
	3.00		265.47	2.87	1473.42	1476.29		
72.00		216.95					1523.03	1186.64
	3.00		187.49	2.02	1463.47	1465.50		
75.00		158.02					1522.77	1036.85
	3.00		136.20	1.47	1454.30	1455.77		

78.00		114.39					1522.53	903.21
	3.00		110.13	1.19	1446.01	1447.20		
81.00		105.86					1522.32	794.58

v, Far future (2071-2100) of RCP8.5 Reservoir routing Baro I

Time (hr)	Δt (hr)	Inflow I (cumes)	(I1+I2)/2	((I1+I2)/2)*Δt (MCM)	S-QΔt/2 (MCM)	S+QΔt/2 (MCM)	Elevation (m)	Outflow (cumec)
0.00		105.86				1355.80	1520.00	0.00
	3.00		106.16	1.15	1355.80	1356.95		
3.00		106.46					1520.03	4.73
	3.00		129.03	1.39	1356.90	1358.29		
6.00		151.59					1520.06	10.27
	3.00		248.65	2.69	1358.18	1360.86		
9.00		345.72					1520.13	20.89
	3.00		527.72	5.70	1360.64	1366.34		
12.00		709.72					1520.27	43.48
	3.00		939.36	10.15	1365.87	1376.01		
15.00		1169.00					1520.53	83.40
	3.00		1445.32	15.61	1375.11	1390.72		
18.00		1721.64					1520.90	195.58
	3.00		2045.36	22.09	1388.61	1410.70		
21.00		2369.08					1521.41	376.92
	3.00		2657.30	28.70	1406.63	1435.33		
24.00		2945.52					1522.03	610.40
	3.00		3076.39	33.23	1428.73	1461.96		
27.00		3207.27					1522.69	940.91
	3.00		3173.28	34.27	1451.80	1486.07		
30.00		3139.30					1523.28	1280.97
	3.00		3018.02	32.59	1472.24	1504.83		
33.00		2896.75					1523.74	1577.28
	3.00		2729.94	29.48	1487.80	1517.28		
36.00		2563.14					1524.04	1748.32
	3.00		2383.90	25.75	1498.40	1524.14		
39.00		2204.67					1524.20	1896.91
	3.00		2032.69	21.95	1503.66	1525.61		
42.00		1860.71					1524.24	1918.68
	3.00		1707.17	18.44	1504.89	1523.33		
45.00		1553.63					1524.18	1884.77
	3.00		1430.53	15.45	1502.97	1518.42		
48.00		1307.43					1524.07	1763.99
	3.00		1204.43	13.01	1499.37	1512.38		
51.00		1101.43					1523.92	1680.96
	3.00		1006.27	10.87	1494.22	1505.09		
54.00		911.11					1523.74	1580.85
	3.00		823.89	8.90	1488.02	1496.91		

57.00		736.66					1523.54	1468.53
	3.00		651.59	7.04	1481.05	1488.09		
60.00		566.53					1523.32	1347.31
	3.00		488.22	5.27	1473.54	1478.81		
63.00		409.91					1523.10	1190.16
	3.00		348.30	3.76	1465.96	1469.72		
66.00		286.69					1522.88	1076.38
	3.00		245.78	2.65	1458.10	1460.75		
69.00		204.87					1522.65	964.12
	3.00		180.08	1.94	1450.34	1452.28		
72.00		155.29					1522.45	833.29
	3.00		136.33	1.47	1443.28	1444.76		
75.00		117.36					1522.26	749.57
	3.00		111.61	1.21	1436.66	1437.87		
78.00		105.86					1522.09	672.94

vi. Present future (2014-2034) of RCP4.5 Reservoir routing Baro II

Time (hr)	Δt (hr)	Inflow I (cumes)	(I1+I2)/2	((I1+I2)/2)*Δt (MCM)	S-QΔt/2 (MCM)	S+QΔt/2 (MCM)	Elevation (m)	Outflow (cumec)
0		0.00				45.96	1320.00	0.00
	3		0.54	0.01	45.96	45.97		
3		1.09					1320.00	0.06
	3		3.02	0.03	45.97	46.00		
6		4.95					1320.00	0.40
	3		7.37	0.08	45.99	46.07		
9		9.79					1320.01	1.20
	3		13.60	0.15	46.06	46.21		
12		17.40					1320.01	2.61
	3		25.24	0.27	46.18	46.45		
15		33.09					1320.02	5.20
	3		51.10	0.55	46.40	46.95		
18		69.11					1320.05	10.44
	3		109.66	1.18	46.83	48.02		
21		150.21					1320.10	21.78
	3		226.93	2.45	47.78	50.23		
24		303.65					1320.22	45.21
	3		424.81	4.59	49.75	54.33		
27		545.98					1320.42	88.58
	3		713.35	7.70	53.38	61.08		
30		880.73					1320.75	200.93
	3		1088.09	11.75	58.91	70.66		
33		1295.46					1321.20	398.73
	3		1488.62	16.08	66.36	82.43		
36		1681.78					1321.75	692.09
	3		1837.00	19.84	74.96	94.80		

39		1992.22					1322.31	1045.34
	3		2084.87	22.52	83.51	106.03		
42		2177.51					1322.81	1399.25
	3		2201.15	23.77	90.91	114.69		
45		2224.78					1323.18	1690.66
	3		2229.15	24.07	96.43	120.50		
48		2233.52					1323.44	1893.20
	3		2220.12	23.98	100.06	124.03		
51		2206.72					1323.59	2020.40
	3		2173.35	23.47	102.21	125.68		
54		2139.99					1323.66	2081.35
	3		2078.85	22.45	103.21	125.66		
57		2017.71					1323.66	2080.36
	3		1940.88	20.96	103.19	124.15		
60		1864.04					1323.59	2024.78
	3		1782.27	19.25	102.28	121.53		
63		1700.50					1323.48	1929.07
	3		1617.36	17.47	100.70	118.17		
66		1534.22					1323.33	1811.83
	3		1452.17	15.68	98.60	114.28		
69		1370.12					1323.17	1676.56
	3		1291.45	13.95	96.17	110.12		
72		1212.79					1322.99	1532.48
	3		1140.67	12.32	93.57	105.89		
75		1068.55					1322.80	1394.86
	3		1003.75	10.84	90.83	101.67		
78		938.94					1322.61	1249.50

vii. Mid (2034-2070) of RCP4.5 Reservoir routing Baro II

Time (hr.)	Δt (hr)	Inflow I (cumes)	(I1+I2)/2	((I1+I2)/2)*Δt (MCM)	S-QΔt/2 (MCM)	S+QΔt/2 (MCM)	Elevation (m)	Outflow (cumec)
0		0.00				45.96	1320.00	0.00
	3		1.41	0.02	45.96	45.98		
3		2.82					1320.00	0.16
	3		8.07	0.09	45.97	46.06		
6		13.32					1320.01	1.06
	3		21.78	0.24	46.05	46.28		
9		30.24					1320.02	3.43
	3		47.68	0.51	46.25	46.76		
12		65.12					1320.04	8.49
	3		111.31	1.20	46.67	47.87		
15		157.51					1320.10	20.23
	3		267.69	2.89	47.65	50.55		
18		377.88					1320.23	48.50
	3		565.89	6.11	50.02	56.13		

21		753.91					1320.51	109.55
	3		1024.25	11.06	54.95	66.01		
24		1294.60					1320.99	291.98
	3		1625.79	17.56	62.86	80.42		
27		1956.98					1321.66	637.87
	3		2301.03	24.85	73.53	98.38		
30		2645.07					1322.47	1152.44
	3		2887.25	31.18	85.93	117.12		
33		3129.43					1323.29	1775.25
	3		3207.71	34.64	97.94	132.59		
36		3285.98					1323.95	2335.98
	3		3204.49	34.61	107.36	141.97		
39		3123.00					1324.35	2697.70
	3		3081.33	33.28	112.83	146.11		
42		3039.66					1324.51	2845.69
	3		2980.85	32.19	115.38	147.57		
45		2922.04					1324.54	2871.39
	3		2840.86	30.68	116.56	147.24		
48		2759.69					1324.53	2865.58
	3		2662.83	28.76	116.29	145.05		
51		2565.97					1324.48	2817.28
	3		2364.29	25.53	114.62	140.16		
54		2162.60					1324.27	2627.55
	3		1816.33	19.62	111.78	131.40		
57		1470.05					1323.90	2292.07
	3		1342.71	14.50	106.64	121.14		
60		1215.36					1323.46	1915.51
	3		1143.40	12.35	100.46	112.80		
63		1071.43					1323.10	1625.10
	3		994.80	10.74	95.25	106.00		
66		918.17					1322.80	1398.30
	3		834.59	9.01	90.89	99.91		
69		751.02					1322.54	1200.30
	3		685.67	7.41	86.95	94.35		
72		620.33					1322.29	1031.92
	3		509.75	5.51	83.21	88.71		
75		399.18					1322.03	863.22

vii. Far future (2071-2100) of RCP4.5 Reservoir routing Baro II

Time (hr)	Δt (hr)	Inflow I (cumes)	(I1+I2)/2	((I1+I2)/2)*Δt (MCM)	S-QΔt/2 (MCM)	S+QΔt/2 (MCM)	Elevation (m)	Outflow (cumec)
0		0.00				45.96	1320.00	0.00
	3		0.55	0.01	45.96	45.97		
3		1.09					1320.00	0.06
	3		3.13	0.03	45.97	46.00		

6		5.16						1320.00	0.41
	3		8.34	0.09	45.99	46.08			
9		11.51						1320.01	1.32
	3		17.67	0.19	46.07	46.26			
12		23.83						1320.02	3.19
	3		36.16	0.39	46.23	46.62			
15		48.49						1320.03	6.95
	3		75.15	0.81	46.54	47.35			
18		101.81						1320.07	14.74
	3		157.62	1.70	47.19	48.90			
21		213.43						1320.15	31.07
	3		304.78	3.29	48.56	51.85			
24		396.13						1320.30	62.34
	3		526.64	5.69	51.18	56.87			
27		657.16						1320.55	123.11
	3		816.09	8.81	55.54	64.35			
30		975.02						1320.91	261.32
	3		1133.27	12.24	61.53	73.77			
33		1291.51						1321.35	470.88
	3		1424.92	15.39	68.68	84.07			
36		1558.32						1321.82	736.15
	3		1653.07	17.85	76.12	93.98			
39		1747.81						1322.27	1020.69
	3		1800.88	19.45	82.95	102.40			
42		1853.96						1322.65	1281.37
	3		1868.40	20.18	88.56	108.74			
45		1882.85						1322.92	1487.56
	3		1866.59	20.16	92.68	112.83			
48		1850.34						1323.10	1626.18
	3		1813.28	19.58	95.27	114.86			
51		1776.23						1323.19	1696.55
	3		1726.92	18.65	96.53	115.18			
54		1677.61						1323.21	1707.97
	3		1620.07	17.50	96.74	114.23			
57		1562.54						1323.16	1674.91
	3		1494.69	16.14	96.14	112.29			
60		1426.85						1323.08	1607.13
	3		1354.69	14.63	94.93	109.56			
63		1282.54						1322.96	1514.24
	3		1231.58	13.30	93.21	106.51			
66		1180.62						1322.83	1414.96
	3		1120.79	12.10	91.23	103.33			
69		1060.97						1322.69	1311.63
	3		1002.11	10.82	89.17	99.99			
72		943.25						1322.54	1202.91
	3		889.84	9.61	87.00	96.61			
75		836.43						1322.39	1099.45
	3		788.98	8.52	84.73	93.25			
78		741.53						1322.24	999.14

viii. Present future (2014-2034) of RCP8.5 Reservoir routing Baro II

0.00		0.00				45.96	1320.00	0.00
	3.00		0.55	0.01	45.96	45.97		
3.00		1.10					1320.00	0.06
	3.00		3.09	0.03	45.97	46.00		
6.00		5.08					1320.00	0.41
	3.00		7.77	0.08	45.99	46.08		
9.00		10.45					1320.01	1.25
	3.00		15.01	0.16	46.06	46.23		
12.00		19.57					1320.01	2.82
	3.00		29.07	0.31	46.20	46.51		
15.00		38.57					1320.03	5.82
	3.00		61.31	0.66	46.45	47.11		
18.00		84.06					1320.06	12.16
	3.00		136.46	1.47	46.98	48.45		
21.00		188.86					1320.13	26.36
	3.00		283.89	3.07	48.17	51.23		
24.00		378.92					1320.27	55.78
	3.00		529.23	5.72	50.63	56.35		
27.00		679.53					1320.52	113.49
	3.00		883.86	9.55	55.12	64.67		
30.00		1088.19					1320.92	267.13
	3.00		1318.26	14.24	61.78	76.02		
33.00		1548.33					1321.45	523.14
	3.00		1752.27	18.92	70.37	89.29		
36.00		1956.21					1322.06	880.64
	3.00		2083.07	22.50	79.78	102.28		
39.00		2209.93					1322.64	1277.42
	3.00		2278.24	24.60	88.48	113.09		
42.00		2346.54					1323.11	1635.02
	3.00		2380.25	25.71	95.43	121.14		
45.00		2413.96					1323.46	1915.31
	3.00		2421.28	26.15	100.45	126.60		
48.00		2428.60					1323.70	2115.18
	3.00		2415.05	26.08	103.76	129.84		
51.00		2401.50					1323.84	2234.67
	3.00		2372.22	25.62	105.71	131.33		
54.00		2342.95					1323.90	2289.48
	3.00		2302.16	24.86	106.60	131.46		
57.00		2261.37					1323.91	2294.53
	3.00		2202.95	23.79	106.68	130.47		
60.00		2144.53					1323.86	2258.04
	3.00		2054.74	22.19	106.09	128.28		
63.00		1964.95					1323.77	2177.03
	3.00		1862.38	20.11	104.77	124.88		
66.00		1759.81					1323.62	2051.65
	3.00		1658.77	17.91	102.72	120.64		

69.00		1557.73						1323.44	1897.88
	3.00		1462.35	15.79	100.14	115.93			
72.00		1366.96						1323.24	1734.07
	3.00		1280.32	13.83	97.20	111.03			
75.00		1193.69						1323.03	1563.41
	3.00		1117.95	12.07	94.15	106.22			
78.00		1042.20						1322.81	1405.61
	3.00		976.21	10.54	91.04	101.58			
81.00		910.22						1322.61	1254.79

ix. Mid (2034-2070) of RCP8.5 Reservoir routing Baro II

0.00		0.00					45.96	1320.00	0.00
	3.00		0.55	0.01	45.96	45.97			
3.00		1.09						1320.00	0.05
	3.00		3.03	0.03	45.97	46.00			
6.00		4.96						1320.00	0.31
	3.00		7.42	0.08	45.99	46.07			
9.00		9.88						1320.01	0.93
	3.00		13.99	0.15	46.06	46.22			
12.00		18.11						1320.01	2.07
	3.00		27.33	0.30	46.19	46.49			
15.00		36.55						1320.03	4.29
	3.00		60.50	0.65	46.44	47.10			
18.00		84.45						1320.06	9.21
	3.00		142.87	1.54	47.00	48.54			
21.00		201.28						1320.13	20.91
	3.00		313.85	3.39	48.31	51.70			
24.00		426.41						1320.29	46.55
	3.00		613.05	6.62	51.20	57.82			
27.00		799.68						1320.60	108.98
	3.00		1061.45	11.46	56.64	68.11			
30.00		1323.21						1321.11	264.53
	3.00		1606.23	17.35	65.25	82.60			
33.00		1889.25						1321.80	545.62
	3.00		2098.67	22.67	76.71	99.37			
36.00		2308.09						1322.58	933.78
	3.00		2444.68	26.40	89.29	115.69			
39.00		2581.27						1323.33	1366.60
	3.00		2679.81	28.94	100.93	129.87			
42.00		2778.35						1323.97	1775.79
	3.00		2876.52	31.07	110.69	141.76			
45.00		2974.68						1324.50	2142.01
	3.00		3015.86	32.57	118.63	151.20			
48.00		3057.04						1324.68	2270.52
	3.00		3032.24	32.75	126.68	159.42			
51.00		3007.45						1324.83	2382.55

	3.00		2950.42	31.86	133.69	165.56		
54.00		2893.40					1324.94	2466.07
	3.00		2842.20	30.70	138.92	169.62		
57.00		2791.00					1325.01	2517.50
	3.00		2732.09	29.51	142.43	171.94		
60.00		2673.17					1325.04	2539.25
	3.00		2605.91	28.14	144.51	172.66		
63.00		2538.64					1325.05	2544.19
	3.00		2465.21	26.62	145.18	171.80		
66.00		2391.79					1325.04	2538.00
	3.00		2305.96	24.90	144.39	169.30		
69.00		2220.14					1325.01	2494.07
	3.00		2104.98	22.73	142.36	165.10		
72.00		1989.83					1324.93	2459.79
	3.00		1854.64	20.03	138.53	158.56		
75.00		1719.44					1324.81	2370.78
	3.00		1596.33	17.24	132.96	150.20		
78.00		1473.22					1324.66	2256.88
	3.00		1368.52	14.78	125.82	140.60		
81.00		1263.82					1324.45	2106.09

X. Far future (2071-2100) of RCP8.5 Reservoir routing Baro II

0.00		0.00				45.96	1320.00	0.00
	3.00		0.55	0.01	45.96	45.97		
3.00		1.09					1320.00	0.05
	3.00		3.13	0.03	45.97	46.00		
6.00		5.17					1320.00	0.32
	3.00		8.36	0.09	46.00	46.09		
9.00		11.54					1320.01	1.02
	3.00		17.75	0.19	46.07	46.27		
12.00		23.95					1320.02	2.49
	3.00		36.06	0.39	46.24	46.63		
15.00		48.18					1320.03	5.42
	3.00		74.67	0.81	46.57	47.38		
18.00		101.16					1320.07	11.49
	3.00		158.40	1.71	47.25	48.96		
21.00		215.64					1320.15	24.35
	3.00		304.61	3.29	48.70	51.99		
24.00		393.58					1320.31	48.88
	3.00		515.11	5.56	51.46	57.03		
27.00		636.64					1320.56	97.61
	3.00		792.90	8.56	55.97	64.54		
30.00		949.17					1320.93	205.43
	3.00		1110.97	12.00	62.32	74.31		
33.00		1272.78					1321.41	376.92
	3.00		1409.63	15.22	70.24	85.47		

36.00		1546.48					1321.94	606.07
	3.00		1641.25	17.73	78.92	96.65		
39.00		1736.03					1322.46	838.44
	3.00		1800.42	19.44	87.59	107.04		
42.00		1864.81					1322.94	1130.61
	3.00		1881.62	20.32	94.83	115.15		
45.00		1898.42					1323.31	1351.69
	3.00		1879.24	20.30	100.55	120.85		
48.00		1860.05					1323.56	1511.30
	3.00		1813.52	19.59	104.52	124.11		
51.00		1767.00					1323.71	1606.95
	3.00		1722.35	18.60	106.75	125.36		
54.00		1677.71					1323.77	1643.47
	3.00		1627.50	17.58	107.61	125.18		
57.00		1577.28					1323.76	1638.42
	3.00		1521.46	16.43	107.49	123.92		
60.00		1465.65					1323.70	1601.40
	3.00		1402.00	15.14	106.63	121.77		
63.00		1338.35					1323.61	1538.29
	3.00		1268.23	13.70	105.15	118.85		
66.00		1198.10					1323.47	1453.79
	3.00		1138.33	12.29	103.15	115.44		
69.00		1078.56					1323.32	1359.83
	3.00		1019.45	11.01	100.76	111.77		
72.00		960.34					1323.15	1258.44
	3.00		901.81	9.74	98.18	107.92		
75.00		843.29					1322.98	1127.71
	3.00		798.40	8.62	95.74	104.36		
78.00		753.52					1322.81	1061.85

E. RCM data Projected simulated flow for frequency Analysis

E.1 Maximum daily annual flow of simulated RCP4.5

Year	**Annual Daily Max. flow Q**	**Year**	**Annual Daily Max. flow Q**	**Year**	**Annual Daily Max. flow Q**
2014	906.9	2043	769.3	2072	1081
2015	4211	2044	2732	2073	836.3
2016	1506	2045	1924	2074	987.3
2017	2127	2046	938.1	2075	1442
2018	1281	2047	2206	2076	2498
2019	1899	2048	1380	2077	974.9
2020	806	2049	2507	2078	2076
2021	2276	2050	736.5	2079	3274
2022	2692	2051	1527	2080	1036

2023	1589	2052	1172	2081	1617
2024	692.8	2053	2303	2082	2060
2025	2259	2054	747.6	2083	1340
2026	1964	2055	2200	2084	3477
2027	1322	2056	1252	2085	2640
2028	1855	2057	1207	2086	1308
2029	1855	2058	482	2087	1443
2030	954.7	2059	2179	2088	2339
2031	1578	2060	775.4	2089	2378
2032	1211	2061	1435	2090	2275
2033	1740	2062	1248	2091	2193
2034	2066	2063	1818	2092	1675
2035	1794	2064	999	2093	1665
2036	1270	2065	1560	2094	2364
2037	928	2066	797.5	2095	1672
2038	955.9	2067	2584	2096	3148
2039	2271	2068	2511	2097	3362
2040	2514	2069	1175	2098	1861
2041	2847	2070	1754	2099	2517
2042	1123	2071	1213	2100	570.8

E.2 Maximum daily annual flow of simulated RCP8.5

Year	Annual Daily Max. flow Q	Year	Annual Daily Max. flow Q	Year	Annual Daily Max. flow Q
2014	2715	2043	2690	2072	3632
2015	2921	2044	1552	2073	1979
2016	1147	2045	1264	2074	3780
2017	1389	2046	1252	2075	1968
2018	1422	2047	956.7	2076	1765
2019	1726	2048	1889	2077	1622
2020	1056	2049	2208	2078	1769
2021	1823	2050	2075	2079	3084
2022	1823	2051	878.8	2080	1065
2023	1829	2052	2620	2081	1286
2024	1222	2053	2395	2082	1919
2025	2074	2054	996.5	2083	858.2
2026	3216	2055	626.2	2084	3144
2027	2094	2056	1906	2085	2170
2028	1664	2057	1752	2086	2180
2029	3573	2058	2179	2087	3135

2030	1455	2059	1549	2088	925
2031	1699	2060	1440	2089	2291
2032	2415	2061	918.3	2090	3080
2033	1742	2062	3000	2091	739.7
2034	794.6	2063	3322	2092	1506
2035	2412	2064	3752	2093	1617
2036	1277	2065	1356	2094	1223
2037	1758	2066	596.4	2095	1832
2038	1251	2067	2692	2096	1235
2039	2130	2068	1869	2097	2608
2040	1890	2069	3445	2098	1074
2041	1075	2070	1161	2099	2603
2042	1596	2071	1299	2100	3000

F. Best fit Distribution Calculation Simulated Output for Two Scenarios (RCP4.5 and RCP8.5)

F.1. Parameters and L-moment Distribution for RCP4.5 (β)

Present future

Rank of Data (i)	**βo = ppt (j)**	**β1 =((n-j)*X_j)/(n*(n-1))**	**β2 =((n-j)(n-j-1)Xj)/(n*(n-1)(n-2))**	**β3 =((n-j)(n-j-1)(n-j-2)*Xj)/(n*(n-1)(n-2)(n-3))**
1	4211	210.550	210.550	210.550
2	2692	127.516	120.432	113.347
3	2276	101.821	90.508	79.860
4	2259	95.116	79.263	65.276
5	2127	83.961	65.303	49.937
6	1964	72.358	52.258	36.888
7	1899	64.966	43.311	28.024
8	1855	58.579	35.798	21.058
9	1855	53.697	29.832	15.793
10	1740	45.789	22.895	10.774
11	1589	37.634	16.726	6.887
12	1578	33.221	12.919	4.560
13	1506	27.742	9.247	2.720
14	1322	20.874	5.798	1.364
15	1281	16.855	3.746	0.661
16	1211	12.747	2.125	0.250
17	954.7	7.537	0.837	0.049
18	906.9	4.773	0.265	0.000
19	806	2.121	0.000	0.000
20	692.8	0.000	0.000	0.000

Mean	**1736.270**			
Sum	**34725.4**	**1077.858**	**801.813**	**647.999**

Mid future

Rank of Data (i)	**βo = ppt (j)**	**β1 =((n-j)*Xj)/(n*(n-1))**	**β2 =((n-j)(n-j-1)Xj)/(n*(n-1)(n-2))**	**β3 =((n-j)(n-j-1)(n-j-2)*Xj)/(n*(n-1)(n-2)(n-3))**
1	2847	76.946	76.946	76.946
2	2732	71.787	69.736	67.685
3	2584	65.958	62.189	58.531
4	2514	62.284	56.945	51.921
5	2511	60.324	53.430	47.144
6	2507	58.346	50.011	42.656
7	2303	51.869	42.977	35.393
8	2271	49.444	39.555	31.411
9	2206	46.372	35.773	27.356
10	2200	44.595	33.127	24.358
11	2179	42.533	30.381	21.445
12	2066	38.776	26.589	17.987
13	1924	34.667	22.781	14.741
14	1818	31.392	19.732	12.187
15	1794	29.631	17.778	10.458
16	1754	27.653	15.802	8.830
17	1560	23.423	12.716	6.732
18	1527	21.782	11.202	5.601
19	1435	19.392	9.419	4.432
20	1380	17.613	8.051	3.552
21	1270	15.255	6.538	2.692
22	1252	14.099	5.640	2.156
23	1248	13.117	4.872	1.720
24	1207	11.780	4.039	1.307
25	1175	10.586	3.327	0.978
26	1172	9.679	2.765	0.732
27	1123	8.431	2.168	0.510
28	999	6.750	1.543	0.318
29	955.9	5.741	1.148	0.203
30	938.1	4.930	0.845	0.124
31	928	4.180	0.597	0.070
32	797.5	2.994	0.342	0.030
33	775.4	2.329	0.200	0.012

34	769.3	1.733	0.099	0.003
35	747.6	1.123	0.032	0.000
36	736.5	0.553	0.000	0.000
37	482	0.000	0.000	0.000
Mean	**1586.170**			
Sum	**58688.3**	**988.064**	**729.296**	**580.222**

Far Future

Rank of Data (i)	**βo = ppt (j)**	**β1 =((n-j)*Xj)/(n*(n-1))**	**β2 =((n-j)(n-j-1)Xj)/(n*(n-1)(n-2))**	**β3 =((n-j)(n-j-1)(n-j-2)*Xj)/(n*(n-1)(n-2)(n-3))**
1	3477	115.900	115.900	115.900
2	3362	108.202	104.338	100.474
3	3274	101.607	94.349	87.360
4	3148	94.078	83.998	74.665
5	2640	75.862	65.025	55.391
6	2517	69.434	57.035	46.473
7	2498	66.039	51.888	40.357
8	2378	60.133	45.100	33.407
9	2364	57.062	40.759	28.682
10	2339	53.770	36.487	24.325
11	2275	49.684	31.940	20.110
12	2193	45.372	27.548	16.324
13	2076	40.566	23.180	12.878
14	2060	37.885	20.296	10.524
15	1861	32.086	16.043	7.724
16	1675	26.954	12.514	5.562
17	1672	24.984	10.707	4.362
18	1665	22.966	9.022	3.342
19	1617	20.445	7.302	2.434
20	1443	16.586	5.331	1.580
21	1442	14.917	4.262	1.105
22	1340	12.322	3.080	0.685
23	1308	10.524	2.255	0.418
24	1213	8.366	1.494	0.221
25	1081	6.213	0.888	0.099
26	1036	4.763	0.510	0.038
27	987.3	3.404	0.243	0.009
28	974.9	2.241	0.080	0.000
29	836.3	0.961	0.000	0.000
30	570.8	0.000	0.000	0.000
Mean	**1910.777**			

Sum	57323.3	1183.328	871.575	694.449

F.2. Parameters and L-moment Distribution for RCP4.5 (λ, τ)

Parameters	Present future	Mid future	Far future
λ1 = βo =	1736.27	1586.170	1910.777
λ2 = 2 β1 − βo =	419.445	389.958	455.879
λ3 = 6 β2 − 6 β1 + βo	80.001	33.560	40.259
λ4 = 20β3 − 30 β2+12 β1 - βo	127.673	44.845	57.039
τ = λ 2/ λ 1	0.242	0.246	0.239
τ3 = λ 3 / λ 2 (Skewness)	0.191	0.086	0.088
τ4 = λ4/λ2 (Kurtosis)	0.165	0.115	0.125

F.3. Parameters and L-moment Distribution for RCP8.5 (β)

Present Future

Rank of Data (i)	**βo = ppt (j)**	**β1 =((n-j)*Xj)/(n*(n-1))**	**β2 =((n-j)(n-j-1)Xj)/(n*(n-1)(n-2))**	**β3 =((n-j)(n-j-1)(n-j-2)*Xj)/(n*(n-1)(n-2)(n-3))**
1	3573	178.650	178.650	178.650
2	3216	152.337	143.874	135.411
3	2921	130.676	116.157	102.491
4	2715	114.316	95.263	78.452
5	2415	95.329	74.145	56.699
6	2094	77.147	55.718	39.330
7	2074	70.953	47.302	30.607
8	1829	57.758	35.296	20.763
9	1823	52.771	29.317	15.521
10	1823	47.974	23.987	11.288
11	1742	41.258	18.337	7.550
12	1726	36.337	14.131	4.987
13	1699	31.297	10.432	3.068
14	1664	26.274	7.298	1.717
15	1455	19.145	4.254	0.751
16	1422	14.968	2.495	0.293
17	1389	10.966	1.218	0.072
18	1222	6.432	0.357	0.000
19	1147	3.018	0.000	0.000
20	1056	0.000	0.000	0.000
Mean	**1950.250**			

Sum	39005	1167.605	858.232	687.651

Mid Future

Rank of Data (i)	βo = ppt (j)	β1 =((n-j)*Xj)/(n*(n-1))	β2 =((n-j)(n-j-1)Xj)/(n*(n-1)(n-2))	β3 =((n-j)(n-j-1)(n-j-2)*Xj)/(n*(n-1)(n-2)(n-3))
1	3752	101.405	101.405	101.405
2	3445	90.522	87.935	85.349
3	3322	84.796	79.950	75.247
4	3000	74.324	67.954	61.958
5	2692	64.673	57.282	50.543
6	2690	62.605	53.662	45.770
7	2620	59.009	48.893	40.265
8	2412	52.514	42.011	33.362
9	2395	50.345	38.838	29.700
10	2208	44.757	33.248	24.447
11	2179	42.533	30.381	21.445
12	2130	39.977	27.413	18.544
13	2075	37.387	24.569	15.897
14	1906	32.911	20.687	12.777
15	1890	31.216	18.730	11.017
16	1889	29.782	17.018	9.510
17	1869	28.063	15.234	8.065
18	1758	25.077	12.897	6.448
19	1752	23.676	11.500	5.412
20	1596	20.369	9.312	4.108
21	1552	18.643	7.990	3.290
22	1549	17.444	6.977	2.668
23	1440	15.135	5.622	1.984
24	1356	13.234	4.537	1.468
25	1277	11.505	3.616	1.063
26	1264	10.438	2.982	0.789
27	1252	9.399	2.417	0.569
28	1251	8.453	1.932	0.398
29	1161	6.973	1.395	0.246
30	1075	5.649	0.968	0.142
31	996.5	4.489	0.641	0.075
32	956.7	3.591	0.410	0.036
33	918.3	2.758	0.236	0.014
34	878.8	1.979	0.113	0.003
35	794.6	1.193	0.034	0.000
36	626.2	0.470	0.000	0.000

37	596.4	0.000	0.000	0.000
Mean	**1797.959**			
Sum	**66524.5**	**1127.295**	**838.789**	**674.017**

Far Future

Rank of Data (i)	**βo = ppt (j)**	**β1 =((n-j)*X_j)/(n*(n-1))**	**β2 =((n-j)(n-j-1)Xj)/(n*(n-1)(n-2))**	**β3 =((n-j)(n-j-1)(n-j-2)*Xj)/(n*(n-1)(n-2)(n-3))**
1	3780	126.000	126.000	126.000
2	3632	116.892	112.717	108.543
3	3144	97.572	90.603	83.892
4	3135	93.690	83.651	74.357
5	3084	88.621	75.961	64.707
6	3080	84.966	69.793	56.868
7	3000	79.310	62.315	48.467
8	2608	65.949	49.462	36.639
9	2603	62.831	44.879	31.582
10	2291	52.667	35.738	23.825
11	2180	47.609	30.606	19.270
12	2170	44.897	27.259	16.153
13	1979	38.670	22.097	12.276
14	1968	36.193	19.389	10.054
15	1919	33.086	16.543	7.965
16	1832	29.480	13.687	6.083
17	1769	26.433	11.329	4.615
18	1765	24.345	9.564	3.542
19	1622	20.508	7.324	2.441
20	1617	18.586	5.974	1.770
21	1506	15.579	4.451	1.154
22	1299	11.945	2.986	0.664
23	1286	10.347	2.217	0.411
24	1235	8.517	1.521	0.225
25	1223	7.029	1.004	0.112
26	1074	4.938	0.529	0.039
27	1065	3.672	0.262	0.010
28	925	2.126	0.076	0.000
29	858.2	0.986	0.000	0.000
30	739.7	0.000	0.000	0.000
Mean	**2012.963**			
Sum	**60388.9**	**1253.446**	**927.940**	**741.665**

F.4. Parameters and L-moment Distribution for RCP8.5 (λ, τ)

Parameters	Present Future	Mid Future	Far Future
$\lambda_1 = \beta_o =$	1950.25	1797.959	2012.963
$\lambda_2 = 2\,\beta_1 - \beta_o =$	384.961	456.630	493.929
$\lambda_3 = 6\,\beta_2 - 6\,\beta_1 + \beta_o$	94.008	66.925	59.924
$\lambda_4 = 20\beta_3 - 30\,\beta_2 + 12\,\beta_1 - \beta_o$	75.067	71.407	58.778
$\tau = \lambda_2 / \lambda_1$	0.197	0.254	0.245
$\tau_3 = \lambda_3 / \lambda_2$ (Skewness)	0.244	0.147	0.121
$\tau_4 = \lambda_4/\lambda_2$ (Kurtosis)	0.195	0.156	0.119

F.5. the computed values of the skewness and kurtosis for the selection of the frequency analysis for RCP4.5

Present Future

Skewness	Kurtosis		
	Log normal distribution	General extreme value	Pearson type III
0	0.123	0.107	0.122
0.05	0.125	0.115	0.123
0.07	0.127	0.119	0.124
0.09	0.129	0.124	0.125
0.11	0.132	0.129	0.126
0.13	0.136	0.136	0.128
0.15	0.140	0.143	0.130
0.17	0.145	0.150	0.132
0.19	0.151	0.158	0.134
0.191	0.151	0.159	0.135

Mid Future

Skewness	Kurtosis		
	Log normal distribution	General extreme value	Log Pearson type III
0	0.123	0.107	0.122

0.01	0.123	0.108	0.122
0.02	0.123	0.110	0.123
0.03	0.124	0.111	0.123
0.04	0.124	0.113	0.123
0.05	0.125	0.115	0.123
0.06	0.126	0.117	0.123
0.07	0.127	0.119	0.124
0.08	0.128	0.121	0.124
0.083	0.128	0.122	0.125
0.086	0.129	0.123	0.125

Far Future

Skewness	Kurtosis		
	Log normal distribution	General extreme value	Log Pearson type III
0	0.123	0.107	0.122
0.01	0.123	0.108	0.122
0.02	0.123	0.110	0.123
0.03	0.124	0.111	0.123
0.04	0.124	0.113	0.123
0.05	0.125	0.115	0.123
0.06	0.126	0.117	0.123
0.07	0.127	0.119	0.124
0.08	0.128	0.121	0.124
0.083	0.128	0.122	0.125
0.088	0.129	0.123	0.125

F.6. the computed values of the skewness and kurtosis for the selection of the frequency analysis for RCP8.5
Present Future

Skewness	Kurtosis		
	Log normal distribution	General extreme value	Pearson type III
0	0.123	0.107	0.122
0.05	0.125	0.115	0.123
0.07	0.127	0.119	0.124
0.09	0.129	0.124	0.125
0.11	0.132	0.129	0.126
0.13	0.136	0.136	0.128

0.15	0.140	0.143	0.130
0.17	0.145	0.150	0.132
0.19	0.151	0.158	0.134
0.21	0.157	0.167	0.137
0.24	0.168	0.182	0.143
0.244	0.169	0.184	0.144

Mid Future

Skewness	Kurtosis		
	Log normal distribution	General extreme value	Pearson type III
0	0.123	0.107	0.122
0.02	0.123	0.110	0.123
0.04	0.124	0.113	0.123
0.06	0.126	0.117	0.123
0.08	0.128	0.121	0.124
0.1	0.131	0.127	0.126
0.11	0.132	0.129	0.126
0.12	0.134	0.132	0.127
0.13	0.136	0.136	0.128
0.14	0.138	0.139	0.129
0.147	0.140	0.141	0.129

Far Future

Skewness	Kurtosis		
	Log normal distribution	General extreme value	Log Pearson type III
0	0.123	0.107	0.122
0.01	0.123	0.108	0.122
0.02	0.123	0.110	0.123
0.03	0.124	0.111	0.123
0.04	0.124	0.113	0.123
0.05	0.125	0.115	0.123
0.06	0.126	0.117	0.123
0.07	0.127	0.119	0.124
0.08	0.128	0.121	0.124
0.09	0.129	0.124	0.125
0.1	0.131	0.127	0.126
0.12	0.134	0.132	0.127
0.121	0.134	0.133	0.127